國立中央大學天文研究所
鹿林天文台年報

2008

No.6

國立中央大學天文研究所編

目錄

研究報告

The Observations of Comets 17P/Holmes, C/2007 W1 (Boattini), and C/2007 N3 (Lulin)

C.H. Lin(林建賢),Z.Y. Lin(林忠義),W.H. Ip(葉永烜),T.W. Chen(陳婷琬),Y.C. Cheng(鄭宇棋),
C.S. Lin(林啟生),C.Y. Shih(施佳佑),H.Y. Hsiao(蕭翔耀),H.C. Lin(林宏欽)
Graduate Institute of Astronomy, National Central University

17P/Holmes

At the October 24 2007, the short-period comet **17P/Holmes** was observed to brighten up extremely and reached magnitude 2.5th from 17th within 42 hours. This comet whose period is 6.88 yrs had passed its perihelion (2.053AU) at May in 2007, and the outburst happened near the perigee (1.62AU on Nov. 6). We have observed 17P with LOT since last Oct. 24 and continued monitoring it in the following months. Except for the BVRI broad-band filters, we also used the Rosetta narrow-band filters including CN, NH_2, H_2O^+, C_2, Rc, Bc in several days.

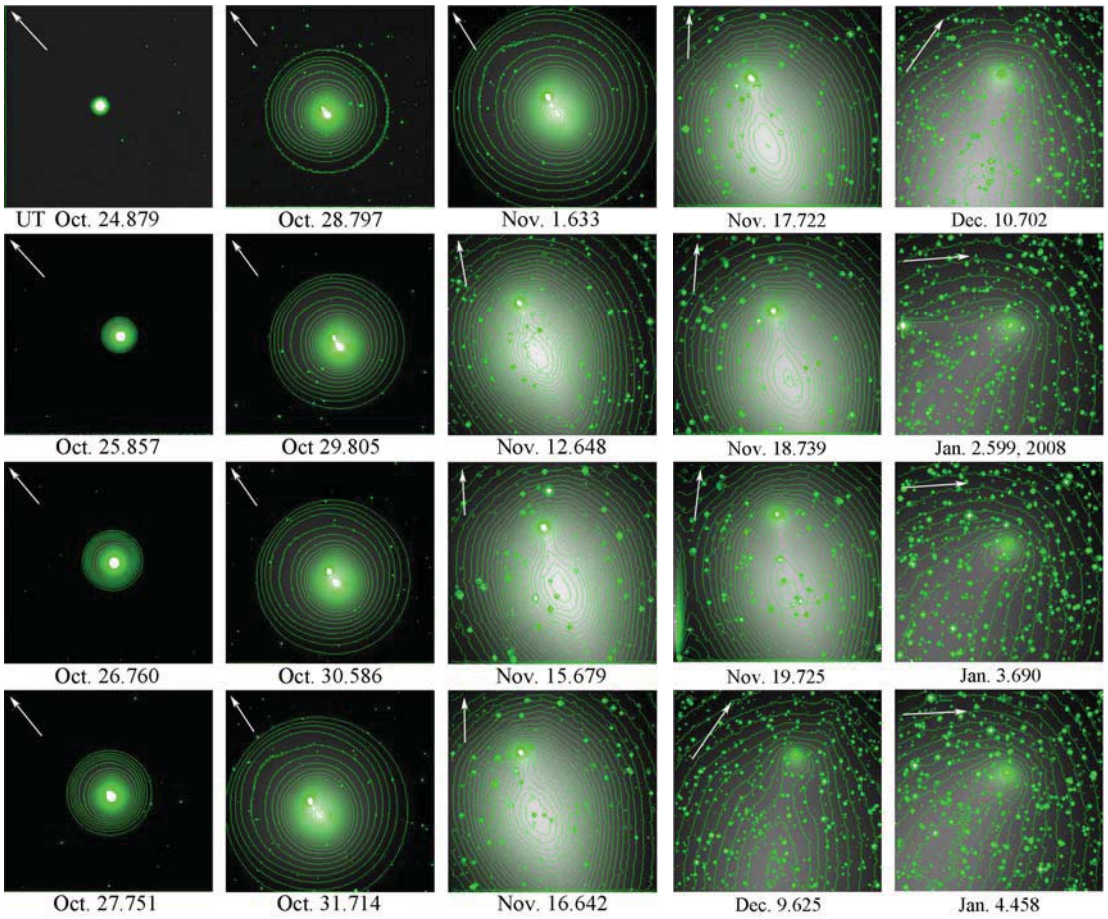

Figure 1: The contour plot of R-band images of 17P/Holmes from Oct. 24, 2007 to Jan. 4, 2008. The white arrows point out the projected solar direction. The FOV of all

frames is 11' x 11'. Every step of the contour is 3% of the brightness.

As shown in Figure.1, at the first day of Oct 24, 17P just looked like a small fuzzy spot. In the following days, there was an apparent condensation cloud, so-called the coma blob, traveling apart from the cometary nucleus and also expanding spherically in early evolution. In the latter phase after the mid-November, the coma blob was no longer like a circular condensation part but diffused and dragged by the gravity of the Sun into a drill shape.

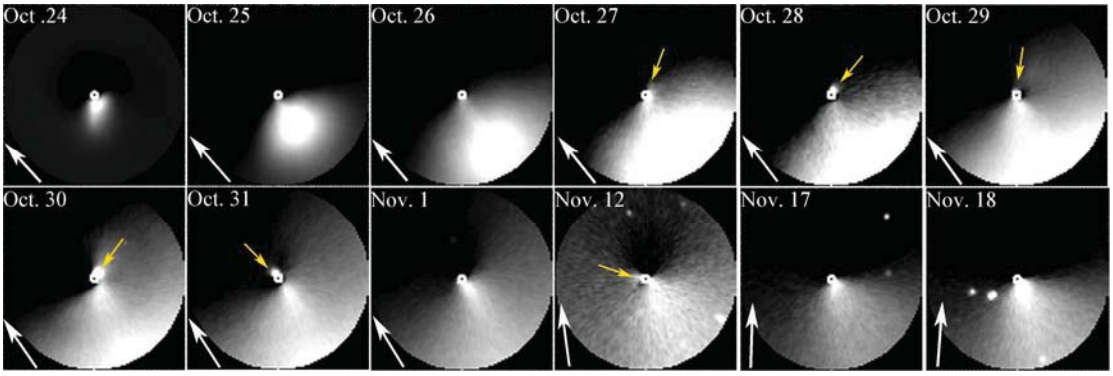

Figure 2: The series of images processed by ring masking method from Oct.24 to Nov.18. FOV is 0.86' x 0.86', about 60,000 km in width. The yellow arrows point out the minor jets.

One of the image procession we use here is *Azimutahl Media Subtraction (ring masking)*, and this method will reveal the detailed structure around the nuclear region. Except for the main eruption region for the 2007 outburst in our resulted images (Figure 2), we also find a minor jet revealing since Oct. 27 relative another active region on the nucleus surface. This minor jet has lasted for at least two weeks.

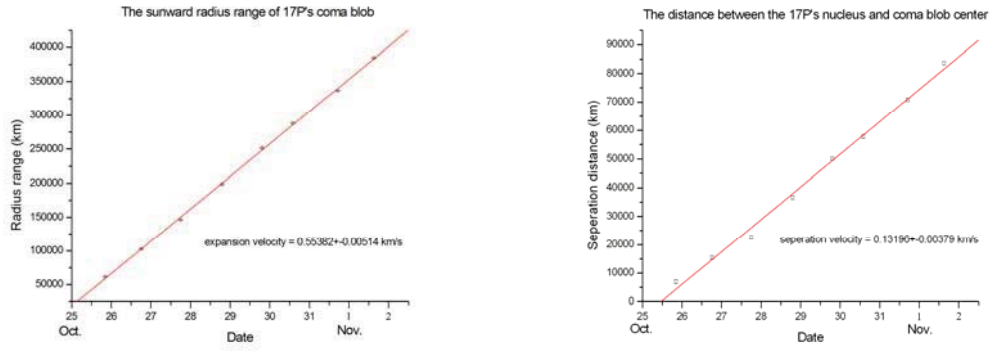

Figure 3: The left diagram shows the separating distance between the nucleus and the coma blob and is estimated to be a constant rate as 0.132±0.004km/s. The right diagram shows the radial distance of the sunward coma and is also estimated to be a constant rate as 0.554±0.005km/s.

We also roughly estimated the ejected mass of the very first outburst to be about 0.25% of the total nuclear mass and the gas production rate with Afρ (related to dust production rate) of the inner coma.

The paper of these results has been submitted to *The Astronomical Journal* (AJ).

C/2007 W1 (Boattini)

The comet **C/2007 W1 (Boattini)** reached perihelion on June 24, 2008. It was a naked-eye object when it was close to Sun with m~6. The filters of LOT applied to this new comet also contain broad-band and Rosetta narrow-band filters. Therefore it could be very useful in the detailed study of the outgassing activity and production rates of daughter species, dust to gas ratios.

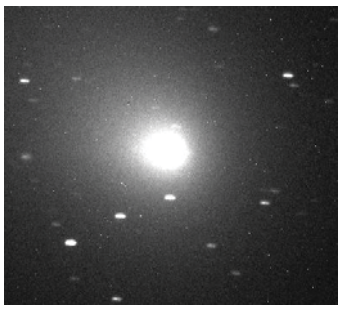

Figure 4: The R-band image of C/2007 W1 (Boattini) taken on May 3, 2008.

C/2007 N3 (Lulin)

The new comet **C/2007 N3 (Lulin)**, hereafter comet Lulin, is the first discovery of a comet by Lulin Observatory with 41cm telescope (SLT) in Taiwan on July 11, 2007. It reached the perihelion with 1.21 AU from the sum on Jan. 10, 2009. And this comet may be the most luminous comet of the year on Feb. 24, which is in the perigee phase. We have monitored comet Lulin for a long time scale since its discovery with both LOT and SLT. The original magnitude as we first saw is about 19 only and it reached the brightest value to be about 6 when the comet traveled close the Earth.

We applied Rosetta narrow-band filters consisting CN, NH_2, H_2O^+, H_2O-continuum, C_2, R-continuum, and B-continuum to observe comet Lulin for a shorter period observation with LOT. It will help us to evaluate the production rate of molecular gas and the correlated dust color. It revealed high production rate and Afρ since the existence of the apparent jets around the cometary nucleus (see Figure 5).

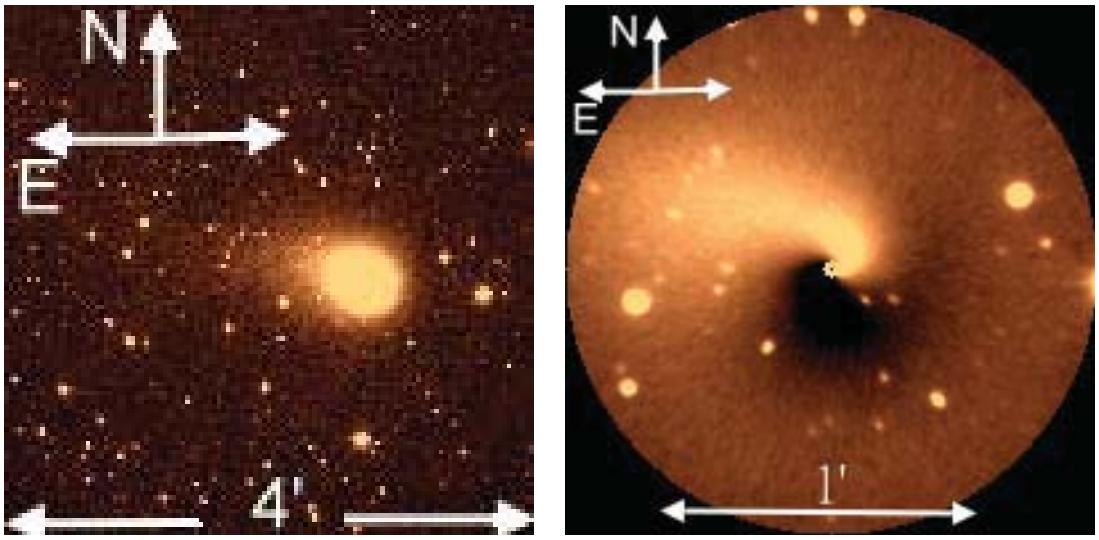

Figure 5: The left diagram is the unfilter image of comet Lulin taken by H.C. Lin on July 23, 2008. The right diagram is the same enlarged image with the left frame but processed by Azimuthal media subtraction (Ring masking).

We can already see that the coma of comet Lulin in the left diagram of Figure 5 is nearly in spherical shape and with a tiny anti-tail. It may be caused by the cometary orbit to which parallel the ecliptic. And after the procession of the original image centered on the nucleus, we see an apparent spiral jet due to the rotation of the nucleus (see the right frame of Figure 5). By different narrow bands of the images after the subtraction of continuous flux, the detailed structures of different daughter species can be revealed. We will estimate the more precise gas production rate calibrated by the spectroscopic standard stars and derive more detailed the evolution of both coma and tails from the enormous data set of comet Luin in the future.

The Astrophysical Journal, 685: L157–L160, 2008 October 1

FIRST RESULTS FROM THE TAIWANESE-AMERICAN OCCULTATION SURVEY (TAOS)

Z.-W. Zhang,[1] F. B. Bianco,[2,3] M. J. Lehner,[4,3] N. K. Coehlo,[5] J.-H. Wang,[1,4] S. Mondal,[1] C. Alcock,[3] T. Axelrod,[6] Y.-I. Byun,[7] W. P. Chen,[1] K. H. Cook,[8] R. Dave,[9] I. de Pater,[10] R. Porrata,[10] D.-W. Kim,[7] S.-K. King,[4] T. Lee,[4] H.-C. Lin,[1] J. J. Lissauer,[11] S. L. Marshall,[12,8] P. Protopapas,[3] J. A. Rice,[5] M. E. Schwamb,[13] S.-Y. Wang,[4] and C.-Y. Wen[4]

Received 2008 March 24; accepted 2008 August 21; published 2008 September 9

ABSTRACT

Results from the first 2 years of data from the Taiwanese-American Occultation Survey (TAOS) are presented. Stars have been monitored photometrically at 4 or 5 Hz to search for occultations by small (~3 km) Kuiper Belt objects (KBOs). No statistically significant events were found, allowing us to present an upper bound to the size distribution of KBOs with diameters 0.5 km $< D <$ 28 km.

Subject headings: Kuiper Belt — occultations — solar system: formation

1. INTRODUCTION

The study of the Kuiper Belt has exploded since the discovery of 1992 QB1 by Jewitt & Luu (1993). The brightness distribution of objects with R magnitude brighter than ~26 is relatively well established by many surveys, most recently by Fraser et al. (2008) and references therein. The brightness distribution is adequately described by a simple cumulative luminosity function $\Sigma(< R) = 10^{\alpha(R-R_0)}$ deg^{-2}, where $R_0 \sim 23$ and $\alpha \sim 0.6$, for objects with magnitude $R < 26$. There is clear evidence for a break to a shallower slope for fainter objects: the deepest survey, conducted using the Advanced Camera for Surveys on the *Hubble Space Telescope* (Bernstein et al. 2004), extended to $R = 28.5$, and found a factor of ~25 fewer objects than would be expected if the same distribution extended into this range.

The size distribution of Kuiper Belt objects (KBOs) is believed to reflect a history of *agglomeration* during the planetary formation epoch, when relative velocities between particles were low and collisions typically resulted in particles sticking together, followed by *destructive collisions* when the relative velocities were increased by dynamical processes after the giant planets formed (Stern 1996; Davis & Farinella 1997; Stern & Colwell 1997; Kenyon & Luu 1999a, 1999b; Kenyon & Bromley 2004; Pan & Sari 2005). The slope of the distribution function for larger objects reflects the early phase of agglomeration, while the shallower distribution for smaller objects reflects a subsequent phase of destructive collisions. The location of the break moves to larger sizes with time, while the distribution for smaller objects is expected to evolve toward a steady state collisional cascade (Kenyon & Bromley 2004; Pan & Sari 2005). Models for the spectrum of small bodies differ between Pan & Sari (2005) who derived a double-power-law distribution, and Kenyon & Bromley (2004) whose simulations show more structure, depending on material properties.

Thus, the size spectrum encodes information about the history of planet formation and dynamics. However, the size spectrum for small KBOs is not constrained by the imaging surveys because the objects of interest are too faint for direct detection using presently available instruments. These small objects may, however, be detected indirectly when they pass between an observer and a distant star (Bailey 1976; Dyson 1992; Axelrod et al. 1992; Brown & Webster 1997; Roques & Moncuquet 2000; Cooray & Farmer 2003; Nihei et al. 2007). The challenge confronting any survey exploiting this technique is the combination of very low anticipated event rate and short duration of the events (typically <1 s).

Other groups are attempting similar occultation surveys. Roques et al. (2006) reported three events in 10 star-hours of photometric data sampled at 45 Hz, which they modeled as objects at 15, 140, and 210 AU, respectively, placing the inferred objects outside the Kuiper Belt. Bickerton et al. (2008) reported results of 5 star-hours of data sampled at 40 Hz, during which no events were detected. Chang et al. (2006) reported a surprisingly high rate of possible occultation events in *RXTE* X-ray observations of Sco X-1, but many of these events have since been attributed to instrumental effects (Jones et al. 2008; Chang et al. 2007).

We report here the first results of the Taiwanese American Occultation Survey (TAOS). TAOS differs from the previously reported projects primarily in the extent of the photometric time series, a total of 1.53×10^5 star-hours, and in that data are collected simultaneously with three telescopes. Some compromises have been made in regard to the signal-to-noise ratio (S/N), which is typically lower than in previously reported surveys, and in cadence, which is 4 or 5 Hz, in contrast with the higher rates mentioned above. The substantial increase in exposure more than compensates for the lower cadence and S/N, and we are able to

[1] Institute of Astronomy, National Central University, No. 300, Jhongda Road, Jhongli City, Taoyuan County 320, Taiwan; s1249001@cc.ncu.edu.tw.
[2] Department of Physics and Astronomy, University of Pennsylvania, 209 South 33rd Street, Philadelphia, PA 19104.
[3] Harvard-Smithsonian Center for Astrophysics, 60 Garden Street, Cambridge, MA 02138.
[4] Institute of Astronomy and Astrophysics, Academia Sinica, P.O. Box 23-141, Taipei 106, Taiwan.
[5] Department of Statistics, University of California, 367 Evans Hall, Berkeley, CA 94720.
[6] Steward Observatory, 933 North Cherry Avenue, Room N204, Tucson, AZ 85721.
[7] Department of Astronomy, Yonsei University, 134 Shinchon, Seoul 120-749, Korea.
[8] Institute of Geophysics and Planetary Physics, Lawrence Livermore National Laboratory, Livermore, CA 94550.
[9] Initiative in Innovative Computing, Harvard University, 60 Oxford Street, Cambridge, MA 02138.
[10] Department of Astronomy, University of California, 601 Campbell Hall, Berkeley, CA 94720.
[11] Space Science and Astrobiology Division 245-3, NASA Ames Research Center, Moffett Field, CA 94035.
[12] Kavli Institute for Particle Astrophysics and Cosmology, 2575 Sand Hill Road, MS 29, Menlo Park, CA 94025.
[13] Division of Geological and Planetary Sciences, California Institute of Technology, 1201 East California Boulevard, Pasadena, CA 91125.

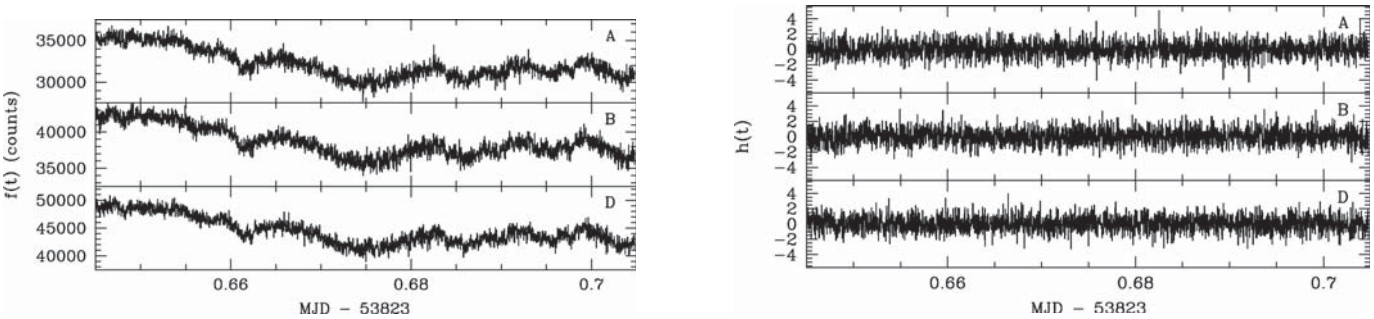

FIG. 1.—Demonstration of detrending by the filtering process. The left panel shows a raw light curve set $f(t)$, and the right panel shows the light curve set $h(t)$ after filtering. The total number points in the light curve set is 26,622, corresponding to 89 minutes. Here only one of every 10 points is plotted, for readability.

probe significant ranges of the model space for small KBOs. We have also developed a statistical analysis technique which allows efficient use of the multitelescope data to detect brief occultation events that would be statistically insignificant if observed with only one telescope.

2. DATA AND ANALYSIS

TAOS has been collecting scientific data since 2005. Observations are normally carried out simultaneously with three 50 cm telescopes (A, B, and D, separated by distances of 6 m and 60 m; this system is described by Lehner et al. 2008). Over 15 TB of raw images have been taken. We report here on the first 2 years of data taken simultaneously with all three telescopes. The data set comprises 156 *data runs*, where a data run is defined as a series of three-telescope observations of a given field for durations of ~90 minutes. Thirty data runs with a 4 Hz sampling rate were taken before 2005 December 15, and 126 data runs were collected subsequently with a sampling rate of 5 Hz. Only fields with ecliptic latitudes $|b| < 10°$ were analyzed. Over 93% of the data were collected in fields with $|b| < 3°$, so the results of our analysis are relevant to the sum of the cold and excited KBO populations (Bernstein et al. 2004). No data run was included unless each star was sampled more than 10,000 times in each telescope. The angle from opposition in these data runs is distributed from 0° to 90°. The number of stars (with $R < 13.5$, which typically gives a S/N ≥ 5) monitored in the data runs ranges between 200 and 2000.[14]

The images were analyzed using an aperture photometry package (Z.-W. Zhang et al. 2008, in preparation) devised exclusively for TAOS images. Light curves were produced for each star by assembling the photometric information into a time series. A star in each data run has a light curve from each of the three telescopes. The data presented in this Letter comprise 110,895 *light curve sets* (where a light curve set is defined as a set of three light curves, one for each telescope, for the same star in a single data run), containing 7.1×10^9 individual photometric measurements.

The photometric data are not calibrated to a standard system. Changes in atmospheric transparency during a data run produce flux variations (Fig. 1) that could undermine our occultation search algorithm. Such low-frequency trends in a light curve can be removed by a numerical high-pass filter that preserves information of a brief occultation event, typically with a duration less than 1–2 data points with the TAOS sampling rate. Our filter takes a time series of f_i measured at time t_i to produce an intermediate series $g_i = f_i - \bar{f}_i$ where $\bar{f}_i$ is the running average of 33 data points centered on t_i. The series g_i is then scaled by the local fluctuation, $h_i = g_i/\sigma(g_i)$ with $\sigma(g_i)$ being the standard deviation of g_i of 151 data points centered at t_i. Both the mean and standard deviation are calculated using *3 σ clipping*. This filtering proves effective to remove slow-varying trends in the light curve, while preserving high-frequency fluctuations that we aim to detect, as illustrated in Figure 1.

We now confront the two central challenges in the search for extremely rare occultation events in these data: (1) *to search for events simultaneously in three parallel data streams*, and (2) *to determine the statistical significance of any rare events that are found*. The second is not straightforward because the statistical distribution of our photometric measurements is not known in advance; approximations based on Gaussian statistics are unreliable far from the mean. This motivates a nonparametric approach.

We thus found it useful to represent each data point by its *rank* in the filtered, rescaled light curve data h_i. That is, the rank of a data point ranges from $r = 1$ (lowest h) to $r = N_P$ (highest h), for a data run comprising N_P photometric measurements taken with telescope A, B, or D. The *rank triples* (r_i^A, r_i^B, r_i^D) form the basis of further analysis of the multitelescope data. The statistical distribution of these ranks is known exactly, since each rank must occur exactly once in each time series. Thus, the probability that a given rank will occur at time t_i is $P(r_i) = 1/N_P$. When the photometric data are uncorrelated, the probability that a particular rank triple will occur is simply $P(r_i^A, r_i^B, r_i^D) = 1/N_P^3$. This allows a straightforward test for correlation between the photometric data taken in the three telescopes: the rank triples should be distributed uniformly in a cube with sides of length N_P. A nonuniform pattern in the cube, on the other hand, indicates correlation. Figure 2 shows an example of the rank series of one telescope

[14] Information on the TAOS fields is available at http://taos.asiaa.sinica.edu.tw/taosfield/.

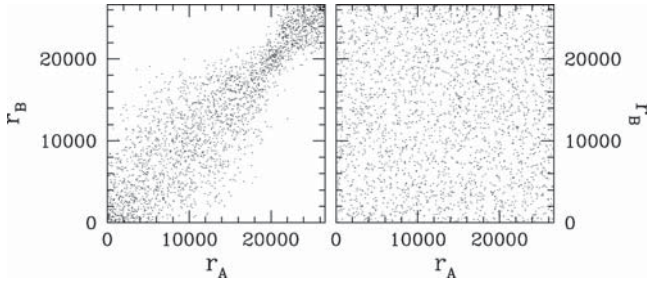

FIG. 2.—Rank-rank plots of the light curve set shown in Fig. 1. Each point shows the ranks at a single time point for telescopes A and B. The ranks from the raw light curves (Fig. 1, *left*) are shown in the left panel, and the ranks from the filtered light curves (Fig. 1, *right*) are shown in the right panel.

against another; this indicates that the raw photometric data f_i are strongly correlated, but the filtered data h_i are not.

Given that the rank triples are uncorrelated, the ranks can be used to search for possible occultation events, as follows: *A true occultation event will exhibit anomalous, correlated low ranks in all three telescopes*. The rank triples thus allow an elegant test for the statistical significance of a candidate event. Consider the quantity

$$\eta_i = -\ln (r_i^A r_i^B r_i^D / N_P^3).$$

Since the ranks are uncorrelated (unless we have an occultation event), we can calculate the exact probability density function[15] for η. This in turn allows us to compute the probability that a given triple of low ranks randomly occurred in an uncorrelated light curve set; this is our measure of statistical significance. An illustration of the power of this approach is shown in Figure 3, where a simulated occultation event is readily recovered.[16]

We thus screened all of our series of rank triples for events with low ranks in all three telescopes. In the analysis reported here, we considered only events for which $P(\eta \geq c) \leq 10^{-10}$, which leads to an expected value of 0.24 false positive events in the entire data set of 2.4×10^9 rank triples. *No statistically significant events emerged from this analysis*.[17]

3. EFFICIENCY TEST AND EVENT RATE

While the example event shown in Figure 3 is readily recovered, objects with smaller diameters or which do not directly cross the line of sight might not be so easily detected. An efficiency calculation is thus necessary for understanding the detection sensitivity of our data and analysis pipeline to different event parameters, notably the KBO size distribution. Our efficiency test started with implanting synthetic events into observed light curves, with the original noise. Each original light curve f_i was modified by the implanted occultation, $k_i = f_i - (1 - d_i)\bar{f}_i$, where d_i is the simulated event light curve (with baseline $d_i \rightarrow 1$ far from the event; Nihei et al. 2007), and $\bar{f}_i$ is the average of the original series over a 33 point rolling window. Since we preserved the original noise in the modified light curves, the noise where the implanted occultation event takes place—for which the flux diminishes—would be slightly overestimated; hence our efficiency estimate is conservative.

We assumed spherical KBOs at a fixed geocentric distance of $\Delta = 43$ AU. (Given our sampling rate, varying the KBO distance within the Kuiper Belt has little effect on our simulated light curves.) The event epoch t_0 was chosen randomly and uniformly within the duration E of the light curve set. The angular size θ_* of each star, necessary for the simulated light curve calculation, was estimated using stellar color and apparent magnitude taken from the USNO-B (Monet et al. 2003) and 2MASS (Skrutskie et al. 2006) catalogs. The impact parameter of each event was chosen, again randomly and uniformly, between 0 and $H/2$, where H is the *event cross section* (Nihei et al. 2007),

$$H = 2[(\sqrt{3}F)^{3/2} + (D/2)^{3/2}]^{2/3} + \theta_* \Delta.$$

Here D is the diameter of the occulting object, and F is the *Fresnel scale*, $F = (\lambda\Delta/2)^{1/2}$, where $\lambda = 600$ nm is the median wavelength in the TAOS filter. The relative velocity between the Earth and KBO $v_{\rm rel}$, necessary for the conversion of the occultation diffraction pattern to a temporally sampled light curve, is calculated based on the angle from opposition during each data run.

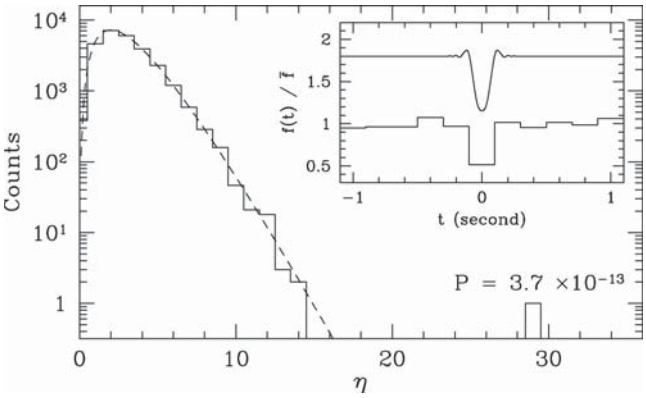

FIG. 3.—Histogram of η for a light curve set implanted with a *simulated* occultation by a 3 km KBO. Each light curve comprises 26,637 points and the ranks from the three telescopes are found to be 1, 3, and 1. The event is clearly visible at $\eta = 29.47$, and the probability of a rank product of 3 or lower from random chance is $P = 3.7 \times 10^{-13}$. The overlaid dashed line is the theoretical distribution of η. The theoretical and implanted light curves are shown in the inset, offset vertically for clarity.

To adequately cover a wide range of parameter space, two efficiency runs were completed in which we implanted each light curve set with exactly one simulated occultation event. For each event, the diameter of the KBO was chosen randomly according to a probability, or weighting factor, w_D. In the first run, objects of diameters $D = 0.4$, 0.5, 0.6, 0.7, 0.8, and 0.9 km were added with $w_D = 1/6$ for each diameter. In the second run, objects of diameters $D = 1$, 2, 3, 5, 10 and 30 km were added with weights $w_D = \{100, 100, 100, 30, 5, 1\}/336$. The modified light curves k_i were reprocessed using the same procedure described in § 2. The recovered events and the event parameters were then used to calculate the number of expected occultation event in our survey. That is, we calculated the quantity

$$\Omega_e(D) = w_D^{-1} \sum_j [E_j v_{\rm rel_j} H_j(D)/\Delta^2],$$

where the sum is over all light curve sets where a simulated event is successfully recovered in the reanalysis (Fig. 4). Essentially $\Omega_e(D)$ is the *effective solid angle* of our survey, insofar as TAOS can be considered equivalent to a survey that is capable of counting every KBO of diameter D in a solid angle Ω_e with 100% efficiency.

The expected number of detected events by KBOs with sizes ranging from D_1 to D_2 can then be written as

$$N_{\rm exp} = \int_{D_2}^{D_1} \frac{dn}{dD} \Omega_e(D) dD, \quad (1)$$

[15] For small η, this distribution can be approximated by a Γ distribution of the form $P(\eta) = \eta^{N_T - 1} e^{-\eta}/(N_T - 1)!$, where $N_T = 3$ is the number of telescopes.

[16] Details of our statistical methodology will be described in M. J. Lehner et al. (2008, in preparation).

[17] A candidate event was reported in Chen et al. (2007). This event had a significance of 3.7×10^{-10}, which did not pass our cut on η. We expect to have ~1 false positive event at that significance level or higher.

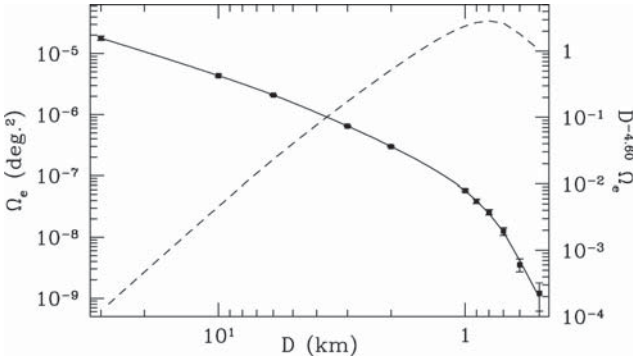

FIG. 4.—Effective solid angle of the TAOS survey as a function of KBO diameter D (*solid line*), and the product of the upper limit of the differential surface density by the effective solid angle (*dashed line*, in arbitrary units).

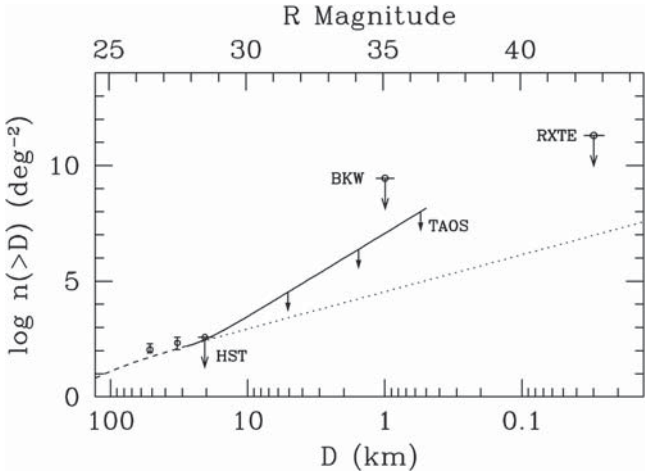

FIG. 5.—TAOS upper limit to the size spectrum (*solid line*) assuming a power-law distribution; double-power-law fit from Bernstein et al. (2004) (*dashed line*; extrapolation at $D < 28$ km shown with dotted line). Results from Bernstein et al. (2004) are shown as data points. Upper limits from Bickerton et al. (2008) (BKW) and Jones et al. (2008) (RXTE) are also shown. An albedo of 4% is assumed for computing magnitude.

where dn/dD is the differential surface number density of KBOs. The integrand of equation (1) contains two factors: the *model-dependent* size distribution dn/dD, and the *model-independent* effective solid angle $\Omega_e(D)$, which describes the sensitivity of the survey to objects of diameter D. Given the observed number of events and the value of $\Omega_e(D)$ resulting from the efficiency calculation, we can place model-dependent limits on the population of KBOs. Based on the absence of detections in this data set, any model with a size distribution such that $N_{\rm exp} \geq 3.0$ is inconsistent with our data at the 95% confidence level.

Note that there are an infinite number of models that satisfy the above requirement. We thus make the reasonable choice of a power-law size distribution $dn/dD = n_{\rm B}(D/28\ {\rm km})^{-q}$, where $n_{\rm B}$ is chosen such that the cumulative size distribution is continuous at 28 km with the results of Bernstein et al. (2004). We integrate equation (1) from $D_2 = 28$ km down to our detection limit of $D_1 = 0.5$ km, and solve equation (1) with $N_{\rm exp} = 3$, to find $q = 4.60$. Our null detection thus eliminates any power-law size distribution with $q > 4.60$ at the 95% c.l., setting a stringent upper limit (see Fig. 5) to the number density of KBOs.

4. CONCLUSION

We have surveyed the sky for occultations by small KBOs using the three telescope TAOS system. We have demonstrated that a dedicated occultation survey using an array of small telescopes, an innovative statistical analysis of multitelescope data, and a large number of star-hours, can be used as a powerful probe of small objects in the Kuiper Belt, and we are thus able to place the strongest upper bound to date on the number of KBOs with 0.5 km $< D <$ 28 km. We continue to operate TAOS, soon with an additional telescope, and will report more sensitive survey results in the future.

Work at NCU was supported by the grant NSC 96-2112-M-008-024-MY3. Work at the CfA was supported in part by the NSF under grant AST 05-01681 and by NASA under grant NNG04G113G. Work at ASIAA was supported in part by the thematic research program AS-88-TP-A02. Work at UCB was supported by the NSF under grant DMS-0405777. Work at Yonsei was supported by the KRCF grant to Korea Astronomy and Space Science Institute. Work at LLNL was performed under the auspices of the US DOE in part under contract W-7405-Eng-48 and contract DE-AC52-07NA27344. Work at SLAC was performed under US DOE contract DE-AC02-76SF00515. Work at NASA Ames was funded by NASA/PG&G.

REFERENCES

Axelrod, T. S., et al. 1992, in ASP Conf. Ser. 34, Robotic Telescopes in the 1990s, ed. A. V. Filippenko (San Francisco: ASP), 171
Bailey, M. E. 1976, Nature, 259, 290
Bernstein, G. M., et al. 2004, AJ, 128, 1364
Bickerton, S. J., Kavelaars, J. J., & Welch, D. L. 2008, AJ, 135, 1039
Brown, M. J. I., & Webster, R. L. 1997, MNRAS, 289, 783
Chang, H.-K., et al. 2006, Nature, 442, 660
———. 2007, MNRAS, 378, 1287
Chen, W. P., et al. 2007, in IAU Symp. 236, Near Earth Objects, Our Celestial Neighbors: Opportunity and Risk, ed. G. B. Valsecchi & D. Vokrouhlický (Cambridge: Cambridge Univ. Press), 65
Cooray, A., & Farmer, A. J. 2003, ApJ, 587, L125
Davis, D. R., & Farinella, P. 1997, Icarus, 125, 50
Dyson, F. J. 1992, QJRAS, 33, 45
Fraser, W. C., et al. 2008, Icarus, 195, 827
Jewitt, D., & Luu, J. 1993, Nature, 362, 730
Jones, T. A., Levine, A. M., Morgan, E. H., & Rappaport, S. 2008, ApJ, 677, 1241
Kenyon, S. J., & Bromley, B. C. 2004, AJ, 128, 1916
Kenyon, S. J., & Luu, J. X. 1999a, AJ, 118, 1101
———. 1999b, ApJ, 526, 465
Lehner, M. J., et al. 2008, PASP, submitted (arXiv:0802.0303)
Monet, D. G., et al. 2003, AJ, 125, 984
Nihei, T. C., et al. 2007, AJ, 134, 1596
Pan, M., & Sari, R. 2005, Icarus, 173, 342
Roques, F., & Moncuquet, M. 2000, Icarus, 147, 530
Roques, F., et al. 2006, AJ, 132, 819
Skrutskie, M. F., et al. 2006, AJ, 131, 1163
Stern, S. A. 1996, AJ, 112, 1203
Stern, S. A., & Colwell, J. E. 1997, AJ, 114, 841

The Astrophysical Journal, 679: L5–L8, 2008 May 20

EARLY OPTICAL BRIGHTENING IN GRB 071010B

J. H. Wang,[1] M. E. Schwamb,[2] K. Y. Huang,[1] C. Y. Wen,[1] Z. W. Zhang,[3] S. Y. Wang,[1] W. P. Chen,[3] F. B. Bianco,[4] R. Dave,[5] M. J. Lehner,[1,4] S. L. Marshall,[6,7] R. Porrata,[8] C. Alcock,[5] Y. I. Byun,[9] K. H. Cook,[7] S. K. King,[1] T. Lee,[1] and Y. Urata[1,10]

Received 2008 March 7; accepted 2008 April 7; published 2008 April 24

ABSTRACT

We report the detection of early (60–230 s) optical emission of the gamma-ray burst afterglow of GRB 071010B. No significant correlation with the prompt γ-ray emission was found. Our high time resolution data combining with other measurements within 2 days after the burst indicate that GRB 071010B is composed of a weak early brightening ($\alpha \sim 0.6$), probably caused by the peak frequency passing through the optical wavelengths, followed by a decay ($\alpha \sim -0.51$), attributed to continuous energy injection by patchy jets.

Subject headings: gamma rays: bursts — gamma rays: observations

Online material: color figures

1. INTRODUCTION

With the launch of the *Swift* γ-ray explorer (Gehrels et al. 2004) in late 2004, great progress has been made in the study of early optical afterglow of gamma-ray bursts (GRBs). Two broad classes have been proposed (Vestrand et al. 2006) for the optical emission detected during the first few minutes after a GRB: (1) prompt optical emission correlated in time with the prompt γ-ray emission (e.g., GRB 041219 and GRB 050820a; Vestrand et al. 2005, 2006); (2) early optical afterglow after the γ-ray emission (e.g., GRB 990123 and GRB 050401; Akerlof et al. 1999; Rykoff et al. 2005).

The standard relativistic blast wave ("fireball") model (e.g., Sari & Piran 1997a; Meśzaŕos 2002) attributes the prompt γ-ray emission to the internal shocks in the ultrarelativistic jet generated by the central engine (Narayan et al. 1992; Rees & Meśzaŕos 1994; Sari & Piran 1997b). The prompt optical emission is known to vary simultaneously with the prompt γ-ray emission, indicative of their common origin. The early optical afterglow, on the other hand, is considered to arise from interaction between the internal shocks and the surrounding medium (so-called "external shocks"; Rees & Meśzaŕos 1992; Meśzaŕos & Rees 1993; Katz 1994; Sari & Piran 1995). The early optical afterglow may start during the prompt γ-ray emission, and persist for 10 minutes or longer after the prompt γ-ray emission has faded. So far, only GRB 050820a has been observed to show a temporal correlation between the two different optical components. Such a correlation suggests that the early afterglow is associated with the impulsive energy released by the prompt emission, which is consistent with what is expected in the fireball model for an external forward shock. Fast photometry in the early phase of emission is therefore important to reveal the two optical components and to study the interaction of the GRB ejecta with the surrounding medium.

In this Letter, we report on our high time resolution detection of the optical emission of GRB 071010B in the first few minutes with the TAOS (Taiwanese-American Occultation Survey) telescopes (Alcock et al. 2003; Chen et al. 2007).

2. THE TAOS OBSERVATION AND RESULTS

The TAOS system consists of an array of four robotic telescopes, TAOS-A, TAOS-B, TAOS-C, and TAOS-D, with separations ranging from 6 to 65 m. Each telescope has a 50 cm aperture imaging to a corrected Cassegrain focus at f/1.9 with a 5000–7200 Å passband. Each telescope is equipped with a Spectral Instruments Series 800 CCD camera with a 2048 × 2052 E2V CCD 42-40 chip with two readout channels. The optical system gives a 3 deg^2 field of view. More details about the TAOS telescope system are described by Lehner et al. (2008). The main scientific goal of the TAOS project is to detect and characterize the small (a few km across) objects beyond Neptune, but the robotic system is well suited to respond efficiently to GRBs.

Upon arrival of a GCN alert, the TAOS scheduler daemon makes the decision whether to interrupt the regular observing session to follow up on the GRB, based on the observability of the target, duplicate packets, alert retracted by the GCN, etc. Currently the TAOS system responds to, weather permitting, any GRB above 25° elevation, within 2 hours of the burst. The advantage of the TAOS system for the GRB studies is its capability to respond rapidly to an alert with fast photometry. This allows us to study early optical behavior of a GRB. Currently our system can point to the burst coordinates provided by *Swift* in less than 30 s and start observing. A GRB alert is followed up for 30 minutes, with each TAOS telescope taking a different exposure time, i.e., with different cadences between telescopes, from a fraction of a second to tens of seconds. Targets brighter than $R \sim 18$ mag can be readily detected. This setup of multiple telescopes taking different exposure times maximizes the chance to detect various types of GRB optical

[1] Institute of Astronomy and Astrophysics, Academia Sinica, P.O. Box 23-141, Taipei 106, Taiwan.
[2] Division of Geological and Planetary Sciences, California Institute of Technology, 1201 East California Boulevard, Pasadena, CA 91125.
[3] Institute of Astronomy, National Central University, Chung-Li 32054, Taiwan.
[4] Harvard-Smithsonian Center for Astrophysics, 60 Garden Street, Cambridge, MA 02138.
[5] Initiative in Innovative Computing, Harvard University, 60 Oxford Street, Cambridge, MA 02138.
[6] Kavli Institute of Particle Astrophysics and Cosmology, 2575 Sand Hill Road, MS 29, Menlo Park, CA 94025.
[7] Institute of Geophysics and Planetary Physics, Lawrence Livermore National Laboratory, Livermore, CA 94550.
[8] Department of Physics, University of California, Berkeley, CA 94270.
[9] Department of Astronomy, Yonsei University, 134 Shinchon, Seoul 120-749, Korea.
[10] Department of Physics, Saitama University, Shimookubo, Saitama 338-8570 Japan.

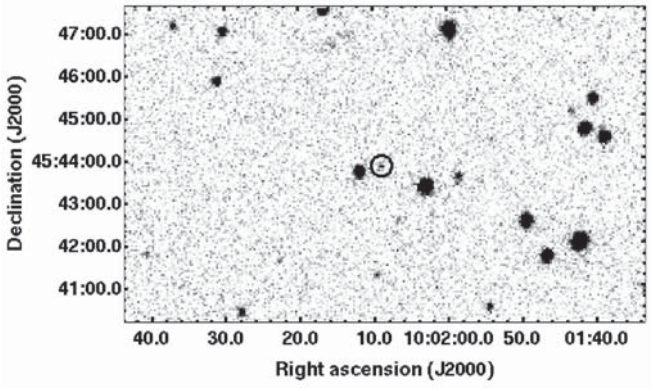

FIG. 1.—One of the TAOS afterglow images taken with the TAOS-B telescope at 60 s after the burst of GRB 071010B. The integration time was 5 s.

counterparts and enables cross-checking of photometric reliability.

On 2007 October 10, the *Swift* Burst Alert Telescope (BAT) detected GRB 071010B at 20:45:47 UT. This burst showed a main FRED (fast rise–exponential decay) pulse lasting ~20 s, with a precursor some 45 s before the main pulse, an extended tail emission, and a third, weak peak around 95 s after the burst (Markwardt et al. 2007). The T_{90} duration of this event is 35.74 ± 0.5 s in the 15–350 keV range (Markwardt et al. 2007). *Suzaku* WAM also detected the main spike (Kira et al. 2007; Y. Urata et al. 2008, in preparation).

A bright X-ray afterglow was detected by the *Swift* X-Ray Telescope (XRT) 6800 s after the burst (Kennea et al. 2007). In addition, a bright optical afterglow was detected by several ground-based telescopes (Oksanen 2007; Kann et al. 2007a; Im et al. 2007a; Kocevski et al. 2007; Xin 2007; Klunko et al. 2007; Rumyantsev & Pozanenko 2007). The spectral measurements of the afterglow by the Gemini North telescope (Cenko et al. 2007) and Keck telescope (Stern et al. 2007) indicate a redshift of $z = 0.947$ for this event. A jet break was also detected with late-time observations (Kann et al. 2007c; Im et al. 2007a; Y. Urata et al. 2008, in preparation).

The TAOS telescopes began to observe GRB 071010B about 38 s after the GCN alert—or 52 s after the burst. A sequence of 1, 5, and 25 s exposures were taken, respectively, by TAOS-A, TAOS-B, and TAOS-D. The sky conditions were favorable but observations were terminated after 3 minutes because of the twilight shutdown set by the scheduler. Such a constraint has since been lifted to allow completion (30 minutes) of a GRB follow-up, with the fourth TAOS telescope now designated to take 0.25 s data.

The images were processed by a standard routine including bias subtraction and flat-fielding using IRAF. Detection was clearly seen in the individual images of TAOS-B and TAOS-D, but not in TAOS-A. The images of TAOS-A were co-added to increase the signal-to-noise ratio in the analysis. The DAOPHOT package (Stetson 1987) was then used to perform point-spread function (PSF) photometry. In each image, six stars around the GRB position were used to create the PSF model. For photometric calibration, we used nine reference stars ($0.29 < V - R < 0.61$) in the GRB field given by Henden (2007). Our photometric results, including those of individual images by TAOS-B (Fig. 1) and TAOS-D, and of stacked images by TAOS-A, are listed in Table 1. Both the photometric and systematic calibration errors were included in the magnitude error. A similar result was obtained with differential photometry by the SExtractor software package 2.3 (Bertin & Arnouts 1996) using a nearby reference star (USNOB1 1355.0217787, R.A. = $10^h02^m23.577^s$, decl. = +45°34′54.38″, $R2 = 15.12$ mag). The detection threshold was that an object must have at least 3–10 connected pixels and a flux in excess of 1.5 times the local background noise. The MAGAPER estimator in SExtractor was used to determine the magnitude of the source. The TAOS camera employs a broad, nonstandard filer, with an effective wavelength close to standard R (Lehner et al. 2008). Zero point transformation to standard R can be effected with a deviation of ~0.007 to the result in Henden (2007).

TABLE 1
LOG OF GRB 071010B OPTICAL AFTERGLOW OBSERVATIONS

t_{start}	t_{end}	Exposure (s)	Magnitude	Telescope
60.28	65.28	5	16.88 ± 0.15	TAOS-B
64.87	145.19	1 s × 20	16.64 ± 0.19	TAOS-A
68.48	73.48	5	16.84 ± 0.19	TAOS-B
76.78	81.78	5	17.01 ± 0.19	TAOS-B
80.38	105.38	25	16.66 ± 0.05	TAOS-D
84.98	89.98	5	16.95 ± 0.19	TAOS-B
93.28	98.28	5	16.74 ± 0.15	TAOS-B
101.59	106.59	5	16.70 ± 0.14	TAOS-B
108.59	133.59	25	16.59 ± 0.06	TAOS-D
109.79	114.79	5	16.63 ± 0.13	TAOS-B
118.09	123.09	5	16.60 ± 0.13	TAOS-B
126.29	131.29	5	16.42 ± 0.12	TAOS-B
134.49	139.49	5	16.41 ± 0.11	TAOS-B
136.90	161.90	25	16.52 ± 0.06	TAOS-D
142.80	147.80	5	16.51 ± 0.09	TAOS-B
149.49	226.41	1 s × 19	16.55 ± 0.18	TAOS-A
151.10	156.10	5	16.67 ± 0.12	TAOS-B
159.30	164.30	5	16.53 ± 0.12	TAOS-B
165.20	190.20	25	16.68 ± 0.07	TAOS-D
167.50	172.50	5	16.50 ± 0.12	TAOS-B
175.80	180.80	5	16.86 ± 0.20	TAOS-B
184.00	189.00	5	16.59 ± 0.14	TAOS-B
192.20	197.20	5	16.48 ± 0.13	TAOS-B
193.51	218.51	25	16.68 ± 0.08	TAOS-D
200.41	205.41	5	16.67 ± 0.14	TAOS-B
208.61	213.61	5	16.65 ± 0.12	TAOS-B
216.91	221.91	5	16.88 ± 0.17	TAOS-B
225.11	230.11	5	16.57 ± 0.15	TAOS-B

Figure 2 shows the optical light curves of GRB 071010B taken by the three TAOS telescopes during 60–230 s after the burst. Our data from three telescopes showed consistently a mild increase in flux, with a best-fit power-law index $\alpha = 0.10 \pm 0.07$ ($\chi^2/\nu = 1.15$ for $\nu = 26$), defined by $F(t) \propto t^{\alpha}$, where F is the flux at time t after the burst. Following this mild brightening, GRB 071010B appeared to show a shallow decay ($\alpha \sim -0.48$) during 1020–21,600 s after the burst (Templeton et al. 2007). To combine our TAOS measurements with GCN reports covering up to 2 days after the burst (Oksanen 2007; Kann et al. 2007b; Kocevski et al. 2007; Im et al. 2007b; Klunko et al. 2007; Antonyuk et al. 2007), we recalibrated all the data using the reference stars in Henden (2007) in the GRB 071010B field. The data of Oksanen (2007) and Im et al. (2007b) were calibrated by USNO B1.0 stars with red magnitude; the USNO B1.0 values are on average 0.09 mag fainter than those reported by Henden. The reference star (R.A. = $10^h02^m09.93^s$, decl. = +45°41′41.1″) reported by Kann et al. (2007b), Klunko et al. (2007), and Antonyuk et al. (2007) is 0.227 mag fainter than that given by Henden. The entire, rescaled light curve, covering from 1 minute to almost 2 days after the burst, was then fitted with a broken power-law function, $F(\nu, t) = F_{\nu}^{*}/[(t/t_b)^{-\alpha_1} + (t/t_b)^{-\alpha_2}]$, where t_b is the break

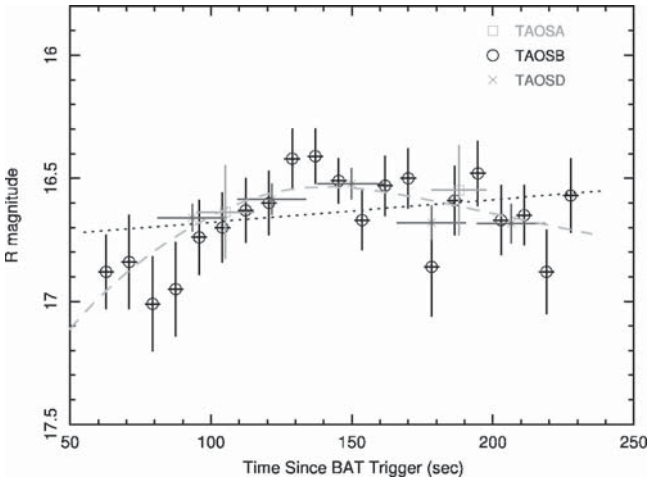

FIG. 2.—Early optical light curves of GRB 071010B taken with TAOS-A (*squares*; stacked images), TAOS-B (*circles*), and TAOS-D (*asterisks*). The linear least-squares fit (*dotted line*) to all TAOS data shows a mild increase of flux. The dashed line is the best broken power-law fit with other measurements as shown in Fig. 3. [*See the electronic edition of the Journal for a color version of this figure.*]

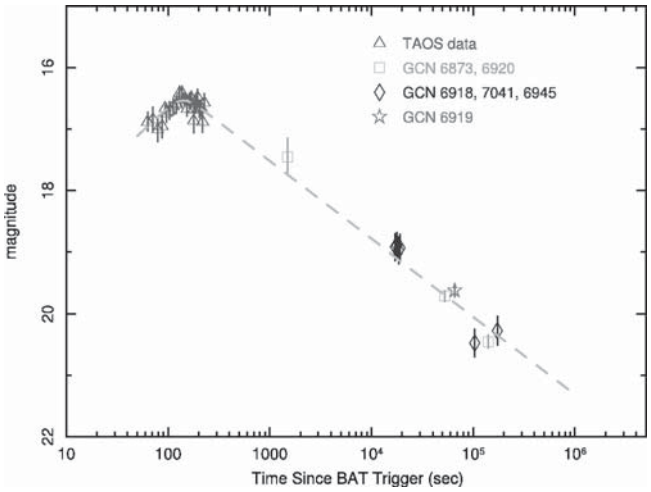

FIG. 3.—Optical light curve of GRB 071010B. The dashed line indicates the best fit by the broken power-law function to the TAOS observations in the first 3 minutes (this work) and data from the literature up to 2 days after the burst (Oksanen 2007; Kann et al. 2007b; Kocevski et al. 2007; Im et al. 2007b; Klunko et al. 2007; Antonyuk et al. 2007). [*See the electronic edition of the Journal for a color version of this figure.*]

time, α_1 and α_2 are the power-law indices before and after t_b, and F_ν^* is the flux at t_b (Beuermann et al. 1999). Figure 3 shows the TAOS and recalibrated measurements, together with the best-fit broken power-law function. It is seen that the light curve has an initially rising phase ($\alpha_1 = 0.62 \pm 0.34$) followed by a decay ($\alpha_2 = -0.51 \pm 0.01$) after the break time $t_b = 137.0 \pm 19.0$ s ($\chi^2/\nu = 0.98$ for $\nu = 31$). For clearance, the best broken power-law fit is also shown in Figure 2 with TAOS data only.

3. DISCUSSION AND CONCLUSIONS

The TAOS light curve was compared with the γ-ray observations for possible temporal correlation. The preliminary high-level BAT data (15–350 keV), downloaded from the *Swift* Data Center (SDC),[11] were binned to 5 s in order to compare with the TAOS-B 5 s data set (Fig. 4). The optical and γ-ray light curves appear quantitatively similar. In particular the optical brightening during 80–140 s after the burst seems to correspond to the weak, third peak at 95 s in the BAT light curve reported by Markwardt et al. (2007). The γ-ray signal was, however, already too weak in this time interval for the optical emission to be the counterpart of the prompt γ-ray emission.

The early optical emission of GRB 071010B, with a brightening followed by a shallow decay, is unusual. The initial deceleration of the fireball by the reverse shock would produce a bright peak, such as observed in the well-known GRB 990123, which exhibited a sharp brightening of ~3 mag within 25 s, until 50 s after the burst (Akerlof et al. 1999). The reverse shock is short-lived and subsequent cooling results in a fast decay, e.g., $\alpha_2 \sim -2.5$ for GRB 990123 (Akerlof et al. 1999). In comparison, GRB 071010B brightened only 0.6 mag in 80 s, and had a later break time ($t_b \sim 140$ s) plus a much shallower decay ($\alpha_2 \sim -0.51$). The reverse shock therefore should not be responsible for the optical emission that we detected.

Electrons accelerated in the shock emit synchrotron radiation. As the fireball slows down, the synchrotron peak frequency moves progressively to a lower frequency. The optical weak brightening that we detected could arise when the synchrotron peak frequency passed through the optical wavelengths. The optical light curve of the forward-shock emission is expected to show an initial rising ($t^{0.5}$), followed by a normal decay $t^{3(1-p)/4}$, where p is the power-law index of the electron spectrum with $p > 2$ (e.g., GRB 041006; Urata et al. 2007). The optical light curve of GRB 071010B has a rising rate ($\alpha_1 = 0.62 \pm 0.34$) consistent with what is expected from the forward-shock mechanism.

On the other hand, considering the case of $\nu_m < \nu_{\rm opt} < \nu_c$, the decay phase of the light curve ($\alpha_2 = -0.51 \pm 0.01$) would give $p = 1.68$ for the uniform ISM case and $p = 1.01$ for the preburst wind case in the standard afterglow model. These values are smaller than the expected value ($p > 2$). Moreover, if we consider the afterglow with a flat-spectrum electron distribution ($1 < p < 2$), the obtained value $p = 0.74$ for the uniform ISM case and $p = -3.92$ for the preburst wind case are also inconsistent with the theoretical value (Dai & Cheng

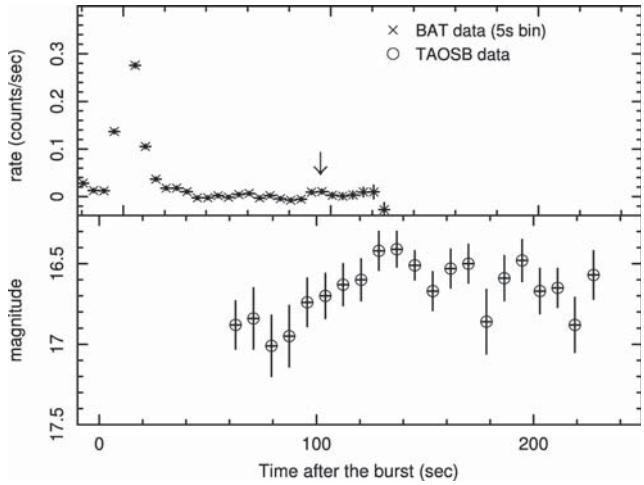

FIG. 4.—*Swift* 15–350 keV BAT light curve (5 s binning) and the TAOS-B light curve (5 s sampling). The inserted arrow denotes the weak third peak of the BAT data.

[11] See http://heasarc.gsfc.nasa.gov/docs/swift/sdc/data_products.html.

2001). The decay phase in GRB 071010B therefore cannot be well explained by the standard afterglow model. Without spectral or other multiband measurements in the early phase of GRB 071010B, it is not possible to verify whether the brightening was indeed caused by the synchrotron peak frequency, but even if it was, an additional mechanism is probably needed to account for the shallow decay after the brightening.

GRB 071010B was detected to have a jet break (Kann et al. 2007c; Im et al. 2007c; Y. Urata et al. 2008, in preparation), suggesting a viewing angle nearly along the jet axis. This excludes the possibility that a tail of prompt emission combined with an afterglow could produce a shallow decay when observing outside the edge of the jet (Eichler & Granot 2006) in GRB 071010B.

The standard GRB afterglow model assumes an initially steady energy. The GRB is produced by the "internal shocks," i.e., a series of collisions between shells moving at different velocities. The energy hence changes when the slow material starts to be left behind. As the initially high-speed material is slowed down by the surrounding environment, the slower material eventually catches up and produces refreshed shocks. Significant continuous energy injection is possible and influences the fireball during the deceleration phase. The forward shocks will be refreshed and decelerate slower than in the standard scenario. This would change the decay slope of the light curve from the canonical one to a shallower one, as is evidenced in GRB 071010B.

Energy injection is expected if the energy distribution over the fireball surface is not uniform. The two-component jet and the patchy jet model have been proposed to explain the nonuniformity. The two-component jet model requires one component to be ultrarelativistic to power the GRB, whereas the other component is a moderately relativistic cocoon (Meśzaŕos & Rees 1993; Berger et al. 2003; Zhang et al. 2004; Huang et al. 2004; Granot 2005). The afterglow of the cocoon contains more energy than the narrow component, thereby producing a noticeable "bump" in the light curve, instead of just changing the rate of the flux decay, but such a bump should be visible only after 10^4 s after the burst (e.g., GRB 030329; Huang et al. 2006). It is obvious that the two-component jet model cannot explain the GRB 071010B light curve.

Alternatively, the light curve of GRB 071010B can be explained by the patchy jet model (Kumar & Piran 2000), which assumes the initial fireball ejecta to have large energy fluctuations in angular direction. This results in jets with distributed values of the Lorentz factor (Γ), so observers along different viewing angles would receive different fluxes. Furthermore, with diversified values of $1/\Gamma$, emission from different patches becomes observable at different time, thus rendering a shallow afterglow light curve as detected in GRB 071010B.

In summary, the prompt optical emission for GRB 071010B was detected within 1 minute after the burst. No significant correlation with the prompt γ-ray emission was found. Our data of the first 3 minutes combined with measurements made by other groups within 2 days after the burst show the temporal evolution of GRB 071010B to consist of a slight brightening followed by a shallow decay. It is likely that the synchrotron peak frequency passed through the optical wavelengths and caused the early brightening, whereas the continuous injection by patchy jets was responsible for the slow decay that followed. The detection of GRB 071010B demonstrates the potential of the TAOS system to respond efficiently to a GRB alert to detect both prompt optical emission and early afterglow.

We acknowledge the use of public data from the *Swift* data archive and C. Markwardt for discussions. Work at NCU was supported by the grant NSC 96-2112-M-008-024-MY3. Work at the CfA was supported in part by the NSF under grant AST 05-01681 and by NASA under grant NNG04G113G. Work at ASIAA was supported in part by the thematic research program AS- 88-TP-A02 and Acdemia Sinica. Work at Yonsei was supported by Korea Astronomy and Space Science Institute. Work at LLNL was performed under the auspices of the US DOE in part under contract W-7405-Eng-48 and contract DE-AC52-07NA27344. Work at SLAC was performed under US DOE contract DE-AC02-76SF00515.

REFERENCES

Akerlof, C., et al. 1999, Nature, 398, 400
Alcock, C., et al. 2003, Earth Moon Planets, 92, 459
Antonyuk, K., Rumyantsev, V., & Pozanenko, A. 2007, GCN Circ. 7041
Berger, E., et al. 2003, Nature, 426, 154
Bertin, E., & Arnouts, S. 1996, A&AS, 117, 393
Beuermann, K., et al 1999, A&A, 352, L26
Cenko, S. B., Cucchiara, A., Fox, D. B., Berger, E., & Price, P. 2007, GCN Circ. 6888
Chen, W. P., et al. 2007, in IAU Symp. 236, Near Earth Objects, Our Celestial Neighbors: Opportunity and Risk, ed. G. B. Valsecchi & D. Vokrouhlický (Cambridge: Cambridge Univ. Press), 65
Dai, Z. G., & Cheng, K. S. 2001, ApJ, 558, L109
Eichler, D., & Granot, J. 2006, ApJ, 641, L5
Gehrels, N., et al. 2004, ApJ, 611, 1005
Granot, J. 2005, ApJ, 631, 1022
Henden, A. 2007, GCN Circ. 6909
Huang, Y. F., Cheng, K. S., & Gao, T. T. 2006, ApJ, 637, 873
Huang, Y. F., Wu, X. F., Dai, Z. G., Ma, H. T., & Lu, T. 2004, ApJ, 605, 300
Im, M., Lee, I., & Urata, Y. 2007a, GCN Circ. 6897
———. 2007b, GCN Circ. 6920
———. 2007c, GCN Circ. 6969
Kann, D. A., Hoegner, C., & Filgas, F. 2007a, GCN Circ. 6884
———. 2007b, GCN Circ. 6918
Kann, D. A., et al. 2007c, GCN Circ. 6935
Katz, J. I. 1994, ApJ, 422, 248
Kennea, J. A., et al. 2007, GCN Circ. 6878
Klunko, E., Marchenkov, A., Eselevich, M., Shulga, A., & Pozanenko, A. 2007, GCN Circ. 6945
Kira, Y., et al. 2007, GCN Circ. 6931
Kocevski, D., Perley, D. A., Bloom, J. S., Modjaz, M., & Poznanski, D. 2007, GCN Circ. 6919
Kumar, P., & Piran, T. 2000, ApJ, 532, 286
Lehner, M. J., et al. 2008, PASP, in press (arXiv:0802.0303)
Markwardt, C. B., et al. 2007, GCN Rep. 92.1
Meśzaŕos, P. 2002, ARA&A, 40, 137
Meśzaŕos, P., & Rees, M. J. 1993, ApJ, 405, 278
Narayan, R., Paczyński, B., & Piran, T. 1992, ApJ, 395, L83
Oksanen, A. 2007, GCN Circ. 6873
Rees, M. J., & Meśzaŕos, P. 1992, MNRAS, 258, 41P
———. 1994, ApJ, 430, L93
Rumyantsev, V., & Pozanenko, A. 2007, GCN Circ. 6977
Rykoff, E. S., et al. 2005, ApJ, 631, L121
Saril, R., & Piran, T. 1995, ApJ, 455, L143
———. 1997a, ApJ, 485, 270
———. 1997b, MNRAS, 287, 110
Stern, D., Perley, D. A., Reddy, N., Prochaska, J. X., Spinrad, H., & Dickinson, M. 2007, GCN Circ. 6928
Stetson, P. B. 1987, PASP, 99, 191
Templeton, M., Kann, D. A., Oksanen, A., & Henden, A. 2007, GCN Circ. 6903
Urata, Y., et al. 2007, ApJ, 655, L81
Vestrand, W. T., et al. 2005, Nature, 435, 178
———. 2006, Nature, 442, 172
Xin, L. P. 2007, GCN Circ. 6924
Zhang, W., Woosley, S. E., & Herger, A. 2004, ApJ, 608, 365

The Astrophysical Journal, 693:564–585, 2009 March 1 doi:10.1088/0004-637X/693/1/564

2006 WHOLE EARTH TELESCOPE OBSERVATIONS OF GD358: A NEW LOOK AT THE PROTOTYPE DBV

J. L. Provencal[1,2], M. H. Montgomery[2,3], A. Kanaan[4], H. L. Shipman[1], D. Childers[5], A. Baran[6], S. O. Kepler[7], M. Reed[8], A. Zhou[8], J. Eggen[8], T. K. Watson[9], D. E. Winget[3], S. E. Thompson[1,2], B. Riaz[1], A. Nitta[10], S. J. Kleinman[10], R. Crowe[11], J. Slivkoff[11], P. Sherard[11], N. Purves[11], P. Binder[11], R. Knight[11], S. -L. Kim[12], Wen-Ping Chen[13], M. Yang[13], H. C. Lin[13], C. C. Lin[13], C. W. Chen[13], X. J. Jiang[14], A. V. Sergeev[15], D. Mkrtichian[16,17], M. Andreev[15], R. Janulis[18], M. Siwak[19], S. Zola[6,19], D. Koziel[19], G. Stachowski[6], M. Paparo[20], Zs. Bognar[20], G. Handler[21], D. Lorenz[21], B. Steininger[21], P. Beck[21], T. Nagel[22], D. Kusterer[22], A. Hoffman[22], E. Reiff[22], R. Kowalski[22], G. Vauclair[23], S. Charpinet[23], M. Chevreton[24], J. E. Solheim[25], E. Pakstiene[26], L. Fraga[4], and J. Dalessio[1,2]

[1] University of Delaware, Department of Physics and Astronomy, Newark, DE 19716, USA; jlp@udel.edu
[2] Delaware Asteroseismic Research Center, Mt. Cuba Observatory, Greenville, DE 19807, USA
[3] Department of Astronomy, University of Texas, Austin, TX-78712, USA; mikemon@rocky.as.utexas.edu
[4] Departamento de Física Universidade Federal de Santa Catarina, C.P. 476, 88040-900, Florianópolis, SC, Brazil; ankanaan@gmail.com
[5] Department of Math and Science, Delaware County Community College, 901 S. Media Rd, Media, PA-19063, USA; dpc@udel.edu
[6] Mount Suhora Observatory, Cracow Pedagogical University, Ul. Podchorazych 2, 30-084 Krakow, Poland; zola@astro1.as.ap.krakow.pl
[7] Instituto de Físisica UFRGS, C.P. 10501, 91501-970 Porto Alegre, RS, Brazil; kepler@if.ufrgs.br
[8] Missouri State University and Baker Observatory, 901S. National, Springfield, MO 65897, USA; MikeReed@missouristate.edu
[9] Southwestern University, Georgetown, TX, USA; tkw@southwestern.edu
[10] Gemini Observatory, Northern Operations Center, 670 North A'ohoku Place, Hilo, HI 96720, USA; atsuko.nittakleinman@gmail.com
[11] University of Hawaii, Hilo, HI 96720, USA; rcrowe@hubble.uhh.hawaii.edu
[12] Korea Astronomy and Space Science Institute, Daejeon 305-348, Korea; slkim@kasi.re.kr
[13] Lulin Observatory, National Central University, Taiwan; wchen@astro.ncu.edu.tw
[14] National Astronomical Observatories, Academy of Sciences, Beijing 100012, People's Republic of China; xjjiang@bao.ac.cn
[15] Ukrainian National Academy of Sciences, Main Astronomical Observatory, Golosiiv, Kiev 022 252650, Ukraine; sergeev@terskol.com
[16] Astronomical Observatory, Odessa National University, Shevchenko Park, Odessa 65014, Ukraine; david@arcsec.sejong.ac.kr
[17] Astrophysical Research Center for the Structure and Evolution of the Cosmos, Sejong University, Seoul 143-747, Korea, davidm@sejong.ac.kr
[18] Institute of Theoretical Physics and Astronomy, Vilnius University, Vilnius, Lithuania; jr@itpa.lt
[19] Astronomical Observatory, Jagiellonian University, ul. Orla 171, 30-244 Cracow, Poland
[20] Konkoly Observatory, P.O. Box 67, H-1525 Budapest XII, Hungary; paparo@konkoly.hu
[21] Institut für Astronomie Universität Wien, Türkenschanzstrasse 17, 1180, Austria; handler@astro.univie.ac.at
[22] Institut für Astronomie und Astrophysik, Universiät Tübingen, Sand 1, 72076 Tübingen, Germany; nagel@astro.uni-tuebingen.de
[23] Laboratoire d'Astrophysique de Toulouse-Tarbes, Université de Toulouse, CNRS, 14 avenue Edouard Belin, F314000 Toulouse, France; gerardv@srvdec.obs-mip.fr
[24] Observatoire de Paris, LESIA, 92195 Meudon, France
[25] Institute of Theoretical Astrophysics, University of Oslo, P.O. Box 1029, Oslo, Norway; janerik@phys.uit.no
[26] Institute of Theoretical Physics and Astronomy, Astronomical Observatory, Gostauto 12, Vilnius LT 2600, Lithuania; erika@itpa.lt

Received 2008 August 19; accepted 2008 November 4; published 2009 March 2

ABSTRACT

We report on the analysis of 436.1 hr of nearly continuous high-speed photometry on the pulsating DB white dwarf GD358 acquired with the Whole Earth Telescope (WET) during the 2006 international observing run, designated XCOV25. The Fourier transform (FT) of the light curve contains power between 1000 and 4000 μHz, with the dominant peak at 1234 μHz. We find 27 independent frequencies distributed in 10 modes, as well as numerous combination frequencies. Our discussion focuses on a new asteroseismological analysis of GD358, incorporating the 2006 data set and drawing on 24 years of archival observations. Our results reveal that, while the general frequency locations of the identified modes are consistent throughout the years, the multiplet structure is complex and cannot be interpreted simply as $l = 1$ modes in the limit of slow rotation. The high-k multiplets exhibit significant variability in structure, amplitude and frequency. Any identification of the m components for the high-k multiplets is highly suspect. The $k = 9$ and 8 modes typically do show triplet structure more consistent with theoretical expectations. The frequencies and amplitudes exhibit some variability, but much less than the high-k modes. Analysis of the $k = 9$ and 8 multiplet splittings from 1990 to 2008 reveal a long-term change in multiplet splittings coinciding with the 1996 *sforzando* event, where GD358 dramatically altered its pulsation characteristics on a timescale of hours. We explore potential implications, including the possible connections between convection and/or magnetic fields and pulsations. We suggest future investigations, including theoretical investigations of the relationship between magnetic fields, pulsation, growth rates, and convection.

Key words: stars: evolution – stars: individual (GD358) – stars: oscillations – white dwarfs

1. INTRODUCTION

Asteroseismology of stellar remnants is traditionally the study of the interior structure of pulsating white dwarfs and subdwarfs as revealed by global stellar oscillations. The oscillations allow a view beneath the photosphere, and contain information about basic physical parameters, such as mass, rotation rate, internal transition profiles, and compositional structure. This information (see, for example, Nather et al. 1990; Winget et al. 1991; Winget et al. 1994; Kepler et al. 2000; Kanaan et al. 2005) provides important constraints on fields ranging from stellar formation and evolution, chemical evolution in our galaxy, the age of the galactic disk, the physics of Type Ia supernovae, and neutrino physics (Winget et al. 2004).

Asteroseismology is now expanding its focus to attack problems that at first consideration may not seem best suited for the technique. Convection remains one of the largest sources of theoretical uncertainty in our understanding of stars. This lack of understanding leads to considerable systematic uncertainties in such important quantities as the ages of massive stars where convective overshooting is important (Di Mauro et al. 2003) and the temperatures and cooling ages of white dwarfs (Prada et al. 2002; Wood 1992). One important early result from the Canadian asteroseismology mission Microvariability and Oscillations of Stars (*MOST*) is the difficulty in detecting predicted oscillations in Procyon A, implying possibly serious incompleteness in our understanding of stars even slightly different from the Sun (Matthews et al. 2004; Marchenko 2008).

Montgomery (2005) shows how precise observations of variable star light curves can be used to characterize the convection zone in a pulsating star. Montgomery bases his approach on important analytical (Goldreich & Wu 1999; Wu 2001) and numerical precursor calculations (Brickhill 1992). The method is based on three assumptions: (1) the flux perturbations are sinusoidal below the convection zone, (2) the convection zone is so thin that local angular variations of the nonradial pulsations may be ignored, i.e., we treat the pulsations locally as if they were radial, and (3) the convective turnover time is short compared with the pulsation timescale, so the convection zone can be assumed to respond instantaneously. Using high signal-to-noise light curves to model nonlinear effects, this approach can observationally determine the convective time scale τ_0, a temperature dependence parameter N, and, together with an independent $T_{\rm eff}$ determination, the classical convective efficiency parameter (the mixing length ratio) α.

Montgomery (2005) applies this theoretical construct to two large amplitude, monoperiodic white dwarf variables where it is possible to fold long light curves to obtain high signal-to-noise pulse shapes. The test candidates are a hydrogen atmosphere DAV (G29−38) and a helium atmosphere DBV (PG1351+489). G29−38 is a well-studied DAV known for the complexity of its pulsations (Kleinman et al. 1998). However, G29−38 was nearly monoperiodic during the 1988 Whole Earth Telescope (WET) campaign (Winget et al. 1990). PG1351+489 is dominated by a single mode and its harmonics, and was WET target in 1995 (Alves et al. 2003). Using folded light curves, Montgomery (2005) obtained results for these two stars which are consistent with mixing length theory (MLT) and other calculations of convective transport.

This significant theoretical advance offers the first empirical determination of convection parameters in stars other than the Sun. However, a result from one star in each white dwarf instability strip provides an insufficient basis for global statements about the nature of the convection zones for all white dwarfs. The next logical step is to map a population spanning a range of temperatures and masses across each instability strip, enabling us to determine the depth of their convection zones as a function of $T_{\rm eff}$ and log g.

PG1351+489 and G29−38 are examples of relatively rare, large amplitude, monoperiodic pulsators where it is possible to fold long light curves to obtain a high signal-to-noise pulse shapes. Simulations by Montgomery (2006) show that this approach is not sufficient for the more common pulsators demonstrating variable complexity in their pulsation spectra. In these cases, we require at least 5 hr of very high signal-to-noise photometry (S/N $\approx$ 1000) coupled with accurate real time frequency, amplitude, and phase information for the pulsations present in the high S/N light curve. The frequency, amplitude, and phase information, provided by a long timebase, multisite observing run, is used to fit the high S/N light curve and extract the convection parameters. The criteria for such a candidate star include nonlinear pulsations, a fairly bright target, and prior knowledge of the l and m values of the pulsations. The bright ($m_{\rm v}$ = 13.5) DB GD358 fits these criteria. GD358 is the best studied DB pulsator, and the only DB with existing, detailed asteroseismology (Winget et al. 1994, hereafter W94; Bradley & Winget 1994; Kepler et al. 2003, hereafter K03; Metcalfe et al. 2003).

In cooperation with the Delaware Asteroseismic Research Center (Provencal et al. 2005), we organized a WET run in May of 2006 (XCOV25) with GD358 as the prime target for Montgomery's light curve fitting technique. Our purpose was twofold: (1) obtain at least 5 hr of S/N $\approx$ 1000 photometry and (2) accurately identify the frequencies, amplitudes and phases present in GD358's current pulsation spectrum. The 2006 XCOV25 data set contains $\approx$436 hr of observations, with $\approx$29 hr of high S/N photometry. While GD358 is the best studied DB pulsator, the star's behavior is by no means well understood. The 2006 data set contains a great deal of interesting information on GD358's pulsational behavior. Before we can proceed with detailed lightcurve fitting, we must thoroughly understand the data set, examine GD358's pulsation spectrum, and extract accurate frequency, amplitude, and phase information. In the following, we will present an overview of the data set and reduction procedures. Our discussion will expand the existing asteroseismological analysis of GD358, exploring the 2006 XCOV25 identified modes, combination frequencies, and multiplet structure. We will compare our results with previous observations and examine the complexity and evolution of GD358's pulsations over time. Our investigation will lead us to consider connections between GD358's pulsations, its convection zone, and a possible surface magnetic field. The remarkable event that occurred in 1996 August (K03) will play an important role in this discussion. Finally, we present implications for our understanding of GD358's physical properties and suggest future investigations.

2. OBSERVATIONS AND DATA REDUCTION

GD358 (V777 Her), the brightest ($m_{\rm v}$ = 13.7) and best studied helium atmosphere white dwarf pulsator, was the target of the 25th Whole Earth Telescope (WET) run (XCOV25), the first sponsored by the Delaware Asteroseismic Research Center (DARC). The observations span 2006 May 12 to June 16, with the densest coverage between May 19 and May 31. Nineteen observatories distributed around the globe contributed a total of 88 individual runs (Table 1). The final XCOV25 light curve contains 436.1 hr of high speed photometry.

A goal of any WET run is to minimize data artifacts by obtaining as uniform a data set as possible (Nather et al. 1990). Early WET runs (e.g., Winget et al. 1991) comprised mainly 3-channel blue-sensitive photomultiplier tube (PMT) photometers that monitored the target variable, a comparison star, and sky brightness. CCDs now bring improved sensitivity and better sky measurements, but individual CCDs have distinct effective bandpasses resulting in different measured amplitudes from different observing sites. Recent WET runs (examples include Kanaan et al. 2005 and Vuckovic et al. 2006) comprise a mixture of CCD and PMT observations, and XCOV25 is no exception. CCDs were employed at sixteen observatories, and 3-channel PMT photometers at the remaining three sites. We attempt to minimize bandpass issues by using CCDs with similar detectors

Table 1
Journal of 2006 XCOV25 Observations

Run Name	Telescope	Instrument	Date	Length (hr)
konk20060512	Konkoly 1.0 m	CCD	2006 May 12	6.8
konk20060515	Konkoly 1.0 m	CCD	2006 May 15	6.3
mole20060515	Moletai 1.65 m	PMT	2006 May 15	1.3
mole20060517	Moletai 1.65 m	PMT	2006 May 17	3.5
konk20060517	Konkoly 1.0 m	CCD	2006 May 17	5.3
cuba20060517	Mt. Cuba 0.6 m	CCD	2006 May 18	5.4
kpno20060518	KPNO 2.1 m	CCD	2006 May 18	7.0
ctio20060518	CTIO 0.9 m	CCD	2006 May 19	4.4
kpno20060519	KPNO 2.1 m	CCD	2006 May 19	7.3
hawa20060518	Hawaii 0.6 m	CCD	2006 May 19	2.2
luln20060519	Lulin 1.0 m	CCD	2006 May 19	5.0
cuba20060519	Mt. Cuba 0.6 m	CCD	2006 May 20	2.5
ctio20060519	CTIO 0.9 m	CCD	2006 May 20	2.1
kpno20060520	KPNO 2.1 m	CCD	2006 May 20	7.6
hawa20060519	Hawaii 0.6 m	CCD	2006 May 20	1.7
ters20060520	Peak Terskol 2.0 m	CCD	2006 May 20	5.8
cuba20060520	Mt. Cuba 0.6 m	CCD	2006 May 21	7.1
kpno20060521	KPNO 2.1 m	CCD	2006 May 21	7.3
ctio20060520	CTIO 0.9 m	CCD	2006 May 21	0.7
hawa20060520	Hawaii 0.6 m	CCD	2006 May 21	3.5
ters20060521	Peak Terskol 2.0 m	CCD	2006 May 21	6.0
tueb20060521	Tuebingen 0.8 m	CCD	2006 May 21	6.6
lapa20060521	La Palma WHT 4.2 m	CCD	2006 May 22	0.9
cuba20060521	Mt. Cuba 0.6 m	CCD	2006 May 22	4.4
ctio20060521	CTIO 0.9 m	CCD	2006 May 22	4.5
kpno20060522	KPNO 2.1 m	CCD	2006 May 22	1.0
cuba20060521	Mt. Cuba 0.6 m	CCD	2006 May 22	1.7
hawa20060521	Hawaii 0.6 m	CCD	2006 May 22	7.8
luln20060522	Lulin 1.0 m	CCD	2006 May 22	4.5
konk20060522	Konkoly 1.0 m	CCD	2006 May 22	4.2
ters20060522	Peak Terskol 2.0 m	CCD	2006 May 22	1.3
mcdo20060523	McDonald 2.1 m	CCD	2006 May 23	7.4
kpno20060523	KPNO 2.1 m	CCD	2006 May 23	2.9
hawa20060522	Hawaii 0.6 m	CCD	2006 May 23	6.6
boao20060523	BOAO 1.8 m	CCD	2006 May 23	7.1
mcdo20060524	McDonald 2.1 m	CCD	2006 May 24	7.2
cuba20060523	Mt. Cuba 0.6 m	CCD	2006 May 24	4.0
hawa20060523	Hawaii 0.6 m	CCD	2006 May 24	3.7
boao20060524	BOAO 1.8 m	CCD	2006 May 24	6.7
ters20060524	Peak Terskol 2.0 m	CCD	2006 May 24	6.1
haut20060524	OHP 1.93 m	PMT	2006 May 24	2.3
mcdo20060525	McDonald 2.1 m	CCD	2006 May 25	6.4
hawa20060524	Hawaii 0.6 m	CCD	2006 May 25	5.7
ters20060525	Peak Terskol 2.0 m	CCD	2006 May 25	7.1
haut20060525	OHP 1.93 m	PMT	2006 May 25	4.2
ctio20060525	CTIO 0.9 m	CCD	2006 May 26	4.0
hawa20060525	Hawaii 0.6 m	CCD	2006 May 26	8.8
haut20060526	OHP 1.93 m	PMT	2006 May 26	4.0
ters20060526	Peak Terskol 2.0 m	CCD	2006 May 27	7.1
ctio20060526	CTIO 0.9 m	CCD	2006 May 27	4.3
hawa20060526	Hawaii 0.6 m	CCD	2006 May 27	9.1
chin20060527	BAO 2.16 m	PMT	2006 May 27	4.5
haut20060527	OHP 1.93 m	PMT	2006 May 27	4.6
cuba20060527	Mt. Cuba 0.6 m	CCD	2006 May 28	6.2
lna20060528	Itajuba 1.6 m	CCD	2006 May 28	3.1
mcdo20060528	McDonald 2.1 m	CCD	2006 May 28	0.7
mcdo20060528b	McDonald 2.1 m	CCD	2006 May 28	7.2
hawa20060527	Hawaii 0.6 m	CCD	2006 May 28	7.8
chin20060528	BAO 2.16 m	PMT	2006 May 28	5.2
haut20060528	OHP 1.93 m	PMT	2006 May 28	5.2
vien20060528	Vienna 1.0 m	CCD	2006 May 28	2.2
cuba20060528	Mt. Cuba 0.6 m	CCD	2006 May 29	3.4
mcdo20060529	McDonald 2.1 m	CCD	2006 May 29	8.2
cuba20060528	Mt. Cuba 0.6 m	CCD	2006 May 29	2.6
hawa20060528	Hawaii 0.6 m	CCD	2006 May 29	9.1

Table 1
(Continued)

Run Name	Telescope	Instrument	Date	Length (hr)
ters20060529	Peak Terskol 2.0 m	CCD	2006 May 29	6.0
haut20060529	OHP 1.93 m	PMT	2006 May 29	5.3
cuba20060529	Mt. Cuba 0.6 m	CCD	2006 May 30	2.7
ters20060530	Peak Terskol 2.0 m	CCD	2006 May 30	6.9
haut20060530	OHP 1.93 m	PMT	2006 May 30	4.2
hawa20060530	Hawaii 0.6 m	CCD	2006 May 31	8.7
chin20060531	BAO 2.16 m	PMT	2006 May 31	3.9
ters20060531	Peak Terskol 2.0 m	CCD	2006 May 31	7.0
nord20060606	NOT 2.7 m	CCD	2006 Jun 6	5.9
tueb20060607	Tuebingen 0.8 m	CCD	2006 Jun 7	4.2
nord20060607	NOT 2.7 m	CCD	2006 Jun 7	7.1
tueb20060608	Tuebingen 0.8 m	CCD	2006 Jun 8	4.7
nord20060608	NOT 2.7 m	CCD	2006 Jun 8	8.0
tueb20060609	Tuebingen 0.8 m	CCD	2006 Jun 9	5.4
nord20060609	NOT 2.7 m	CCD	2006 Jun 9	7.9
tueb20060610	Tuebingen 0.8 m	CCD	2006 Jun 10	5.2
tueb20060611	Tuebingen 0.8 m	CCD	2006 Jun 11	5.1
tueb20060612	Tuebingen 0.8 m	CCD	2006 Jun 12	4.5
lapa20060613	La Palma WHT 4.2 m	CCD	2006 Jun 13	1.8
tueb20060613	Tuebingen 0.8 m	CCD	2006 Jun 13	5.2
lapa20060614	La Palma WHT 4.2 m	CCD	2006 Jun 14	1.4
lapa20060615	La Palma WHT 4.2 m	CCD	2006 Jun 15	2.6
lapa20060616	La Palma WHT 4.2 m	CCD	2006 Jun 16	2.0

and equipping each CCD with a BG40 or S8612 filter to normalize wavelength response and reduce extinction effects. The bi-alkali photomultiplier tubes are blue sensitive, so no filters are required. We also made every attempt to observe the same comparison star at each site, but given plate scale differences, that is not always possible.

We employ a 10 s contiguous integration time with the PMT photometers, while the cycle time for the CCD observations, including exposure and readout times, varies for each instrument. To illustrate the extremes, the Argos camera (Nather & Mukadam 2004) at McDonald Observatory uses a frame-transfer CCD and 5 s integrations with negligible deadtime, while the camera on the CTIO 0.9m telescope operated by the SMARTS consortium uses 10 s integration and a 25 s readtime for a total cycle time of ≈35 s.

Data reduction for the PMT observations follows the prescription outlined in Nather et al. (1990) and W94. In most cases, a third channel continuously monitored sky, allowing point by point sky subtraction. For two channel observations, the telescope is occasionally moved off the target/comparison for sky observations. We examined each light curve for photometric quality, and marked and discarded "bad" points. "Bad" points are those dominated by external effects such as cosmic rays or clouds. We divided GD358's light curve by the comparison star to remove first order extinction and transparency effects. If necessary, we fit a low order polynomial to the individual light curves to remove remaining low frequency variations arising from differential color extinction. We divided by the mean light curve value and subtracted 1, resulting in a light curve with amplitude variations as fractional intensity (mmi). The unit is a linear representation of the fractional intensity of modulation (1 mmi ≈ 1 mmag). We present our Fourier transforms (FT) in units of modulation amplitude (1 mma = 1×10^{-3} ma).

XCOV25 marked an evolution of WET headquarters' role in CCD data reduction. A standard procedure for a WET run is for observers to transfer observations to headquarters for analysis

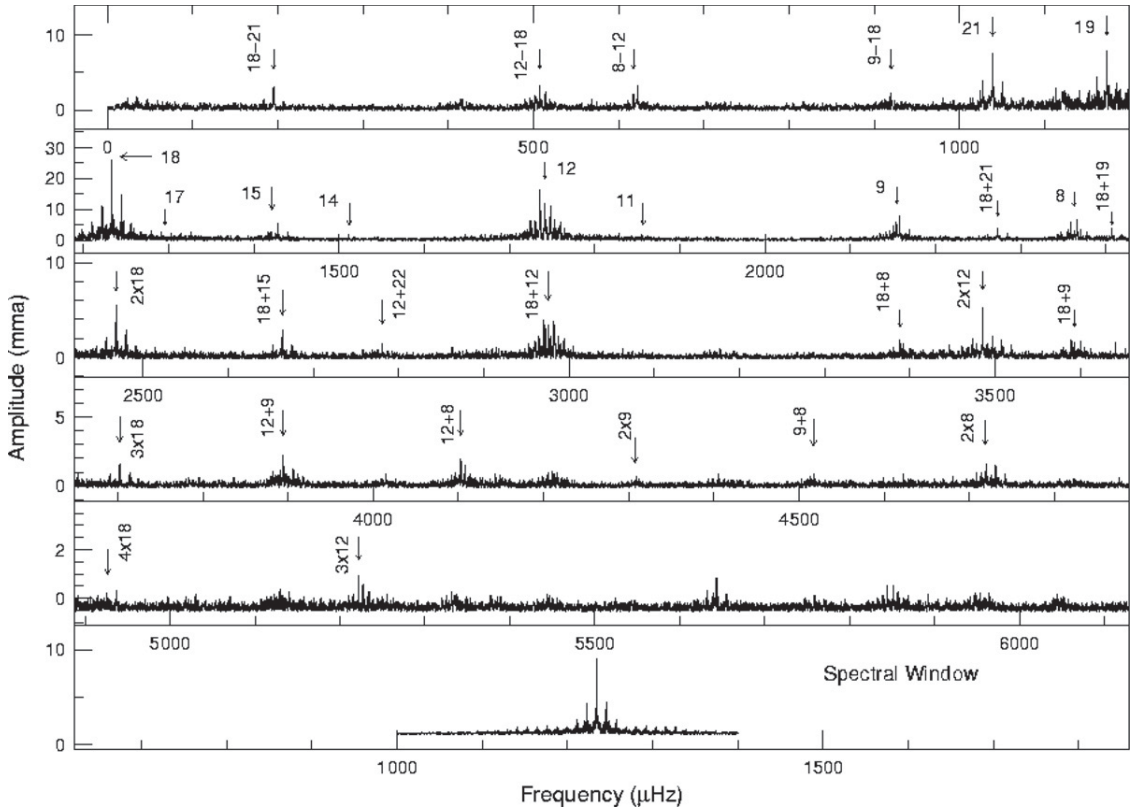

Figure 1. Fourier Transform of the 2006 GD358 photometry observations (note vertical scale in each panel). Arrows are labeled with *k* values for independent modes (single values) and first order combination frequencies. The unlabeled peaks are second and third order combinations. The spectral window is plotted in the last panel. Table 2 lists exact identifications.

at the end of each night. In the past, CCD observers completed initial reductions (bias, flat, and dark removal) at their individual sites, performed preliminary aperture photometry, and transferred the result to WET headquarters. For XCOV25, the majority of participants transferred their raw images, enabling headquarters to funnel data through a uniform reduction pipeline. The few sites unable to transfer images nightly performed preliminary reductions on site using the same procedures as those at headquarters, and sent their images at a later date.

CCD data reduction follows the pipeline described by Kanaan et al. (2002). We corrected each image for bias and dark counts, and divided by the flat-field. Aperture photometry with a range of aperture sizes was performed on each image for the target and selected comparison stars. For each individual nightly run, we chose the combination of aperture size and comparison star producing the highest signal/noise as the final light curve. Each reduced CCD light curve consists of a list of times and fractional intensities. As with the photometer observations, we examined each light curve for photometric quality and discarded "bad" points.

Finally, we combined the individual PMT and CCD light curves to produce the complete light curve for XCOV25. This last step requires detailed assessment of overlapping observations. We make two assumptions in this process: (1) our observational technique is not sensitive to periods longer than a few hours, and (2) we assume GD358 oscillates about a mean light level. These assumptions allow us to carefully identify and correct vertical offsets in overlapping segments.

This data set does contain a significant fraction of overlapping lightcurves. We experimented with the effects of overlapping data on the FT by computing FTs with (1) all data included, (2) no overlapping data, where we kept those data with higher signal-to-noise ratio, and (3) weighting the overlapping light curves by telescope aperture size. We found no significant differences between the noise levels or FTs of overlapping versus non-overlapping versus weighted data.

Despite the favorable weather enjoyed by many participating sites, there are gaps within our light curve, especially near the beginning and end of XCOV25 when fewer telescopes were on-line. These gaps produce spectral leakage in the amplitude spectrum, resulting in a pattern of alias peaks associated with each physical mode that is not of astrophysical origin. To quantify this, we sampled a single sinusoid exactly as our original data and calculated its amplitude spectrum. The "spectral window" is the pattern produced by a single frequency in our data set. The Fourier transform and spectral window of the final complete light curve are given in Figure 1.

3. FREQUENCY IDENTIFICATION

3.1. Stability

Before we can look in detail at the 2006 XCOV25 FT, we must investigate GD358's amplitude and frequency stability over the entire timebase. GD358 is known for large scale changes in amplitudes and small but not insignificant frequency variations on a variety of timescales (K03). Amplitude and/or frequency variations produce artifacts in FTs, greatly complicating any analysis. We divided the data set into three chunks spanning ≈180 hr and calculated the FT of each chunk (Figure 2). For

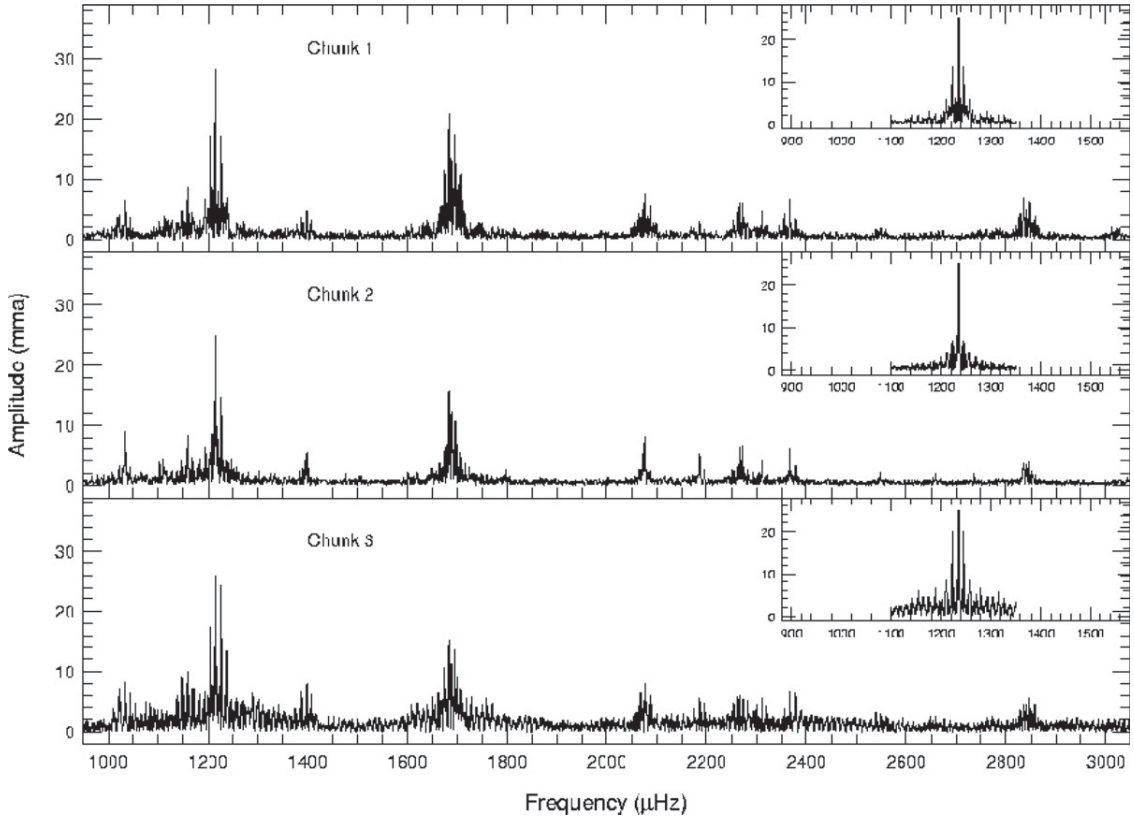

Figure 2. FTs of the 2006 data set subdivided into three chunks of ≈180 hr each. The changes in each FT can be explained as differences in the window structure/resolution for each chunk. GD358 was relatively stable over this time frame.

the dominant peak, the frequencies are consistent to within measurement error and the amplitudes remain stable to within 3σ. The differences between each FT are explained by variation in window structure and resolution from chunk to chunk. We are confident that GD358 was fairly stable over the length of XCOV25.

3.2. The 2006 Fourier Transform

To select the statistically significant peaks in the Fourier transform, we adopt the criterion that a peak have an amplitude at least 4.0 times greater than the average noise level in the given frequency range. This leads to a 99.9% probability that the peak is a real signal present in the data, and is not due to noise (Scargle 1982; Breger et al. 1993, K03, for example). Here, "noise" is defined as the average amplitude after prewhitening by the dominant frequencies in the FT, and is frequency dependent. This is a conservative estimate, as it is impossible to ensure that all of the "real" frequencies are removed when calculating the noise level. This is most certainly the case in GD358, where the FT contains myriad combination frequencies. Figure 3 displays the average amplitude, specified as the square root of the average power after prewhitening by 50 frequencies, as a function of frequency, for 2006, and previous WET runs on GD358 in 2000, 1994, and 1990.

The amplitude limit we select is very important in determining "real'signals. To confirm our uncertainty estimates, we performed several Monte Carlo simulations using the routine provided in *Period04*, software devoted to the statistical analysis of time series photometry (Lenz & Breger 2005). The Monte Carlo routine generates a set of light curves using the original times, the fitted frequencies and amplitudes, and added Gaussian noise. A least-squares fit is performed on each simulated light curve, with the distribution of fit parameters giving the uncertainties. Our Monte Carlo results are consistent with our average amplitude noise estimates (Table 2), confirming our use of the average amplitude after prewhitening.

For both Fourier analysis and multiple least squares fitting, we use the program *Period04*. The basic method involves identifying the largest amplitude resolved peak in the FT, subtracting that sinusoid from the original light curve, recomputing the FT, examining the residuals, and repeating the process. This technique is fraught with peril, especially in multiperiodic stars, where it is possible for overlapping spectral windows to conspire to produce alias amplitudes larger than real signals. Elimination of this alias issue was the driving motivation behind the development of the WET, whose goal is to obtain nearly continuous coverage over a long time baseline. Our current data set on GD 358 does contain gaps, but we have minimized the alias problem.

To illustrate the procedure we followed, let us examine the region of dominant power at 1234 μHz (Figure 4). Comparison of this region with the spectral window demonstrates that most of the signal is concentrated at 1234 μHz. We fit the data with a sine wave to determine frequency, amplitude, and phase, and subtract the result from the original light curve. The second panel of Figure 4 shows the FT prewhitened by this frequency. Careful examination reveals two residual peaks (arrows) that are clearly not components of the spectral window. We next subtract a simultaneous fit of the 1234 μHz frequency and these two additional frequencies, with the results displayed in panel 3 of Figure 4. At this point, we must proceed with extreme caution. The remaining peaks, which correspond closely with aliases in the spectral window, are significant and cannot be ignored.

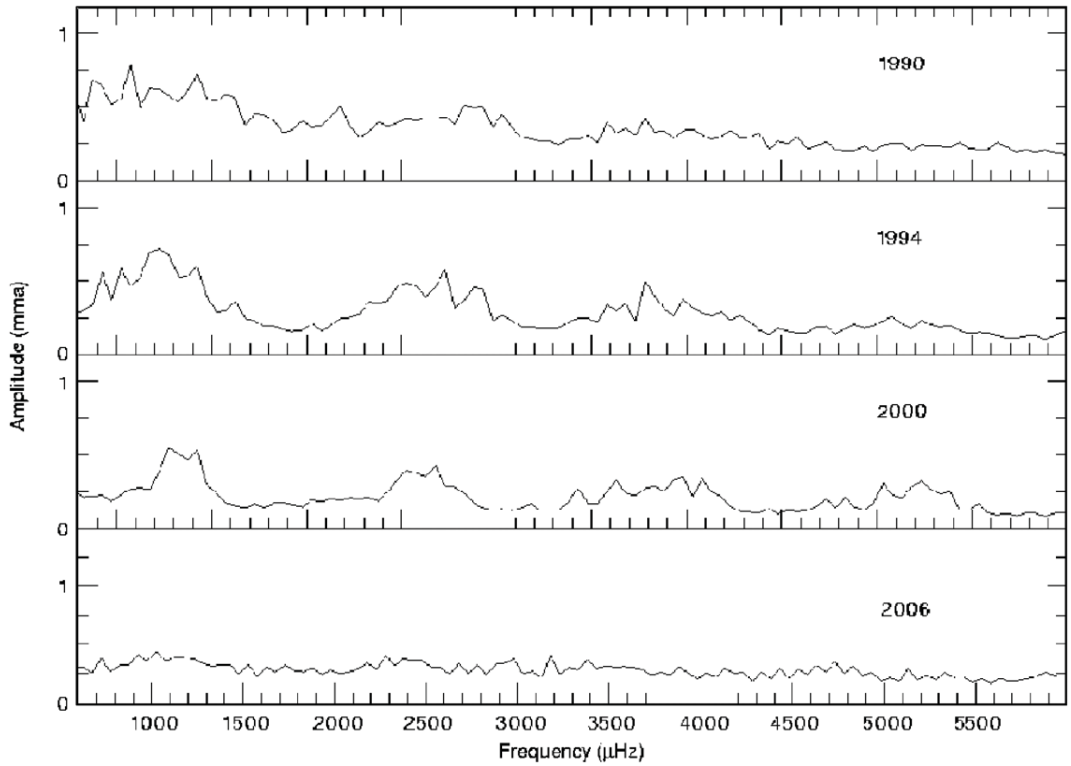

Figure 3. A comparison of the average noise from the 1990, 1994, 2000, and 2006 WET runs. Each data set was prewhitened by the 50 largest amplitude frequencies. This is a conservative estimate of the noise in each data set.

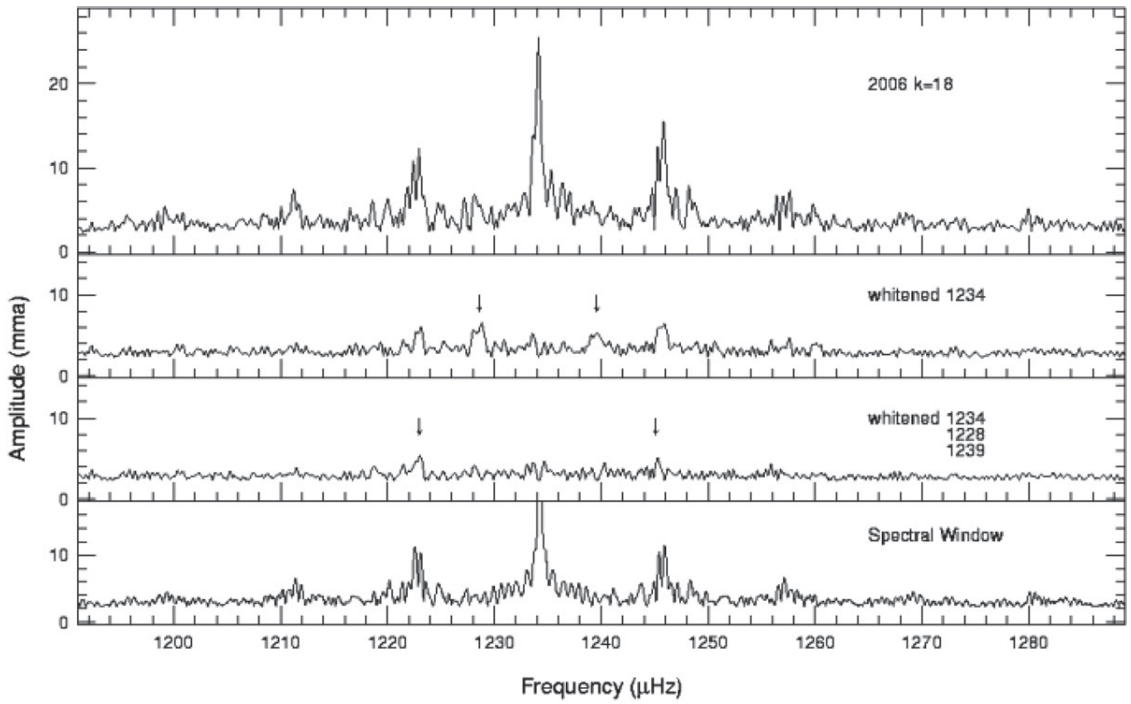

Figure 4. Demonstration of prewhitening using the dominant 1234 μHz mode in the 2006 FT. We begin with the removal of the largest amplitude resolved peak, a careful comparison of the residuals with the spectral window (last panel), and the subsequent removal of additional peaks.

We are faced with two possibilities: (1) these peaks represent real signals, and (2) amplitude modulation is present. While we have ruled out large modulations in frequency/amplitude during XCOV25, small scale amplitude modulation may be intrinsic to GD358, or artificially present in the data set. An examination of data from individual sites reveals that although the frequencies from each site are the same within the statistical uncertainties, two observatories, one using a CCD and one a

Table 2
Table of 2006 Independent Frequencies

$k(l=1)$	2006 Frequency (μHz)	Amp (mma)	S/N	MC σ_{amp} (mma)
21	1039.076 ± 0.002	7.96 ± 0.07	27	0.08
19	1173.042 ± 0.002	7.28 ± 0.07	25	0.08
18	1222.751 ± 0.001	5.0 ± 0.07	18	0.6
18	1228.792 ± 0.002	5.7 ± 0.07	19	0.07
18	1234.124 ± 0.001	24 ± 0.07	88	0.09
18	1239.540 ± 0.002	4.7 ± 0.07	18	0.07
18	1245.220 ± 0.003	4.7 ± 0.07	17	0.6
17	1295.533 ± 0.008	1.4 ± 0.08	5	0.6
15	1421.012 ± 0.008	2.8 ± 0.08	7	0.07
15	1423.942 ± 0.008	1.3 ± 0.08	6	0.07
15	1429.210 ± 0.002	5.6 ± 0.07	23	0.07
15	1434.784 ± 0.008	1.4 ± 0.07	4.4	0.06
15	1440.622 ± 0.008	1.4 ± 0.07	4.3	0.06
14	1512.010 ± 0.007	3.6 ± 0.08	8	0.07
12	1736.302 ± 0.001	17.0 ± 0.07	75	0.07
12	1737.962 ± 0.007	5.6 ± 0.07	8	0.08
12	1741.665 ± 0.001	10.9 ± 0.07	50	0.07
12	1743.738 ± 0.002	5.6 ± 0.07	8	0.07
12	1746.673 ± 0.007	1.8 ± 0.08	8	0.08
12	1749.083 ± 0.001	12.9 ± 0.07	50	0.07
11	1856.845 ± 0.009	1.4 ± 0.08	6.4	0.08
9^{-1}	2150.395 ± 0.003	4.2 ± 0.07	17	0.07
9^{0}	2154.222 ± 0.002	5.5 ± 0.07	22	0.07
9^{+1}	2158.071 ± 0.002	7.2 ± 0.07	29	0.07
8^{-1}	2359.064 ± 0.002	5.87 ± 0.07	22	0.07
8^{0}	2363.058 ± 0.007	1.82 ± 0.08	6	0.07
8^{+1}	2366.523 ± 0.002	6.54 ± 0.07	23	0.07

PMT, report consistently lower amplitudes, probably due to beating effects. Removing the suspect observations from the data set does not alter the prewhitening results for the 1234 μHz region. As an additional test, we closely examined the FTs from Figure 2. Prewhitening the 1234 μHz regions of each chunk consistently produces the same five peaks. Finally, we note that one of these peaks appears in combination with other modes (Table 3). Therefore, we believe our first possibility is most probable, all five peaks are real and are listed in Table 2.

We employed this procedure to identify frequencies satisfying our criteria of amplitudes 4σ above the average noise. The large amplitude power at 1740 μHz is particularly complex. Unlike our example at 1234 μHz, this mode contains three peaks with amplitudes over 10 mma and contains as many as nine frequencies (Figure 5). Figure 6 demonstrates the prewhitening results for modes at 2154 and 2362 μHz.

Our final identifications result from a simultaneous nonlinear least squares fit of 130 frequencies, amplitudes, and phases. We adopt the $l = 1$ mode identifications for GD358 established in W94. We emphasize, however, that k, representing the number of nodes in the radial component of displacement from the center to the stellar surface, cannot be observationally determined and may not correspond precisely to the values given here. Tables 2 lists 27 identified independent frequencies. Table 3 presents significant combination frequencies. In the interest of space, we do not list all of the combination frequencies.

Table 3
2006 Combination Frequencies

Frequency (μHz)	Combination(s) k	$f_{obs} - f_{calc}$ (μHz)	Amp (mma)	(S/N)	R_c
195.085	1234 − 21	0.04	2.7	7.7	...
507.523	1741.7 − 1234	−0.02	3.0	8.2	...
622.798	2358.1 − 1736.3	−1.0	2.8	7.5	...
920.039	9^0 − 1234	−0.06	1.9	4.5	...
2078.187	2 × 1039.1	−0.1	0.74	3.2	2.4
2273.244	1234 + 21	0.05	4.2	10.8	9.6
2407.205	1234 + 19	0.07	3.8	9.7	9.1
2462.989	1234 + 1228.8	0.07	3.7	8.2	11.4
2468.282	2 × 1234	0.034	5.1	13.1	1.8
2479.358	1234 + 1245.2	0.014	1.5	4.1	5.6
2663.369	1234 + 1429.2	0.04	2.9	7.3	9.4
2780.786	1741.7 + 1039.1	0.014	1.4	4.0	7.1
2909.416	1736.3 + 19	0.1	1.0	2.6	3.5
2964.917	1228.8 + 1736.3	−0.18	1.1	2.8	5.0
	1222.8 + 1741.7	−0.46	1.1	2.8	
2970.400	1234 + 1736.3	0.025	3.0	7.6	3.1
	1228.8 + 1741.7	−0.057			
2972.085	1234 + 1737.9	0.036	2.82	7.6	8.8
	1222.8 + 1749.1	−0.22			
2975.814	1234 + 1741.7	−0.024	3.4	8.7	5.5
	1239.5 + 1736.3	−0.039			
2977.885	1228.8 + 1749.1	0.01	1.7	4.4	11.9
	1234 + 1743.8	0.02			
2981.032	1239.5 + 1741.7	0.17	1.3	4.0	11.2
2981.947	1245.2 + 1736.3	−0.45	3.5	7.9	20.6
2983.266	1234 + 1749.1	0.057	3.1	7.9	4.66
2988.643	1239.5 + 1749.1	−0.42	1.1	3.9	9.36
3388.400	1234 + 9^0	0.052	1.5	4.0	4.75
3392.185	1234 + 2150.4	−0.013	1.7	4.4	7.35
3472.552	2 × 1736.3	−0.052	1.5	4.8	1.2
3477.939	1736.3 + 1741.7	0.06	1.7	4.5	4.0
3485.387	1741.7 + 1743.7	−0.02	5.7	16.7	11.6
	1736.3 + 1749.1	0.003	5.7	16.8	
3490.720	1741.7 + 1749.1	0.03	1.3	4.0	
3593.136	1234 + 2359.1	−0.041	1.6	4.2	4.8
3600.577	1234 + 2366.5	−0.071	1.7	4.5	4.5
3702.443	3 × 1234	0.071	2.0	5.3	
3890.607	1736.3 + 9^0	0.08	1.5	4.8	7.0
3894.392	1736.3 + 2158.1	0.016	2.7	7.7	6.8
3907.140	1749.083 + 2158.1	−0.014	1.6	5	7.7
4095.326	1736.302 + 2359.1	−0.03	1.2	4.0	5.2
4102.850	1736.302 + 2366.5	0.024	2.2	7.3	4.0
4108.130	1749.083 + 2359.1	−0.06	1.7	5.6	9.8
4209.941	2 × 1234 + 1741.7	0.028	1.3	4.8	
4308.536	2 × 9^0	−0.092	1.0	4.6	11.7
4517.044	8^0 + 9^0	−0.24	1.1	4.7	48.5
	2359.1 + 2158.1	0.13			
	2150.4 + 2366.5	−0.08			
4719.483	2 × 2359.064	−1.4	2.1	7.2	13.2
4718.268	2 × 2359.064	−0.14	1.1	4.7	
5221.734	1736.3 + 1741.7 + 1743.7	0.034	1.3	4.2	
	2 × 1736.3 + 1749.1	−0.049			
5643.452	1736.3 + 1749.1 + 2158.1	0.05	1.2	4.1	

4. GD358 IN 2006

4.1. Independent Modes

The 2006 XCOV25 data set illustrates GD358's continuing tendency for changing the distribution of amplitudes among its excited modes. Using the k identifications established in W94, we detect power at $k = 21, 19, 18, 17, 15, 14, 12, 11, 9$, and 8. The principal frequency is at 1234 μHz ($k = 18$) with an amplitude

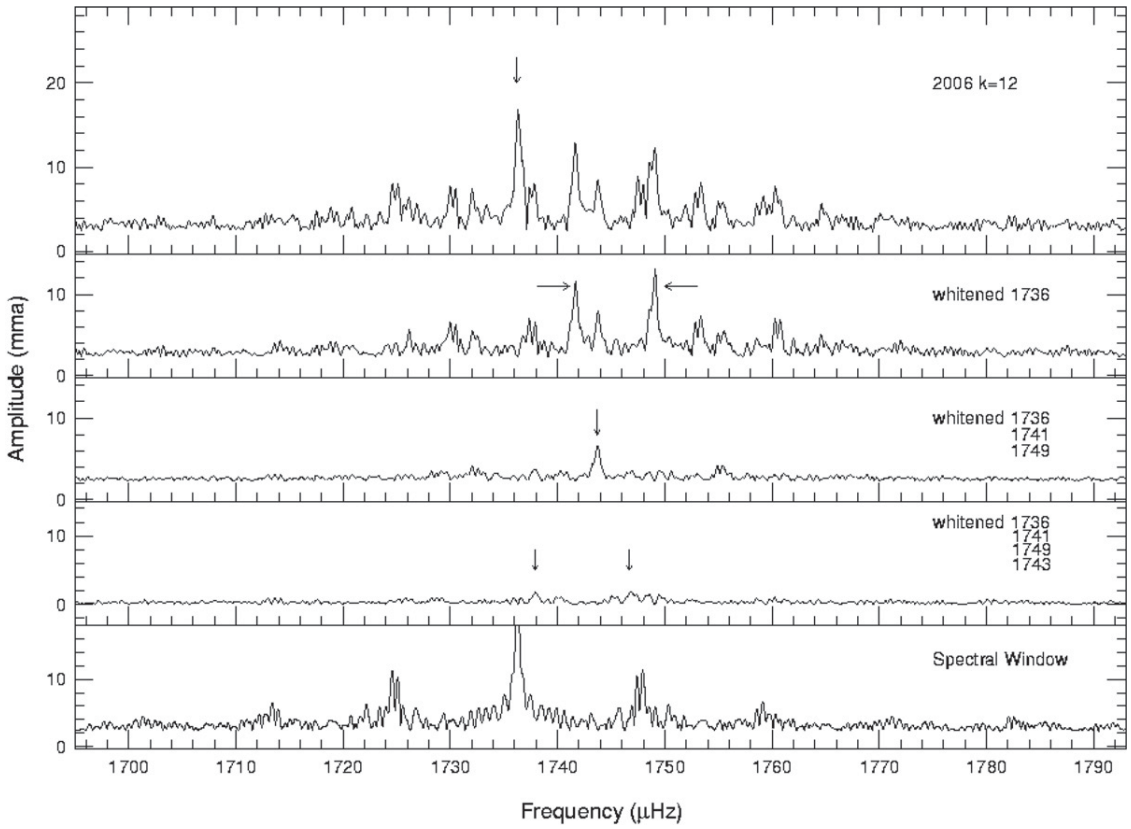

Figure 5. Prewhitening of the complex $k = 12$ mode. We find three peaks over 10 mma at 1736, 1741 and 1749 μHz, and numerous additional peaks (Table 2). This mode could contain as many as 9 components.

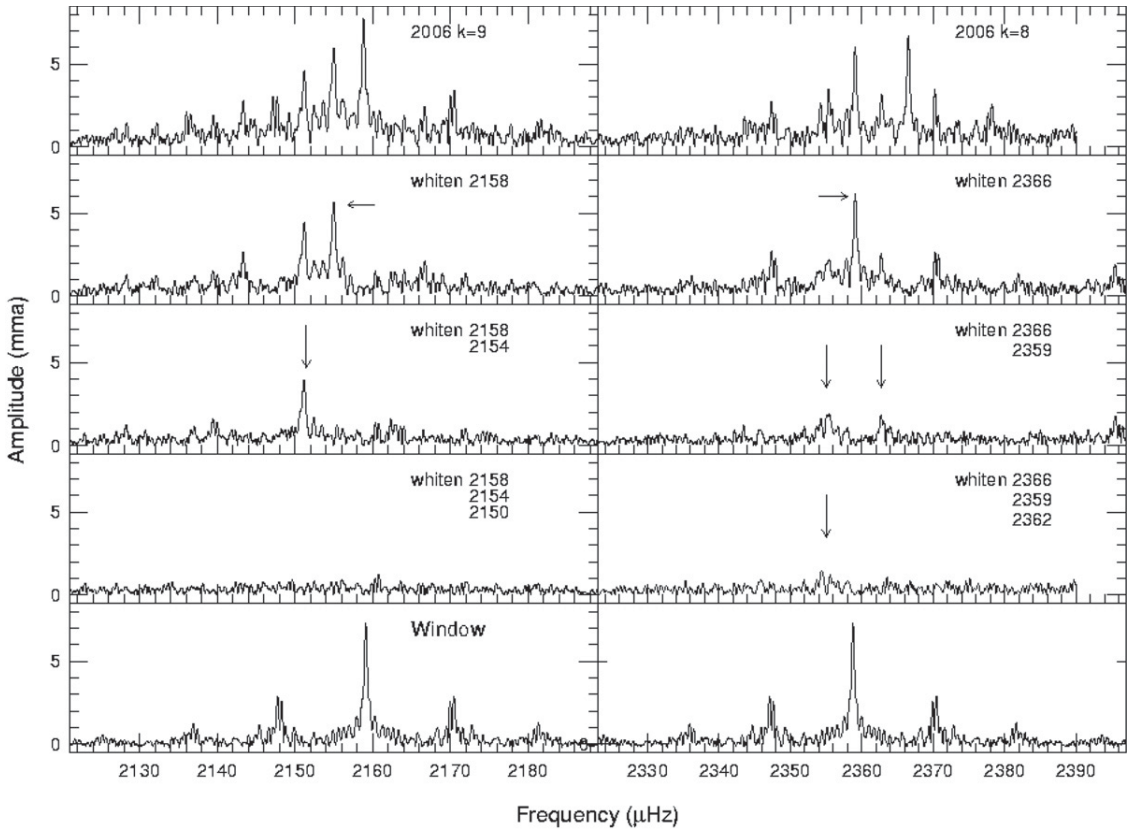

Figure 6. Prewhitening of the $k = 9$ and 8 modes. These modes are triplets consistent with previous reports of W94 and K03.

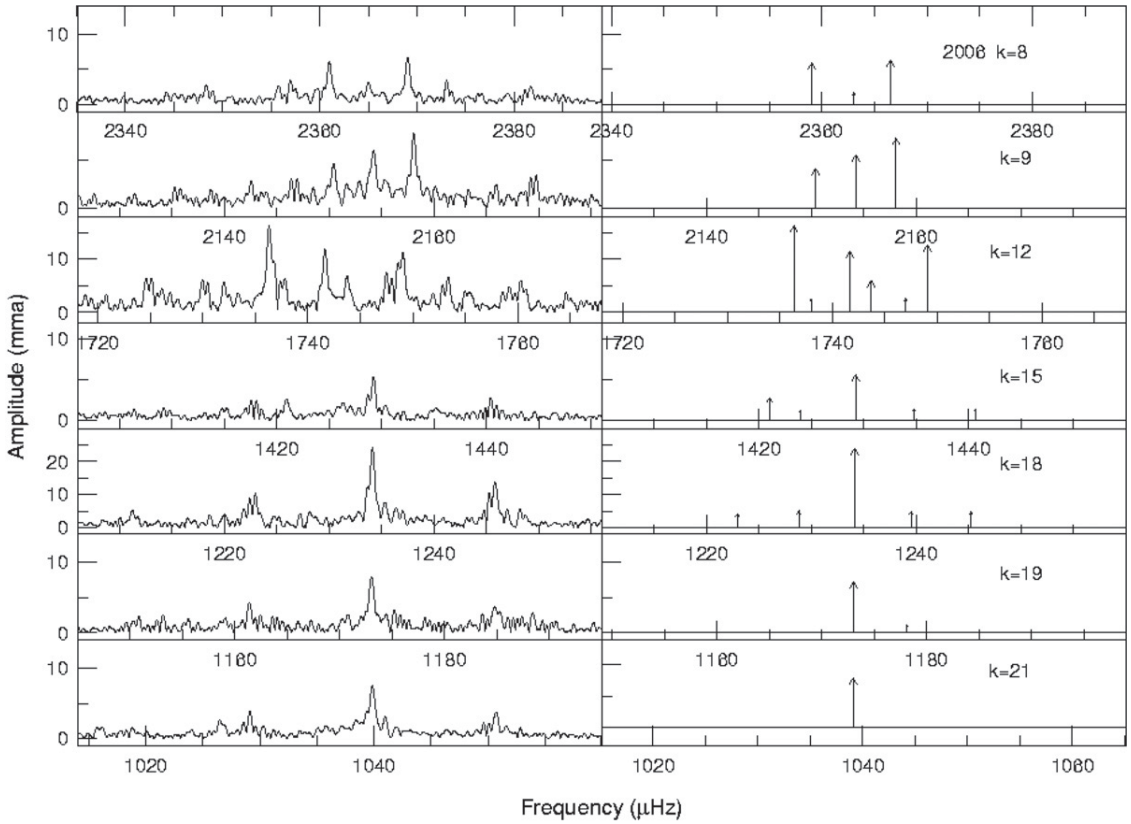

Figure 7. A "snapshot" of the 2006 largest amplitude modes and their multiplet structure. The left panels plot the observed FT, and the right panels presents the prewhitening results. The 1σ frequency errors are $\approx$0.001 μHz. Each panel spans 50 μHz. Note the changes in y scale.

of 24 mma. The previously dominant $k = 17$ and 15 modes (K03) are greatly diminished in amplitude (1.4 and 5.6 mma, respectively), and we do not detect the $k = 16$ or $k = 13$ modes reported by W94 and K03. We cannot identify the suspected $l = 2$ mode at 1255.4 μHz or $k = 7$ at 2675.5 μHz noted by K03). K03 suggest that $k = 7$ may have been excited to visibility via resonant coupling with $k = 17$ and 16. Since neither has significant amplitude in 2006 (Figure 1), it logically follows that this mode would not be detected. Perhaps the greatest surprise from XCOV25 is the appearance of prominent power at the predicted value for $k = 12$, a region of the FT previously devoid of significant peaks.

Figure 7 presents a "snapshot" of multiplet structure in the XCOV25 FT. The only modes exhibiting structure with splittings in agreement with previous observations are $k = 9$ and 8. We find average multiplet splittings of 3.83 and 3.75 μHz, respectively. The dominant $k = 18$ is a quintuplet with an average splitting of 5.6 μHz. The 5.6 μHz splitting also appears in the $k = 15$ and $k = 12$ modes. The $k = 15$ mode contains five peaks, only three of which are split by 5.6 μHz. The $k = 12$ mode could contain as many as nine components, if we relax our 4.0 σ detection criteria slightly. A possible interpretation for $k = 12$ is two, perhaps three, overlapping triplets, each with $\approx$ 5.6 μHz splitting. An $l = 2$ mode is predicted at $\approx$1745μHz, so a second possible interpretation is an overlap of $l = 1$ and $l = 2$ modes. We point out that the other high-k modes (17, 16, 14, and 13) reported by W94 to have frequency splittings of $\approx$ 6 μHz are either not detected here, or do not have sufficient amplitude to investigate multiplet structure.

Our goal for XCOV25 is the identification/confirmation of l and m values for modes in GD358's 2006 light curve. This information is required to fit our high signal-to-noise lightcurve using Montgomery's technique. However, the 2006 multiplet structure proves to be puzzling. In the limit of slow rotation, we expect each mode to be split into $2l + 1$ components. Except for $k = 9$ and $k = 8$, we do not find the distinct triplets attributable to $l = 1$. Indeed, $k = 18$ is a quintuplet at first glance suggesting $l = 2$, and $k = 15$ and 12 are both complex but lacking equal splittings. We cannot confirm the l or m designations of W94 and K03 based on multiplet structure alone. Fortunately, the identification of the spherical degree of GD358's pulsation modes as $l = 1$ does not rely solely on multiplet structure. Table 4 presents the mean period spacing for XCOV25, as well as WET runs from 1990, 1991, 1994, and 2000. The average period spacing, which is dependent on stellar mass, is 38.6 s. If GD358's modes are consecutive $l = 1$, the period spacing corresponds to a stellar mass of $\approx 0.6\ M_o$, in agreement with spectroscopic results (Beauchamp et al. 1999). If they are consecutive $l = 2$ modes, the derived stellar mass becomes $\approx 0.2\ M_o$, making GD358 one of the lowest mass field white dwarfs known and incompatible with the spectroscopic log g. In addition, the distance of 42 ± 3pc derived from GD358 models assuming $l = 1$ is consistent with the trigonometric distance of 36 ± 4pc. The distance derived derived from models assuming $l = 2$ is $\approx$75 pc (Bradley & Winget 1994). Is it possible that we have an amalgam of $l = 1$ and 2 modes? $l = 2$ modes are predicted to be quintuplets, fitting with our results for $k = 18$. However, we expect the ratio of rotational splittings between $l = 1$ and $l = 2$ to be $R_{1,2} = 0.60$ (Winget et al. 1991). Assuming

Table 4
Mean Period Spacing

Year	Time BJED	ΔP_{av} (s)
1990	2440831.772	38.60 ± 0.3
1991	2448356.716	38.39 ± 0.3
1994	2449474.998	38.67 ± 0.3
2000	2451702.402	38.77 ± 0.3
2006	2453868.311	38.77 ± 0.3

Notes. The spacing from the "period transform is given as PT, and the value from the subtracting of low- and high-k periods is "K."

$k = 8$ and 9 are $l = 1$ as indicated by their triplet structure, we expect an $l = 2$ splitting of 6.3 μHz, much larger than the observed 5.6 μHz splitting. We have no easy explanation for the 5.6 μHz splitting, and hesitate to identify $k = 18$ as an $l = 2$ mode solely on the basis of a quintuplet. The $k = 12$ and $k = 15$ modes contain the mysterious 5.6 μHz splitting, but the splittings are unequally spaced. The "best fit" pulsation models do predict $l = 2$ modes at 1250 μHz (near $k = 18$) and 1745 μHz (near $k = 12$) (Metcalfe et al. 2003). The 1250 μHz mode is not detected in this data set. Some of the complex peaks at $k = 12$ could correspond to an underlying $l = 2$ mode, but the splittings do not support this conclusion. Finally, optical and UV radial velocity variations have been used to determine the l values for several modes in GD358, including $k = 18$. Kotak et al. (2003) identified radial velocities corresponding to $k =$ 18, 17, 15, 9, and 8 in their time-resolved optical spectra. They determined that these modes all share the same l value, which is probably $l = 1$. Castanheira et al. (2005) use *HST* UV time resolved spectroscopy to determine that $k = 9$ and 8 are best explained as $l = 1$.

While we are fairly certain that the majority of GD358's modes are $l = 1$, except for $k = 9$ and 8, we cannot directly provide m identifications for the observed multiplet components or confirm the m identifications of W94 and K03. For this data set, we must resort to indirect means. In the next section, we examine the combination frequencies, and, limiting ourselves to $l = 1$, explore their potential for pinning down the multiplet m components in GD358.

4.2. Combination Frequencies

GD358's 2006 FT contains a rich distribution of combination frequencies, from differences to simple harmonics to fourth order combinations. Combinations peaks are typically observed in the FTs of large amplitude pulsators (Dolez et al. 2006; Yeates et al. 2005; Thompson et al. 2003; Handler et al. 2002, W94). Their frequencies correspond to integer multiples of a single frequency (harmonics), combinations (both sums and differences) of different components of a given multiplet, or combinations (again both sums and differences) of components of different modes (cross combinations). The general consensus on the origin of these combinations dictates that they are not independent modes, but are the result of nonlinear mixing induced by the convection zone in the outer layers of the star (Brickhill 1992; Wu 2001; Ising & Koester 2001). The convection zone varies its depth in response to the pulsations, distorting and delaying the original sinusoidal variations, and redistributing some power into combination frequencies. While combinations themselves do not provide additional direct information about the interior structure of the star, they are sensitive to mode geometry, making them potential tools for identifying l and/or m values and orientation for each mode.

Wu (2001) provides a theoretical overview of combinations and their interpretation. Handler et al. (2002) and Yeates et al. (2005) apply Wu's approach to several ZZ Ceti (DA) stars. Yeates et al. (2005) focus on the dimensionless ratio R_c first introduced by van Kerkwijk et al. (2000). The theoretical value of R_c is given as $R_c = F(\omega_i, \omega_j, \tau_{c_0}, 2\beta + \gamma)G(l, m, \theta)$. The first term, F, includes the frequencies of the parent modes (ω_i, ω_j), as well as properties inherent to the star, such as the depth of the stellar convection zone at equilibrium (τ_{c_0}) and the sensitivity of the convection zone to changes in temperature (β, γ). The second term, G, includes geometric factors such as the l and m values of the parent modes, and the inclination angle of the pulsation axis. Both Wu (2001) and Yeates et al. (2005) present theoretical predictions for various combinations of l and m values.

The observed value of R_c is defined as the ratio between the observed amplitude of a combination and the product of the observed amplitudes of its parent modes, including a correction factor incorporating the bolometric correction and an estimate for the convective exponent. The convective exponent appears in theoretical estimations of the thermal response timescale of the convection zone. From Montgomery (2008), we estimate the bolometric flux correction for GD358 to be 0.35 and the convective exponent to be 25. For harmonic combinations, this produces a corrective factor of 0.22. Cross combinations include an additional factor of 2, resulting in a correction of 0.44. With this formalism, and limiting ourselves to the previous identification of the principal modes as $l = 1$, and with the smorgasbord of combination frequencies present in GD358, it should be possible to determine m values of the parent modes, to provide limits on the inclination angle, and to further study convection in white dwarfs. However, interpretation of the combination frequencies is not as straightforward as we would hope.

The analysis of R_c for harmonic combinations is simplified by the fact that we are certain that the combination contains a single parent, and so single values for l and m. In the 2006 data set, we detect the dominant 1234 μHz mode's first, second, and third harmonics, and place upper amplitude limits of $\approx$ 0.3 mma on higher orders. The first harmonic, at 2468.282 μHz with an amplitude of 5.1 mma, is the 12th highest amplitude peak in the FT and the second highest amplitude combination frequency observed.

The second largest mode and most complicated multiplet in the 2006 FT is $k = 12$. Focusing on its three large amplitude components (Table 3), we find the first harmonic of 1736 μHz, near 3472 μHz with an amplitude of 1.5 mma. Interestingly, the largest peak near 3472 μHz is actually a sum of $k = 12$ components (see Table 3), not a simple harmonic, a behavior distinctly different from $k = 18$. We place an upper limit of 0.5 mma for a 1st harmonic of 1741.67 μHz, 0.6 mma for 1749.08 μHz, and upper limits of 0.3 mma for all higher orders for all other components of $k = 12$.

For the remaining modes in Table 2, we detect the first harmonic of 1039 μHz ($k = 21$) with an amplitude of 0.7 mma. For $k = 19$, 17, 15, 14, and 11, we place upper limits of 0.5 mma for their first harmonics. The 2154 μHz peak, identified as $k = 9$, $m = 0$ ($k = 9^0$) in W94, has a first harmonic with an amplitude of 1.0 mma. It is surprising that we do not detect a harmonic of the larger amplitude $k = 9^{+1}$ component. We place upper limits of 0.4 mma for harmonics of the $k = 9^{\pm 1}$ components. Finally, the 2359 μHz component of $k = 8$, identified as $k = 8^{-1}$ in W94, has a first harmonic at 4719.483 μHz (2.1 mma). We place upper limits of 0.4 mma for harmonics of the $k = 8^0$ and

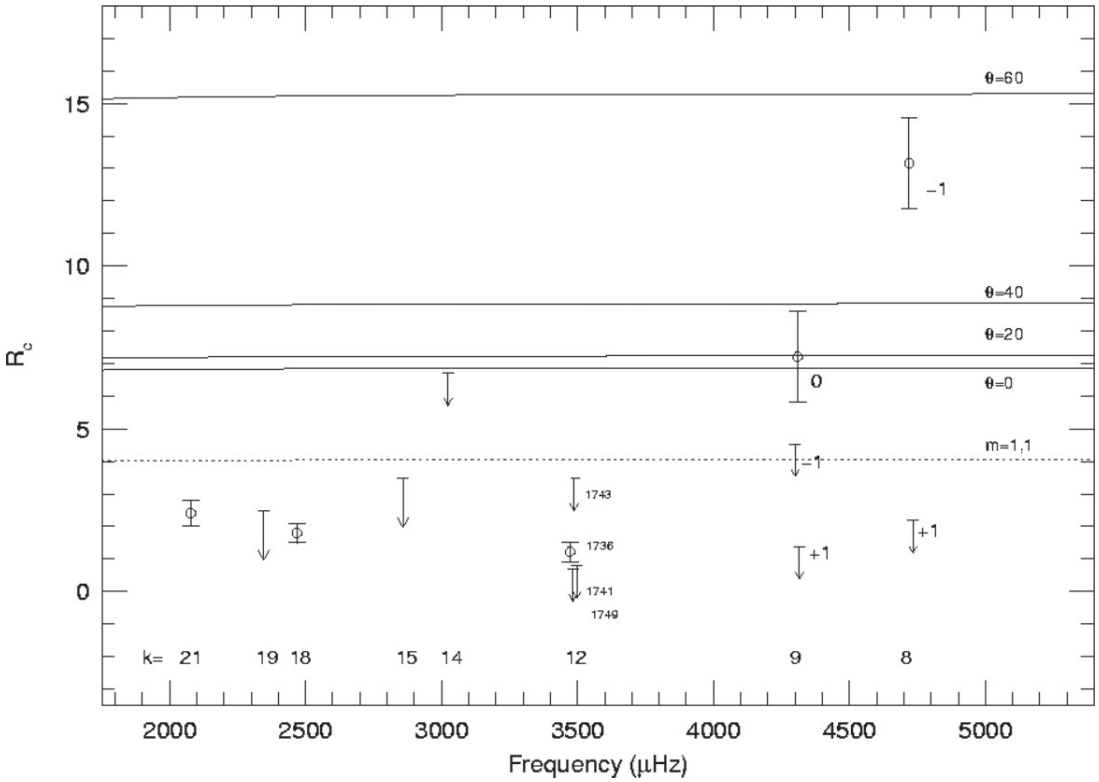

Figure 8. Observed R_c values (ratio of amplitude of the combination to the product of the parent amplitudes) for detected harmonics. The open circles denote detected harmonics with estimated errors, and the vectors plot upper limits on other harmonics. The solid lines represent theoretical values for the harmonics of $m = 0$ modes for inclinations of 0, 20, 40, and 60°. The dotted line gives the theoretical value for the harmonics of $m = 1$ and $m = -1$ modes, which do not depend on inclination. We rely on previous identifications of m values for $k = 9$ and 8.

$k = 8^{+1}$ components. We note again that the larger amplitude $k = 8^{+1}$ does not have a significant harmonic.

We begin by plotting the observed values of R_c for first order harmonics in Figure 8. If no harmonic is detected, we present upper limits. Since we do not have m identifications for most modes but we know that m must be the same for harmonic parents, we plot theoretical predictions for $l = 1$, $m = 0, 0$ combinations for inclinations of 0, 20, 40, and 60° (solid lines) and $l = 1$, $m = 1, 1$ and $m = -1, -1$ (dotted line). R_c values for $m = 1, 1$ and $m = -1, -1$ combinations do not depend on inclination. Surprisingly, the observed R_c values and upper limits for the high-k modes are lower than the theoretical predictions. We could argue that, under the theoretical assumptions of Wu (2001), the detected high-k multiplet components are not consistent with $m = 0$.

From the $k = 9$ harmonics, we find behavior closer to theoretical predictions. The $k = 9^0$ harmonic is consistent with an inclination of between 0 and 40°, while the $k = 9^{\pm 1}$ components are in the direction of theoretical predictions. However, for $k = 8$, the $k = 8^{-1}$ harmonic has a larger value of R_c than the $k = 8^{+1}$ upper limit, something that is difficult to explain using current theory and simple viewing arguments. The upper limit of R_c for $k = 8^0$ is 29, and is not shown in Figure 8.

The most eye-catching example of cross combination peaks is found near 3000 μHz (Figure 1), corresponding to linear combinations between the two largest multiplets, $k = 18$ and $k = 12$. Our resolution and sensitivity are sufficient to reveal nine combinations, with amplitudes ranging from 3.4 mma to 1.1 mma. In several cases, multiple parent identifications are possible for each mode. For the following discussion, we include identifications for detected combinations involving at least one large amplitude parent, with most including the 1234 μHz mode in combination with components of $k = 12$ (Table 3). The 1234 μHz mode also produces large amplitude combinations (4.2 and 3.8 mma) with the 1039 ($k = 21$) and 1173 ($k = 19$) μHz modes.

Figure 9 presents observed R_c values and upper limits for first order cross combinations including the dominant 1234 μHz mode as one parent. We include the same theoretical predictions as in Figure 8, adding predictions for $l = 1$, $m = +1, -1$ combinations for inclinations of 20, 40, and 60° (dotted lines), and $m = 0, \pm 1$ combinations (dot/dash line). The R_c values for combinations of 1234 μHz with the high-k modes 21, 19, 15, and one component of $k = 12$ (1739 μHz) are consistent with either $m = 0, 0$ combinations with an inclination of roughly 40° or $m = +1, -1$ combinations with an inclination closer to 50°. Recalling that the harmonic combinations (Figure 8) argue that none of the high-k modes are $m = 0$, the second choice of $m = +1, -1$ combinations seems more likely. This further implies that 1234 μHz is either $m = +1$ or $m = -1$, and the other modes are all the remaining value.

The relative values of R_c among the 3000 μHz combinations ($k = 18$+12), while independent of most model parameters, do depend on inclination, and should reflect their respective projection in our line of sight. We should find R_c values corresponding to combinations of $m = 0, \pm 1$, $m = 0, 0$, $m = -1, +1$, and $m =$ same. However, even incorporating our tenuous identification of 1234 μHz as $m = -1$, given the number of multiplet components and large uncertainties in the inclination angle, our analysis based on Wu (2001) predictions produces no clear identification.

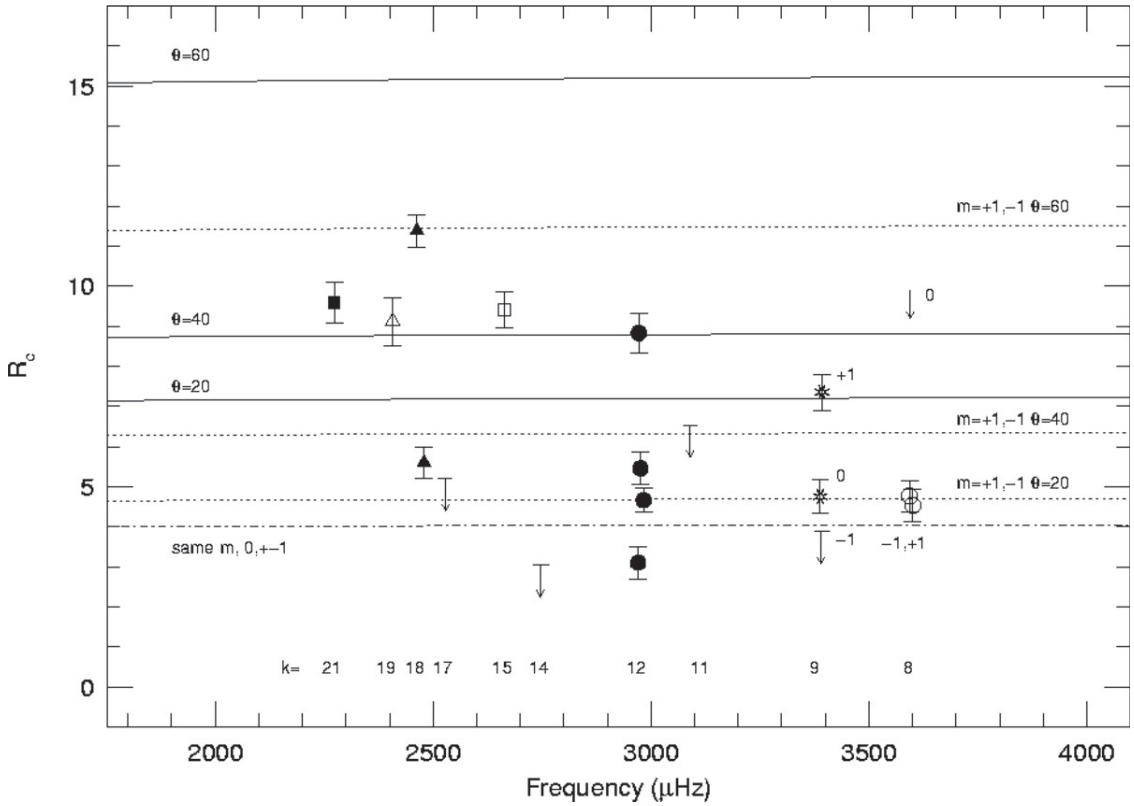

Figure 9. Observed R_c values (ratio of amplitude of the combination to the product of the parent amplitudes) for cross combinations including 1234 μHz as one parent mode. The k value of the second parent is given along the bottom of the figure, and different point types indicate combinations of 1234 μHz with different ks. The solid lines represent theoretical predictions for $m = 0, 0$ combinations with inclinations of 20, 40, and 60°, the dotted lines are for $m = +1, -1$ combinations with the same inclinations, and the dot/dash line represents $m = 1, 1$ and $m = -1, -1$, and $m = 0, \pm 1$ combinations. Error bars are 1σ formal errors.

Our analysis of GD358's combination frequencies is complex. We find a very tenuous identification for the 1234 μHz mode of $m = \pm 1$, requiring the remaining high-k modes' largest component to be the remaining value. We find no clear m identifications for the components of $k = 12$. This mode is clearly more complex than the simple multiplet structure expected in the limit of slow rotation.

There are multiple reasons why GD358's combination frequencies defy simple interpretation. First, this star simply has too many principal modes simultaneously excited to large amplitude. The cross-talk between them is large, and the perturbative treatment of Wu (2001) may not be valid. Second, both Wu (2001) and Yeates et al. (2005) assume the intrinsic amplitudes are the same for every component in a multiplet, and this may simply not be the case for GD358. Third, the theoretical value of R_c relies on correct identification of l and m, although in simpler cases, as in Yeates et al. (2005), it can be used as a mode identification technique. While we are fairly certain that GD358's pulsations are $l = 1$, the assumption of a classical triplet split by rotation is not valid for GD358's high-k modes. Finally, we raise a possibility suggested by the $k = 9$ and 8 components and their harmonics: to first order, the $m = 0$ components sample the radial direction, and the $m = \pm 1$ components sample azimuthal direction. Components of the same mode have the same inclination, so cancellation effects should be the same. The $k = 9$ and 8 multiplet amplitudes and presence/absence of harmonics argue that something is interrupting the azimuthal symmetry of GD358. It is possible that the pulsations do not all share the same inclination, in which case they would not combine as expected by Wu (2001). The oblique pulsator model is well known, especially in the case of roAp stars. For example, Bigot & Dziembowski (2002) show that the main mode of HR 3831, a pulsating roAp star, departs from alignment with the magnetic axis. GD358's combinations are trying to tell us something important about the pulsation geometry, but we do not yet understand how to interpret it.

While the general frequencies of the high-k multiplets agree with the identifications of W94 and K03, the 2006 multiplets themselves are complex, and cannot be explained by simply invoking rotation using standard theory and simple geometric viewing arguments. Except for the $k = 9$ and $k = 8$ modes, we do not find triplet structure as reported in W94 and cannot provide m identifications. The facts that the multiplets do change and the 2006 combinations do not conform to theoretical predictions leads us to expand our investigation to include archival observations of GD358. In the following, we will examine the structure of GD358's multiplets in detail over timescales of years.

5. MULTIPLET STRUCTURE CHANGE AND COMPLEXITY

Each multiplet in GD358's FT should represent a quantized g-mode pulsation, described theoretically by a spherical harmonic of index l and overtone k, which has been split into multiple components ($2l + 1$) by the star's rotation. As component frequencies are determined by the star's structure and rotation rate, we would expect the multiplet structure to remain stable over long time periods. The classic example is the DO pulsator PG1159-035, which exhibits prototypical triplets, cor-

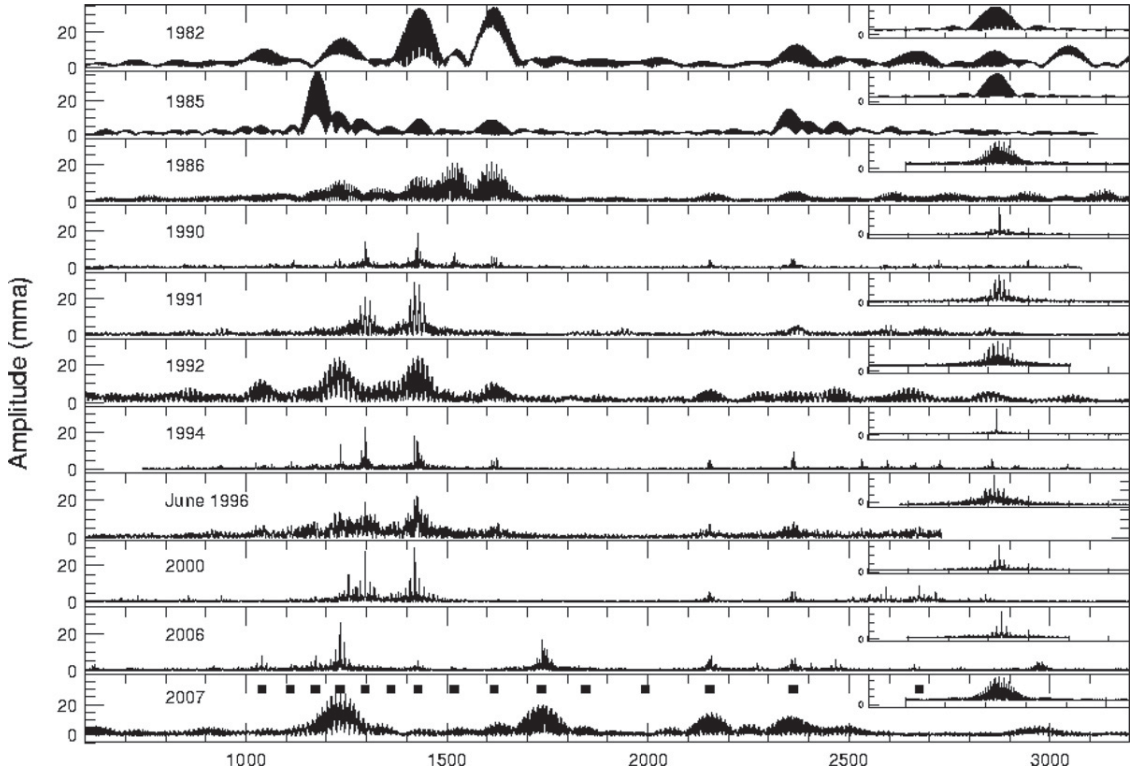

Figure 10. FTs of GD358 from 1982 to 2007, with each spectral window given in the upper right corner of each panel. Each panel spans 2800 μHz. The filled squares in the bottom panel mark the predicted locations of GD358's pulsation modes ($l = 1$). GD358 changes its distribution of amplitudes of the excited modes, but the modes are consistently in the same general locations. High-k modes exhibit the largest variation in amplitude. Note the appearance of $k = 12$ in 2006.

responding to $l = 1$, and quintuplets, corresponding to $l = 2$ (see Figures 5 and 6 in Winget et al. 1991).

W94 based the first asteroseismological analysis of GD358 on the identified modes and multiplet structure in the 1990 data set. The frequency splittings within the 1990 multiplets range from 3.5 to 6.5 μHz, vary as a function of the radial number k, and are not always symmetric with respect to the central frequency. W94 interpreted the trend with k as differential rotation within the star, and used the splitting asymmetry to determine an average magnetic field strength of 1300 $\pm$ 300 G. If we assume that GD358's structure is constant in time, then we would expect to find similar multiplet structure in other observing seasons, including XCOV25.

Figure 10 displays FTs for seasons spanning GD358's 1982 discovery to 2007. The 1990 (W94), 1991, 1994, 2000 (K03), and 2006 FTs are from WET runs, while the other FTs are single site, obtained from McDonald Observatory or Mt. Cuba Observatory (2007 season). The large amplitude peaks are consistently found between 1000 and 1800 μHz, and individual modes are close to predicted values for $l = 1$ (the filled boxes in the last panel of Figure 10 marks the periods of the best fit model from Metcalfe et al. 2003). Using the 2006 data set, we calculated an average period spacing of 38.77 s using the measured periods of the lowest and highest k modes. This is consistent with results from previous observations (Table 4), demonstrating that GD358's general internal structure is largely unchanged.

We extracted the $k = 8$, 9, 15, and 17 multiplets from the 1990, 1991, 1992, 1994, 1996, 2000, and 2006 seasons, using the techniques discussed in Section 3. The multiplets are plotted in Figures 11, 12, 13, and 14. The low-order $k = 8$ and 9 modes consistently display the triplet structure expected for $l = 1$ g-modes in the limit of slow rotation (Figures 11 and 12). While the component amplitudes vary from season to season, the frequencies and splitting within the triplets remain roughly the same. The story changes for the $k = 15$ and 17 multiplets (Figures 13 and 14). The multiplet structure of these modes exhibit dramatic changes from year to year. If rotational splitting is the dominant mechanism producing the high-k multiplets, we expect them to share the same splitting with other detected modes within the same data set. We have shown that this is not the case (Figure 7).

We now turn our attention to the frequency stability of the $k = 8$, 9, 15, and 17 mode components. Both W94 and K03 report small but significant frequency changes within the identified multiplets, and Figures 11–14 support this finding. For $k = 8$, 9, and 17 we select the component identified as $m = 0$ in W94. For $k = 15$, however, we choose $m = -1$ since a peak was present near this frequency more often than the $m = 0$ frequency. Figure 15 plots the frequencies of the identified peaks versus time. In all cases, the frequencies shift by several times the statistical errors, where the average error for all the data sets is $\sigma = 0.06$ μHz. The high-k frequencies wander by over 30 σ, much more than the detected 8 σ changes for $k = 8$ and 9. While these variations are small, they point to very definite changes in the g-mode propagation cavity in this star.

Summarizing our results, we find a clear difference between high- and low-k modes. The high-k multiplets are highly variable in amplitude and frequency, and exhibit large changes in multiplet structure. The multiplets within these modes appear to be almost randomly present with the $m = 0$ component not necessarily preferred. The low-k modes typically show a stable triplet structure, but the amplitudes of the components are moderately variable. All the multiplets exhibit significant

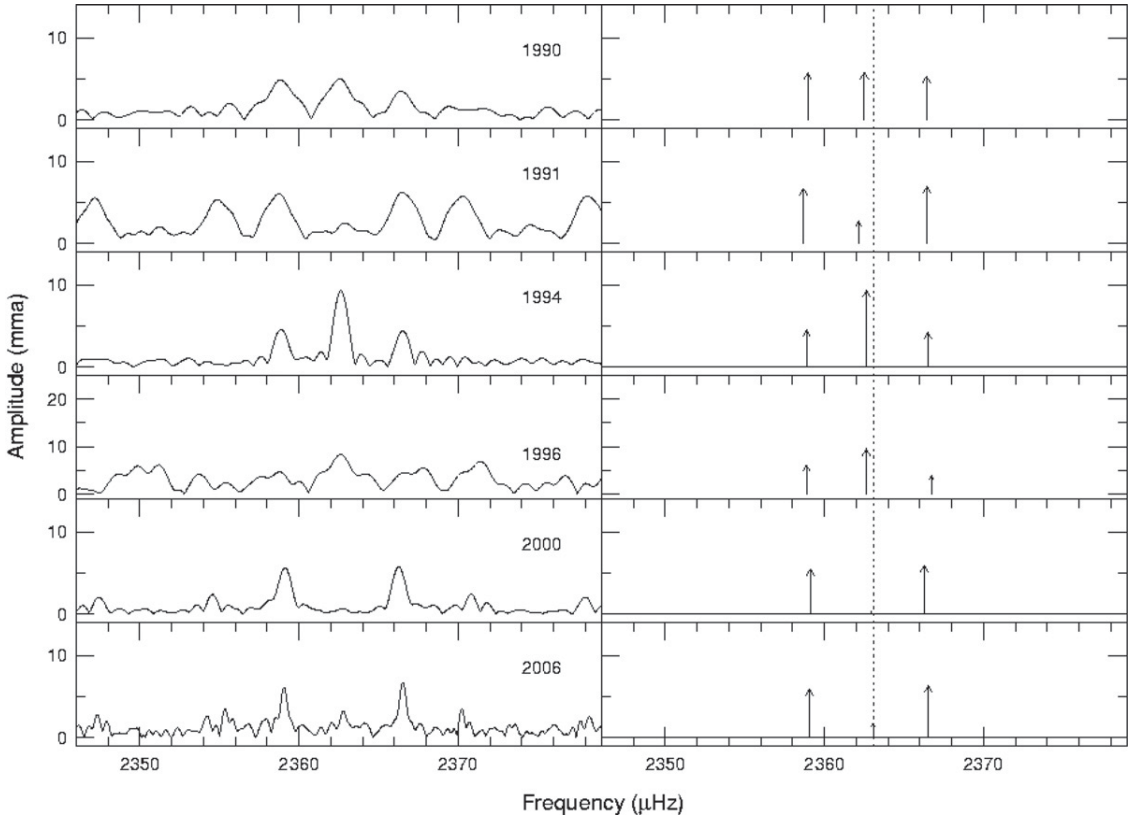

Figure 11. Multiplet structure associated with the $k = 8$ mode in GD358 from different observing seasons. The left panels plot the original FTs, and the right panels give the prewhitening results. The largest 1σ frequency error bar is 0.06 μHz (1996). Each panel spans 18 μHz. The horizontal line through each right panel gives the noise level for that season, and the dotted line marks the 2006 detected frequency.

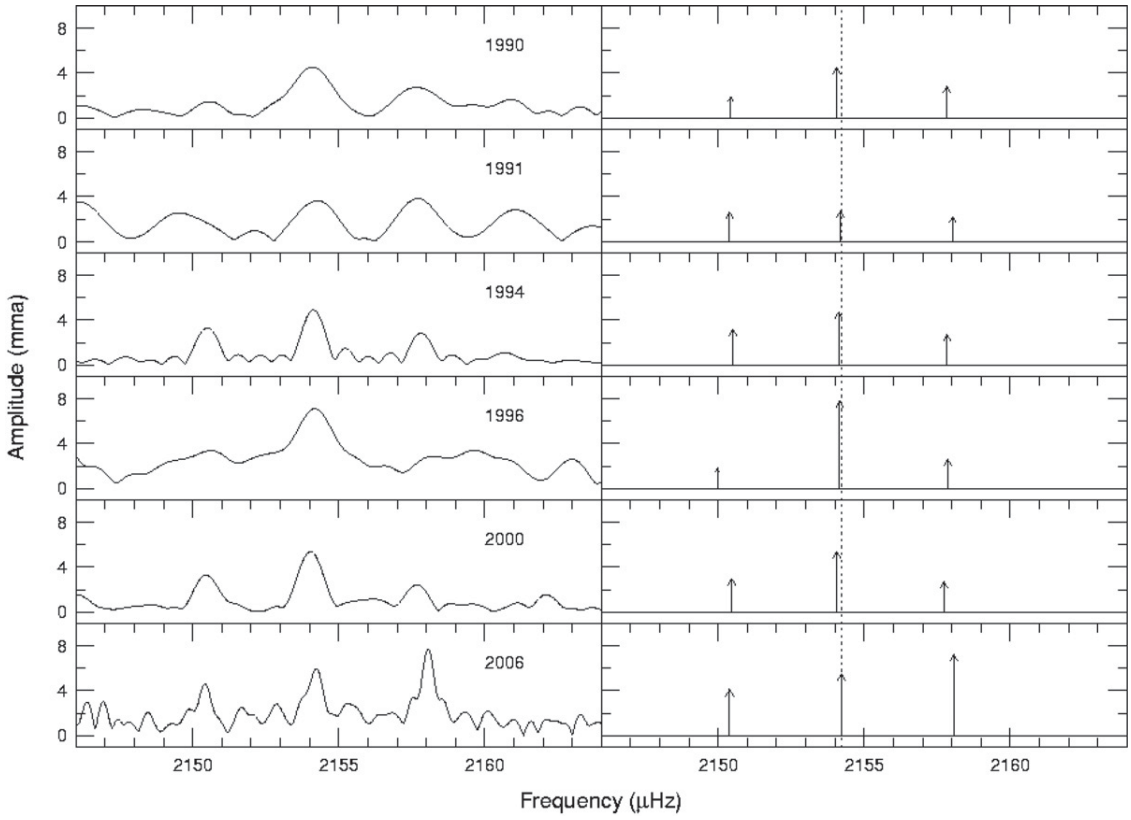

Figure 12. Multiplet structure associated with the $k = 9$ mode in GD358 from different observing seasons. The left panels plot the original FTs, and the right panels give the prewhitening results. The largest 1σ frequency error bar is 0.06 μHz (1996). Each panel spans 18 μHz. The horizontal line through each right panel gives the noise level for that season, and the dotted line marks the 2006 detected frequency.

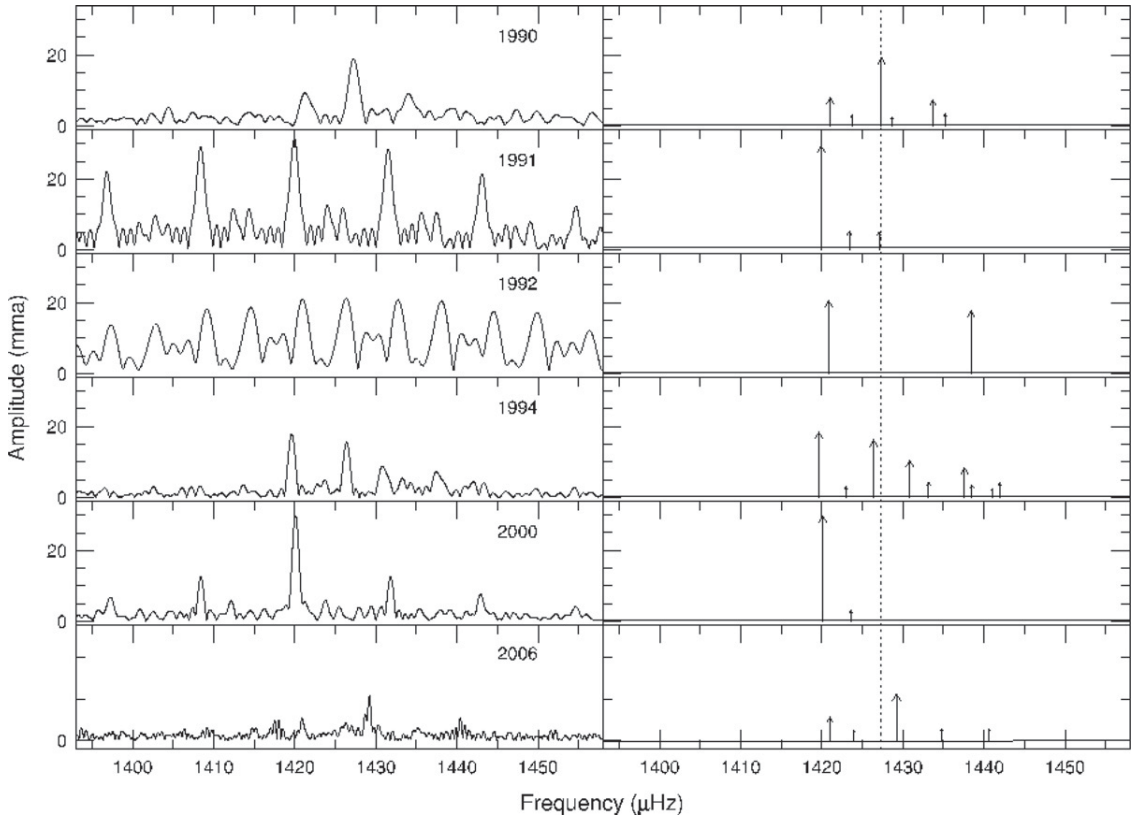

Figure 13. Multiplet structure associated with the $k = 15$ mode in GD358 from different observing seasons. The left panels plot the original FTs, and the right panels give the prewhitening results. The largest 1σ frequency error bar is 0.06 μHz (1992). Each panel spans 65 μHz. The horizontal line through each right panel gives the noise level for that season, and the dotted line marks the 1990 detected frequency.

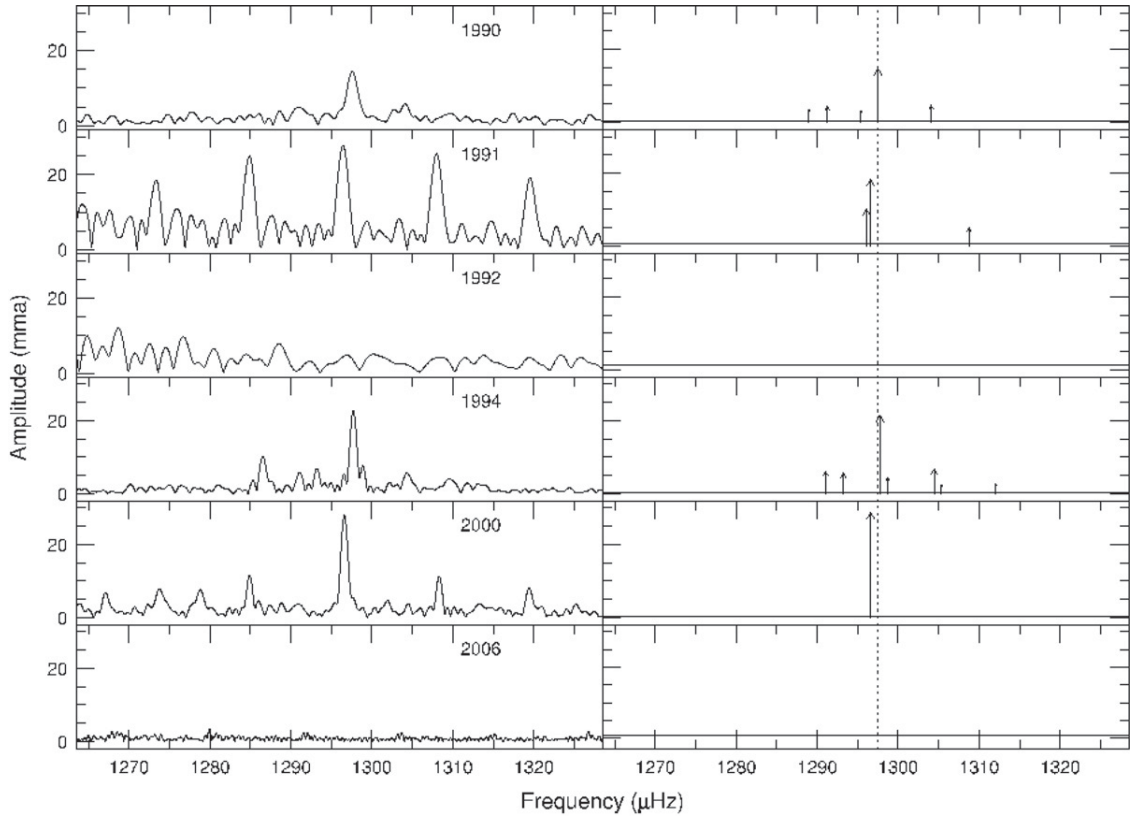

Figure 14. Multiplet structure associated with the $k = 17$ mode in GD358 spanning 1990 to 2006. The left panels present the yearly FTs, and the right panels represent the prewhitening results. The largest 1σ frequency error bar is 0.06 μHz (1992). Each panel spans 65 μHz. The horizontal line through each right panel gives the noise level for that season, and the dotted line marks the 1990 detected frequency. The 2006 peak is difficult to detect due to the *y* scale.

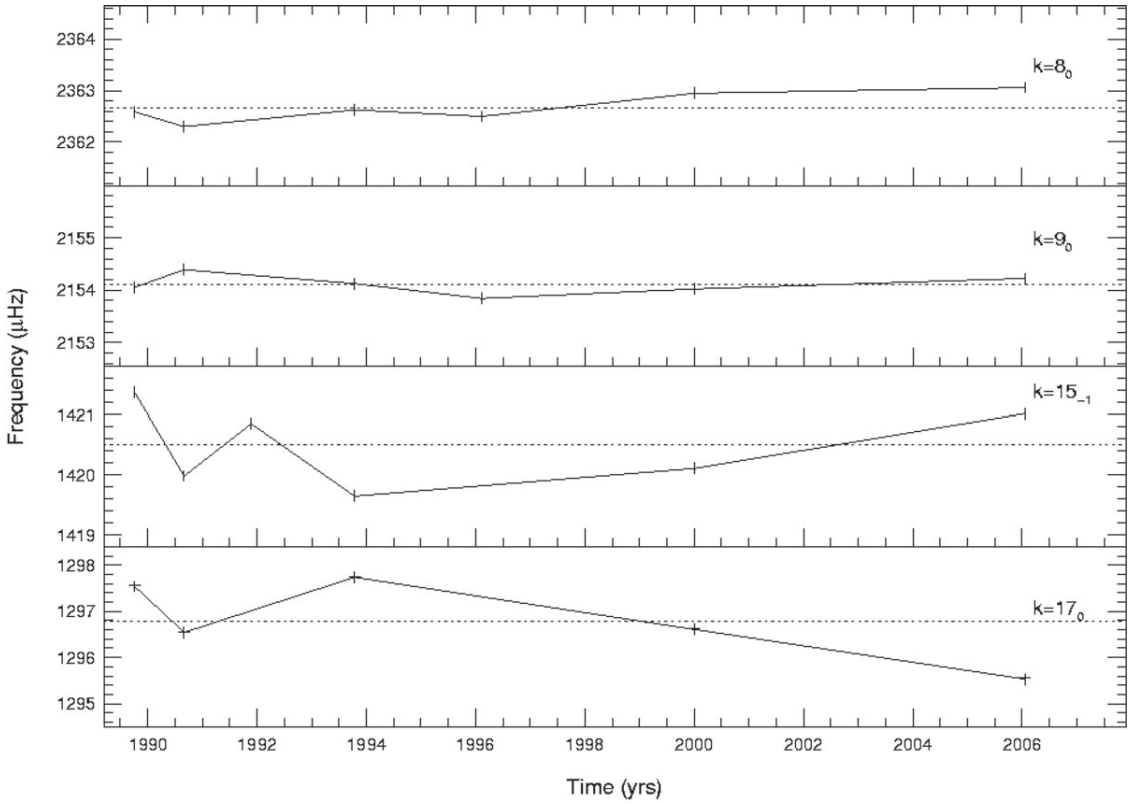

Figure 15. Frequency of the largest component for the $k = 17$, 15, 9, and 8 modes. For $k = 17$, 9, and 8, the $m = 0$ component was selected. For $k = 15$, the $m = -1$ mode was detected more often at larger amplitude. While all modes exhibit some variation in frequency, the high-k modes wander by over 30 σ. The dotted lines mark the reported 1990 frequencies (W94).

wanderings in frequency, with the frequency changes observed in the high-k modes being much larger than those seen in the low-k modes.

6. IMPLICATIONS FOR GD358

GD358's 2006 FT contains 27 independent frequencies distributed in 10 excited modes. The locations of the modes agree with previous observations and predicted values for $l = 1$ g-mode pulsations. The average period spacing $\Delta P_{\rm av}$, calculated using the lowest-k and highest-k modes, is identical from 1990 to 2006 (Table 4). As $\Delta P_{\rm av}$ is fixed by stellar mass and temperature, GD358's basic physical properties have remained unchanged over a timescale of years, as expected. The changes we observe in GD358's pulsation spectra and multiplet structure are not due to gross changes in structure or temperature.

We have shown that the standard model of a pulsating white dwarf in the limit of slow rotation cannot adequately explain the observations of GD358's multiplet structure and behavior. The fine structure of the high-k modes is inconsistent with the expectations of slow rotational splitting, the amplitudes of multiplet components for all ks cannot be explained using simple viewing arguments, and the observed frequency variations imply changes in the g-mode propagation medium that are much more rapid than expected from evolutionary changes.

The qualitative behavior of the low-k and high-k modes can be explained in the context of a general model. g-modes are standing waves of buoyancy in a spherical cavity, and they are thought of as superpositions of traveling waves bouncing back and forth between an inner and an outer turning point. These turning points depend on the mode's period: short period (low-k) modes have deeper outer turning points than long period (high-k) modes, so high-k modes sample the outer regions of the star more than low-k modes. If we introduce an additional, non-spherical structure in the star's outer layers, due to magnetic fields or convection, for example, the effect should be much larger on the high-k modes. In effect, GD358 is telling us where this perturbation to its structure must be, but it is still incumbent upon us to diagnose the actual cause.

We do find a clear difference in the photometric behavior of GD358's high- and low-k modes, leading us to consider a connection between the outer layers and its pulsation changes. The following discussion requires that we draw into the mix a remarkable sequence of events that occurred over ≈30 days in 1996. We follow Castanheira et al. (2005) in calling the event the *sforzando*. In classical music, *sforzando* is an abrupt change in the character of music, usually accompanied by an increase in volume. We begin with a description of the *sforzando*. We will examine the implications and connections between our asteroseismic results, the *sforzando* and two possibilities that may affect GD358's photometric behavior: a surface magnetic field and the convection zone.

6.1. GD358 in 1996

In 1996 June, GD358's light curve (third panel, Figure 16) was typically nonlinear, with a dominant frequency of 1297 μHz corresponding to $k = 17$, and a peak to peak intensity variation of ≈15%. The $k = 9$ and 8 modes were present with amplitudes of 8 and 9 mma, respectively. On August 10 (suh-0055, second panel Figure 16), the light curve was again typical, with a 20% peak to peak intensity varia-

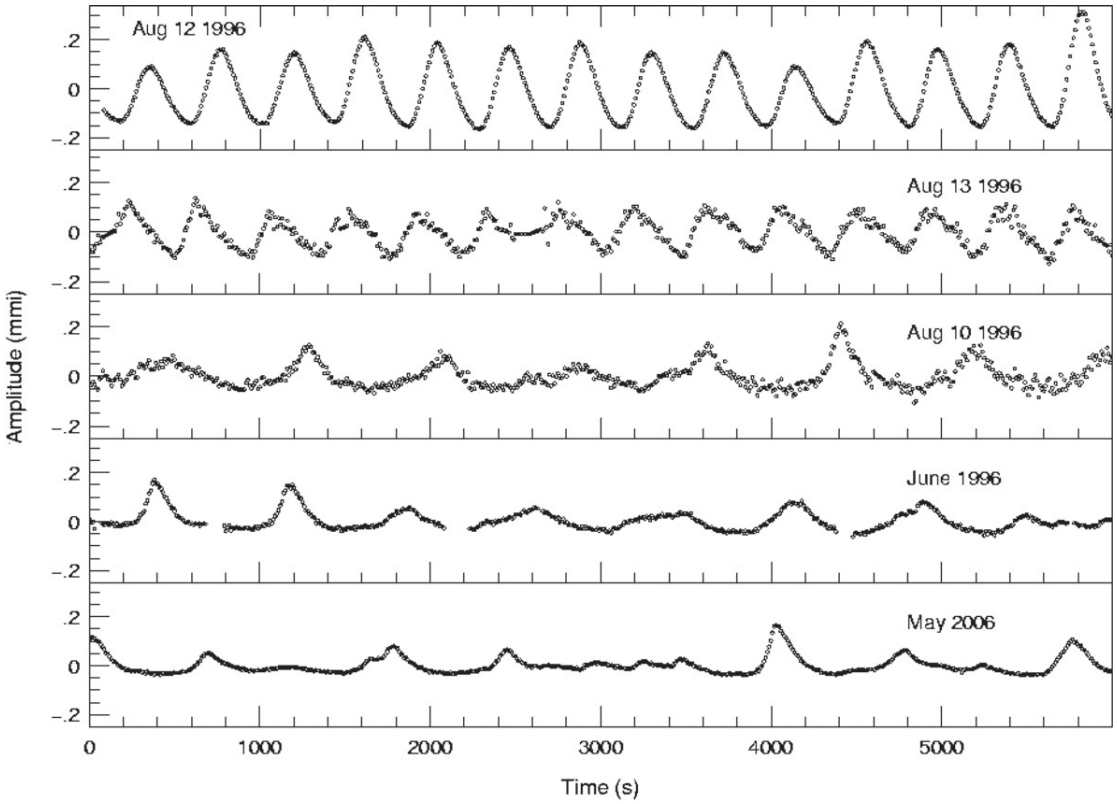

Figure 16. Light curve of GD358 on August 12 (an-0034, top panel) and August 13 (suh-056, second panel), during the 1996 *sforzando*. On 1996 August 10 (suh-0055, third panel), the light curve was typically nonlinear, as it was in 1996 June (fourth panel), and 2006 May (bottom panel).

tion, and main frequencies consistent with previously observed high-k modes. The $k = 9$ and 8 modes had upper amplitude limits of 8 mma. On August 12, 27 hr later, GD358 exhibited completely altered pulsation characteristics (an-0034, top panel Figure 16). The lightcurve was remarkably sinusoidal, with an increased peak to peak intensity variation of ≈50%. The $k = 8$ mode dominated the lightcurve with a amplitude of 180 mma, the highest ever observed for GD358. The $k = 9$ mode was also present, with an amplitude of ≈20 mma. The high-k modes, dominant 27 hr prior, had upper detection limits of 7 mma. Over the next 24 hr, the $k = 8$ mode began to decrease in amplitude (Figure 17). Between Aug 13 and 14, $k = 9$ grew in amplitude as $k = 8$ decreased, reaching a maximum of ≈57 mma, and then began to decrease as the $k = 8$ mode continued to dissipate. By August 16, a mere 96 hr after the *sforzando* began, GD358 was an atypically low amplitude pulsator, with power detected in the $k = 9$ and 8 modes at amplitudes of ≈7 mma, and upper limits of less than 5 mma for the high-k modes. By September 10, less than a month after the start of the *sforzando*, the high-k modes had reappeared, with the dominant mode at ≈1085 μHz at an amplitude of 29 mma.

The only observations we have during the maximum *sforzando* are the PMT photometry (Table 5) observations. Differential photometry does not measure standard stars. However, we can calculate the ratio between the average counts from GD358 and its comparison star, assuming the same comparison star was used each night, and accounting for factors such as extinction and sky variation. In the following, we calculate ratios based on sky subtracted counts obtained within ±1.5 hr of the zenith. We focus on the McDonald 2.1 m runs an-0034, an-0036, an-0038, and an-0040. The ratio between GD358 and the comparison star decreased from 1.23 during the height of the *sforzando* (an-0034, Aug 12) to 1.01 on Aug 15 (an-0040). We also examined observations from Mt. Suhora (Table 5). Suh-0055 was obtained ≈24 hr before the *sforzando*, and the ratio between GD358 and the comparison star was 0.11. Suh-0056 took place 18 hr after the *sforzando* maximum but before the pulsations had completely decayed. For suh-0056, the ratio between GD358 and the comparison star increased to 0.16. For the remaining Mt. Suhora observations, obtained during the

Table 5
GD358 1996 August

Run	CH1 GD358	CH2 Comp	CH1/CH2	Time (BJED)	Date	Length (hr)
McDonald						
an-0034	343727	279268	1.23	2450307.6170160	Aug 12	4.7
an-0036	308308	290898	1.06	2450308.6309639	Aug 13	3.2
an-0038	269937	251923	1.07	2450309.6362315	Aug 14	3.5
an-0040	250813	248479	1.01	2450310.6294625	Aug 15	3.5
Mt. Suhora						
suh-0055	12786	114746	0.11	2450306.4793479	Aug 10	4.8
suh-0056	29408	181597	0.16	2450308.3533174	Aug 12	3.0
suh-0057	20271	158035	0.12	2450309.3015281	Aug 13	5.9
suh-0058	15974	130814	0.12	2450310.4729899	Aug 14	1.0
suh-0059	15434	127672	0.12	2450314.3776294	Aug 18	3.0

Notes. Observations made with McDonald 2.1 m. The same comparison star was used in each instance.

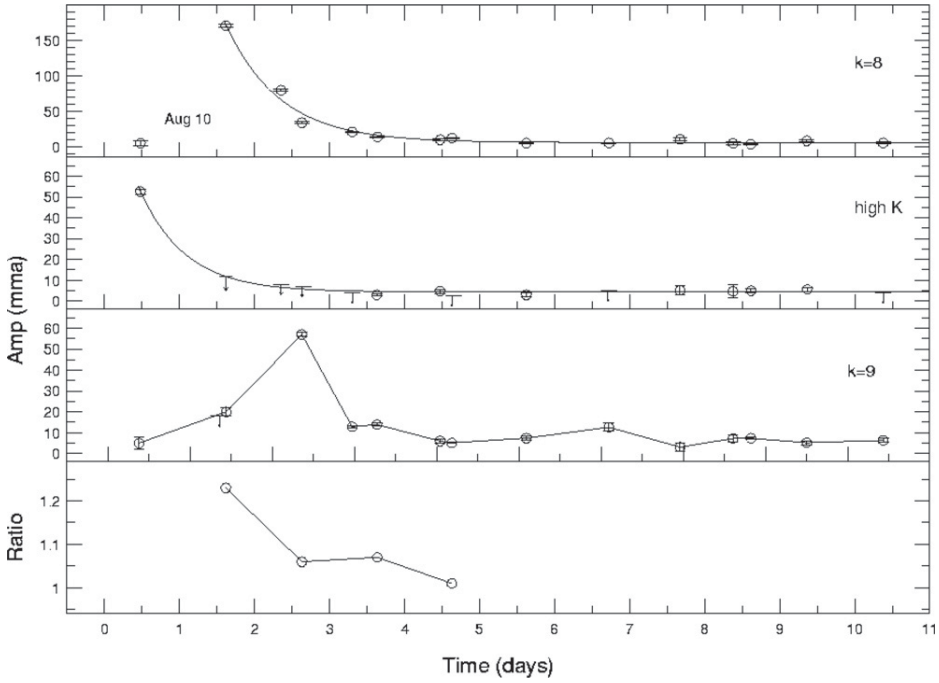

Figure 17. The first three panels give the measured amplitudes for $k = 8$ (top panel), the high-k modes, and $k = 9$ during the 1996 *sforzando*. The solid lines give fits using a simple exponential decay model. For $k = 8$ and the high-k modes, the damping time was 1.4 days. Note that the "high-k" points do not correspond to any particular k value, but give the highest amplitude (or upper limit) between 1000 and 1500 μHz at that time. The $k = 9$ mode grew in amplitude as $k = 8$ decayed. The last panel gives the ratio between GD358 and its comparison star from the McDonald 2.1 m photometry. Note the change in y-axis units.

following days, the ratio between GD358 and the comparison star decreased to 0.12. Observation logbooks at Mt. Suhora demonstrate that the same comparison star, but not the same one used at McDonald, was used each night (Zola 2008). While we cannot pin down any exact numbers due to the nature of differential photometry, the observations of GD358 are consistent with a flux increase in the observed bandpass during the maximum *sforzando*.

6.2. Convection and GD358

The onset of convection goes hand in hand with the initiation of pulsation in both hydrogen and helium white dwarfs (Brickhill 1991; Wu 2000; Montgomery 2005). A primary goal of XCOV25 is to use GD358's nonlinear lightcurve to characterize its convection zone, improving the empirical underpinnings of convective heat transport theory. Our asteroseismological investigation points to evidence that something in the star's outer surface layers is influencing its pulsation modes. The convection zone lies in the outermost regions of GD358, so we are led to consider the relationship between the star's convection zone and its photometric behavior, both typical and during the *sforzando*.

In general, theoretical studies of convective energy transport are based on the mixing length theory (MLT) (Bohm-Vitense 1958). Originally intended to depict turbulent flows in engineering situations, MLT enjoys success in describing stellar convection (Li & Yang 2007). It remains, however, an incomplete model with unresolved problems. The actual mixing length is not provided by the theory itself, but is defined as (αH_p), where H_p is the pressure scale height, and α is an adjustable variable. This adjustable parameter undermines the ability of theoretical models to make useful predictions. Advances in convection theory include stellar turbulent convection (Canuto & Mazzitelli 1991; Canuto et al. 1996), which establishes a full range of turbulent eddy sizes. Work is currently underway employing helioseismology to compare MLT and turbulent convection models (Li & Yang 2007). Our work with convective light curve fitting will also provide important tests for convection theory.

Physical conditions in white dwarf atmospheres differ by orders of magnitude from those in envelopes of main sequence stars like the Sun. For GD358, models indicate that the convection zone is narrow, with a turnover time of ≈1 second and a thermal relaxation timescale of ≈300 s (Montgomery 2008). The pressure scale height is small, limiting the vertical height of the convective elements. Montgomery & Kupka (2004), employing an extension of stellar turbulent convection, calculate that 40–60% of GD358's flux is carried by convection, depending on the adopted effective temperature.

Convective lightcurve fitting is based on the assumption that the convection zone, by varying its depth in response to the pulsations, is responsible for the nonlinearities typically observed in GD358's lightcurves (Montgomery 2005). During the *sforzando*, within an interval of 27 hr, GD358's lightcurve became sinusoidal, arguing that the convection zone was inhibited, at least as sampled by the $k = 8$ mode. For example, if this large amplitude mode was the $m = 0$ member of the triplet, then its brightness variations would be predominantly at the poles and not the equator. Thus, all that is required to produce a sinusoidal lightcurve is a mechanism to inhibit convection near the poles.

How could convection in any star be decreased on such short timescales? The obvious method, but not necessarily the most physical, is to raise GD358's effective temperature, forcing it to the blue edge of the instability strip, and decreasing convection. Such a temperature increase has the observable consequence of increasing the stellar flux. A flux increase of 20% in our effective photometric bandpass would produce an equivalent change in the bolometric flux of ≈40%, corresponding to a temperature change of ≈2200 K. The *sforzando* photometry is consistent

with such an increase in flux, and Weidner & Koester (2003) find that $T_{eff} \approx 27,000$ K is required to simulate GD358's light curve during the maximum *sforzando*. Castanheira et al. (2005) use FOS spectroscopy of GD358 obtained on 1996 August 16 to determine $T_{eff} = 23900 \pm 1100$ K, a number not inconsistent with previous observations (Beauchamp et al. 1999). However, the FOS spectra were acquired after the pulsations had greatly decreased in amplitude (Figures 16 and 17). It is possible that GD358 had cooled by this point. Recent theoretical evidence also indicates that simply "turning off" convection would have minimal observable effects on GD358's spectrum (Koester 2008).

The connection between convection and pulsation during the *sforzando* may also depend on the origin of the event. Was the *sforzando* a short-term change, such as a collision, or a more global event intrinsic to GD358? The growth and dissipation of modes during the *sforzando* could be connected to pulsation growth timescales, or may be governed by a completely different mechanism. Pulsation theory predicts that growth rates for high-k modes are much larger than for low-k modes. This simply means that high-k modes are easier to excite and have growth times (and decay times) of days rather than years (Goldreich & Wu 1999). This makes sense for GD358, where we typically find the high-k modes to be much more unstable in amplitude over time than $k = 9$ and 8 (Figure 10). Figure 17 plots the amplitudes for the $k = 8$, $k = 9$, and "high-k" modes during the *sforzando*. We note that the "high-k" points do not correspond to any particular k value, but give the highest amplitude (or upper limit) between 1000 and 1500 μHz. We fit the observed amplitudes for $k = 8$ and the high ks with a simple exponential decay model $A(t) = A_0 e^{-t/\tau_d} + c$, where A(t) is the amplitude at time t and τ_d is the damping constant. Our fits give a damping timescale of $\tau_d = 1.5 \pm 0.2$ days for both the $k = 8$ mode and the high ks. The $k = 9$ mode, which actually grew in amplitude later, as $k = 8$ decayed, has an upper limit of $\tau_{9^d} < 1.1$ days. We only have a few points measuring the growth timescale (τ_g) of $k = 8$ and 9, so we place an upper limits for $k = 8$ of $\tau_{8^g} \leqslant 1.2$ days. For $k = 9$, we find an upper limit of $\tau_{9^g} \leqslant 2.2$ days. These timescales are all roughly equivalent, are all much longer than the dynamical timescale, and not distributed as predicted by theoretical pulsation growth rates. The results for $k = 9$ and 8 are much shorter than the expected pulsation damping timescale of about two months (Montgomery 2008a), arguing that the source of the *sforzando* was capable of interacting with the pulsations to produce changes on faster timescales than theoretical growth rates.

Our purpose in entering this discussion of the *sforzando* was to provide insight into connections between convection and pulsation in GD358. We find evidence that convection diminished during the *sforzando*. The decreased convection was accompanied by the rapid disappearance of GD358's high-k modes and the transfer of energy to the $k = 8$ and 9 modes. The photometry is consistent with a temperature increase, which would inhibit convection. The sudden transfer of energy from the high-k modes to $k = 9$ and 8 argues that a mechanical (radial or azimuthal) or thermal structural change altered GD358's outer layers, modifying mode selection. We find that the growth/damping timescales during the *sforzando* for the $k = 9$ and 8 modes do not agree with the expectations of pulsation theory, and may be governed by a completely different mechanism.

Magnetic fields have long been known to be capable of inhibiting convection. For example, localized fields associated with sunspots in the Sun are observed to inhibit convection in the surrounding photosphere (Biermann 1941; Houdek et al. 2001). Winget (2008) estimates that the magnetic decay time at the base of the convection zone is ≈3 days. In the next section, we investigate the possible implications of magnetic fields on GD358 and its pulsations.

6.3. Magnetic Fields

Our current understanding of magnetic fields in stars like the Sun invokes the dynamo mechanism, which is believed to function in the narrow region where rotation changes from the latitudinal rotation of the outer convective layers to spherical rotation in the radiative zone (Morin et al. 2008). The solar magnetic field consists of small, rapidly evolving magnetic elements displaying large scale organization, with a cycle time of 22 years during which the polarity of the field switches. Localized fields, with strengths hundreds of times stronger than the global field, exert non-negligible forces on charged particles, influencing convective motion. Solar pulsations are observed to vary in frequency with the solar cycle in these regions (Schunker & Cally 2006). Although the exact mechanism is uncertain, the frequency shifts are interpreted as representing change in the Sun's internal structure or driving (Woodward & Noyes 1985; Kuhn 1998; Houdek et al. 2001).

A pulsating white dwarf represents an extreme environment. The atmosphere and the convection zone are thin, the surface gravity orders of magnitude higher, and differential rotation may or may not play a role (Kawaler et al. 1999). The magnetic field in a typical white dwarf is confined to the nondegenerate outer layers. The field may dominate near the surface, but deeper in the atmosphere, gas pressure will prevail. Drawing an analogy with the Sun, a surface magnetic field in GD358 probably has an associated cycle time similar to the solar cycle. Hansen et al. (1977) and Jones et al. (1989) discuss this topic from a theoretical perspective, predicting cycle times ranging from two to six years.

What are the observable consequences of a magnetic field on white dwarf pulsations? Jones et al. (1989) find that, in the presence of a weak field, defined as strong enough to perturb but not dominate mass motions, multiplet frequencies are increased with respect to the central mode in a manner proportional to m^2. The $m = 0$ mode is also shifted, unlike the case for rotation. Each g-mode pulsation samples the magnetic field at a different depth. A logical expectation is that, for low-k modes with reflection points below the convection zone, we can treat the magnetic field as a perturbation, while for high-k modes such a treatment is not valid.

Our best candidates to investigate the influence of a magnetic field on multiplet structure are GD358's $k = 9$ and 8 modes. These two modes are consistent with rotationally split triplets and we can examine their multiplet structure in detail over 16 years of observations (Figures 18 and 19). From 1990 to 2006, $k = 9$ had an average multiplet width of 7.7 ± 0.1 μHz, while $k = 8$ is similar, at 7.5 ± 0.1 μHz. Figures 18 and 19 show that the complete multiplet width and the splittings with respect to the central mode wander up to 0.5 μHz from the average values. Both Figures 18 and 19 reveal a dramatic change during the *sforzando*. In June 1996, both multiplets increased in total width by ≈1μHz. Prior to August 1996, the retrograde splitting (0, −1) for $k = 8$ was consistently smaller by ≈0.2 μHz than the prograde splitting (0, +1). After 1996 August, the retrograde splitting became consistently larger by ≈0.5 μHz than the prograde splitting and has remained so through 2007, at the

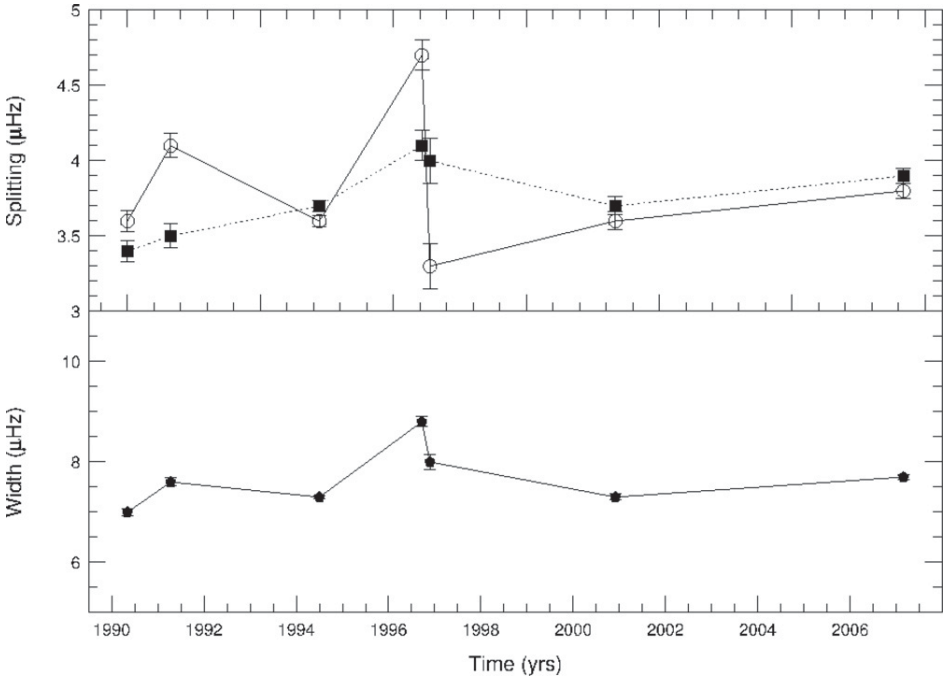

Figure 18. Multiplet structure within the $k = 9$ multiplet. The x-axis is time in years, and the y-axis is in μHz. The bottom panel plots the width of the entire multiplet over time. The top panel examines the $m = 0, +1$ (dotted line) and $m = 0, -1$ (solid line).

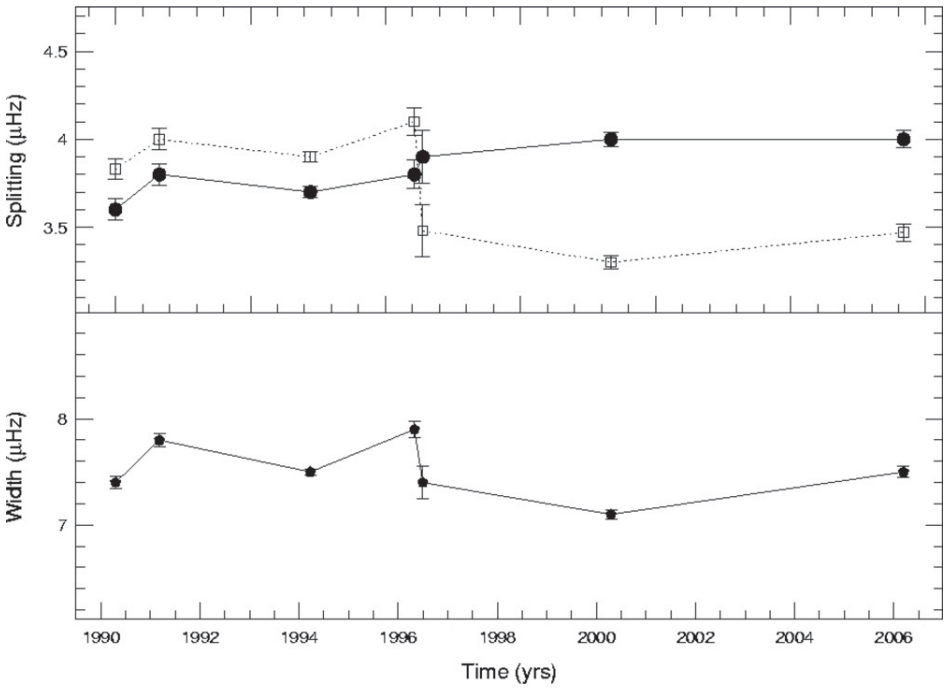

Figure 19. Multiplet structure with $k = 8$ multiplet. The x-axis is time in years, and the y-axis is in μHz. The bottom panel plots the width of the entire multiplet over time. The top panel examines the $m = 0, +1$ (dotted line) and $m = 0, -1$ (solid line).

resolution of our observations. The case is not so straightforward for $k = 9$, but this mode clearly shows a large change in 1996, especially for the $(0, -1)$ splitting (Figure 18). In the previous section, we questioned whether the *sforzando* was a short-term event or a global, enduring change. This analysis of $k = 9$ and 8 points toward a long-term change in GD358's resonance cavity. The changes we observe in the multiplet structure could be explained by a change in magnetic fields.

A magnetic field also introduces an additional symmetry axis. Our analysis of GD358's harmonics and combination frequencies hints that something is disrupting its azimuthal symmetry. It is conceivable that high-k modes would align more or less with the magnetic field, while the low-k modes align with the rotation axis. Wu (2001) & Yeates et al. (2005) do not explore the possibility of multiple axes or the effects of a magnetic field on nonlinear mixing by the convection zone. Future work could

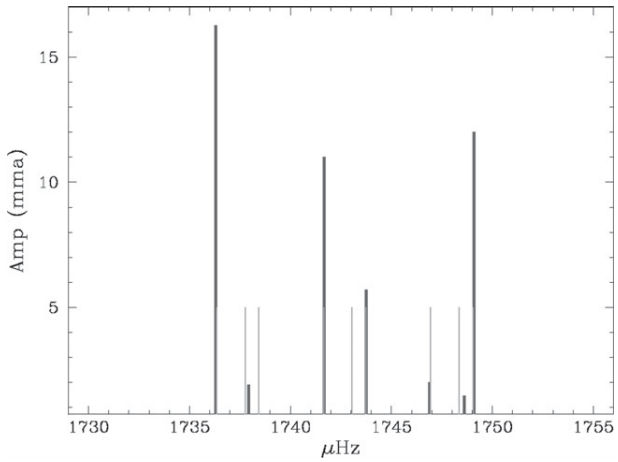

Figure 20. Fit to k=12 components assuming the dominant splitting mechanism is a magnetic field using the model of Unno et al. (1979) rather than rotation. The black lines are the observed multiplet components, including several below our detection limits that are not listed in Table 2. The light gray lines are the theoretical predictions. Theoretical predictions overlap the four largest amplitude peaks, although they are difficult to distinguish in the figure.

explain why GD358's modes do not combine as expected by simple theory.

The presence of the $k = 12$ mode offers a final hint of a possible surface magnetic field. The second largest mode in the 2006 FT, $k = 12$ appears in a region that is normally devoid of significant power. If, for this mode, the magnetic field can no longer be treated as a perturbation, we would expect a multiplet with $(2l + 1)^2$ components, as opposed to the three expected from rotation (Unno et al. 1979). For $l = 1$, this corresponds to nine magnetic components. We do find six peaks above our 4σ limit, with three additional peaks slightly just our criteria. Using the magnetic model of Unno et al. (1979), we are able to match the frequencies of the $k = 12$ mode components, but not the amplitudes (Figure 20).

7. SUMMARY AND CONCLUSIONS

GD358 is the best studied of the DB pulsators, yet our work shows that this object is by no means completely understood. The 2006 XCOV25 observations were obtained with the goal of using GD358's nonlinear lightcurve to characterize its convection zone, but our initial asteroseimological analysis of the data set reveals a great deal of interesting information about GD358's pulsational behavior. Our investigation began with an analysis of GD358's 2006 XCOV25 FT. We explored the identified modes, combination frequencies, and multiplet structure. Difficulties in identifying the m components of the 2006 mode multiplets, both directly and indirectly using the combination frequencies, lead us to examine the multiplet structure in detail over time. Our investigation expanded to include observations of GD358 over the 24 years since its discovery, focusing on the multiplet structure, frequency stability, and photometric behavior of GD358. We summarize our results concerning GD358's pulsation properties:

1. The 2006 FT contains 27 independent frequencies distributed in 10 modes ($k = 21$, 19, 18, 17, 15, 14, 12, 11, 9, and 8). The dominant frequency is at 1234 μHz ($k = 18$) with an amplitude of 24 mma.
2. We find significant power at $k = 12$, a region of the FT previously devoid of significant power.
3. The frequency location of each mode in the 2006 FT is consistent with previous observations and theoretical predictions, assuming $l = 1$.
4. The $k = 9$ and 8 modes exhibit triplets in agreement with theoretical predictions for $l = 1$ in the limit of slow rotation. The amplitudes and frequencies of the components exhibit some variability over time, but much less than the high-k modes.
5. Our analysis of GD358's high-k multiplets over time reveal that they are variable in multiplet structure, amplitude, and frequency. The variability and complexity of the high-k multiplets cannot be interpreted simply as $l = 1$ modes in the limit of slow rotation.
6. We cannot provide m identifications for most of the multiplet components in the 2006 FT, with the exception of $k = 9$ and 8.
7. The 2006 FT contains a rich assortment of combination frequencies. They are potential tools for identifying m values and orientation for each mode. However, their amplitudes do not agree with theoretical predictions from Wu (2001).
8. The $k = 9$ and 8 multiplet amplitudes and presence/absence of harmonics cannot be explained by simple geometric viewing arguments, and argue that something is interrupting GD358's azimuthal symmetry.
9. The linear, sinusoidal shape of the lightcurve indicates that GD358's convection zone was diminished during the 1996 *sforzando*.
10. Photometry taken during the maximum *sforzando* is consistent with a flux increase in the effective bandpass.
11. We find damping/growth timescales during the *sforzando* that are not consistent with the expectations of pulsation theory.
12. Changes in the splittings of the $k = 9$ and 8 multiplets indicate that some mechanism, perhaps a magnetic field, induced a long-term change in the multiplet structure of these modes during the *sforzando*.

Our investigation raises a number of interesting implications for our understanding of the physics of GD358, many beyond the scope of this paper, and some blatantly skirting the realm of speculation. While we cannot pretend that our investigation has unearthed unshakable evidence thereof, we do find tantalizing indications pointing to connections between convection, magnetic fields, and pulsation in GD358. We suggest future investigations:

1. Theoretical investigation of the relationship/connection between magnetic fields, convection, and pulsation will increase our understanding of GD358's photometric behavior. The typical static model of a pulsating white dwarf is too limiting. The dynamic model must accommodate the observed changes in pulsation frequencies and multiplet structure.
2. GD358's multiplets do not conform to theoretical expectations based on rotation. Other mechanisms must be considered. Examination of the influence of a nonspherical asymmetry in the outer layers on the multiplet structure is required to understand GD358's multiplets. Identification of spherical degree by multiplet structure alone should be highly suspect in any large amplitude pulsator.
3. Further work on the theoretical aspects of combination frequencies should explore the effects of multiple symmetry axes and the effects of a magnetic field on nonlinear mixing by the convection zone.

4. Detailed investigation of the FOS spectrum obtained during the *sforzando* for possible metals may provide insight into the mechanism producing the event.
5. Theoretical predictions for growth and damping rates have been calculated using static models. The timing of the growth and decay of $k = 8$ and 9 during the *sforzando* indicates interaction between these two modes. A theoretical examination of growth rates in the presence of other modes, including the interaction of a mode with itself, is necessary to better understand both the growth and dissipation of modes during the *sforzando* and typical mode selection in all large amplitude DB and DA pulsators.
6. A detailed examination of behavior of white dwarf pulsators, both low and high amplitude, spanning both the DA and DB instability strips (and hence a range of convective depths) will improve our understanding of convection's role in mode selection.
7. Theoretical work is needed to improve the treatment of convection. Lightcurve fitting of GD358 and other pulsators is an important step towards that goal.
8. Continued observation of GD358 will better define its dynamic behavior. We would like to observe another *sforzando*.

The practice and theoretical development of asteroseismology of GD358 and other pulsating stars continues to reward us with a rich scientific return. Our focus here on GD358 shows us that stellar seismology can challenge our current paradigm of the interior and behavior of pulsating white dwarfs.

The Delaware Asteroseismic Research Association is grateful for the support of the Crystal Trust Foundation and Mt. Cuba Observatory. DARC also acknowledges the support of the University of Delaware, through their participation in the SMARTS consortium. This work is further supported by the Austrian Fonds zur Förderung der wissenschaftlichen Forschung under grant P18339-N08. We would like to thank the various Telescope Allocation Committees for the awards of telescope time. We also acknowledge the assistance of J. Berghuis, M. David, H. Wade, and U. Burns with the Hawaii 0.6m. D.E.M acknowledges his work as a part of research activity of the Astrophysical Research Center for the Structure and Evolution of the Cosmos (ARCSEC) which is supported by the Korean Science and Engineering Foundation.

Facilities: MCAO:0.6 m, McD:2.1 m, KPNO:2.1 m, UH:0.6 m, BOAO:1.8 m, Lulin:1.8 m, Beijing:2.16 m, Maidanek:1.0 m, Peak Terskol:2.0 m, Moletai:1.65 m, Mt. Suhora:0.6 m, Konkoly:1.0 m, Vienna:0.8 m, Tübingen:0.8 m, OHP:1.93 m, NOT, ING:Herschel, LNA:1.6 m, CTIO:0.9 m, SOAR

REFERENCES

Alves, V. M., et al. 2003, Balt. Astron., 12, 33
Beauchamp, A., Wesemael, F., Bergeron, P., Fontaine, G., Saffer, R., Liebert, J., & Brassard, P. 1999, ApJ, 516, 887
Biermann, L. 1941, Mitt. Ges., 76, 1941
Bigot, L., & Dziembowski, W. A. 2002, A&A, 392, 235
Bohm-Vitense, E. 1958, Z. Astrophys., 46, 108
Bradley, P. A., & Winget, D. E. 1994, ApJ, 430, 850
Breger, M., et al. 1993, A&A, 271, 482
Brickhill, A. J. 1991, MNRAS, 251, 273
Brickhill, A. J. 1992, MNRAS, 259, 519
Canuto, V. M., Goldman, I., & Mazzitelli, I. 1996, ApJ, 473, 550
Canuto, V. M., & Mazzitelli, I. 1991, ApJ, 370, 295
Castanheira, B., Kepler, S. O., Nitta, A., Winget, D. E., & Koester, D. 2005, A&A, 432, 175
Di Mauro, M. P., Christensen-Dalsgaard, J., Kjeldsen, H., Bedding, T. R., & Paterno, L. 2003, A&A, 341
Dolez, N., Vauclair, G., & Kleinman, S. J., et al. 2006, A&A, 446, 237
Goldreich, P., & Wu, Y. 1999, ApJ, 511, 904
Handler, G., Romero-Colmenero, E., & Montgomery, M. H. 2002, MNRAS, 335, 399
Hansen, C. J., Cox, J. P., & Van Horn, H. M. 1977, ApJ, 217, 151
Houdek, G., et al. 2001, MNRAS, 327, 483
Ising, J., & Koester, D. 2001, A&A, 374, 116
Jones, P. W, Pesnell, W. D., Hansen, C. J., & Kawaler, S. D. 1989, ApJ, 336, 403
Kanaan, A., Kepler, S. O., & Winget, D. E. 2002, A&A, 389, 896
Kanaan, A., et al. 2005, A&A, 432, 219
Kawaler, S., Sedekii, T., & Gough, D. 1999, ApJ, 516, 349
Kepler, S. O., et al. 2003, A&A, 401, 639, K03
Kepler, S. O., et al. 2000, ApJL, 534, L185
Kleinman, S. J., et al. 1998, ApJ, 495, 424
Kotak, R., van Kerkwijk, M. H., Clemens, J. C., & Koester, D. 2003, A&A, 397, 1043
Kuhn, J. R. 1998, Proc. SOHO6/GONG 98 Workshop, ESA, SP-418, 871
Lenz, P., & Breger, M. 2005, Commun. Asteroseismol., 146, 53
Li, Y., & Yang, J. Y. 2007, MNRAS, 375, 388
Koester, D. 2008, private communication
Marchenko, S. V. 2008, A&A, 479, 845
Matthews, J. M, et al. 2004, Nature, 430, 51
Metcalfe, T. S., Montgomery, M. H., & Kawaler, S. D. 2003, MNRAS, 344, 88
Montgomery, M., & Kupka, F. 2004, MNRAS, 350, 267
Montgomery, M. H. 2005, ApJ, 633, 1142
Montgomery, M. H. 2006, in ASP Conf. Ser. 352, New Horizons in Astronomy: Frank N. Bash Symp. (San Francisco, CA: ASP), 261
Montgomery, M. H. 2008a, Commun. Asteroseismol., 154, 38
Montgomery, M. H. 2008b, private communication
Morin, J., et al. 2008, MNRAS, 384, 77
Nather, R. E., & Mukadam, A. 2004, ApJ, 605, 846
Nather, R. E., Winget, D. E., & Clemens, J. C. 1990, ApJ, 361, 390
Prada, M., Pier, G., & Straniero, O. 2002, ApJ, 581, 585
Provencal, J. L., et al. 2005, BAAS, 37, 1157
Thompson, S. E., Clemens, J. C., van Kerkwijk, M.H., & Koester, D. 2003, ApJ, 589, 921
Scargle, J. D. 1982, ApJ, 263, 835
Schunker, H., & Cally, P. S. 2006, MNRAS, 372, 551
Unno, W., Osaki, Y., Ando, H, & Shibahashi, H 1979, Nonradial Oscillations of Stars (Tokyo: Univ. Tokyo Press)
van Kerkwijk, M. H., Clemens, J. C., & Wu, Y. 2000, MNRAS, 314, 209
Vuckovic, M., et al. 2006, ApJ, 646, 1230
Weidner, C., & Koeter, D. 2003, A&A, 406, 657
Winget, D. E., et al. 1990, ApJ, 357, 630
Winget, D. E., et al. 1991, ApJ, 378, 326
Winget, D. E., et al. 1994, ApJ, 430, 839, W94
Winget, D. E., Sullivan, D. J., Metcalfe, T. S., Kawaler, S. D., & Montgomery, M. H. 2004, ApJL, 602, 109
Winget, D. E. 2008, private communication
Wood, M. 1992, ApJ, 386, 539
Woodward, M. F., & Noyes, R. W. 1985, Nature, 449, 318
Wu, Y. 2000, ASP Conf. Ser. 203, The Impact of Large-Scale Surveys on Pulsating Star Research, IAU Colloquium 176, ed. L. Szabados & D. Kurtz (San Francisco, CA: ASP), 508
Wu, Y. 2001, MNRAS, 323, 248
Yeates, C. M., Clemens, J. C., Thompson, S. E., & Mullaly, F. 2005, ApJ, 635, 1239
Zola, S. 2008, private communication

Lulin One-meter Telescope Observations for Black Hole Binary Swift J1753.5-0127

C. H. Wu (吳清雄)[1], Y. Chou (周翊)[1], T. C. Yang (楊庭彰)[1], C. P. Hu (胡欽評)[1], P. Cheng (鄭寶玲)[1], T. J. Li (李姿蓉)[1], P. Hsu (徐鵬英)[1], C. J. Chien (簡淨茹)[1], W. Y. Chang (張瑋芸)[1], C. J. Wu (吳承展)[2]

[1] Institute of Astronomy, National Central University, Taiwan, R.O.C

[2]Department of Physics, Chung Yuan Christian University, Taiwan, R.O.C

Abstract

The transient X-ray source Swift J1753.5-0127 is considered as an accreting black hole binary system with a late type mass losing star. It is still in its outburst state since its discovery on 2005 June 30 by the *Swift Burst Alert Telescope* and thus its optical counterpart is bright enough to be observed (*V*~16.6) with small telescope in these years. We report our optical observation results of Swift J1753.5-0127 using *Lulin one-meter telescope* (*LOT*) from May 13 to 17, 2008. Multi-band photometry (*V, R* and *I*) was preformed to study its variability. The light curves of these three bands show complex modulation morphology. A strong ~3.2 hrs period was detected in all three bands. A distinct analysis method, combined with Lomb-Scargle periodogram and multi-frequency sinusoidal fitting, was applied to all the light curves to further reveal its periodicity. The best period evaluated from our method is 3.2527 ±0.0032 hrs, consistent with the one proposed by Zurita et al. (2008) (3.2454±0.0080 hrs). After removing this ~3.2 hrs modulation, no clear side band was found in the spectra of residual light curves so the nature of this variation (orbital or superhump) is still uncertain although Zurita et al. (2008) claimed that it is superhump modulation because of its complex modulation profile. More *LOT* observations are planned to further study the origin of this variation.

Introduction

Superhump phenomenon was first observed in the SU UMa type stars, a subclass of dwarf nova. During the superoutburst state, superhump variation with period ~1% to ~7% longer than its orbital period is detected. The thermal-tidal instability model was proposed by Whitehurst et al. (1988) to explain the phenomenon. As the mass ratio ($q = M_2 / M_1$; M1, M2 : the masses of the accretor and the donor respectively) is less than 0.33, the accretion disk may be larger than the 3:1 resonance radius, and the accretion disk is elongated by the tidal force and starts to precess. Since low-mass X-ray binary (LMXB) is similar to Cataclysmic Variable (CV), superhump may also be detected in LMXB. Because the mass ratio should be less than 0.33, LMXBs with black holes (M_{BH}>3.2$M_{\odot}$) are good candidates to find superhump phenomena.

Swift J1753.5-0127 is a LMXB with a black-hole candidate. It was discovered on 30th June, 2005 by the *Swift Burst Alert Telescope*. Its optical counterpart was found with the *MDM 2.4m telescope* with *R* ~15.8. The *RXTE*/ASM light curve shows it remains bright in X-ray band (~33 mCrab)

since its outburst in 2005 (Fig 1). Therefore, its optical counterpart is also observable with small telescope because the optical emissions of a Soft X-ray Transient (SXT) in outburst state are mainly from the X-ray reprocessing in accretion disk. Zurita et al. (2008) concluded that their detection of ~3.2 hrs periodicity is owing to the superhump variation based on its complex modulation morphology instead of investigating the properties of the period (e.g. stability), the conventional ways to verify orbital and superhump periods. We therefore proposed to perform the multi-band photometry with *Lulin One-meter Telescope* (*LOT*) to do the verification.

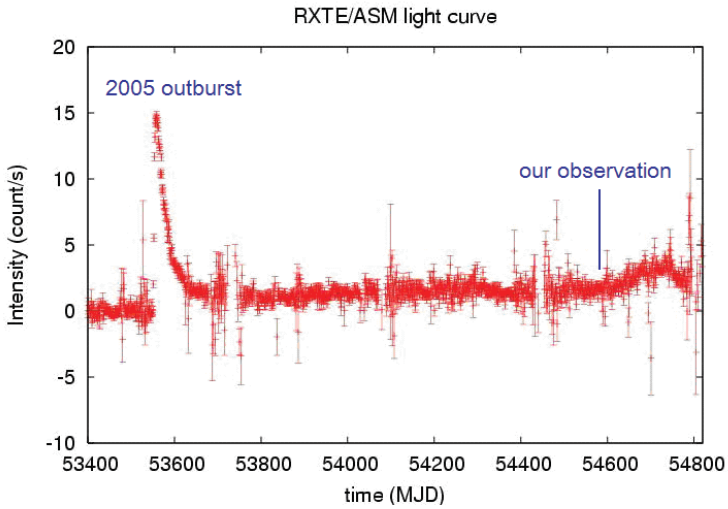

Fig. 1: The X-ray light curve from June 2005 to December 2008.

Observation and data analysis

Observation and data reduction

We observed Swift J1753.5-0127 for 4 nights between May 13 to 17 with *LOT*. The photometry was made in *V*, *R* and *I* bands with exposure time from 60s to 120s depending on the photometric condition and sufficient SNR (>100). All the images were calibrated with bias, dark and flat-field frames with IRAF. Aperture photometry was performed to gain the magnitude and the comparison stars suggested by Zurita et al. (2008) were applied in our analysis. After subtracting the mean magnitude of the comparison stars, daily mean values were removed. Typical light curves are shown in Fig 2.

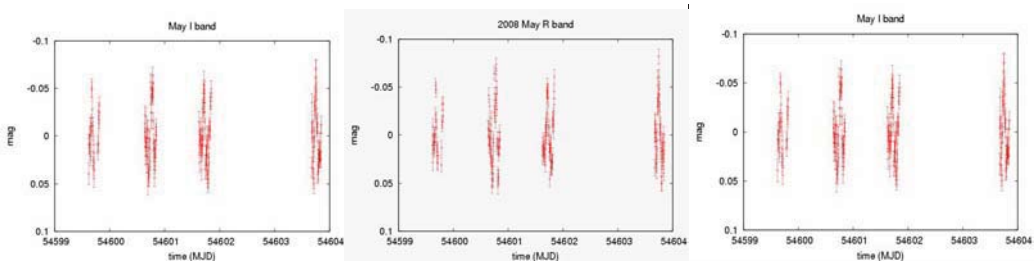

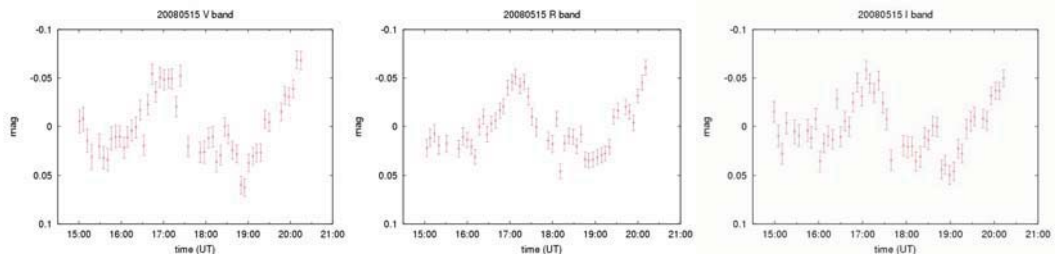

Fig. 2: The *V*, *R* and *I* band light curves of May 2008 (the upper panels). The *V*, *R* and *I* band light curves of May 15, 2008 (the lower panels).

Timing analysis and models

We first attempted to verify the periodicity of these three bands' light curves with Lomb Scargle (LS) periodogram (Lomb, 1976 & Scargle, 1982), which is suitable for smooth variation, and phase dispersion minimization (PDM) (Stellingwerf, 1978), which is more sensitive to non-sinusoidal modulation. Strong detections of ~3.2 hrs periodicity were yielded from all three bands' light curves with both methods (see Fig 3).

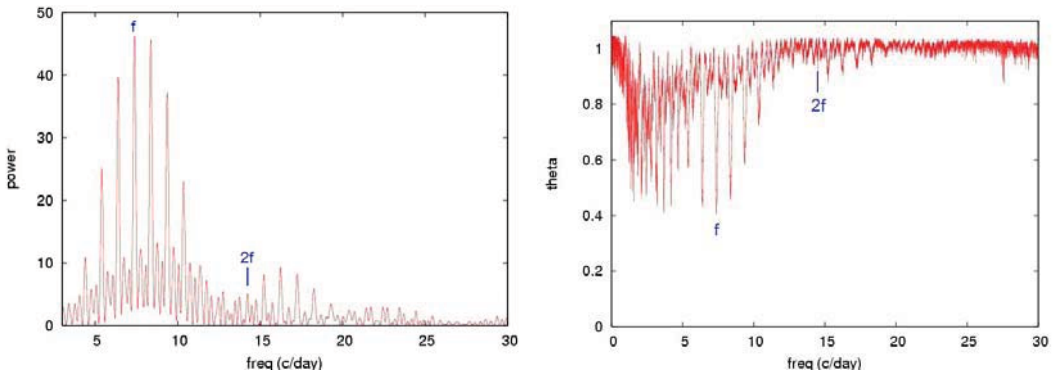

Fig. 3: Left: LS periodogram of *R* band. The frequency with the maximum power is f~7.38 c/day. Right: The PDM result of *R* band.

We further processed multi-frequency sinusoidal fitting using Period04, which allow us to do multi-frequency sinusoidal fitting up to 256 components, to refine the detected periods, obtain their corresponding errors, and minimize the effects of aliases in power spectra due to observation gaps to reveal other possible periodicity with weaker power. We first selected the peak frequency from LS power spectrum as the initial guessing value of primary frequency for single sinusoidal fitting with Period04. This program is able to automatically process the non-linear χ^2 fitting to yield the best frequency, amplitude and phase. The best-fitted model was then subtracted from the original light curve. As shown in the Fig. 4, the frequency of the last step and its aliases are removed. The peak frequency from the power spectrum of residual light curve was chosen as the initial guessing value of secondary frequency. As shown in the Fig. 4, the frequency ~7.38 c/day and its aliases are removed. Combined with the primary result, the double sinusoidal fitting was also performed with Period04. This process above was repeated until the peak power in the LS power spectrum of the residual light curve was less than 12 (< 95% confidence level). The fitting results of three bands' models are shown in table 1.

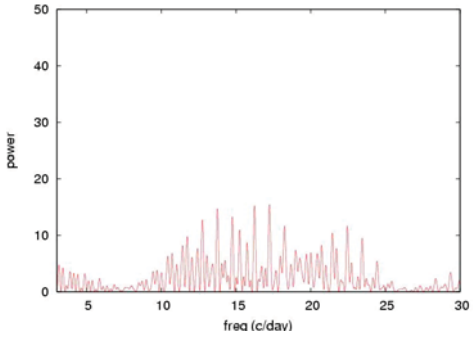

Fig. 4: The frequency ~7.38 c/day and its aliases are removed.

Band	Parameters of Model					Period (hr)	χ_ν^2
	component	Frequency (f) (c/day)	Amplitude (A) (magnitude)	Phase(Φ)	A_0 (magnitude)		
V	1	7.3710±0.0070	0.0330±0.0049	0.5187±0.0099	-0.0015±0.0014	3.2560±0.0058	3.5039
	2	12.7447±0.0185	0.0124±0.0019	0.8759±0.0255			
R	1	7.3866±0.0062	0.0309±0.0036	0.9863±0.0086	-0.0013±0.0011	3.2490±0.0055	3.8020
	2	17.2494±0.0168	0.0113±0.0017	0.3945±0.0233			
	3	12.7428±0.0215	0.0093±0.0016	0.1898±0.0287			
	4	22.4339±0.0197	0.0096±0.0016	0.7668±0.0272			
I	1	7.3773±0.0073	0.0278±0.0037	0.8500±0.0103	-0.0014±0.0012	3.2532±0.0055	2.9776
	2	13.7237±0.0162	0.0131±0.0018	0.1303±0.0215			
	3	17.2541±0.0188	0.0108±0.0017	0.6689±0.0262			

Table 1: The results of models in *V*, *R* and *I* bands by LS periodogram. The models are expressed in the form: $A_0+\sum A_n\times\sin\left(2\pi\times\left(f_n\times t+\phi_n\right)\right)$, and the period is derived from the best-fitted frequency of component 1.

Three best-fitted periods got from all bands were then weight-averaged using the inverse of square of the corresponding errors as weighting factors and obtained the mean period of 3.2527 ±0.0032 hrs. This value is consistent with that proposed by Zurita et al. (2008) (3.2454±0.0080 hrs). The folded light curve (Fig. 5) was made through folding the nightly *R* band light curves with the following ephemeris:

$$T_N=T_0+P\times N$$

where P is the mean period (3.2527 hrs) and the phase zero epoch (T_0=MJD 54599.675) was selected from one of the peak fluxes in *R* band light curve. No clear side-band whose period close to the ~3.2 hrs period was found. However, after removing the f ~7.38 c/day signal, a significant periodic signal with period ~2.95 hrs (f ~8.13 c/day, see Fig 6) can be seen in PDM spectra from R band light curve. This frequency is also shown in LS periodogram of *R* and *I* bands' models, but it's in the form of 2f (~16.2 c/day, the f ~17.2 c/day in the models is the result of one-day alias). If it were the orbital period and the ~3.2 hrs period were superhump, the period exceeding >10%, larger than the 1% to 7% period exceeding for other superhump system. However, if the frequency ~8.13 c/day is in fact just an one-day alias of

$\varepsilon=(P_{sh}-P_{orb})/P_{orb}$

the frequency ~7.13 c/day (period ~3.36 hrs), the period exceeding is only 4%. If this is confirmed, the ~3.2 hrs period will be the orbital period whereas ~3.36 hrs period will be the positive superhump period, contrary to the conclusion of Zurita et al. (2008).

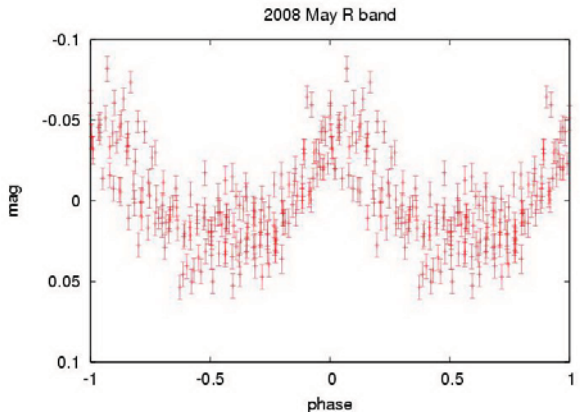

Fig. 5: The fold light curve of *R* band. Folded period is 3.2454 hrs. The phase zero epoch (T_0) is MJD 54599.675.

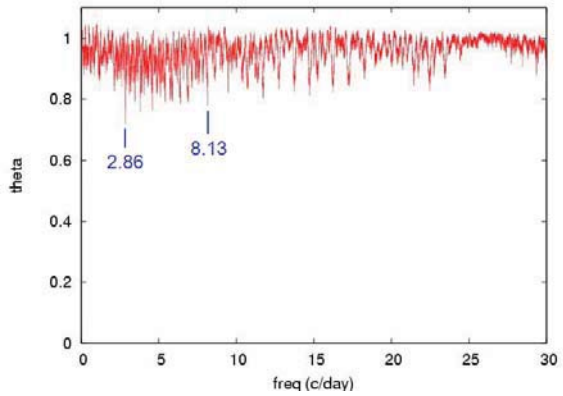

Fig. 6: The frequency ~8.13 (c/day) is the second minimum θ after removing the frequency ~7.38 c/day. The frequency ~2.86 c/day is from the observational time span.

Discussion and conclusion

We have performed multi-band observations for black-hole binary Swift J1753.5-0127 between May 13 to 17 2008 using *LOT*. The ~3.2 hrs periodicity can be detected in the light curves of all three bands. The multi-frequency sinusoidal fitting method was applied to verify other possible periodicity in the light curves. Although no clear side-band is found in the spectra of residual light curves, the nature of this variation (orbital or superhump) is still uncertain. A marginal evidence of a period ~3.36 hrs was inferred from the *R* band light curve. If this period can be confirmed, it is likely that the ~3.2 hrs period is orbital period whereas ~3.36 hrs period is possible superhump period. On the other hand, after significant signals being removed, there is still clear variability in the light curves since the reduced χ^2 are still too large (> 3) to be statistic acceptable, which indicates that the modulation is indeed complex as Zurita et al. (2008) suggested. More observations for Swift J1753.5-0127 are planned to process in April, May and June this year.

Reference

- Bel, C. M. et al., 2008, ApJ, 659, 549
- Durant, M., 2008, ATel, 1599
- Durant, M., 2008, ATel, 1608
- Durant, M. et al., 2008, MNRAS, 391, 1
- Lomb, N. R., 1976, Ap&SS, 39, 447
- Miller, J. M. et al., 2006, ApJ, 652 , 113
- Period04 homepage：http://www.univie.ac.at/tops/Period04/
- Ramadevi, M.C. & Seetha,S., 2007, MNRAS, 378, 182
- Scargle, J. D., 1982, AJ, 302, 757
- Stellingwerf, R. F., 1978, ApJ, 224, 953
- Zurita, C. et al., 2008, ApJ, 681, 1458
- Zhang, G. B. et al., 2007, ApJ, 659, 1511

Optical rebrightening of the blazar AO 0235+16 observed by the GASP

ATel #1785; ***M. Villata and C. M. Raiteri (INAF, Osservatorio Astronomico di Torino, Italy), V. M. Larionov, T. S. Konstantinova, E. N. Kopatskaya, and L. Larionova (Astronomical Institute, St.-Petersburg State University, Russia, and Pulkovo Observatory, Russia), W. P. Chen and E. Koptelova (Institute of Astronomy, National Central University, Taiwan), K. Nilsson and M. Pasanen (Tuorla Observatory, University of Turku, Finland), R. Ligustri (Circolo Astrofili Talmassons, Italy), M. BÄttcher, P. Roustazadeh, and C. Diltz (Astrophysical Institute, Department of Physics and Astronomy, Ohio University, OH, USA), for the GASP Collaboration***
on ***17 Oct 2008; 10:47 UT***
Password Certification: Claudia M. Raiteri (raiteri@oato.inaf.it)

Subjects: Optical, AGN
Referred to by ATel #: 1849

With reference to ATels #1724, #1735, #1744, #1784 on the high radio-to-optical and gamma-ray activity of the blazar AO 0235+16, the GLAST-AGILE Support Program (GASP) of the Whole Earth Blazar Telescope (WEBT) reports on the recent observation of a strong optical rebrightening of the source. After the optical peak of R ~ 14.2 reached on September 24.1, 2008, the brightness rapidly decreased by 2 mags in the following 10 days. Since then, the source has been quickly rebrightening toward the R ~ 14.5 level achieved on October 13.1 and maintained, with slight variations, on October 14 and 15. Further observations in the last two nights have been prevented by the close full Moon. The preliminary GASP light curve can be seen at http://www.oato.inaf.it/blazars/webt/gasp/lc/g0235r.png.

Optical and near-IR brightening of the blazar 3C 66A detected by the GASP

ATel #1755; ***V. M. Larionov (Astronomical Institute, St.-Petersburg State University, Russia, and Pulkovo Observatory, Russia), M. Villata and C. M. Raiteri (INAF, Osservatorio Astronomico di Torino, Italy), D. Gorshanov, T. S. Konstantinova, E. N. Kopatskaya, and L. Larionova (Astronomical Institute, St.-Petersburg State University, Russia, and Pulkovo Observatory, Russia), W. P. Chen and E. Koptelova (Institute of Astronomy, National Central University, Taiwan), for the GASP Collaboration***
on ***2 Oct 2008; 13:36 UT***
Password Certification: Claudia M. Raiteri (raiteri@oato.inaf.it)

Subjects: Infra-Red, Optical, AGN
Referred to by ATel #: 1759

With reference to ATel #1753 announcing the detection of >100 GeV gamma-ray emission from the blazar 3C 66A in September 25 √ October 1, the GLAST-AGILE Support Program (GASP) of the Whole Earth Blazar Telescope (WEBT) reports on the observation of an optical and near-IR brightening of the source occurred in the same period: from R ~ 14.3 on September 24 to R ~ 13.7 on September 30, while the J mag varied from about 12.8 to 12.3.

GASP observation of a spectacular optical-to-radio brightening of the blazar AO 0235+16

ATel #1724; ***M. Villata and C. M. Raiteri (INAF, Osservatorio Astronomico di Torino, Italy), D. Carosati (Armenzano Astronomical Observatory, Italy), W. P. Chen and E. Koptelova (Institute of Astronomy, National Central University, Taiwan), V. M. Larionov, D. Gorshanov, T. S.***

Konstantinova, E. N. Kopatskaya, and L. Larionova (Astronomical Institute, St.-Petersburg State University, Russia, and Pulkovo Observatory, Russia), K. Nilsson and M. Pasanen (Tuorla Observatory, University of Turku, Finland), M. A. Gurwell (Harvard-Smithsonian Center for Astrophysics, MA, USA), P. Leto (INAF, Istituto di Radioastronomia Sezione di Noto, Italy), C. S. Buemi, C. Trigilio, and G. Umana (INAF, Osservatorio Astrofisico di Catania, Italy), M. F. Aller and H. D. Aller (Department of Astronomy, University of Michigan, MI, USA), for the GASP Collaboration
*on **19 Sep 2008; 14:23 UT***
Password Certification: Claudia M. Raiteri (raiteri@oato.inaf.it)

Subjects: Radio, Millimeter, Infra-Red, Optical, AGN
Referred to by ATel #: 1735, 1744, 1785, 1849

The GLAST-AGILE Support Program (GASP) of the Whole Earth Blazar Telescope (WEBT) reports on the recent observation of a spectacular optical-to-radio brightening of the blazar AO 0235+16, reaching levels comparable to those of the 2006-2007 outburst (see Raiteri et al. 2008, A&A, 480, 339). On August 12, 2008, the source was at R ~ 17.5 and brightened by 1 mag in the next 3 days; after an oscillating and increasing trend it was at R ~ 16.1 on September 8, and a further brightening led to R ~ 14.75 on September 17.8, followed by a slight dimming to R ~ 15.1 at September 18.0. Last night (September 18-19) the level was more or less the same, but the bright close Moon prevented precise measurements. The same behaviour has been observed in the near-IR (Campo Imperatore), with the September 18.0 peak at J ~ 12.55. At mm wavelengths (SMA), the source has been around 3 Jy in the last 30 days, and previously showed a progressive flux increase from the base level of ~ 0.5 Jy following the 2006-2007 outburst. Similarly, at 43 GHz (Noto) and 14.5-4.8 GHz (UMRAO) the source brightened from about 1 Jy in early 2008 to 4-5 Jy and 3.5-2.5 Jy, respectively, in mid 2008, then remaining in a bright state.

GASP detection of a bright optical flare and mm-cm activity from the blazar 3C 454.3

ATel #1625; ***M. Villata and C. M. Raiteri (INAF, Osservatorio Astronomico di Torino, Italy), V. M. Larionov and E. N. Kopatskaya (Astronomical Institute, St.-Petersburg State University, Russia), M. A. Gurwell (Harvard-Smithsonian Center for Astrophysics, MA, USA), K. Nilsson and M. Pasanen (Tuorla Observatory, Finland), M. Lister (Purdue University, USA) and the MOJAVE Collaboration, M. F. Aller, A. Arkharov, P. Calcidese, D. Carosati, W. P. Chen, E. FornИ, E. Koptelova, P. Leto, and the GASP Collaboration***
*on **22 Jul 2008; 11:30 UT***
Password Certification: Claudia M. Raiteri (raiteri@oato.inaf.it)

Subjects: Radio, Millimeter, Infra-Red, Optical, AGN, Quasars
Referred to by ATel #: 1628, 1849

The GLAST-AGILE Support Program (GASP) of the Whole Earth Blazar Telescope (WEBT) reports on the recent observation of a very bright optical flare from the blazar 3C 454.3. After a moderate flare in June 2008, the source rebrightened from R ~ 15 to ~ 13.4 between the end of June and mid July. Noticeable activity has been also observed in the near-IR (Campo Imperatore), at mm wavelengths (SMA), at 43 GHz (Noto) and 14.5 GHz (UMRAO). A VLBA intensity and polarization image of June 25 (MOJAVE) at 15 GHz is shown at
http://www.cv.nrao.edu/2cmVLBA/data/2251+158/2008_06_25/2251+158.u.2008_06_25.pcn.jpg

Observations of (3200) Phaethon and its Possible Fragment

Kinoshita Daisuke
Institute of Astronomy, National Central University

31 March 2009

Abstract

Ohtsuka et al. (2006) carried out numerical integrations of orbits of (3200) Phaethon and (155140) 2005 UD, and pointed out possible association between these two Apollo type near-Earth asteroids from dynamical study. Jewitt and Hsieh (2006) and Kinoshita et al. (2007) performed visible photometric observations of (155140) 2005 UD, and they confirmed bluish surface colors of (155140) 2005 UD are similar to those of (3200) Phaethon suggesting rare F/B-type among near-Earth asteroids, and a possible link between these two objects was also confirmed by observational studies. Furthermore, Kinoshita et al. (2007) pointed out the variation of $(R-I)$ color along the rotation of the body. A part of the surface of (155140) 2005 UD may be originated from the sub-surface of the precursor object. These observational results support the idea that the fragmentation of (3200) Phaethon produced a large amount of dust particles and formed a meteor stream complex. In order to confirm this hypothesis, we carried out observations of (3200) Phaethon and (155140) 2005 UD. Time-resolved low dispersion spectroscopic observation of (3200) Phaethon was performed at Lulin Observatory in Taiwan in Nov./Dec. 2007. Basically, the spectra of (3200) Phaethon exhibit bluish colors with negative spectral gradient for most part of the rotational phase. The change of the spectral gradient was recognized, and a clear trend was seen when we folded the time-series spectral gradient by a possible rotational period estimated by the lightcurve obtained at the same time of the observation in Japan. It could be a signature of the split event on (3200) Phaethon. In Oct. 2008, we carried out intensive time-series photometric observation of (155140) 2005 UD at Lulin Observatory for six nights. The purpose of this observation is to search for the complex rotation of (155140) 2005 UD. If the non-principal axis rotation is detected, it is a strong piece of evidence for the fragmentation process for (3200) Phaethon and (155140) 2005 UD system. The data analysis of this observation is in progress.

1 Background

An Apollo-type near-Earth asteroid, (3200) Phaethon (= 1983 TB), was discovered by the InfraRed Astronomical Satellite (IRAS) in October 1983 (Green & Kowal 1983). Although the appearance of (3200) Phaethon is asteroidal, its orbit is highly eccentric with $e = 0.89$, like those of comets. In addition, (3200) Phaethon is a strong candidate for the Geminid meteor stream (Whipple 1983; Gustafson 1989; Williams & Wu 1993), so it is regarded as one of the most likely dormant cometary nuclei, whose cometary activity is sporadic, or as extinct cometary nuclei whose activity has already stopped. Many attempts have been made to detect the faint coma of this object (Cochran & Barker 1984; Chamberlin et al. 1996; Hsieh & Jewitt 2005). No cometary activity has been observed yet; therefore, (3200) Phaethon seems to be one of the most peculiar and enigmatic objects in the solar system.

On October 22, 2005, an Apollo-type, near-Earth asteroid was discovered by the Catalina Sky Survey, and the provisional designation of (155140) 2005 UD was given to this object (McNaught et al. 2005). Ohtsuka et al. (2005) immediately pointed out that (155140) 2005 UD was probably the parent body of the daytime Sextantids meteor stream, based on the orbital similarity. Thus, (155140) 2005 UD is very likely a large member of the Phaethon-Geminid stream complex. Furthermore, Ohtsuka et al. (2006) performed both forward and backward 10,000-yr numerical integrations of the Kustaanheimo-Stiefel (K-S) regularized equation of motion (Arakida & Fukushima 2000, 2001) for (3200) Phaethon and (155140) 2005 UD. The results of this numerical work show quite similar evolutional behaviors along with the time shift by $\sim$ 4600-yr; hence, they suggest that both bodies are dynamically related and (155140) 2005 UD is most likely a km-sized fragment of (3200) Phaethon. Ohtsuka et al. (2006) also point out that fragmentation processes are important in forming the complex meteor stream.

Jewitt and Hsieh (2006) have reported their analysis of the photometric observation of (155140) 2005 UD. The results of their broadband multi-color photometry support the possible dynamical association between (155140) 2005 UD and (3200) Phaethon. The mass-loss rate from (155140) 2005 UD, based on the point-spread function (PSF) fitting, is found to be very small or negligible. They also mention that a mainbelt comet (MBC) could be a possible origin of (3200) Phaethon and (155140) 2005 UD, although testing their idea currently does not seem to be easy.

Kinoshita et al (2007) carried out observational studies of 2005 UD. The primary aim of observations was to verify the dynamical relationship between (3200) Phaethon and (155140) 2005 UD through the similarity of surface physical properties. If (155140) 2005 UD exhibited photometric properties similar to those of (3200) Phaethon, we can confirm prior research by providing another strong piece of evidence for their genetic relationship. Second, they tried to detect the surface color variation of (155140) 2005 UD. Ohtsuka et al. (2006) concluded (155140) 2005 UD is very likely a km-order fragment from (3200) Phaethon from the standpoint of dynamics; therefore, there may be non-uniformity of photometric properties if the fresh materials are exposed elsewhere on the surface. This sort of exposed fresh materials may create color variations during the rotation of the body. The time-resolved photometry in the R-band showed a rotational period of 5.2310 hours. The lower limit of the axis ratio $a/b \sim 1.50$ is estimated from the amplitude of the lightcurve. The lower limit of the bulk density of (155140) 2005 UD is estimated as 1.5×10^3 kg/m^3. Results of multi-color photometry show a bluish surface for (155140) 2005 UD, which is consistent with (3200) Phaethon, and this supports the hypothesis that (155140) 2005 UD is a km-sized fragment of (3200) Phaethon. Furthermore, surface colors of (155140) 2005 UD exhibit variations during the rotation of the body. This surface inhomogeneity may be associated with the fragmentation or collisional processes.

2 Observation

Apollo-type near-Earth asteroid (3200) Phaethon and (155140) 2005 UD have been suggested to be associated each other. Previous dynamical study and observational results support the idea that the fragmentation of (3200) Phaethon produced a large amount of dust particles and formed a meteor stream complex. In order to confirm this hypothesis, we carried out observations of (3200) Phaethon and (155140) 2005 UD.

2.1 Time-Resolved Spectroscopy of (3200) Phaethon

In 2007B semester, time-resolved low dispersion spectroscopy of (3200) Phaethon was carried out using Lulin One-meter Telescope and the low dispersion spectrograph "Hiyoyu". The aim of this observation is to search for a signature of the split event on the surface of (3200) Phaethon. A 300 gr./mm grating was used to cover the wavelength region of $380 < \lambda < 760$ nm. The visible spectra of (3200) Phaethon were continuously taken for three nights on 30 Nov., 1 Dec., and 2 Dec. in 2007. The geocentric distance of (3200) Phaethon at the time of observation ranged from 0.198 to 0.236 AU. Because of small geocentric distance, the apparent motion of (3200) Phaethon was relatively large. The apparent motions of (3200) Phaethon for RA and Dec. directions ranged from 380 to 515 arcsec per hour and from 140 to 230 arcsec per hour, respectively. The integration time of each exposure is set to be 300 sec. 600 sec integration time was also tested, but the signal-to-noise ratio didn't seem to improve due to poor tracking. A spectrophotometric standard star and a solar analogue star were also observed several times at different airmass on each night. 70 spectra were obtained in total.

2.2 Intensive Time-Resolved Photometry of (155140) 2005 UD

In 2008B semester, intensive time-resolved photometry of (155140) 2005 UD was carried out using Lulin One-meter Telescope and the imaging CCD camera. The purpose of this observation is to search for complex rotation of (155140) 2005 UD. The non-principal axis rotation, or tumbling motion, may be excited by the fragmentation event of an asteroid. After the excitation of tumbling motion, the tumbling motion is damped toward the lowest energy state by the internal stresses. The damping time scale depends on the size and rotation period of the asteroid, and is estimated by

$$\tau \sim \frac{\mu Q}{\rho K_3^2 R^2 \omega^3}, \tag{1}$$

where R is asteroid size, ω is angular velocity of the asteroid spin, μ is rigidity, Q is quality factor, and K_3^2 is shape-dependent factor. For an asteroid with $R = 1$ km and $P = 5.2$ hr, the damping timescale is

a few 10^7 years (Fig. 1). On the other hand, a typical dnamical lifetime of a near-Earth asteroid is an order of 10^6 years. (155140) 2005 UD may still have non-principal axis rotation. If the non-principal axis rotation is detected, it is a strong piece of evidence for the fragmentation process for (3200) Phaethon and (155140) 2005 UD system.

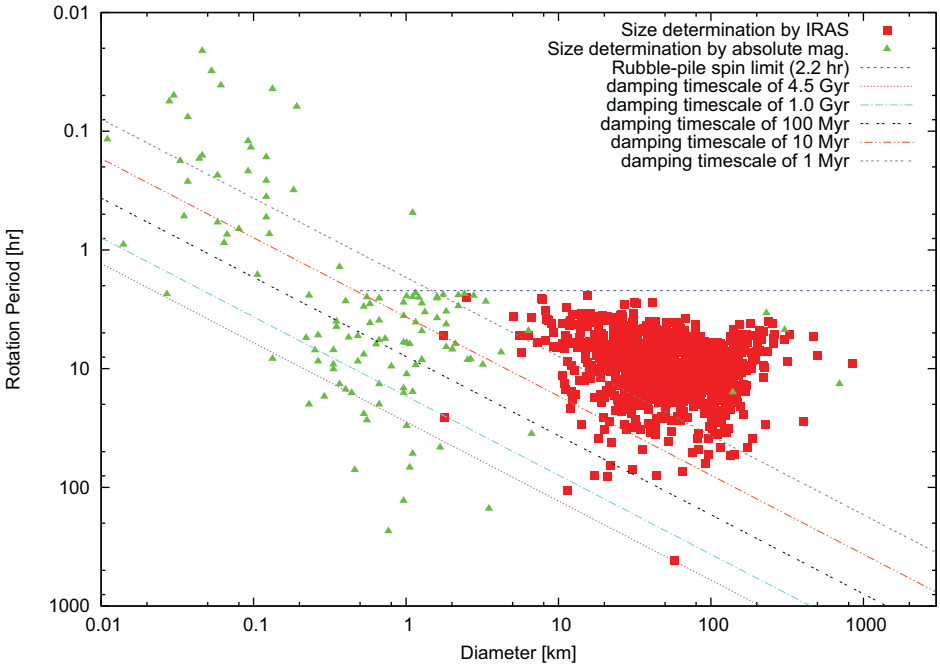

Figure 1: The size and rotation period of asteroids are plotted. Red squres denote asteroids with size estimation by IRAS infrared data, and green triangle denote asteroids with size estimation by the absolute magnitude under the assumption of typical albedo. The damping timescale of 1 Myr, 10 Myr, 100 Myr, 1.0 Gyr, and 4.5 Gyr are overlayed on the figure.

We had seven nights allocated for our observing program from 22 to 28 October 2008. We had six observable nights. on each night, time-resolved photometry of (155140) 2005 UD was carried out. The apparent magnitude of (155140) 2005 UD at the time of observation was about $V \sim 18.7$ mag. In order to search for complex rotation, one has to perform the periodicity analysis to the residual of the periodicity analysis. This analysis requires excellent quality of the data. Hence, The target signal-to-noise ratio of this observation was about 100, and the integration time was set to 300 sec. R-band filter was used for this observation. 324 images of (155140) 2005 UD were obtained in total.

3 Preliminary Results

The data reduction and analysis of spectroscopic data obtained in 2007B semester has been completed. Basically, the spectra of (3200) Phaethon exhibit bluish colors with negative spectral gradient for most part of the rotational phase. The change of the spectral gradient was recognized, and a clear trend was seen when we folded the time-series spectral gradient by a possible rotational period estimated by the lightcurve obtained at the same time of the observation in Japan. It could be a signature of the split event on (3200) Phaethon.

The data reduction and analysis of photometric data obtained in 2008B semester is in progress. The CCD data reduction of raw data are completed, and we soon start the periodicity analysis to derive the rotational lightcurve. After the derivation of the rotational lightcurve, we apply the periodicity analysis to the residual of the fitting to search for the non-principal axis rotation.

4 Future Work

For the spectroscopic data of (3200) Phaethon, we are now preparing a paper, and will soon submit a manuscript to a refereed journal.

For the photometric data of (155140) 2005 UD, we plan to complete the data analysis in a few months. We plan to submit a manuscript to a refereed journal by the end of 2009.

Acknowledgement

I am grateful to Mr. Miyasaka Seidai who carried out the imaging observation of (3200) Phaethon in Japan while I was taking visible low dispersion spectra of (3200) Phaethon in Taiwan. His data were used to derive the rotation period of this asteroid. I would like to thank Ms. Lin I-Ling for her support to the observation in October 2008. This work is supported by the research grant from National Science Council (ID: 96-2911-M-008-015-MY3).

References

[1] Arakida, H., Fukushima, T., AJ, 120, 3333 (2000).

[2] Arakida, H., Fukushima, T., AJ, 121, 1764 (2001).

[3] Chamberlin, A. B., McFadden, L.-A., Schulz, R., Schleicher, D. G., Bus, S. J., Icarus, 119, 173 (1996).

[4] Cochran, A. L., Berker, E. S., Icarus, 59, 296 (1984).

[5] Green, S., Kowal, C., IAU Circular, 3878 (1983).

[6] Gustafson, B. A. S., *A&A*, 225, 533 (1989).

[7] Hsieh, H. H., Jewitt, D., ApJ, 624, 1093 (2005).

[8] Jewitt, D. and Hsieh, H., *AJ*, 132, 1624.

[9] Kinoshita, D., Ohtsuka, K., Sekiguchi, T., Watanabe, J., Ito, T., Arakida, H., Kasuga, T., Miyasaka, S., Nakamura, R., Lin, H.-C., *A&A*, 466, 1153.

[10] McNaught, R. H., McGaha, J. E., Young, J., Christensen, E. J., Beshore, E. C., Garradd, G. J., Grauer, A. D., Hill, R. E., Kowalski, R. A., Larson, S. M., Tibbets, D., Hug, G., Hutsebaut, R., Jacques, C., Pimentel, E., Miles, R., Birtwhistle, P., Marsden, B. G., Minor Planet Electronic Circ., 2005-U22 (2005).

[11] Ohtsuka, K., Sekiguchi, T., Kinoshita, D., Watanabe, J.-I., Ito, T., Arakida, H., Kasuga, T., *A&A*, 450, L25 (2006).

[12] Whipple, F. L., IAU Circular, 3881 (1983).

[13] Williams, I. P., Wu, Z., MNRAS, 262, 231 (1993).

鹿林天文台 CCD 相機 PI1300B 的暗電流及增益值測量

黃相輔 [1]、木下大輔 [1]、施佳佑 [2]
[1] 國立中央大學天文研究所
[2] 中央研究院天文及天文物理研究所

摘要

儀器的狀況可能隨時間改變並影響其效能。爲了確保天文觀測的準確度，我們需定期檢視儀器的表現。本實驗中，我們檢測了鹿林天文台CCD PI1300B的暗電流、增益值及讀出噪音。我們使用平場及暗電流影像來估計增益與讀出噪音，並求得不同CCD冷卻溫度下所表現的暗電流產生率。我們所量測的數據與2005年以前的調查結果 (Kinoshita et al. 2005) 相符合，說明CCD PI1300B仍持續穩定運作。

The Dark Current and Gain Measurements of CCD Camera PI1300B at Lulin Observatory

Hsiang-Fu Huang [1], Daisuke Kinoshita [1], and Chia-You Shih [2]
[1] Institute of Astronomy, National Central University
[2] Institute of Astronomy and Astrophysics, Academic Sinica

Abstract

The condition of the instrument may vary through time, and influences the basic properties and performance of instruments. In order to ensure the stable science operation of observation, the characteristics and performance of CCD needs to be re-examined regularly. We have measured the dark current, gain, and readout noise of CCD camera PI1300B mounted on Lulin One-meter Telescope (LOT) at Lulin Observatory. We have obtained dark and flatfield frames to estimate the gain and readout noise. The dark current generation rates at different CCD cooling temperatures were measured. Results are compared with the previous study (Kinoshita et al. 2005), and it is found to be consistent. The instrument is found to be stably operated.

關鍵字 (Key words): 天文儀器 (instrumentation)、CCD: PI1300B、鹿林天文台 (Lulin Observatory)、暗電流 (dark current)、增益 (gain)、讀出雜訊 (readout noise)

Received : 2008.11.07; accepted: 2008.12.12

1. Introduction

Charge-coupled devices (CCD) are the most popular detectors which are used in optical astronomical observations for many advantages. These advantages include low noise, high quantum efficiency, good linearity and high dynamic range. The brief description of the operation of CCD is as follows. The electrons are freed by the energy of incoming photons during the integration. When exposure ends, charges have been collected and the voltage has been converted into digital units. In order to obtain precise measurements for scientific study, observer must know the noise occurred within the instrument first. (Martinez and Klotz 1998; Howell 2000)

The CCD camera PI1300B was mounted on Lulin One-meter Telescope (LOT) at Lulin Observatory being the main instrument after January 2003. Its basic characteristics were surveyed in 2004, and results were reported by Kinoshita et al. (2005). Condition of the instrument may vary with time; so the regular re-estimates are necessary to confirm its stable science operation. We measured the gain, readout noise and dark current generation rate in November 2007 in this work. Table 1 lists the basic properties provided by the manufacturer, Roper Scientific, Inc.

Table 1. The basic properties of CCD PI 1300B provided by the manufacturer (adopted from Kinoshita et al. 2005).

CCD Chip	EEV CCD36-40 (back-side illuminated)
Pixel Number	1340 × 1300
Pixel Size	20 μm × 20 μm
Imaging Area	26.8 mm × 26.0 mm
CCD Grade	Scientific Grade; Grade 1
Full Well	200,000 e^-
AD Conversion	16 bits
Sampling	50 kHz (slow mode), 1 MHz (fast mode)
Readout	36 sec @ 50 kHz 1.8 sec @ 1 MHz
Read Noise	3e− rms @ 50 kHz 10e− rms @ 1 MHz
Dark Current	0.1 e−/sec/pixel @ −40°C 0.5 e−/hr/pixel @ −110°C

2. Measurements and Results

2.1 Gain and Readout Noise

The gain [e^-/ADU] is defined as the number of electrons required to produce a unit of digital number, which is often represented by analog-to-digital unit (ADU), in output image,

$$n_e = G\, n_{ADU} \tag{1}$$

Where n_e is the number of electrons, G is the gain, and n_{ADU} is the value of ADU. The total noise consists of two components. One is the contribution from the Poisson noise, which is square root of the signal. The other is the readout noise. So the relation between total noise N and signal S can be represented as (Motohara et al. 2002; Kinoshita et al. 2005),

$$N = \sqrt{\frac{S}{G} + \left(\frac{R}{G}\right)^2} \tag{2}$$

Where R is readout noise [e^-], the number of electrons introduce into final signal accompanies with data readout. N, S/G and R/G are the total noise, mean signal level, and readout noise, respectively, in the unit of ADU. From Howell (2000), we know that subtracting two flatfields can get the standard deviation which includes both background Poisson and readout noises, and it can be written as,

$$\sigma^2_{F_1-F_2} = 2\left\{\left(\frac{\sqrt{n_e}}{G}\right)^2 + \left(\frac{R}{G}\right)^2\right\} \tag{3}$$

Where $\sigma_{F_1-F_2}$ is the standard deviation of

subtracting two flat field frames. Thus, we can estimate the value of gain and readout noise by using flatfields.

We followed the method used by Kinoshita et al. (2005), to obtain five flatfields and five dark frames under the same CCD temperature and exposure time. Each frame was divided into 4 regions which every subframe contains 300 × 300 pixels. Fig. 1 is the schematic drawing to show locations of subframes. Using the Eq. (2), we can fit data points to estimate the gain and readout noise values. Fig. 2 and Fig. 3 show the fitting results under CCD temperature of -50°C for the fast readout of 1 MHz sampling (hereafter "fast mode") and the slow readout of 50 kHz sampling (hereafter "slow mode"), respectively. The comparison between previous work and our measurement are collated in Table 2.

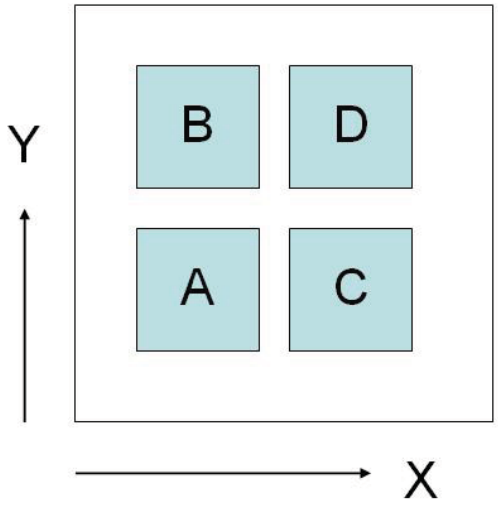

Fig. 1: Sketch of subframes of four regions. Coordinates of four regions are listed as following in the unit of pixel. Region A (301 ≦ X ≦ 600, 301 ≦ Y ≦ 600); Region B (301 ≦ X ≦ 600, 701 ≦ Y ≦ 1000); Region C (701 ≦ X ≦ 1000, 301 ≦ Y ≦ 600); Region D (701 ≦ X ≦ 1000, 701 ≦ Y ≦ 1000).

Fig. 2: The gain and readout noise of different regions for fast mode. Horizontal and vertical axes are the mean signal and noise in the unit of ADU, respectively. G represents gain and R indicates readout noise. Dashed curves are the least square fits to the data using Eq. (2). We used 240 data points to fit, and these data points are roughly uniformly distributed over the signal level.

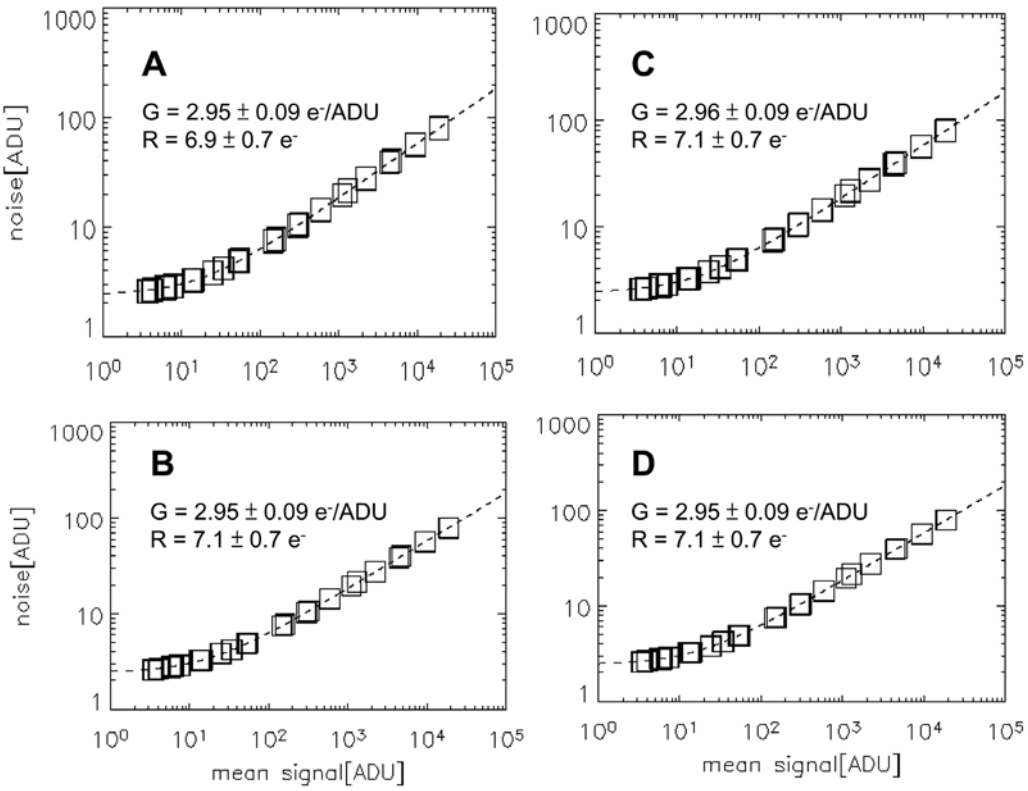

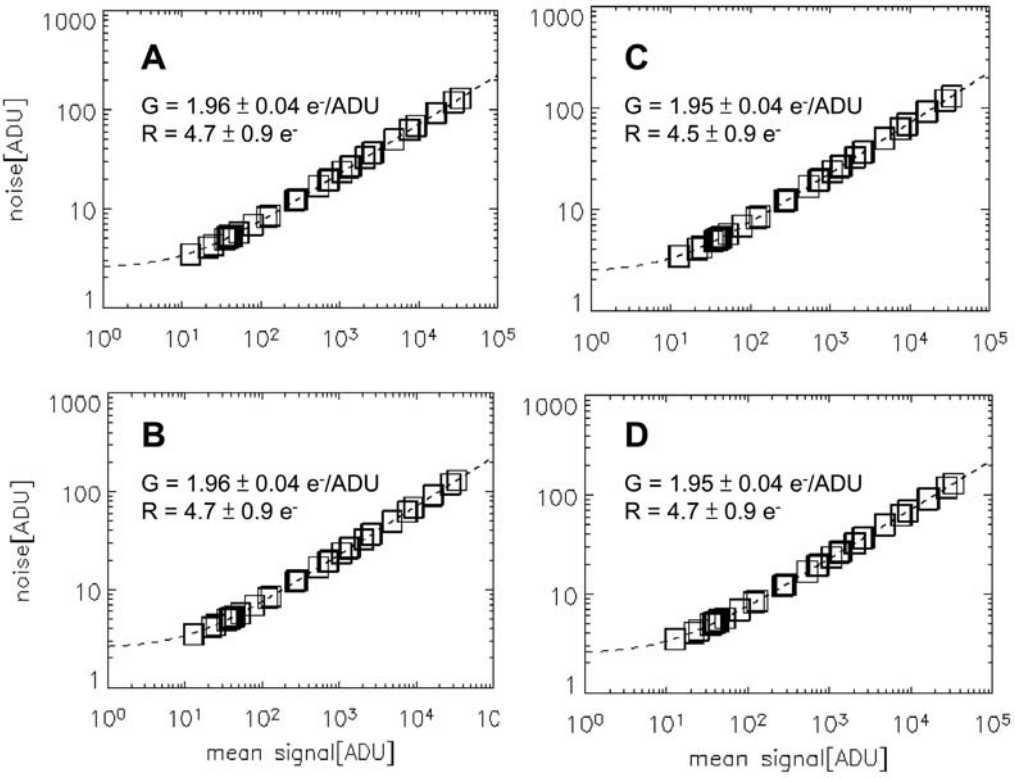

Fig. 3: The gain and readout noise of different regions for slow mode. Legend is as the same as Fig. 2.

Table 2. The average gain and readout noise of CCD PI1300B at -50°C.

		This work	Kinoshita et al. 2005
Fast mode	Gain	2.95 ± 0.05	3.0
	Readout noise	7.0 ± 0.3	7.1 – 7.4
Slow mode	Gain	1.95 ± 0.02	2.0
	Readout noise	4.6 ± 0.5	4.4 – 4.5

2.2 Dark Current

Dark current electrons are electrons generated by thermal influence within instrument. It is usually represented for the generation rate per second per pixel [e^-/s/pix], and has highly correlation with CCD temperature. The theoretical behavior of thermal electron production rate D against temperature can be expressed as Howell (2000),

$$D = CT^{\frac{3}{2}} \exp\left(\frac{-E_g}{2kT}\right) \quad (4)$$

$$E_g = 1.557 - \frac{7.021\times10^{-4}T^2}{1108+T} \quad (5)$$

Where T is temperature, E_g is the band gap energy for silicon, k is the Boltzmann constant, and the C value depends on CCDs.

We took dark frames using slow mode at the temperature from 0°C to -50°C. Six dark and six bias frames were taken for each temperature setting, then we subtracted bias from dark frames to calculate the dark current generation rate. Fig. 4 is our measurement and we use Eq. (4) to fit the data points. For CCD PI1300B, we get the C value = 7.24×10^7. Because the gain depends on the temperature, we used linear fitting to estimate gain values under different CCD temperature conditions, and the fitting result is showed in Fig. 5.

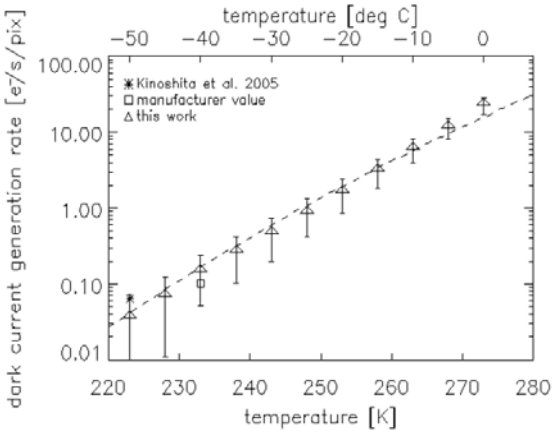

Fig. 4: Dark current performance of CCD PI1300B againsts the CCD cooling temperature. The dashed line is the fitting curve using Eq. (4).

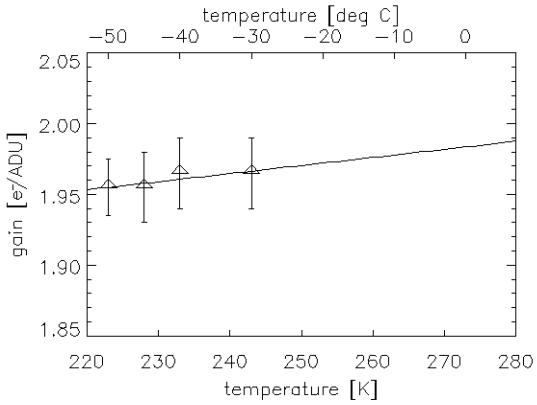

Fig. 5: Gain values at CCD temperature -50, -45, -40, -30°C are labeled as triangle symbols with error bars. The solid line is the linear fitting of these four gains, and we applied this fitting result to estimate dark current in Fig. 4.

3. Discussion

3.1 Comparison with the previous work

We can compare our results with the previous work by Kinoshita et al. (2005). For gain and readout noise, we divide four regions in each image frame in our processing as Fig. 1 shows. This method can help us to check uniformity of the CCD. From the results showed in Fig. 2 and Fig. 3, the CCD PI1300B still performs uniformity well. Our measurements, both for slow and fast mode, are within or quite similar with the range of previous work.

For dark current generation rate, we pick the values from previous work and the manufacturer to check our results. Both the previous work (D = 0.064 e^-/s/pix at -50°C) and the manufacturer value (D = 0.1 e^-/s/pix at -40°C) are within the error range of our measurements. Because we lack direct gain measurements except for -30, -40, -45, -50°C conditions, we adopted gain values from linear fitting based on these four measurements. It may cause errors, especially we have no actual measurements for temperature higher than -30°C.

The influence of dark current can be reduced with lower CCD temperature. Using Eq. (4) and (5), we can estimate dark current generation rate at lower CCD temperature. If the CCD camera can achieve the operation temperature of -100°C, dark current generation rate will be about 0.015 e^-/hr/pix. In other words, effect of dark current is negligible even under long time exposure as one hour.

3.2 Comparison with other instrument

In order to show the comparison between PI1300B and other instruments, here we also summarize the signal-to-noise ratio (SNR) calculations of PI1300B and the other CCD camera once used by LOT.

The previous CCD camera mounted on LOT was AP8, which was manufactured by Apogee Instruments Inc., and became backup camera after PI1300B has started to serve as a main instrument. Kinoshita et al. (2004) has measured its basic performance. AP8 only has one readout mode for 35 kHz sampling. Its gain was estimated as 4.4 ± 0.4

e^-/ADU, and the readout noise was 15.7 ± 4.7 e^-. The dark current generation rate of AP8 was measured as 0.49 e^-/s/pix for the CCD temperature -45°C. Comparing to AP8, PI1300B has much lower readout noise and dark current generation rate. We can use the CCD Equation as Eq. (6) to estimate difference of signal-to-noise ratio between these two CCDs (Mortara and Fowler 1981; Howell 2000),

$$\frac{S}{N} = \frac{N_S}{\sqrt{N_S + n_{pix}(N_B + N_D + N_R^2)}} \qquad (6)$$

Where N_S is the total number of photons from the target, n_{pix} is the number of pixels for calculation, N_B is the total number of photons per pixel from background sky, N_D is the total number of dark current electrons per pixel, N_R is the total number of electrons per pixel from readout noise. First of all, we assume 300 seconds integration in V-band for a source which magnitude is 20 and seeing is 1.5 arcseconds, and then we insert dark current generation rate and readout noise to calculate the ratio of PI1300B to AP8. Under the condition defined above, PI1300B at slow mode achieves 1.1 times higher signal-to-noise ratio than that of AP8.

Similar calculations under different conditions can be made. Fig. 6 shows the signal-to-noise ratios of PI1300B and AP8 with different integration time for a 20 magnitude target. We take ratios of SNRs achieved by PI1300B and AP8, and then Fig. 7 is constructed. Fig. 7 demonstrates the ratio of SNRs achieved by PI1300B and AP8 for different target magnitudes under the integration time of 30, 60, 120, and 300 seconds. We can see that the ratio of SNRs achieved by PI1300B and AP8 are about 1.06 for magnitude range between 12 to14, and become larger when fainter objects are observed. For example, the difference is as large as 15% for 18 magnitude target with 120 seconds integration time. The parameters for the calculation of SNR and limiting magnitude are listed in the Table 3.

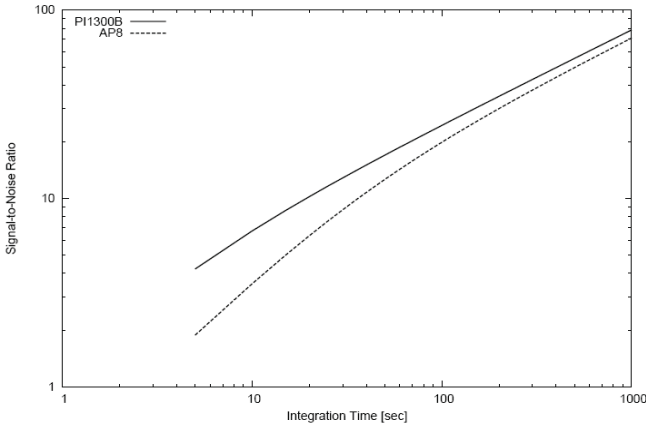

Fig. 6: The signal-to-noise ratio of PI1300B and AP8 versus different integration time for a 20 magnitude target.

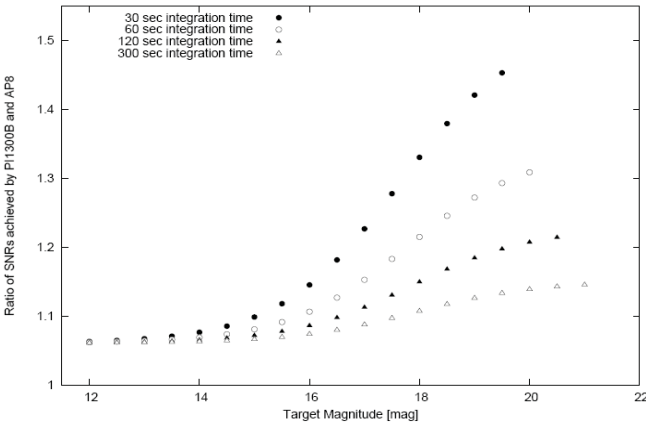

Fig. 7: The ratio of SNRs achieved by PI1300B and AP8 versus target magnitude. Different symbols of data points represent different integration time.

4. Conclusion

We have measured the gain, readout noise of CCD camera PI1300B at 1 MHz and 50 kHz readout mode. Under the CCD cooling

Table 3. Parameters for the Calculation of the relation between SNR and limiting magnitudes.

	AP8	PI1300B
Quantum Efficiency	0.8	0.9
Dark current [e^-/s/pix]	0.49	0.07
Readout noise [e^-]	15.7	4.6
Pixel scale [arcsec/pix]	0.619	0.516
PSF size [arcsec]	1.5	
Aperture size [arcsec]	2.25 (PSF size × 1.5)	
Central wavelength of V-band [Å]	5500	
Bandwidth of V-band [Å]	900	
Zero magnitude flux at V-band [W /m^2/micron]	3.58×10^{-8}	
Sky background brightness at V-band [mag./arcsec^2]	21.0	

temperature of -50°C, the average gains are 1.95 ± 0.02 and 2.95 ± 0.05 e^-/ADU for slow and fast mode, respectively; The average readout noise is 4.6 ± 0.5, and 7.0 ± 0.3 e^- for slow and fast mode, respectively. We have also measured the dark current generation rate for slow mode at difference cooling temperatures. The average value is 0.04 ± 0.04 e^-/s/pix for -50°C. Our measurements are consistent with previous study (Kinoshita et al. 2005), and it is found the instrument is stably operated.

Acknowledgement

This work was partially supported by the project “Comprehensive Understanding of Solar System Small Bodies” (NSC 96-2911 –M -008 -015 –MY3) which Principal Investigator is Daisuke Kinoshita, and it is supported by National Science Council of Taiwan. During our observation, we received many helps from Lulin Observatory staff. Here we present our gratitude to Jin-Chiuan Du, Hao-Wei Shih, Jiun-Shiung Shih, and Rong-Jin Wang for their local support at Lulin Observatory.

References

Howell, S. B., 2000, *Handbook of CCD Astronomy*, Cambridge University Press

Kinoshita, D.; Chen, C.-W.; Lin, H.-C.; Lin, Z.-Y.; Huang, K.-Y.; Chang, Y.-S.; Chen W.-P., 2005, *ChJAA*, 5, 3, 315.

Kinoshita, D.; Huang, K.-Y.; Wu, Y, -L.; Chang, Y.-S.; Urata, Y., 2004, *Annual Report of Lulin Observatory (2003)*, 30.

Martinez, P. and Klotz, A., 1998, *A Practical Guide to CCD Astronomy*, Cambridge University Press.

Mortara, L and Fowler, A., 1981, *Proc. SPIE*, 290, 28.

Motohara, K; Iwamuro, F.; Maihara, T.; Oya, S.; Tsukamoto, H.; Imanishi, M.; Terada, H.; Goto, M.; Iwai, J.; Tanabe, H.; Hata, R.; Taguchi, T.; Harashima, T., 2002, *PASJ*, 54, 2, 315.

超新星巡天與後續觀測

黃立晴、陳婷琬、陳英同、葉永烜、林宏欽、林啓生、蕭翔耀

巡天計畫：

台灣超新星巡天計畫始於 2003 年，中大天文所葉永烜教授所主持，在北京國家天文台的胡景耀博士、裘予雷博士的指導合作下，由碩士生陳英同，博士生黃麗錦、林忠義開始執行。大量的觀測資料使用程式自動化的分析，但仍需仰賴人工判別超新星候選者，由當時還是大學部學生的陳婷琬、李易錫加入團隊分析資料。爾後由升爲碩士生的陳婷琬帶領新的大學部專題生:劉東行、游鎮帆、陳惠雯爲發現新的超新星做努力。計畫進行到 2008 年，碩士生黃立晴加入，但有鑒於大型新一代巡天計畫(Pan-STARRS)-泛星計畫即將上線，歷時 5 年，獨立發現 15 顆新的超新星的台灣超新星巡天計畫宣告結束(參見圖一)。未來將全心做超新星光度變化之後續觀測，以期在超新星的研究課題上有更深入的了解與成果。

2008 年的元旦接續 2007 年的觀測，就在 12/31 的資料中發現了 2007 年最後一顆新的超新星，編號 SN 2007uz。但往後一年卻未再發現新的超新星，檢討後歸責於申請到的觀測次數少，在一年內只有 26 個晚上的觀測時間，平均每個月觀測一次(一次兩天);但又遇上梅雨季與颱風，天氣狀況不佳，實際可觀測天數就更少了。另外是觀測間隔週期過長，導致找到的超新星候選者已被其他人通報發現，例如 SN 2008if。

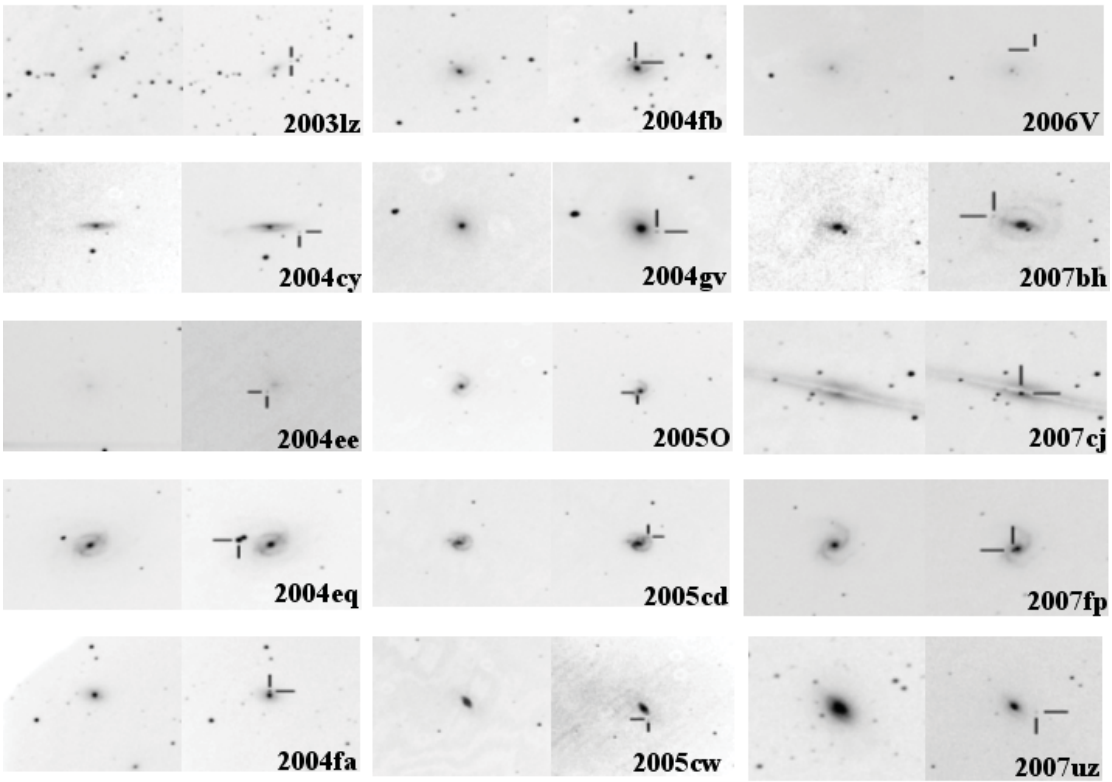

(圖一) 台灣超新星巡天計畫發現的 15 顆超新星影像。

後續觀測：

我們選擇明亮的 IIn 型超新星進行後續光度變化的觀測，使用 SLT 與 LOT 進行此項計畫。其中一顆目標爲超新星 SN 2008ip， 於 2008 年 12 月 31 日由 Takao Kobayashi 發現，其宿主星系爲 NGC4846 (z=0.015124)，天球座標爲 R.A. = 12h57m50s.20, Dec. = +36°22'33".5，發現時的視星等約 15.5 等。

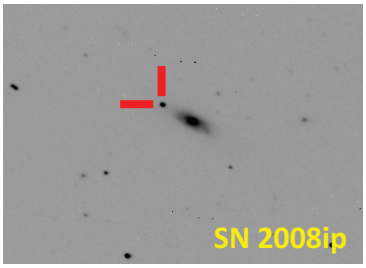

(圖二) SLT 在 2009 年 1 月 6 日以 R 波段拍攝的 SN2008ip，以紅色短線標示其位置。

使用 SLT 及 LOT 對 SN2008ip 進行後續觀測，目前得到 18 個資料點，(圖三)爲其光度變化曲線。

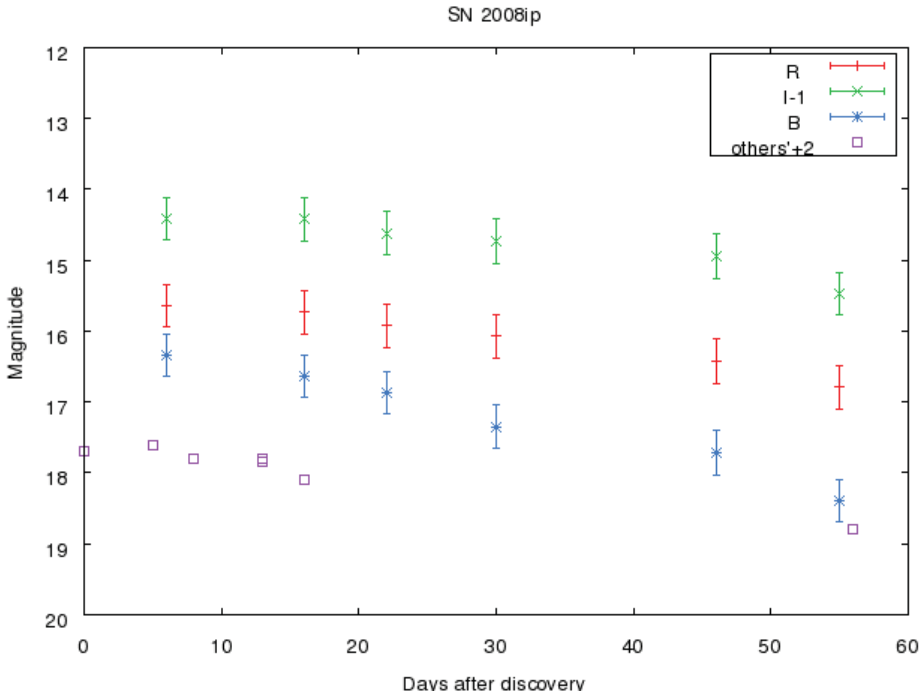

(圖三) 超新星 SN2008ip 在 B、R、I 三個波段的光變曲線。橫軸爲以發現日爲零點的時間軸，單位爲日，縱軸爲視星等。藍色代表 B 波段，紅色代表 R 波段，綠色代表 I 波段。誤差來自於星等轉換（依 USNO-B1 星表做修正）與測光誤差。另外的紫色曲線資料來源於 SN 2008ip 網站: http://www.astrosurf.com/snweb2/2008/08ip/08ipMeas.htm。

Extended Hα halo distribution of planetary nebula with binary nucleus — NGC 1514

香港大學物理系　夏志浩

（1）光暈(Halo)的形成原因與重要性：

根據恆星演化的模型，當恆星演化至水平分支(Horizontal Branch)末期，此時恆星核心的碳、氧核將燃燒殆盡，恆星的核心勢必會收縮，以提升外面殼層的壓力、溫度，因此核心外面的氦殼開始燃燒， 最內部碳氧核的質量增加並且收縮，但由於恆星外部殼層繼續燃燒而恆星的光度增加， 進而使得恆星的殼層膨脹，此時恆星結構處於不穩定的狀態，所以會產生一連串的脈動。這個階段我們稱爲“漸進巨星分支” ，米拉型(Mira) 變星就是這個階段的星體。

根據近年來紅外及毫米波段的觀測顯示，處於AGB 階段恆星的質量損失率(Mass loss Rate)約爲10^{-4}~10^{-5} $M_{\odot}$/yr，這個質量損失率要比一般主序星的質量損失率(10^{-8} $M_{\odot}$/ yr）要大很多， 這麼大的質量損失(Mass loss)也就產生了恆星風(AGB wind；Halo)，而將恆星外面的殼層及周圍的塵埃慢慢吹開， 進而讓內部核心慢慢的露出來。

至於AGB星及其環繞在外圍光暈(Halo)的形態，更是一件有趣的事情，但是，Kwok (2000)利用哈伯太空望遠鏡針對一些原行星狀星雲(PPNe)進行觀測，結果他發現在原行星狀星雲的核心部位是呈現雙極型(Bipolar)，這也就是說行星狀星雲質量損失的方式可能是在AGB的晚期才有明顯的改變(Balick, & Frank 2002)，究竟到底發生什麼事情而使得行星狀星雲的形態改變？一般相信，這與行星狀星雲的中心星爲雙星系統有密切的關連(Soker, 1997)。

我們藉由行星狀星雲的的模型(ISW model)可以知道-行星狀星雲將有較暗的光暈存在(Faint Halo)。而這些光暈存在正是代表著行星狀星雲過去的演化歷史，因爲這些Halo是來自於行星狀星雲前身(漸進巨星分支或是後漸進巨星分支)的質量損失，而這些黯淡的光暈存在行星狀星雲四周這麼長久的時間，有沒有可能它們會與行星狀星雲周圍的星際介質(Interstellar Matter)產生作用呢？事實上，在過去這幾年的時間裡，隨著天文儀器的進步，要把大尺寸的行星狀星雲拍好，已經不是一件難事了！

而在這些行星狀星雲的影像中，有些影像顯示的一些非常有趣的結構或現象。如果行星狀星雲的光暈真的與星際介質(Interstellar Matter)產生交互作用的話，我們勢必會看到一些特徵的結構出現; 比如可以見到光暈的部份會有塊狀、碎片或是絲狀(Filaments)結構出現。不論行星狀星雲是否與星際介質(ISM)進行交互作用，我想這些現象與結構都值得我們加以探討！

（2）行星狀星雲 NGC 1514 的一些性質：

我們之前先分析了行星狀星雲 NGC 1514 的光譜(如下圖一)，經由光譜型態比對之後發現行星狀星雲 NGC 1514 中心星可能爲一組雙星系統(週期約爲 0.4 天)，我們從其光譜中得知，其

伴星可能是一顆光譜型爲 A6 的星，也唯有如此，才能使得我們所觀測到的光譜吸收線才能夠如此的深。除此之外，在影像上 NGC1514 呈現了兩組較亮的團塊，這些團塊分佈的狀況是否與中心星的質量損失有關，這也是一個我們想要研究的課題。

(3) 行星狀星雲 NGC 1514 的多波段觀測：

由於觀測其間天氣不穩定，所以我們只有半個晚上能夠執行我們原先的觀測計畫，如果要按照原先觀測計畫，則必需要連續數天在 H α 波段的觀測，所以，我們臨時改變觀測計畫，改爲數個窄波段影像的觀測([OⅢ]、[NII]、H α 、[SII] …etc)；雖然這也需要極長時間的觀測，但是，也能夠提供給我們一些訊息，比如：一些低游離態物質分佈的狀況、電子密度(Ne)及電子溫度(Te)的狀況…等等。[OIII]、H α 、[NII]、[SII]窄波段影像分別列於(圖二、圖三、圖四、圖五)，由這些窄波段影像中幾乎找不到特殊低游離態的物質存在，這也意味著這個行星狀星雲是高游離態；不管如何，進一步的訊息必須依賴各窄波段的比值(ex: [OIII]/[NII] …etc)才能夠加以精確的判定。

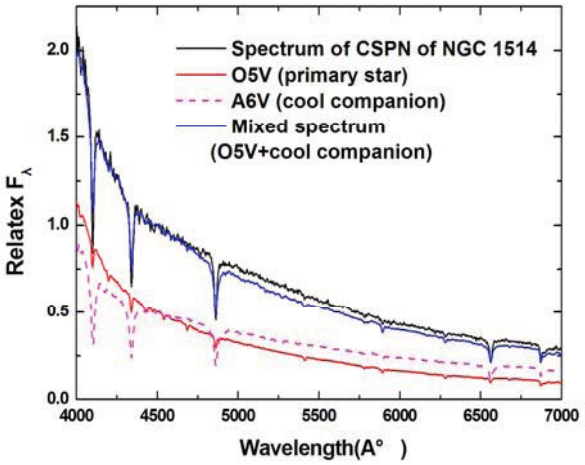

(圖一). NGC 1514 中心星的光譜，我們可以從其光譜中將其較冷伴星的光譜分離出來。

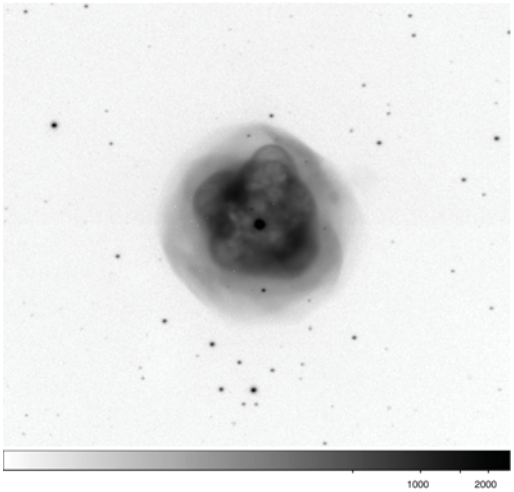

(圖二). NGC 1514 在[OIII] 波段的影像

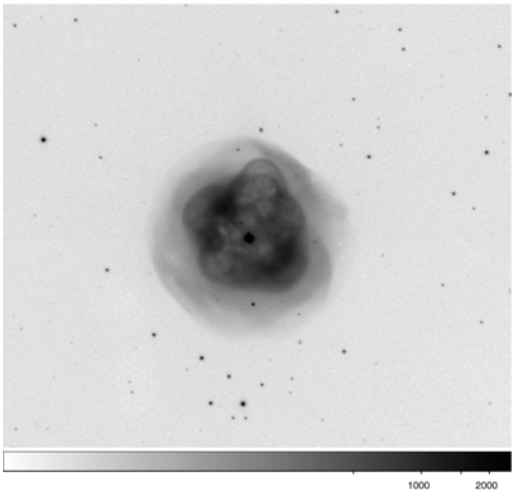

(圖三). NGC 1514 在 H α 波段的影像

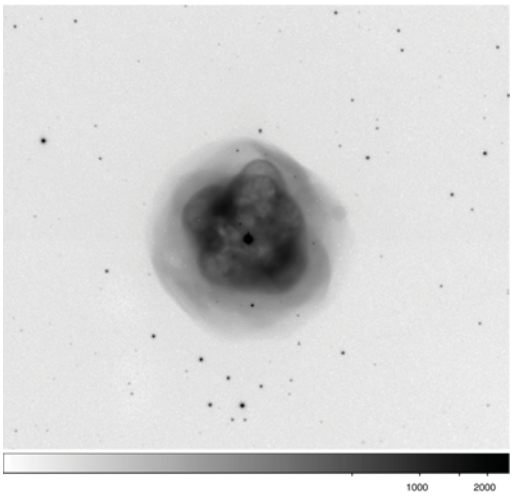

(圖四). NGC 1514 在[NII] 波段的影像

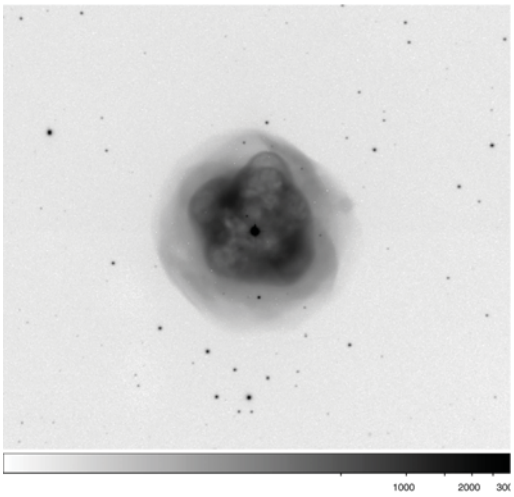

(圖五). NGC 1514 在[SII]波段的影像

TAOS at Lulin in 2008

S.-K. King[a] (金升光), C. Alcock[b], T. Axelrod[c], F. B. Bianco[d,b], Y. I. Byun[e], Y.-H. Chang[f] (張永欣), W.-P. Chen[f] (陳文屏), K. H. Cook[g], R. Dave[d], J. Giammarco[d], L.-J. Huang[a] (黃麗錦), D. W. Kim[e], T. Lee[a] (李太楓), M. J. Lehner[a,b], H.-C. Lin[f] (林宏欽), J. Lissauer[h], S. L. Marshall[i,g], S. Mondal[f], T. C. Nihei[d,b], I. de Pater[j], P. Protopapas[b], J. Rice[k], M. E. Schwamb[l], A. Wang[a] (汪仁鴻), S.-Y. Wang[a] (王祥宇), C.-Y. Wen[a] (溫志懿) and Z.-W. Zhang[f] (張智威)

[a] Institute of Astronomy & Astrophysics Preparatory Office, Academia Sinica, Nankang, Taiwan, ROC
[b] Harvard-Smithsonian Center for Astrophysics, Cambridge, MA, USA
[c] Steward Observatory, University of Arizona, AZ, USA
[d] Department of Physics & Astronomy, University of Pennsylvania, PA, USA
[e] Department of Astronomy, Yonsei University, Korea
[f] Institute of Astronomy, National Central University, Chung-Li, Taiwan, ROC
[g] Institute of Geophysics & Planetary Physics, Lawrence Livermore National Laboratory, CA, USA
[h] NASA Ames Research Center, Mountain View, CA, USA
[i] Kavli Institute for Particle Astrophysics and Cosmology, Menlo Park, CA, USA
[j] Department of Astronomy, University of California, Berkeley, CA, USA
[k] Department of Statistics, University of California, Berkeley, CA, USA
[l] Division of Geological and Planetary Sciences, California Institute of Technology, Pasadena, CA, USA

1. A statistics of the TAOS zipper observation in 2008 is shown in Figure 1. The total observation time (spending in taking TAOS zipper images on a TAOS field) is 878.6 hours where auto-focus, pointing, slewing, special events (e.g. GRB, asteroid, exoplanet, etc.) and overhead are *not* included. Those zipper hours includes 1132 zipper runs in 188 days, where zipper hours longer than 1.5 hours were obtained in 152 days. As TAOS-C running on-line since last August, we have four telescopes running for 349.4 hours in 2008. Joint observation using TAOS-A, B, and D lasted for 615.3 hours (which was 309.7 hours in 2007). For 855.6 hours, we have more than one telescope running (which was 444.8 hours in 2007). Data is under processing.
2. For a possible variable star study, 52 TAOS fields were observed. Among them, 46 have zipper data longer than 1.5 hours from more than one telescope. The next table shows the zipper hours (from more than one telescope) of the seven most observed TAOS fields in 2008.

Field	F060	F054	F133	F074	F043	F146	F061
hours	217.0	118.2	63.3	47.8	47.2	46.1	43.4

3. The first set of data, which was taken in 2005 and 2006, shows no significant event. (See Zhang et al. 2008)
4. Using a special de-trending algorithm, an expected exoplanet event was observed. A flux drop of about 1% was detected. The light curve is shown in Figure 2. The de-trending is described in Kim et al. 2008.

TAOS and Related Publications in 2008 (journal article, preprint, thesis)

1. The Taiwanese-American Occultation Survey: The Multi-Telescope Robotic Observatory, Lehner, M. J. et al., arXiv:0802.0303v1 [astro-ph] (in press)
2. The Early Optical Brightening in the GRB071010B, Wang, J. H. et al., ApJ, 679, L5 (DOI: 10.1086/588814)
3. A Study of the Diffraction Pattern by Trans-Neptunian Objects of Irregular Shape, Kao, Chih-Hao (高至豪), Master's Thesis (in Chinese), National Taiwan University, July, 2008
4. First Results from the Taiwanese-American Occultation Survey (TAOS), Zhang, Z.-W. et al., ApJ, 685, L157 (DOI: 10.1086/592741)
5. De-Trending Time Series for Astronomical Variability Surveys, Kim, Dae-Won et al., arXiv:0812.1010v1 [astro-ph]

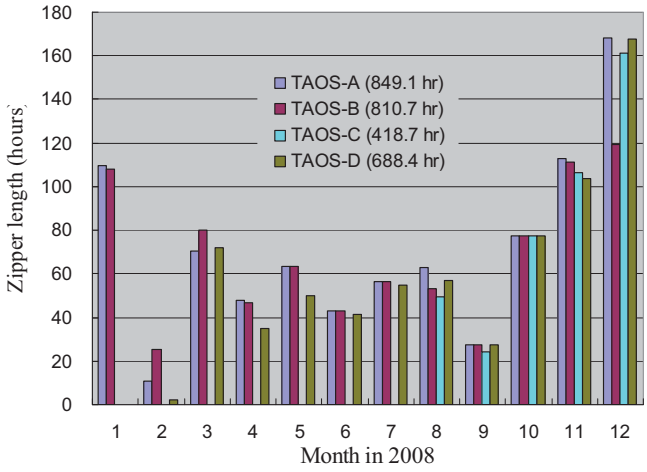

Figure 1. The total hours of TAOS zipper mode data taken by four TAOS telescopes in 2008.

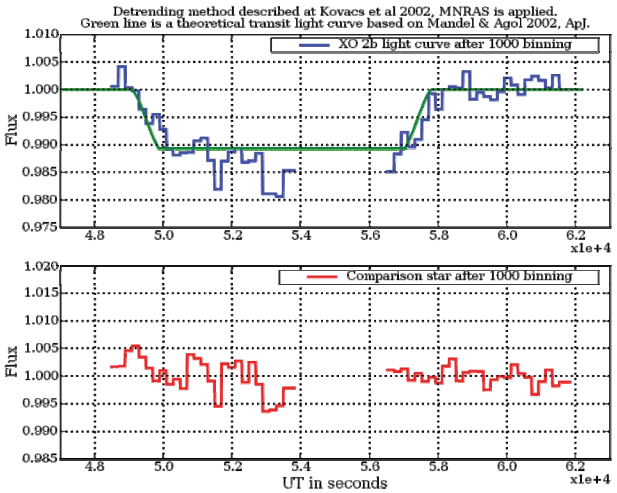

Figure 2. As a test, a predicted transit of an exoplanet XO-2b was observed by the TAOS telescopes on Feb. 9, 2008. The transit depth ~1.15% was well resolved after de-trending and binning. The transit duration was 145 minutes. A 45-minute data in the middle was lost due to manual error. A light curve of a comparison star is shown at the bottom. (Figure prepared by Pavlos Protopapas & Dae-Won Kim.)

2008 年度鹿林巡天成果報告

葉泉志[1]，葉永烜[2]，林宏欽[2]，林啓生[2]，蕭翔耀[2]，施佳佑[2]，石遼珊[3]

1. 中山大學環境科學與工程學院
2. 國立中央大學天文研究所
3. 中山大學物理科學與工程技術學院

從 2008 年 2 月 1 日至 2009 年 1 月 31 日，我們進行了大約 80 個夜晚的觀測，共發現獲得暫定編號的新小行星共 109 顆，獲得觀測資料 21664 條，其中包括 6493 顆小行星、4 顆彗星及 1 顆天然衛星，另外對 6 顆近地小行星進行了測光工作，其中關於 1998 BE7 和(162900) 2001 HG31 的測光結果已經發表在 *Minor Planet Bull.* **39** 上。用於檢測時變天體的程式也在 2008 年 4 月研發完畢並投入使用。

自 2006 年 3 月 5 日開始運行至 2009 年 1 月 31 日止，鹿林巡天共進行了大約 400 個夜晚的觀測，發現獲得暫定編號的新天體 779 顆，包括 775 顆小行星、1 顆新彗星和 3 顆彗星碎片，其中 152 顆小行星已獲得永久編號（其中 62 顆有命名權），12 顆已命名。

MULTI-COLOR PHOTOMETRY OF 1998 BE7

Quanzhi Ye
Department of Atmospheric Science, Sun Yat-sen University, Guangzhou, China (mainland)
tom6740@gmail.com

Liaoshan Shi
School of Physics and Engineering, Sun Yat-sen University, Guangzhou, China (mainland)

Wing-Huen Ip
Graduate Institute of Astronomy, National Central University, Chung-li, Taiwan

Hung-Chin Lin
Graduate Institute of Astronomy, National Central University, Chung-li, Taiwan

(Received: 2008 Nov 11 Revised: 2008 Nov 22)

Multi-color photometry of the high orbital eccentricity asteroid, 1998 BE7, was conducted in the course of Lulin Sky Survey (LUSS) from 2008 October 1 to November 5. These data allowed determination of the rotation period to be 6.6768 ± 0.0001 h, as well as color indices of B-V = 0.727 ± 0.063, V-R = 0.405 ± 0.008, and V-I = 0.897 ± 0.009. These indices suggest that 1998 BE7 could be a D-type asteroid. Assuming a slope parameter G = 0.086 and albedo (p_V) 0.058 ± 0.004, the absolute magnitude H is estimated to be 14.773 ± 0.323, with a corresponding diameter of 5.0-7.0 km.

Asteroid 1998 BE7 was discovered by the NEAT program on 1998 January 24 (Williams, 1998) with orbital elements of a = 3.08, e = 0.51. It made close approaches to Earth in 1998 and 2003 but no photometric observations were made due to unfavorable positions. The asteroid made another close approach to the Earth in 2008 November, reaching V = 15.3 mag – the brightest over the decade. Hence, it was chosen for photometric purpose in the course of Lulin Sky Survey (LUSS). From 2008 October 1 to November 5, 10 nights of data were obtained using our 0.41-m Ritchey-Chretien telescope equipped with a 4-mega pixel back-illuminated CCD. Data from two nights were calibrated with standard fields. The data were reduced with Raab's *Astrometrica* and Warner's *MPO Canopus*. The observations clearly yielded a period of 6.6768 ± 0.0001 h (Figure 1). Considering the relatively large magnitude amplitude (about 0.97 mag) and phase angle of the target at the time (~ 25°), it can be suggested that 1998 BE7 has an elongated shape.

BVRI-filter observations of 1998 BE7 and Landolt fields were made on 2008 November 5. This enabled us to measure the asteroid's color indices. The results are B-V = 0.727 ± 0.0.063, V-R = 0.405 ± 0.008, and V-I = 0.897 ± 0.009. From the asteroid taxonomic method describe by Bus and Binzel (2002), it can be inferred that the color indices of BE7 are consistent with a D-type asteroid. Since VR-filter observations of BE7 and Landolt fields were obtained on both 2008 October 27 and November 5, it was possible to compute the absolute magnitude based on a given slope parameter G. Assuming G = 0.086 (Harris, 1989), the absolute magnitude (H) is estimated to be 14.773 ± 0.323 (Figure 2). We should point out that there is a systematic error among the data due to unsatisfactory quality of the standard field observations, which might be as large as 0.15 mag.

The approximate size of an asteroid can be determined by (Warner 2007):

$$\log D = 3.1235 - 0.2H - 0.5\log(p_V)$$

Where D is diameter of the asteroid in km, H is absolute magnitude, and p_V is albedo of the asteroid. Assuming the asteroid's albedo is 0.058 ± 0.004, which is based on the assumed type, the diameter is estimated to be 5.0-7.0 km.

The lack of calibrated observations caused some difficulties when doing our lightcurve analysis, specifically because different solutions were possible by simply adjusting nightly zero points. This becomes a significant issue for targets without a prominent feature in their lightcurve. We recommend that lightcurve data should always be calibrated, at least on an internal system, in order to rule out false solutions.

Acknowledgements

We would like to thank Alan W. Harris and Petr Pravec for their valuable suggestions and comments and Brian D. Warner and Herbert Raab for their data reduction software. We also thank Hsiang-Yao Hsiao and Chi Sheng Lin for their assistance on obtaining the observations. This work is supported by a 2007 Gene Shoemaker NEO Grant from the Planetary Society. The 0.41-m Ritchey-Chretien telescope is operated with support from the Graduate Institute of Astronomy, National Central University.

Reference

Bus, S.J., and Binzel, R.P. (2002). "Phase II of the Small Main-Belt Asteroid Spectroscopic Survey: A Feature Based Taxonomy." *Icarus* **158**, 146-177.

Harris, A.W. (1989). "The H-G Asteroid Magnitude System: Mean Slope Parameters." *Abstracts of the Lunar and Planetary Science Conference* **20**, 375.

Warner, B.W. (2007). "Initial Results from a Dedicated H-G Project." *Minor Planet Bulletin* **34-4**, 113-119.

Williams, G.V. (1998). "1998 BE7" *MPEC* 1998-B28.

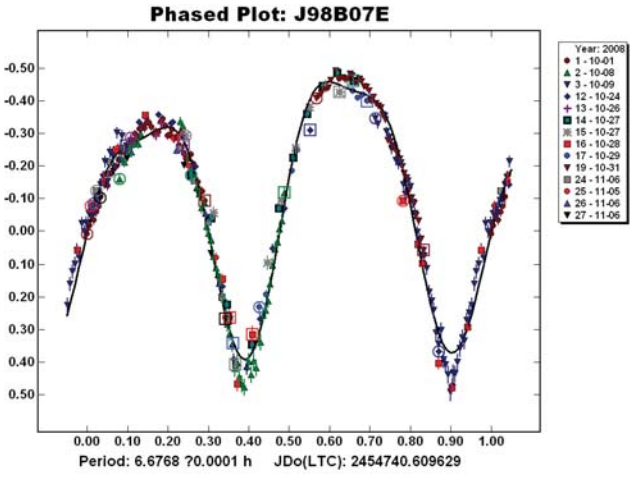

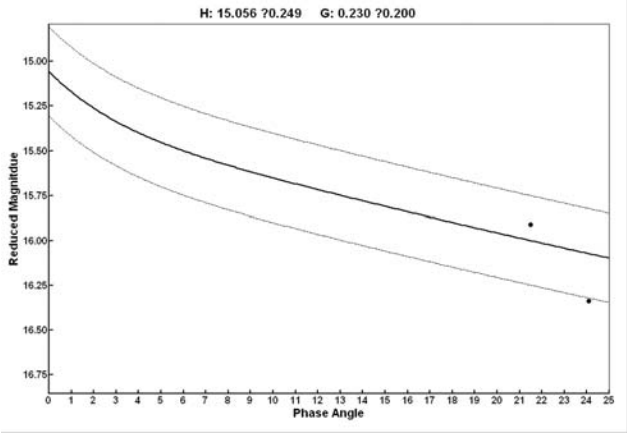

DIGEST OF TEN LIGHTCURVES FROM MODRA

Adrián Galád
Modra Observatory
Department of Astronomy, Physics of the Earth, and Meteorology
FMFI UK, 842 48 Bratislava, SLOVAKIA
and
Astronomical Institute AS CR, 251 65 Ondřejov,
CZECH REPUBLIC
galad@fmph.uniba.sk

(Received: 2009 Jan 11)

Lightcurve analysis of asteroids 3316 Herzberg, 6377 Cagney, 12880 Juliegrady, 14040 Andrejka, (24222) 1999 XW74, 32776 Nriag, (51840) 2001 OH65, (57478) 2001 SW151, (153462) and (190637) is reported. The lightcurves are noisy since most of asteroids were fainter than magnitude 16. The long rotation period of 14040 Andrejka was estimated with the help of MPC data.

Rotations of asteroids of magnitude 16 are usually studied with a 0.60-m f/5.5 telescope and AP8p CCD-camera at Modra. However, the 25'x25' field of view often enables us to study other targets down to magnitude 18 at the same time. The rotation period of such faint asteroids can usually be found only if the amplitude of their lightcurves is large because the noise does not then dominate the total amplitude of the lightcurve. Most of the asteroids presented here are faint with previously unknown rotational properties. The results of lightcurve analysis are summarized in Table I and appropriate lightcurves are in the figures, which include correction for light-travel time.

3316 Herzberg. Only tentative results on the order of 9.6 h for the rotation period and a low amplitude were obtained based on previous observations by Bernasconi in 2006 (Behrend 2009). More recent linked observations at Modra did not shed more light on the result. Since the amplitude of the lightcurve seems to be low (< 0.15 mag), many possible rotation periods fit data. The new tentative result presented here is visually the best one within 2-18 h range. However, linkages to the same instrumental magnitude scale were not perfect and even a tiny shift of individual sessions, or enhancing order of the Fourier fit, produces a completely different best solution.

6377 Cagney and 32776 Nriag. These two asteroids were observed on three consecutive nights as they lay in the same field of view. Their rotation periods were unambiguously derived from those sessions.

12880 Juliegrady. Ascending and descending branches of the asteroid's lightcurve seem to have been obtained during two consecutive nights. The object was extremely faint (fainter than 18 mag), but the large amplitude of the lightcurve was apparent. The period was estimated assuming two extremes in the composite lightcurve.

14040 Andrejka. As a first discovery with a provisional designation and named after my wife, this object was of special personal interest. It reaches magnitude 17 at a favourable opposition, such as in 2008. Three linked sessions at the end of November revealed just the ascending branch of the lightcurve, indicating a long rotation period (P > 200 h). Two previous short sessions were not linked, so they were of limited use, if at all. No other data were obtained from Modra due to weather and other observations of higher priority. However, the large amplitude and long period encouraged me to examine some observations sent to MPC having one-decimal magnitude estimates. Among them were observations in the V band covering six nights from Steward Observatory, Kitt Peak-Spacewatch, that were promising. In combination with the Modra observations these led to P ~ 310 h. Two more stations, Mt. Lemmon Survey and Catalina Sky Survey, also reported observations in the V band. Despite having only two sessions provided by each of these stations, they were not in contrast with previous estimate for P. Each of those observations was just shifted by +0.20 mag to fit other data better. The fit was not expected to be perfect in any case since such small, long-period objects are usually tumblers.

(24222) 1999 XW74 and (51840) 2001 OH65. While three sessions were done every other night, some ambiguity in the rotation period exists for both 18 mag targets. Except for the results reported here, a period of 3.6390 h fits data similarly well for the former, while one of 3.215 h fits just as well for the latter. Moreover, (51840) was at the edge of images in the first session.

(57478) 2001 SW151. This asteroid was also a faint 18 mag target with large lightcurve amplitude. Its rotation period was unambiguously derived from just one long session covering more than a full cycle. The second session on the following night refined the previous result.

(153462) 2001 RE2 and (190637) 2000 WE155. Errors for these two 19 mag asteroids were roughly 0.2 mag. Data were linked to the same instrumental magnitude scale since the sessions were obtained on consecutive nights. Despite the fact that the amplitude of the lightcurves appear to be large, they are only estimated and so the rotation periods are far from being unambiguous. Except for the presented tentative results, a period of 8.90 h fits data similarly well for the former, while one of 15.2 h also fits for the latter.

Acknowledgements

I'm grateful to Petr Pravec, Ondřejov Observatory, Czech Republic, for his ALC software used in data analysis. The work was supported by the Slovak Grant Agency for Science VEGA, Grant 2/0016/09 and the Grant Agency of the Czech Republic, Grant 205/09/1107.

References

Behrend, R. (2009). Observatoire de Geneve web site. http://obswww.unige.ch/~behrend/page_cou.html

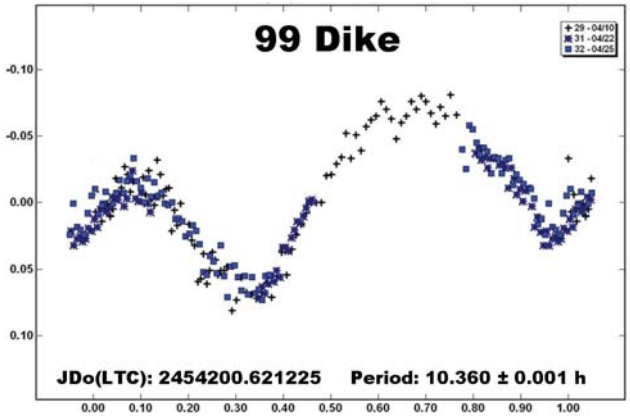

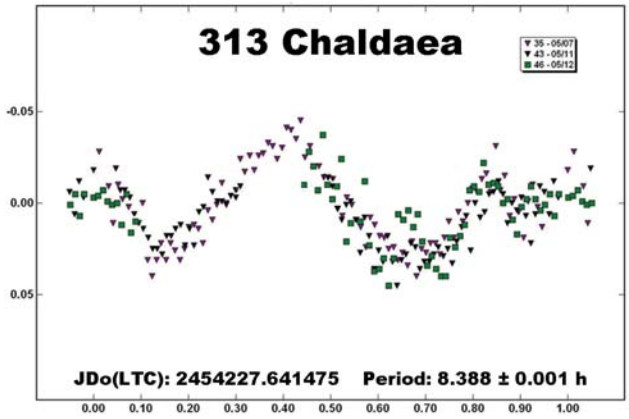

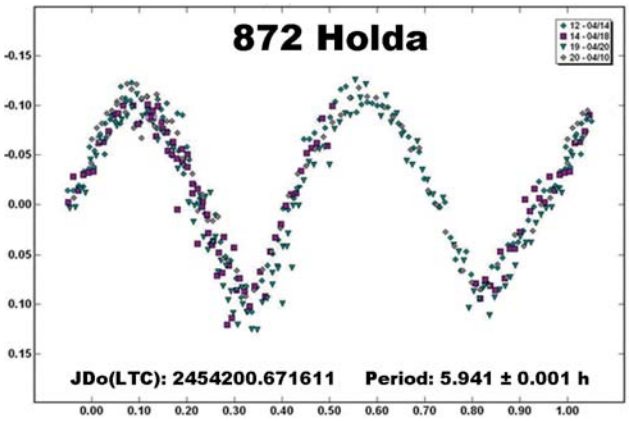

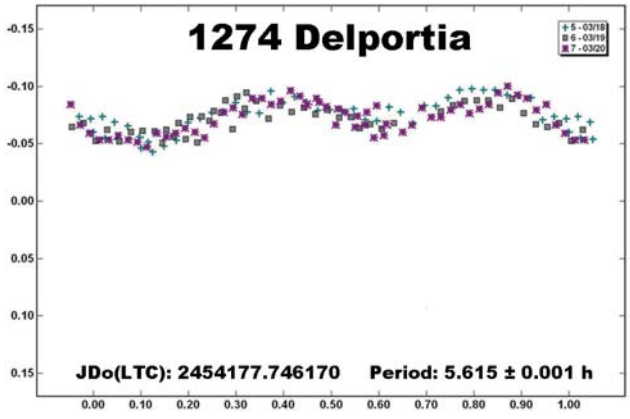

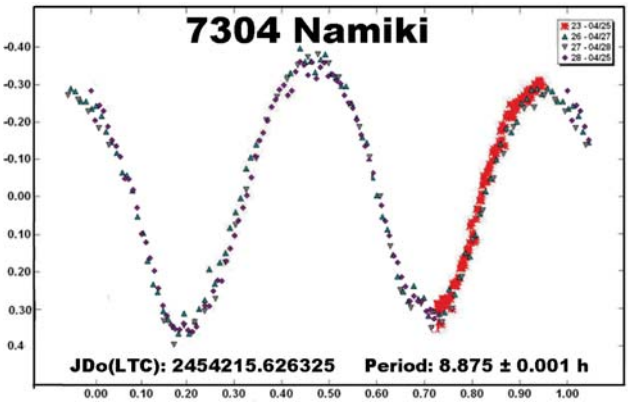

THE CURIOUS CASE OF (162900) 2001 HG31

Brian D. Warner
Palmer Divide Observatory/Space Science Institute
17995 Bakers Farm Rd., Colorado Springs, CO 80908
brian@MinorPlanetObserver.com

Quanzhi Ye
Department of Atmospheric Science, Sun Yat-sen University
Guangzhou, China (mainland)

Liaoshan Shi
School of Physics and Engineering, Sun Yat-sen University
Guangzhou, China (mainland)

Hung-Chin Lin
Graduate Institute of Astronomy, National Central University
Chung-li, Taiwan

Robert D. Stephens
Goat Mountain Astronomical Research Station (GMARS)
Rancho Cucamonga, CA 91737 USA

(Received: 2008 Dec 31)

The near-Earth asteroid (162900) 2001 HG31 was observed by the authors in 2008 October and November. Indications are that the asteroid may be in non-principal axis rotation. Depending on which subset of available data was used, a period of either 59.58 ± 0.01 h or 60.57 ± 0.01 h was found, each with a lightcurve amplitude of 0.60 ± 0.02 mag. No simple, single period could be found that satisfied all observations.

Near-Earth Asteroid (NEA) (162900) 2001 HG31 was observed by the authors in 2008 October and November. With an H magnitude of 14.7 (IAU Minor Planet Center), the size of this object is likely in the range of 3 km. The specific observing dates and instrumentation are listed in Table 1. During the range of dates, the asteroid started at a phase angle (α) of approximately 14°, which decreased to α ~4° on Nov. 15, and increased to α ~ 14° at the end of the observing period. Observations by BDW and RDS were unfiltered with exposures of 240 s and 180 s, respectively. QY observed with V and R filters using exposures of 120 s. All images were measured using *MPO Canopus*, which was also used for period analysis using the Fourier algorithm of Harris et al. (1989).

Night-to-night calibration of the data sets from Warner and Stephens was done using the 2MASS-BVRI conversions developed by Warner (2007) and as described by Stephens (2008) while Ye used calibrations from a standard star reference field to place his observations on a standard system. Ye used his V and R observations from Nov. 4 to determine a V-R = 0.443 ± 0.005. The sessions within the independent data sets could be matched to within 0.03 mag in most cases. However, the matching of the independent sets to a common zero point proved much more difficult and was so uncertain as to prevent unambiguous results. Using the single-period analysis method in *Canopus*, we found two periods that fit most (but not all) of the data when using the same subsets.

Using most of the data from only BDW and QY, we found a period of 59.58 ± 0.01 h with an amplitude of 0.60 mag. Using that same set plus one other session, Petr Pravec of the Astronomical Institute, Czech Republic, also found that period (private communications). That non-fitting additional session from PDO on Nov. 10, gave rise to the possibility that the asteroid was in non-principal axis rotation (NPAR, see Pravec et al., 2005). The lack of sufficient zero-point calibration across the entire data set prevented the determination of the independent periods of a so-called "tumbling" asteroid. In hopes of obtaining sufficient data that could be well-matched, Stephens observed the asteroid in late 2008 November. Using his data from Nov. 30 in combination with a different subset of the previously obtained data, we were able to determine a synodic period of 60.57 ± 0.01 h. Note that the zero-point calibration of some of the previous sessions had to be adjusted anywhere from 0.03 to 0.1 mag in order to obtain the new period. The amplitude of the curve remains at about 0.60 ± 0.02 mag. It's possible that a more thorough analysis using the entire data set with period search code designed to handle non-additive periods, as seen with tumbling asteroids, may find a solution that includes all data points. However, before that is possible, all the data would have to be placed on a common zero point with a much higher degree of certainty.

Acknowledgements

Funding for observations at the Palmer Divide Observatory is provided by NASA grant NNG06GI32G, National Science Foundation grant AST-0607505, and by a 2007 Gene Shoemaker NEO Grant from the Planetary Society. QY thanks Hsiang-Yao Hsiao and Chi Sheng Lin for their assistance on obtaining the observations. His work is at Sun Yat-sen University is supported by a 2007 Gene Shoemaker NEO Grant from the Planetary Society. The 0.41-m Ritchey-Chretien telescope at Lulin Observatory is operated with support from the Graduate Institute of Astronomy, National Central University.

References

Harris, A.W., Young, J.W., Bowell, E., Martin, L.J., Millis, R.L., Poutanen, M., Scaltriti, F., Zappala, V., Schober, H.J., Debehogne, H., and Zeigler, K.W. (1989). "Photoelectric Observations of Asteroids 3, 24, 60, 261, and 863." *Icarus* **77**, 171-186.

Stephens, R.D. (2008). "Long Period Asteroids Observed from GMARS and Santana Observatories." *Minor Planet Bulletin* **35**, 21-22.

Pravec, P., Harris, A.W., Scheirich, P., Kušnirák, P., Šarounová, L., Hergenrother, C.W., and 14 colleagues. (2005). "Tumbling asteriods." *Icarus* **173**, 108-131.

Warner, B.D. (2007). "Preliminary Results from a Dedicated H-G Project." *Minor Planet Bulletin* **34**, 113-119.

Observer	Dates (mm/dd/2008)	Inst.
Warner	10/27-11/02, 07, 08, 15	0.35-m SCT STL-1001E
Ye	11/03, 04, 06	0.41-m R/C 4-Mp CCD
Stephens	11/29, 30	0.35-m SCT, STL-1001E

Table 1. Observer details.

Date (mm/dd/2008)	Phase	PAB_L	PAB_B
10/27	13.7	47.8	0.8
11/15	4.3	53.7	3.8
11/30	13.6	58.6	6.8

Table 2. Observing circumstances for (162900) 2001 HG31 at the start, middle, and end of the observing sessions.

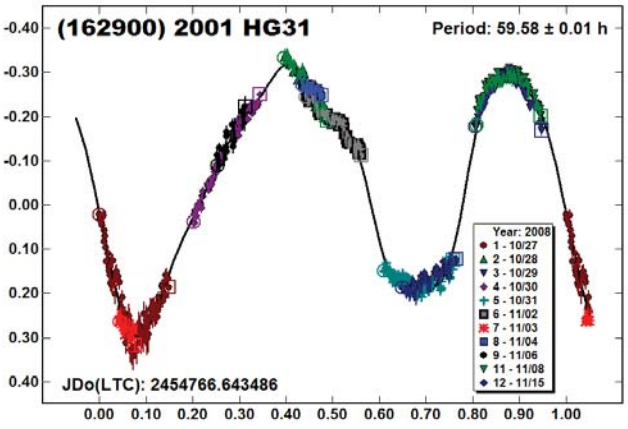

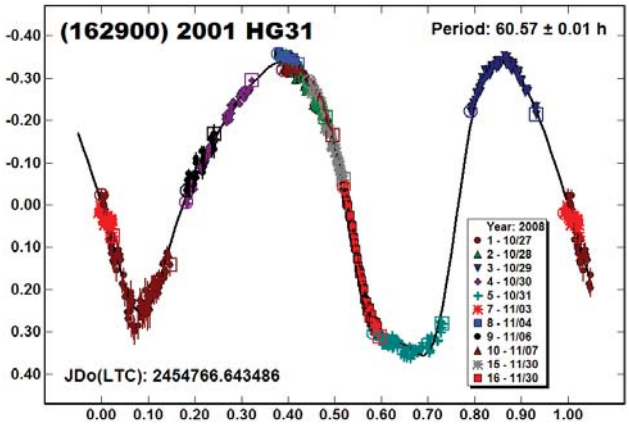

工作報告

鹿林兩米天文望遠鏡儀器研製計畫工作報告

2008 annual report of Lu-lin 2 meter telescope project for developing instruments

吳景煌(Jason Wu)

一、 簡介

本計畫經費來自國科會，計畫主持人為：黃崇源所長。共同主持人為：葉永烜、陳文屏、高仲明、周翊、木下大輔教授。

本計畫主要購置的設備為鍍鏡機、可見光多波段成像儀以及儀器實驗室的建立，本文將依序介紹上項工作內容與現況報告。

1. 鍍鏡機簡介（Coating facility）

兩米為本計畫天文望遠鏡主鏡的直徑，並且該鏡片預計重達1.7公噸以上，在未來建構天文台完成之後，一旦運到鹿林山上，運下山便極困難且風險高，故需設置鍍鏡機於兩米天文台站內，給予該鏡片定期的鍍膜更新。

另外，鏡片鍍膜會因為環境因素漸漸退化，所以世界上許多天文台，都擁有鍍鏡機，並在1到3年的週期重新給予鏡片鍍膜，以維持鏡片鍍膜與觀測品質。本鍍鏡機完成在兩米天文台後，將是本地區唯一海拔最高與最大單一鏡片的鍍膜機，並可兼容鹿林天文台其它較小尺寸鏡片的鍍膜工作，例如一米天文望遠鏡。設計上，並允許鍍鏡機可改變鍍膜材料，例如純鋁、純金或純銀靶材。

（An on-site coating facility is an essential equipment to maintain good performance for the optical/infrared telescope. Most ground-based telescopes mirror coatings are exposed to hostile environment, as the humidity, dust and reactive gases in the air corroding and tarnishing the surface. To keep the mirrors in sufficient high reflectivity for astronomical observations, re-coating every 1 to 3 years is necessary.

Almost all ground-based optical/infrared observatories have their on-site coating facilities to prolong the telescope's lifetime. The facility is required to have the ability to deposit high quality Aluminum (Al) or Silver (Ag) or Gold(Au) to the mirror surface.

For the coating facility of 2m telescope, it must equip with vacuum pumps to retain the pressure as low as 10^{-6} torr during re-coating, as well as a washing tower for stripping off the old coating from mirror and lifter or holder for moving the mirror. There is no such coating system meeting the requirements in Taiwan, and large risk of damage during the transportation, also time and cost consuming.

The facility is designed to locate at the first floor of the 2m telescope's building for convenience. Once the machine set up at Lulin observatory, it does not only serve

as a regular re-coating facility for 2m telescope but also provides coating operations for 1m telescope and other research equipments that require large coating facility in Taiwan.）

2. 可見光多波段成像儀簡介（4-color Simultaneous Imager）

傳統天文望遠鏡在觀測天體可見光不同波段的時候，採用更換濾鏡的方式，會造成每個成像之間除了時間的差異，還有環境因素的差異。

本計畫將設置的可見光多波段成像儀，設計上具備四波段同步觀測的分光鏡與濾鏡架構，將有幾項特色：這將是本地區目前唯一的可見光多波段成像儀、可同步取得四波段可見光的成像、更快速、更精確、更有效率、較不受環境因素影響、較容易的調校以及提升波長較長部分的靈敏度與其觀測的實現。

波長較長部分的觀測，將藉由購置具有深空乏光偶元件的攝像裝置，以及自行開發的全空乏（高阻）光偶元件的攝像裝置，並配以真空泵浦以及機械式冷卻機降到攝氏零下一百度，得以在鹿林天文台實現。這也將是本地區唯一具備的裝置。

（In astronomy, color measurements are often used to characterize physical properties of astronomical objects. As conventional method, one takes the first image with a filter, followed by the second image with another filter. This introduces a time lag between two images, and brings uncertainity in the measurements due to the sky condition change and intrinsic change of the brightness of the target.

We take a new approach for accurate and efficient color measurements. The 4-color simultaneous imager, for r band= 552-689 nm, i band= 691-815 nm, z band= 815-915 nm, y band= 967-1024 nm, which is being built by our group, is realized by dichroic beam splitting and band-pass filters with 3 deep depleted CCD cameras and 1 fully depleted CCD camera. Our 4-color simultaneous imager has uniquenesses and advantages, such as higher observing efficiency, better sensitivity at longer wavelength, better use of poor condition nights, and easier photometric calibration.）

3. 儀器實驗室簡介（Instrument lab）

在開發與購置可見光多波段成像儀之前，必須設置儀器實驗室，以供設計、檢測與組裝設備的使用。其中包含：無塵室、暗房、光學桌、光學裝置、程式設計、電路設計、功能測試、規格檢測、真空裝置、冷卻裝置、電子儀表、各式工具、書籍與加工平台。本實驗室將提供各式儀器在運送到鹿林天文台之前，一個良好的開發環境。

（The instrument lab will provide the facility for the development of a 4-color Simultaneous Imager it will have clean booth, clean bench, dark room, optical and electronic device, hardware and software developing device, vacuum and cooling device, tools and books, it's a buffer for equipments before transported to Lu-lin observatory.）

二、 鍍鏡機

1. 準備工作

(1)技術人員吳景煌參加財團法人國家實驗室研究院儀器科技研究中心的「真空實務技術研討會」課程，除了取得其結業證書，最重要的是能快速建立鍍鏡機所需的基礎知識，以及真空機具相關的符號、定義、術語以及規格要求，以利與廠商訂立規格時的依據，並藉此課程，向講師徵詢國內廠商資訊。其課程大綱為：真空技術概論（蕭健男博士）、真空儀表（林郁洧博士）、真空泵浦簡介（陳峰志博士）、真空測漏與真空泵浦維修實習等（李昭德博士等）。

課後整理心得與未來鍍鏡機需要注意的重點圖示如下。

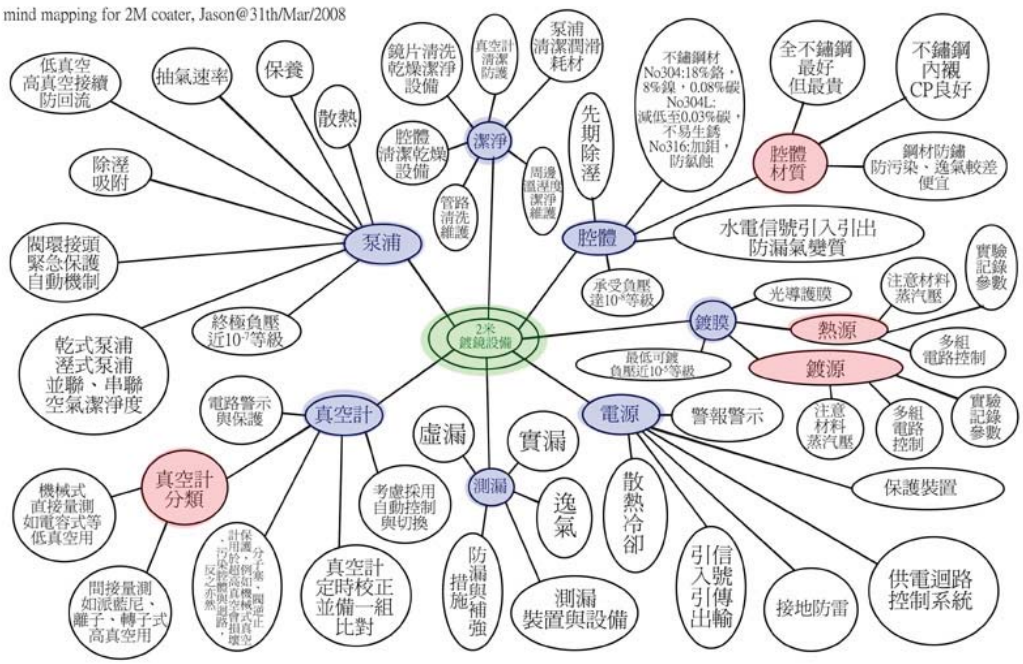

(2)連絡國內相關廠商，研議本計畫鍍鏡機的規格與設計方向，並取得各方的估價與生產時程估算。包括大永、于太、厚昌、富臨、日揚、矽碁、承益、仕貫、龍翩、優貝克、富臨、凌嘉、科敏等真空鍍膜廠商。

(3)觀摩校內外與國內外，與鍍鏡機相關的實驗室與天文台，以及相關展覽，包括國立中央大學光電中心、新竹儀科中心、美國天文台、日本天文台與世貿光電展等。

(4)相關圖示如下：

下圖為大永真空直立式真空腔體概念圖（水平承載鏡片）。

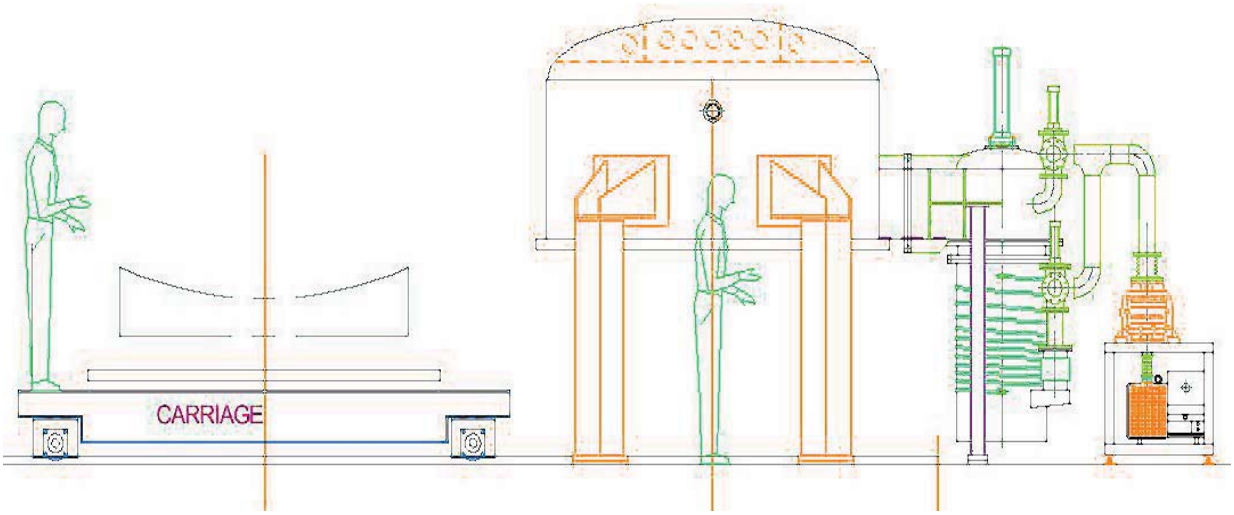

下圖為大永真空水平式真空腔體概念圖（直立承載鏡片）。

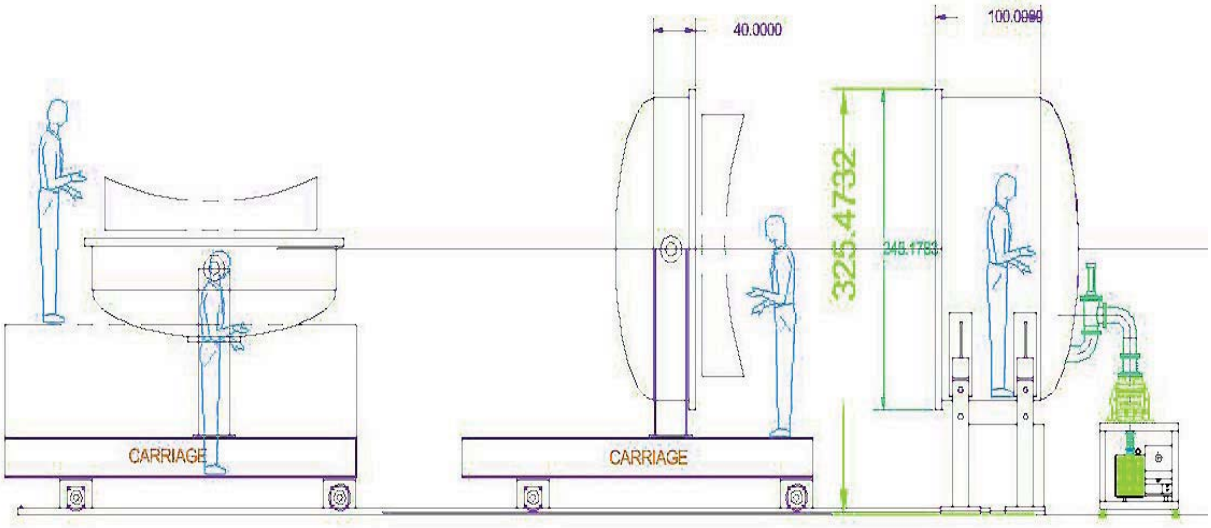

下圖為觀摩國立中央大學光電中心小型蒸鍍與濺鍍設備。

下圖為觀摩美國 Keet-peak 天文台四米蒸鍍機設備（直立腔體）。

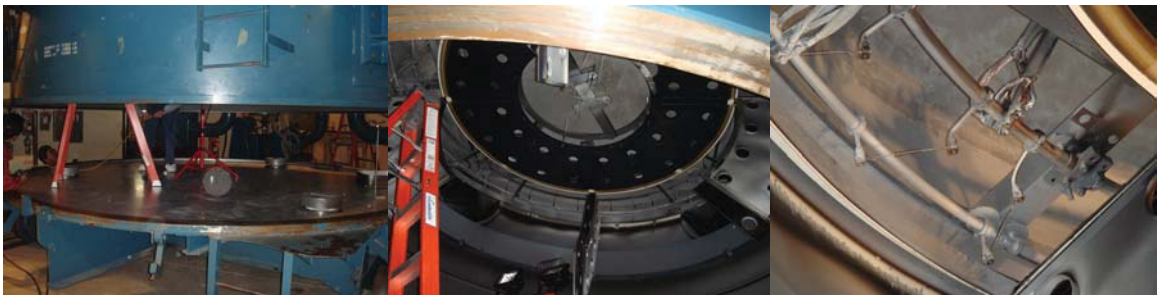

下圖為觀摩美國 Keet-peak 天文台兩米蒸鍍機設備（水平腔體）。


下圖為觀摩日本岡山天文台兩米蒸鍍機設備(水平腔體)。該設計每個電熱絲電源乃貫穿腔體設計，故不用水冷管、腔體較短與成本較低，但是相對線路老化與漏氣風險較高。

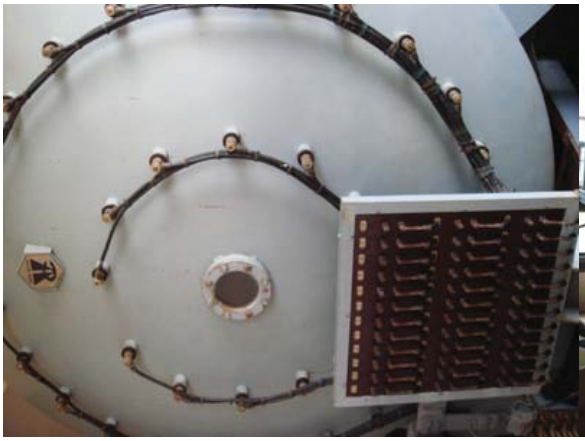


下圖為觀摩日本岡山天文台鏡片表面檢驗之干涉儀裝置。


2. 優缺點比較與規格制定

(1)蒸鍍與濺鍍方式比較：

◎ 蒸鍍優點為，使用歷史較久、製造商較多、參考資料多、技術較簡單、價格較低、靶材費用較低、膜成時間短、鍍源靶材不須移動、不須供應反應氣體。

◎ 濺鍍優點為，功能較多、腔體較小、真空度需求較低、鍵擊能量高附著性好、電力需求可調整、膜厚調整範圍較細、鍍膜密緻與均勻性較優、鍍源無滴落鏡面風險、靶材較多選擇、靶材壽命長、被鍍物較多選擇、熱源控制範圍較細、可保持真空取物。

(2)直立與水平腔體比較：

◎ 直立腔體（鏡片水平）優點為，設備面積較小、全程水平移動對鏡片較安全、鍍膜附著為上下縱向較均勻、相關治具較少。

◎ 水平腔體（鏡片直立）優點為，設備高度較低、腔體較小、機構簡單容易清理保養、鍍源無滴落鏡面風險、更換熱源與靶材較容易、水平清洗鏡片後改直立放置鏡面潔淨度較易維持。

(3)鍍膜品質檢驗：

◎ 目前如此大型鍍膜設備，仍無即時的或全面直接的鍍膜品質檢驗方法。

◎ 蒸鍍機常採用石英晶體振蕩檢測器，其廣泛應用於線上即時定點測量，主要應用於澱積速度與膜厚的監測，還可以回饋訊號用以自動控制。此法最為廉價，但為消耗品，須每次更新。

◎ 濺鍍機常採用 Alpha-stepper，方法是分布試片於腔體中，並半鍍試片（僅一半面積鍍膜，另一半面積擋住不鍍膜），再送入 Alpha-stepper 用以離線檢測鍍膜厚度，其精確度高，但設備昂貴。

◎ 也有採用薄膜反射計，其為線上即時定點測量，其費用較石英晶體振蕩器昂貴許多，技術難度高且較少被採用。尚有干涉顯微鏡法與秤重法，皆為離線測試方式。

(4)規格制定：

◎ 本所會議決定採用濺鍍方式、水平腔體機台。

◎ 蒸鍍機規格另保留備用，濺鍍機規格書亦已備妥。

3. 目前進度

(1)鍍鏡機所需採購、製造、驗收時程為 6 到 8 個月。目前規格皆已確立。

(2)將配合兩米天文台完成部分建築與電力系統，且龍門吊索仍使用的期間，完成採購到驗收的所有程序。

三、 可見光多波段成像儀

1. 準備工作

(1)研讀木下大輔老師提供的相關資料，以了解光偶元件攝像裝置在天文觀測上的需求與規格。

(2)連絡國內外相關廠商，研議光偶元件攝像裝置的規格與設計方向。

(3)觀摩校內外與國內外，與光偶元件攝像裝置相關的實驗室與天文台，以及相關展覽。

(4)相關圖示如下：

下左方塊圖，為日本 Photocoding 設計可見光多波段成像儀光學部分的架構示意圖。

下右圖兩圓筒狀，為美國 Spectrum Instrument 設計光偶元件攝像裝置的外觀示意圖。

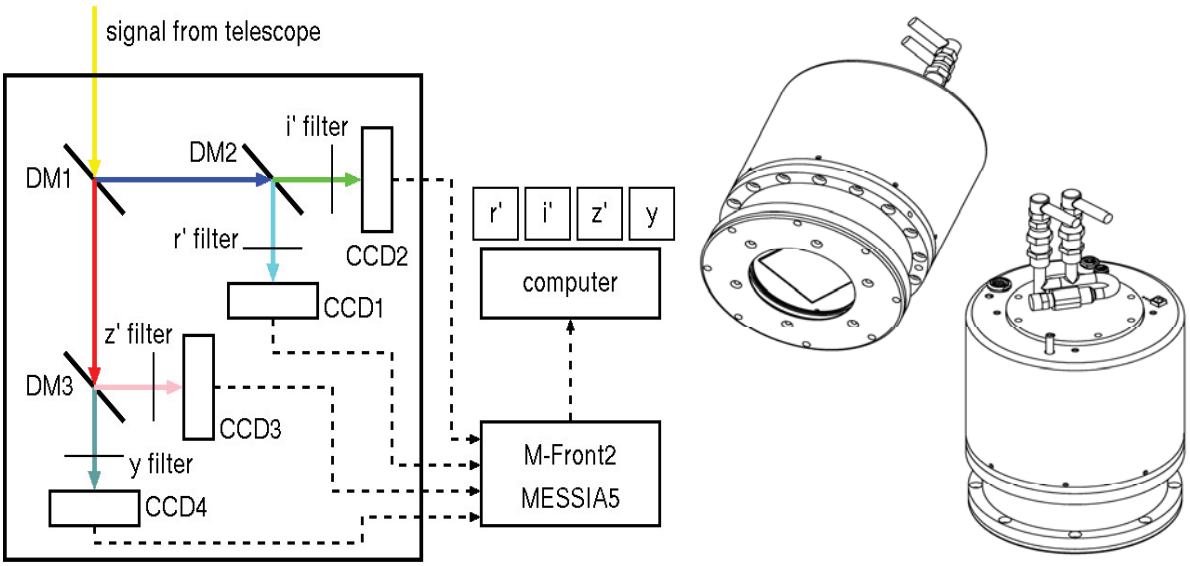

下圖為日本 Photocoding 設計可見光多波段成像儀光學部分的電腦模擬圖。
下右圖表示每個模擬的成像結果皆遠小於 15 μm 直徑。

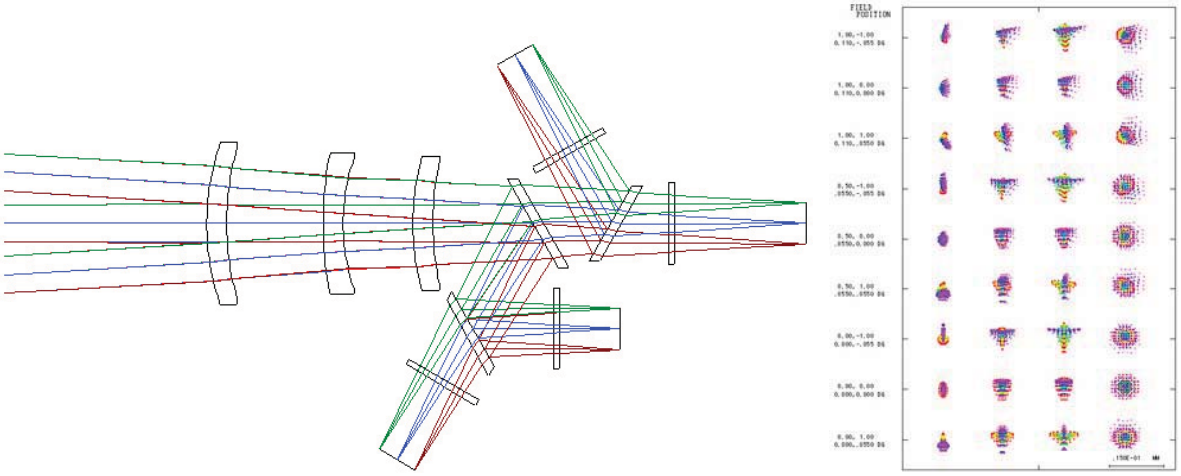

下圖為觀摩日本岡山天文台光偶元件攝像裝置與總成。

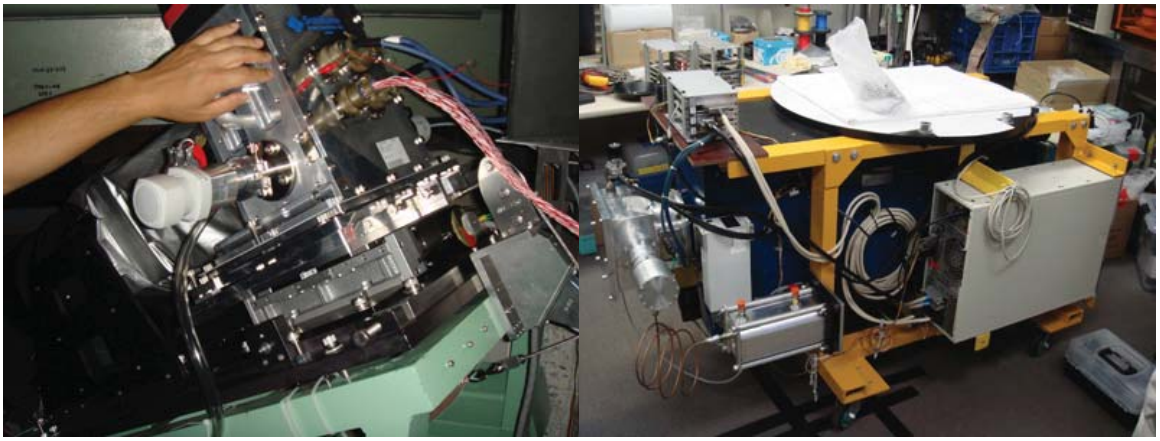

下圖為觀摩日本東廣島天文台光偶元件攝像裝置、讀取電路與腔體總成。

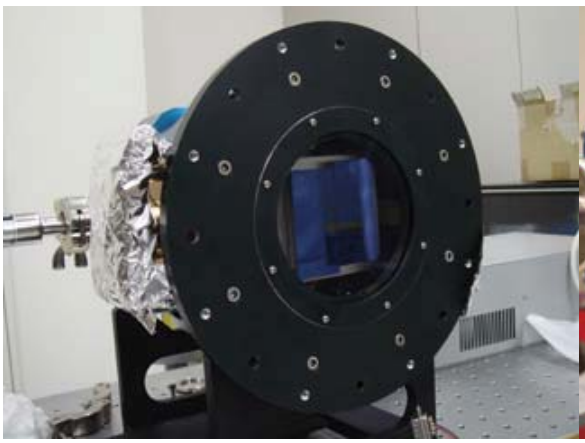
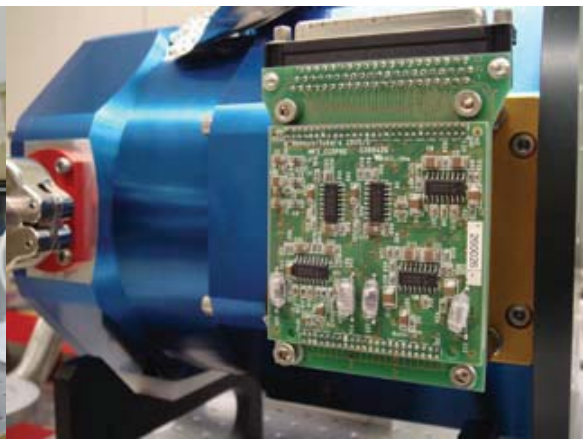

2. 規格制定與目前進度

(1)經所內老師考量經費、時效與最大的研究效益，最後於本所會議決定購置 3 套採用深空乏光偶元件的攝像裝置，以及購置 1 套開發全空乏（高阻）光偶元件攝像裝置與其周邊所需控制器、腔體、泵浦與冷卻機。

(2)3 套深空乏光偶元件攝像裝置之規格書已確立，並已進行採購中。

(3)1 套全空乏（高阻）光偶元件攝像裝置與其周邊所需控制器、腔體、泵浦與冷卻機，以及可見光多波段成像儀光學部分，目前規格制定中。

四、 儀器實驗室

1. 準備工作

(1)研讀相關資料，以了解可見光多波段成像儀在儀器實驗室檢測的需求。

(2)觀摩校內外與國內外相關實驗室與天文台的儀器實驗室與真空組裝環境。

(3)觀摩相關展覽連絡國內外廠商，研究儀器實驗室的需求與設計方向。

(4)相關圖示如下：

下左圖為最初儀器室規劃空間圖。下右圖為觀摩中大光電中心暗棚與光學桌。

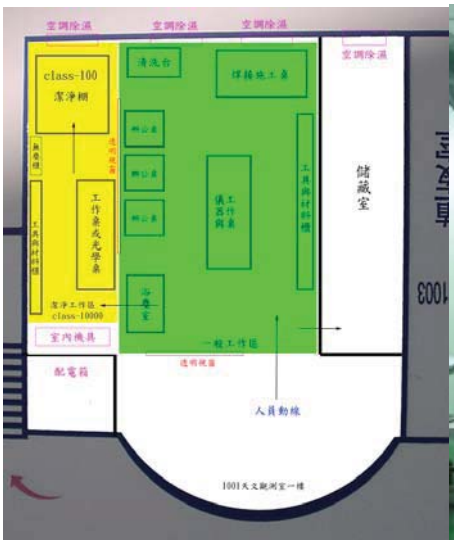

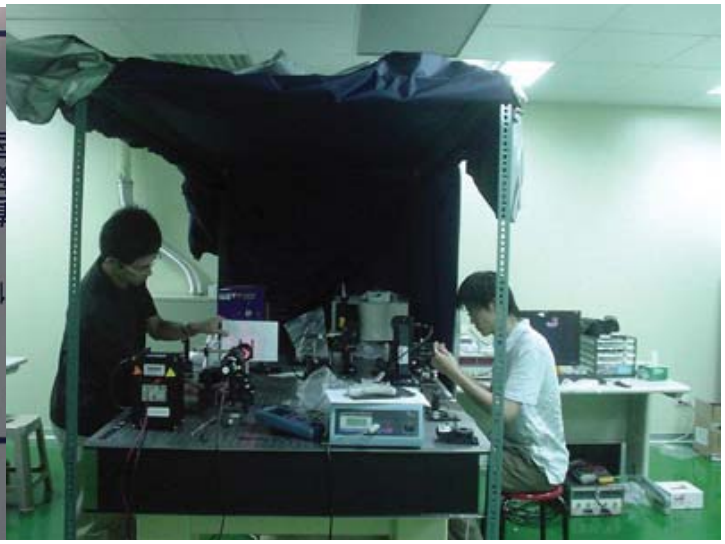

下圖為觀摩日本岡山天文台的無塵棚與光學桌。


下圖為觀摩日本東廣島天文台的無塵棚與攝像裝置的致冷台與腔體。


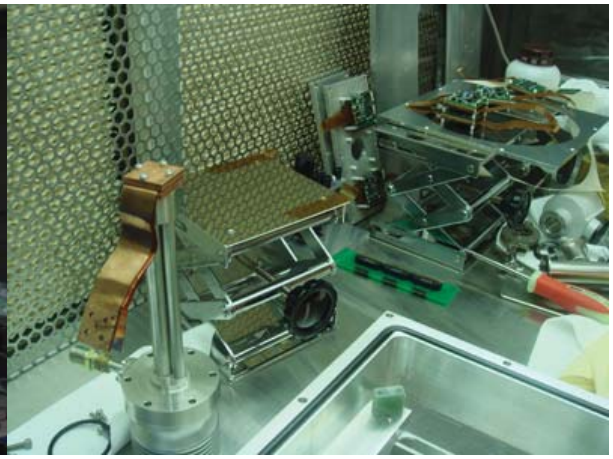

下左圖為日本木曾天文台的暗棚、光學桌與光源。下右圖為日本東廣島天文台的無塵棚。

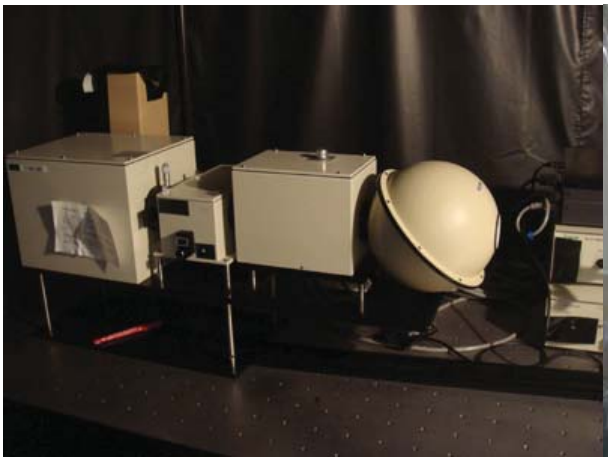


2. 規劃與目前進度

(1)考量經費、效益與本所需求，自行規劃其空間、隔間與組裝。

(2)已完成一級防火輕隔間、輕鋼架、氣密窗、空調、粉刷與空間清理。

(3)首先進行細部空間丈量、設備定位點進行繪製，以利設備進駐定位。

(4)除靜電裝置已確認規格型式，可協助無塵環境靜電的消除，並順利排除微塵，本裝置將與無塵設備同步安裝。

(5)無塵棚、無塵檯配合現有場地，達到 C100 等級，與暗棚，皆已安裝。

(6)採用工業與教學等級氣浮式光學桌，已安裝。

(7)最新儀器室空間規劃圖如下：

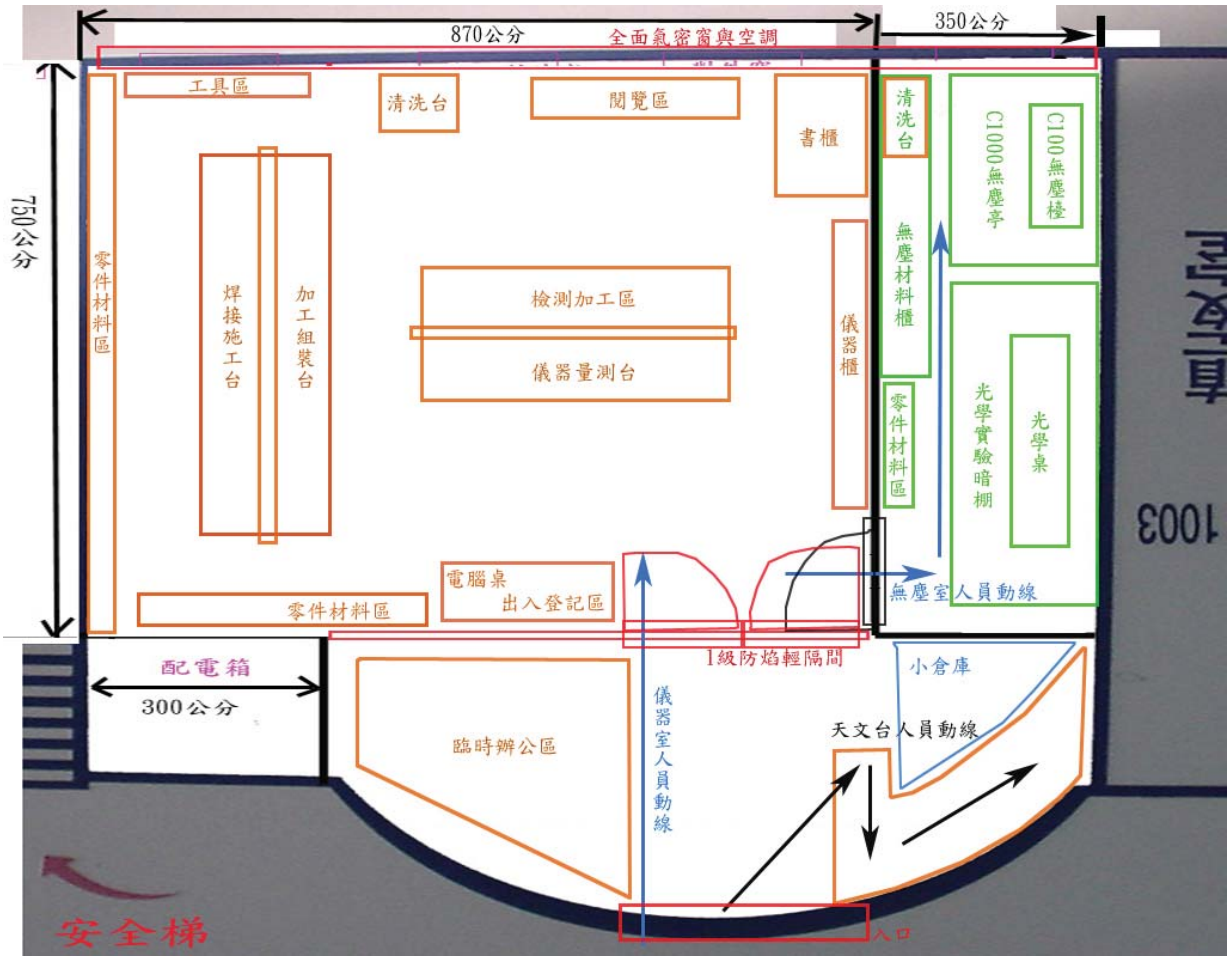

(8)上圖儀器室規劃說明：

◎ 綠色無塵區，具阻抗 $10^5\Omega$ 等級綠色光滑防靜電地墊，以利於微塵靜電消除排放，該區用於組裝 CCD 及其真空腔體等相關元件。

◎ 綠色暗棚區，具阻抗 $10^3\Omega$ 等級黑色粘附防靜電地墊，以利於吸收光線並粘附微塵，該區用於攝像裝置等光學元件之效能檢測。

◎ 藍色小倉庫，提供真空泵浦、機械式冷凍裝置等機械裝置擺放。

◎ 書櫃，相關書籍、工具書等擺放。閱覽區可繪圖與研讀。

◎ 清洗台 2 組，分為無塵區清洗台與一般清洗台。

◎ 儀器與檢測區，完成的電路單元檢測區域，含儀器櫃。

◎ 焊接加工區，電路設計施工與組裝區域。

◎ 零件材料區多組，分無塵區與一般區域。

◎ 電腦桌與登記區，控制電路板設計與使用者出入管制區域。

◎ 本儀器室將陸續設置電子儀器與相關設備，例如示波器、邏輯分析儀、高精度多功能電表、主被動零件檢測表、光源、單光儀、積分球、真空泵浦、機械式冷凍機、靜電量測、微塵檢測、電腦、控制介面、電路設計、電路板設計、電路板加工清洗、焊接加工以及各種光電檢測所需之工具零件等等。

◎ 本空間以提供本所攝像裝置所需研發環境為主，並延伸至其它相關用途，期有

更高的利用率。

(9)目前進度圖示說明：

下圖為無塵區與暗棚區之防靜電地墊與光學桌設備安裝。


下左圖為 C1000 等級無塵棚與暗棚之骨架安裝。下右圖為暗棚安裝完成後。


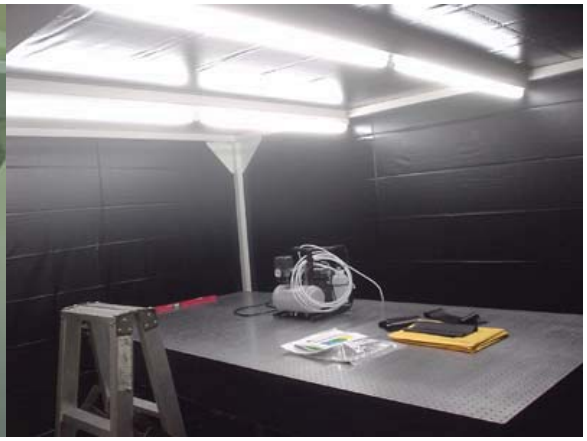

下圖為 C1000 等級無塵棚安裝完成後，C1000 等級定義為『小於 0.5μm 微塵於 1 立方米・分鐘內的數量應少於 1000 個』。


下左圖為微塵檢測儀器之取樣頭，置於出風口下方進行靜態測試。下右圖為其主機。

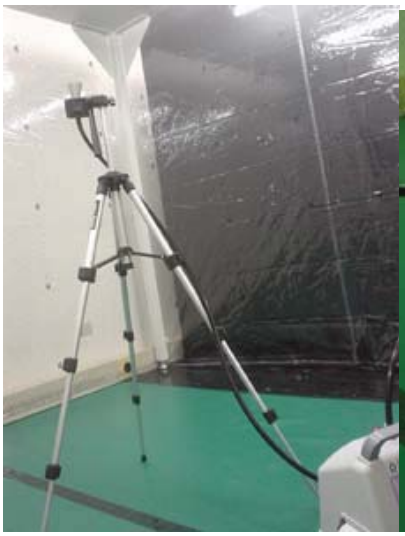

下左圖背景測試，顯示環境中小於 0.5μm 的微塵數量為 12877 個，於 2 秒左右的取樣時間。數據中第一列表示微塵直徑μm，第二列表示單位時間內的微塵數量△，第三列表示單位時間內的微塵數量加總Σ。

下中、右圖顯示該 C1000 無塵棚測試結果，開機 15 分鐘後，第一出風口小於 0.5μm 的微塵數量低於 59 個，第二出風口小於 0.5μm 的微塵數量低於 79 個。

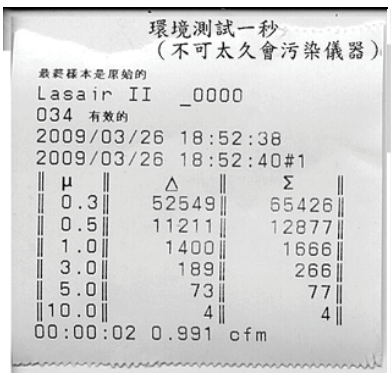

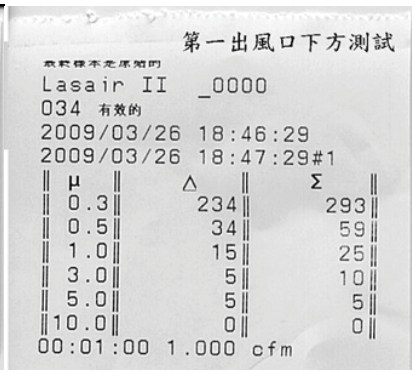

下圖為 C100 等級無塵檯安裝完成後，C100 等級定義為『小於 0.5μm 微塵於 1 立方米・分鐘內的數量應少於 100 個』。

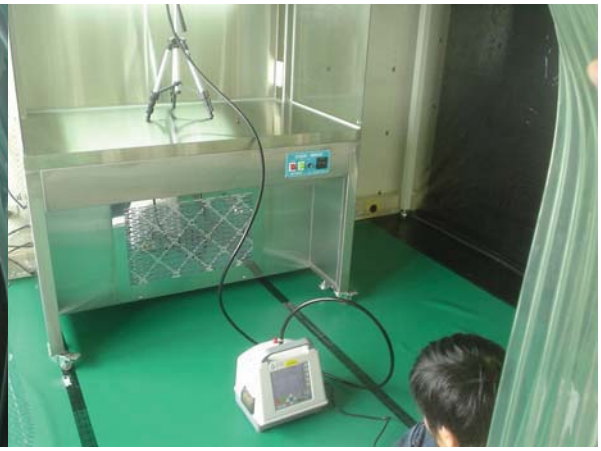

下左、右圖顯示該 C100 無塵棚測試結果，開機 5 分鐘後小於 0.5μm 的微塵數量低於 2 個，開機 8 到 10 分鐘後小於 0.5μm 的微塵數量低於 1 個。

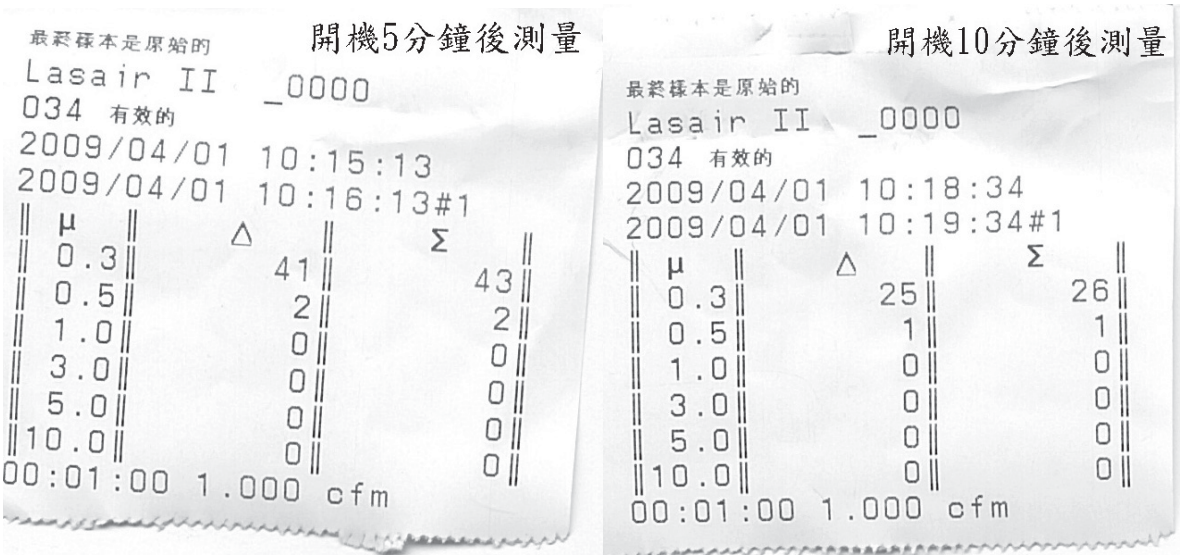

五、 其它

1. 因顧慮科四館天文台圓頂尚有漏水現象，恐雨水過多進入儀器實驗室，本所進行評估後，採用不鏽鋼蒙皮氬焊圓頂，為質輕、經濟又有效的防護措施。相關施工圖示如下：

下圖為發現科四館天文台圓頂蒙皮破損後製作，供本所存檔與廠商估價。

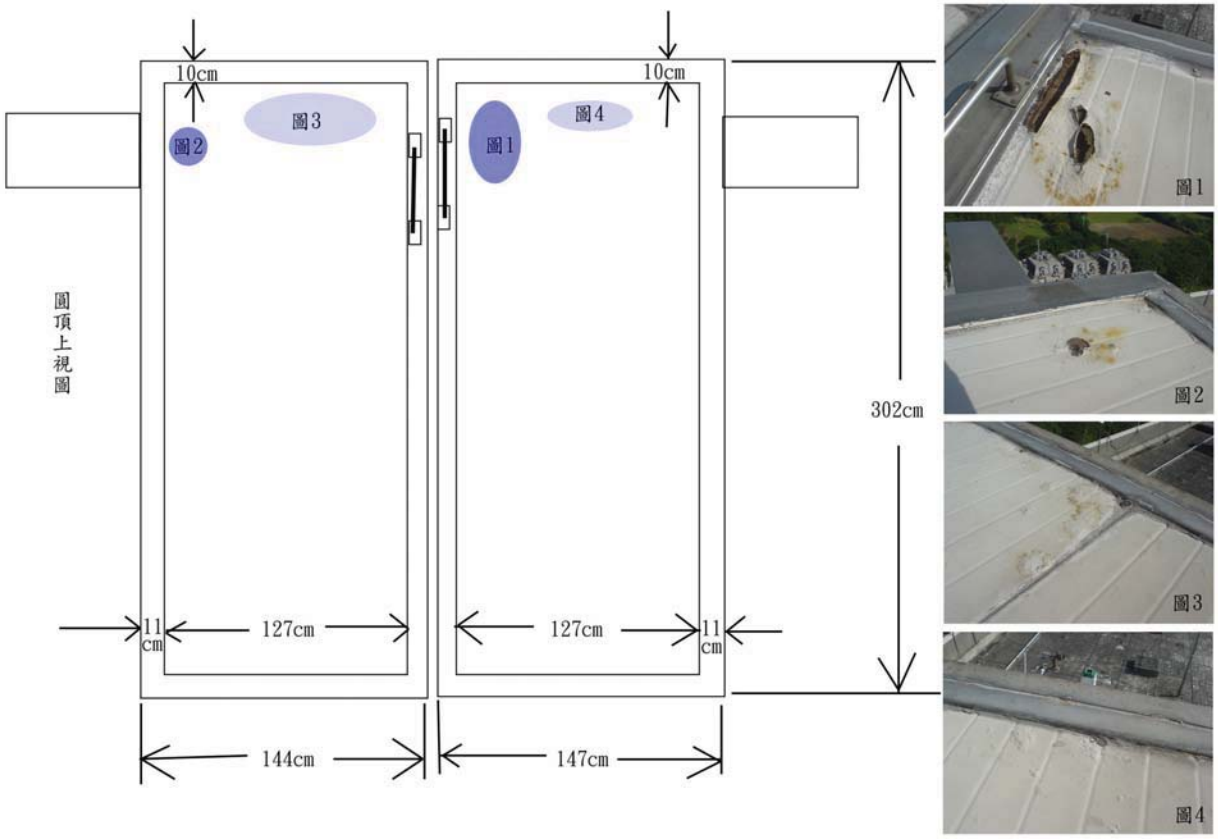

下圖黃色區塊為不鏽鋼蒙皮氬焊範圍圖示，供廠商估價用，完工後共計 19887 元。

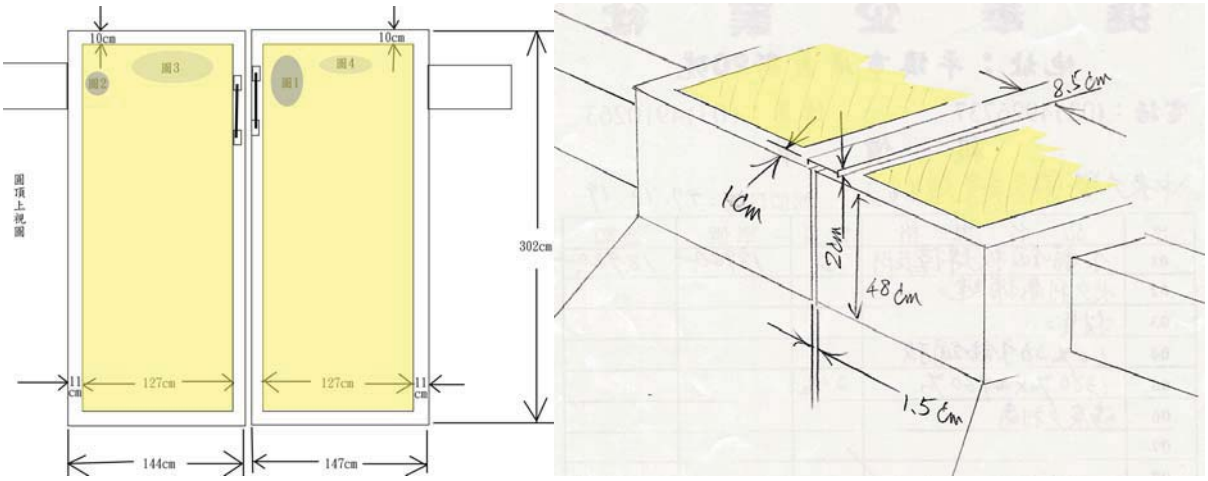

2. 科四館天文台圓頂施工後現況圖示如下：

下圖於施工同後，除了圖中的圓頂頂部，廠商並以矽利康膠加強圓頂全部側面的填縫。

3. 未來鹿林天文台 SLT 與 LOT 圓頂，預計採用相同方式，以保護圓頂之頂部，並希望減輕目前滲漏水現象。
4. 鹿林天文台 LOT 圓頂 encoder 電路改良，完工後材料費共計 998 元，改良成果說明：
   (1)確認『360pulses/1 圈』之 encoder 為最佳解析度，共計『64658pulses/圓頂轉 1 圈』，LOT 之控制器計數上限為『65536pulses/圓頂轉 1 圈』。
   (2)本電路可自動轉換各種型式的 encoder 輸出訊號，如 OC、OD、line-out、push-pull…等型式，皆可相容，並自動轉換。安裝完成之後測試，圓頂轉動誤差較少，不須常常歸零（home）。
   (3)若須更換 encoder 時，僅需拆開圓頂端小黑盒，對接「0V-GND-黑與棕線」、「5V-

紅線」、「AB-黃與橙線」；再到控制室輸入指令「LR」進入學習模式，若圓頂控制器之數字顯示上數則 AB 相位正常，若數字顯示下數則立即切換控制室端大黑盒的開關到反向區段，便可將 AB 相位對調，不需要到圓頂內部更換 AB 相位線。

(4)相關圖示如下：

下左圖為達明企業社免費贊助重新製作的固定片，採 1mm 厚不鏽鋼，較舊型有彈性。

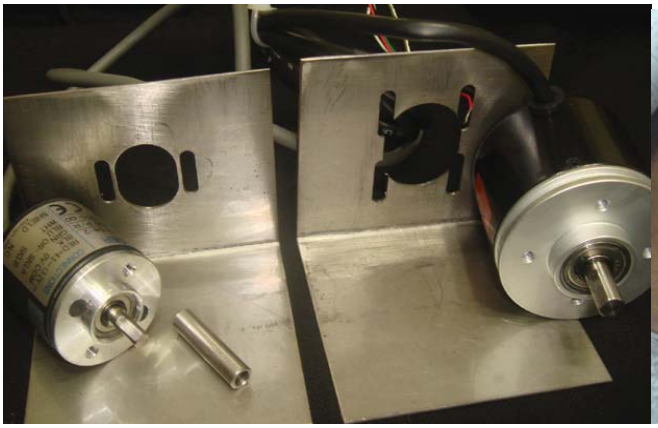


下左圖為 encoder 波形、計數與 AB 相位調換測試。下右圖為圓頂內 encoder 安裝位置。

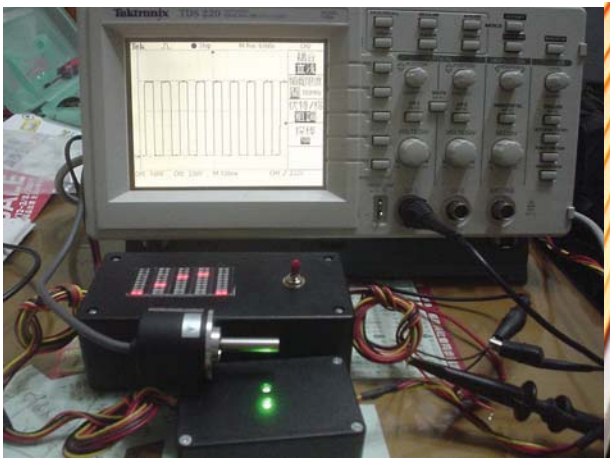
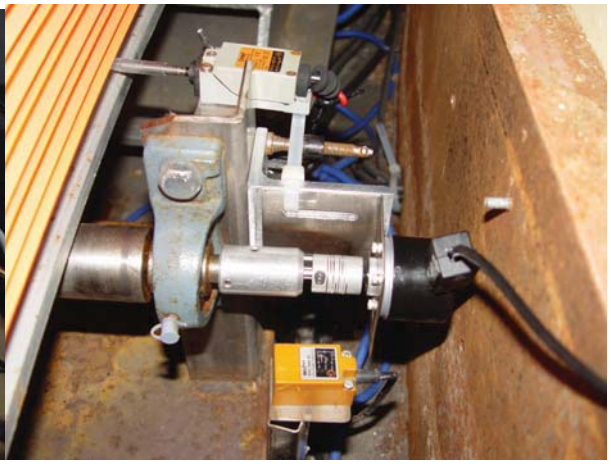

下圖為控制室內部電路的計數器與 AB 相位調換開關外觀。與實際圓頂運作測試。

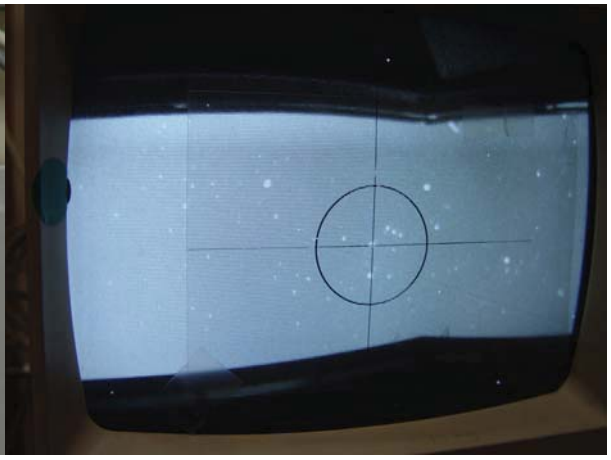

Development of a Visible Four-Color Simultaneous Imager for the Lulin 2-m Telescope

Kinoshita Daisuke, Wu Ching-Huang, and Ip Wing-Huen

first draft on 15 March 2009; revised on 7 April 2009

Abstract

The development of four-color simultaneous imager has been started. This instrument is the first generation astronomical instrument for 2-m telescope which is being built at Lulin observatory in Taiwan. The aim of this instrument is to conduct immediate and intensive follow-up observations for newly discovered objects from Pan-STARRS PS1 sky survey. The reasons we decided to develop four-color simultaneous imager as a first generation instrument is based on the site characteristics and targets of follow-up observations. First, the sky at Lulin observatory is not always stable and we only have limited number of photometric nights. In order to carry out accurate color measurements, we have to complete number of exposures before the sky condition changes. Second, main targets for PS1 follow-up observations are (1) transient objects, such as gamma ray bursts, soft X-ray transients, and supernovae, and (2) moving objects, such as asteroids, comets, and trans-Neptunian objects. These objects change their brightness with time, and simultaneous imaging at two of more bands is essential to perform reliable color measurements. We report the scientific objectives, design of the instrument, development strategy, current status of the development, and future schedule.

Key words: Instrumentation: detectors – Techniques: photometric

1 Introduction

The Institute of Astronomy at National Central University participates PS1 Science Consortium of Pan-STARRS project[1]. PS1 utilizes 1.8-m wide-field telescope and 1.4 giga pixel camera at the summit of Haleakala in Hawaii, and conduct the cyclical sky survey for 3/4 of the whole sky (Kaiser 2004). It is a first trial to image such a wide area of the sky repeatedly in systematic way. It opens new opportunities for knowing the variable universe. Intensive studies of transient objects and moving objects are expected.

In order to maximize the scientific outputs of PS1 sky survey, follow-up observations are essential to investigate physical properties and chemical composition of newly discovered objects. A new 2-m telescope is being built at Lulin observatory for follow-up observations of PS1. The primary mirror has an effective diameter of 2-m, and the manufacturing of the mirror has been completed in late-2008. The focal ratio of the telescope will be F/8, and the 2-m telescope will be able to share some instruments with the existing 1-m telescope at Lulin. The mount of the telescope is chosen to be the alt-az system to reduce the dimension and construction cost of the system. The maximum slew speed is 4 degree per second, and it enables us to do quick pointing right after the trigger of the transient alert.

A visible four-color simultaneous imager was selected to be the first generation instrument for the 2-m telescope. There are two reasons for this decision. First, the site condition of Lulin observatory is not as good as that of excellent astronomical sites, such as Mauna Kea and northern Chile. The sky condition is often unstable, and is variable during the night. We only have limited number of photometric nights. We have to consider how to utilize the observing time on poor condition nights. The simultaneous imager splits the beam from the telescope using dichroic mirrors and records two or more images at different wavelength regions at the same time. It makes the calibration and data analysis easier under the assumption that the transmittance of the cirrus is neutral over the wavelength coverage of the instrument. The use of the simultaneous imager increases the observable nights, and it is critically important for the operation and scientific productivity of Lulin observatory. Second, We focus on the follow-up observations for astronomical objects discovered by PS1 sky survey. Then, the main targets for the 2-m telescope are (1) transient objects, such as gamma ray bursts (hereafter, GRBs), soft X-ray transients, and supernovae, and (2) moving objects, such as asteroids, comets, and trans-Neptunian

[1] http://pan-starrs.ifa.hawaii.edu/

objects. Needless to say, transient objects change the brightness and/or colors by their nature. Moving objects, or small solar system bodies, also have changes in the brightness and/or colors in general due to rotation of irregularly shaped bodies. It means that we need to complete the brightness measurements at two or more pass bands before those objects change their brightness for accurate color determination. A reliable and efficient way to achieve color measurements for transient and moving objects is the use of the simultaneous imager. The images at different wavelength regions are recorded exactly at the same time, and derived colors are less affected by the variability of the atmospheric condition.

In this report, the design of our visible four-color simultaneous imager is described in Section 2, the strategy for the instrument development is introduced in Section 3, the current status of the development is explained in Section 4, and the future schedule of the development is presented in Section 5.

2 Design of Instrument

In astronomy, color measurements are often used to obtain the first look at the physical conditions and chemical composition of astronomical objects. In a conventional method of color measurements, we image the target using a filter, then later re-image the same object using another filter. In this way, there is a time lag between two measurements at different wavelength. Our targets, transient and moving objects, change their brightness with time, and the conventional color measurements may produce false colors.

A different and new approach is proposed here. That is, accurate measurements can be achieved by observing the target at two or more different wavelength regions simultaneously. This is realized by beam splitting using dichroic mirrors. The dichroic mirror is an optical device that reflects the light shorter than the characteristic wavelength and transmits the light longer than the characteristic wavelength. A sample of the transmittance property of a dichroic mirror is shown in Fig. 1. A group of astronomers in Japan produced such an instrument for small telescopes for GRBs studies. They developed tricolor camera named "MITSuME" (Multicolor Imaging Telescopes for Survey and Monstrous Explosions). The instrument is equipped with two dichroic mirrors, and three images at g', R_C, and I_C-band are recorded simultaneously (Kotani et al. 2005). By using three dichroic mirrors and four bandpass filters and detectors, one is able to measure the target flux at four different wavelength regions at the same time.

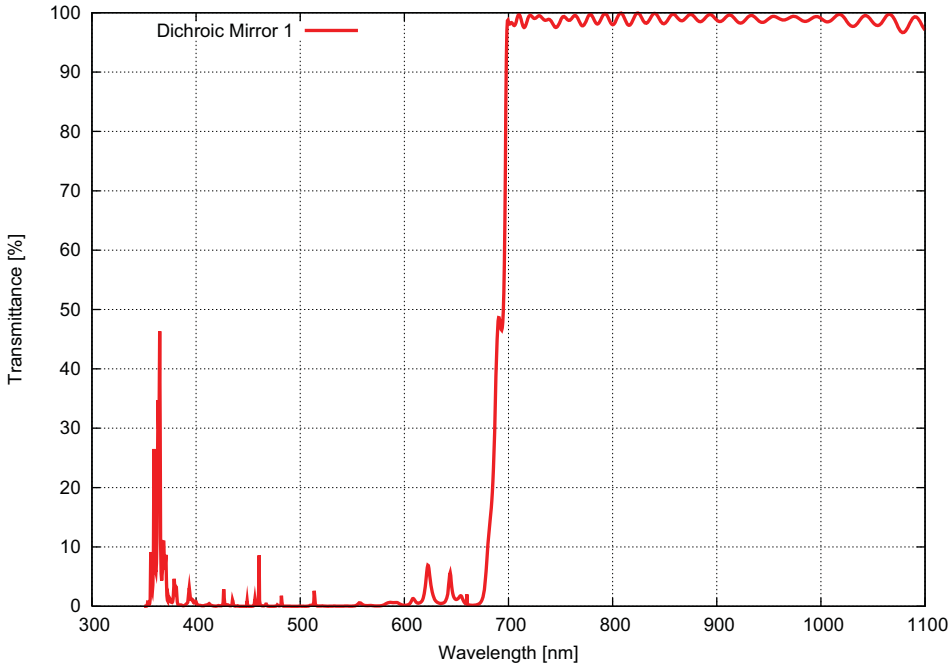

Figure 1: A simulated transmittance property of a dichroic mirror. The simulation is performed by Asahi Spectra, Inc. This dichroic mirror is designed to split the beam for PS1 r'-band and PS1 i'-band, and the characteristic wavelength is set at 700 nm. The light shorter than the wavelength of 700 nm is reflected at the mirror, and the light longer than the wavelength of 700 nm is transmitted.

The conceptual design of the visible four-color simultaneous imager is shown in Fig. 2. Three dichroic mirrors on the optical path split the light from the telescope into four components. These three beams

go through the bandpass filters (PS1 r', i', z', and y filters), and the signals are received by four detectors at the same time. In order to compare data both from PS1 in Hawaii and the 2-m telescope in Taiwan, the filter system of our visible four-color simultaneous imager is designed to be compatible with those of PS1 filter system. The transmittance properties of PS1 r', i', z', and y filters are shown in Fig. 3.

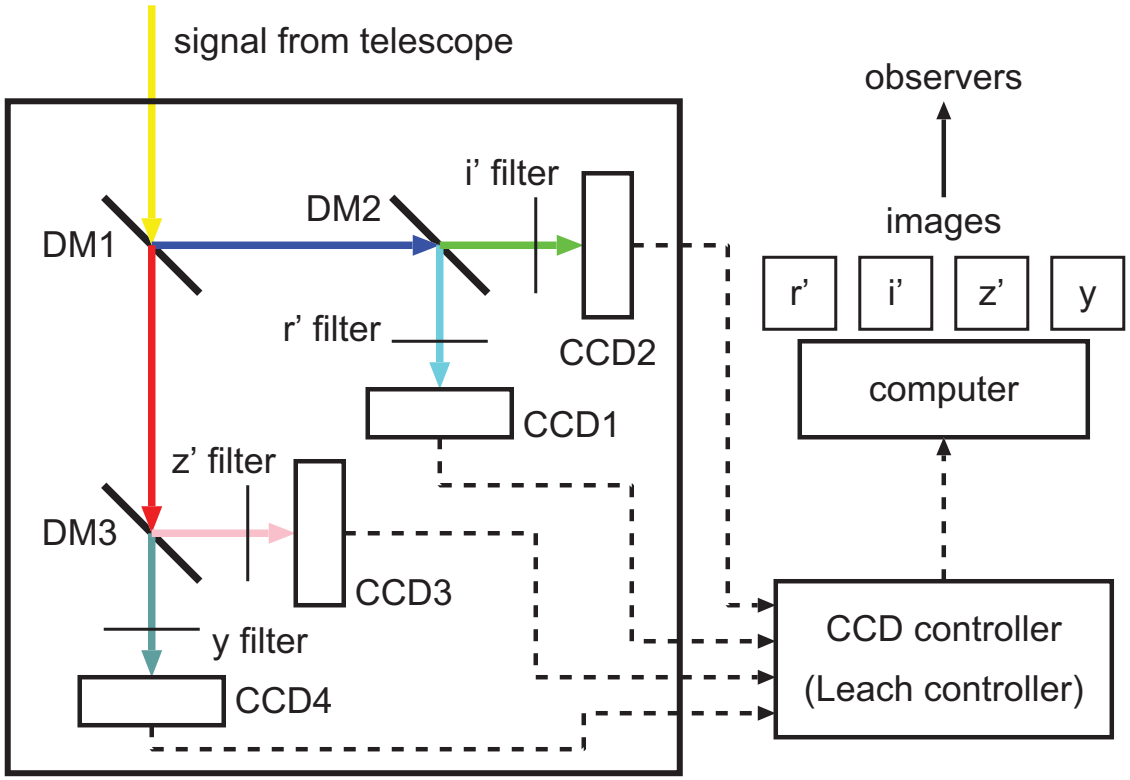

Figure 2: The conceptual design of the visible four-color simultaneous imager. Three dichroic mirrors split the signal from the telescope into four different wavelength regions, and four detectors receive signals at the same time.

The development of the instrument can be devided into two parts, (1) development of CCD cameras, and (2) design and manufacturing of optics and enclosure.

2.1 CCD Cameras and Readout Electronics

Four CCD cameras are the key components of the instrument. Because excellent scientific outputs are more easily produced by an instrument with unique features, we extensively discussed the specifications of CCD cameras to be used for our visible four-color simultaneous imager. The conclusion is that it is critically important to have higher sensitivity at y-band ($\lambda \sim 1.0\ \mu m$) to archieve a big advantage over many other 2-m class telescopes now in existence. For solar system studies, the wavelength of $\lambda \sim 1.0\ \mu m$ is important due to the presence of mineral absorption features. For photometric redshift measurements to estimate the distances of objects at cosmological distances, it is essential to include the y-band data for wide wavelength coverage for reliable distance determination.

Recently, thinned back-illuminated CCDs have been widely used for astronomical observations. Thinned back-illuminated CCDs have high quantum efficiency, and the peak quantum efficiency reaches $\sim 90\%$. The problems of this type of CCDs are (1) poor quantum efficiency at longer wavelength region, say about 10% at $\lambda = 1.0\ \mu m$, and (2) fringe pattern at longer wavelength region which brings larger photometric errors. It is not easy to carry out observations at y-band for small telescopes due to low sensitivity and serious fringe pattern. To overcome these problems, there has been some efforts to develop a new type of CCDs. Lawrence Berkeley National Laboratory[2] has developed fully depleted back-illuminated CCDs (Bebek et al. 2004). The thickness of the CCDs is 200-300 μm, while conventional thinned CCDs has $\sim 15\ \mu m$ thickness. Thanks to the thicker depletion layer, the CCD can reach more than 50% quantum efficiency at $\lambda = 1.0\ \mu m$. This CCD was used for the 4-m telescope and the prime focus spectrograph at

[2]http://www.lbl.gov/

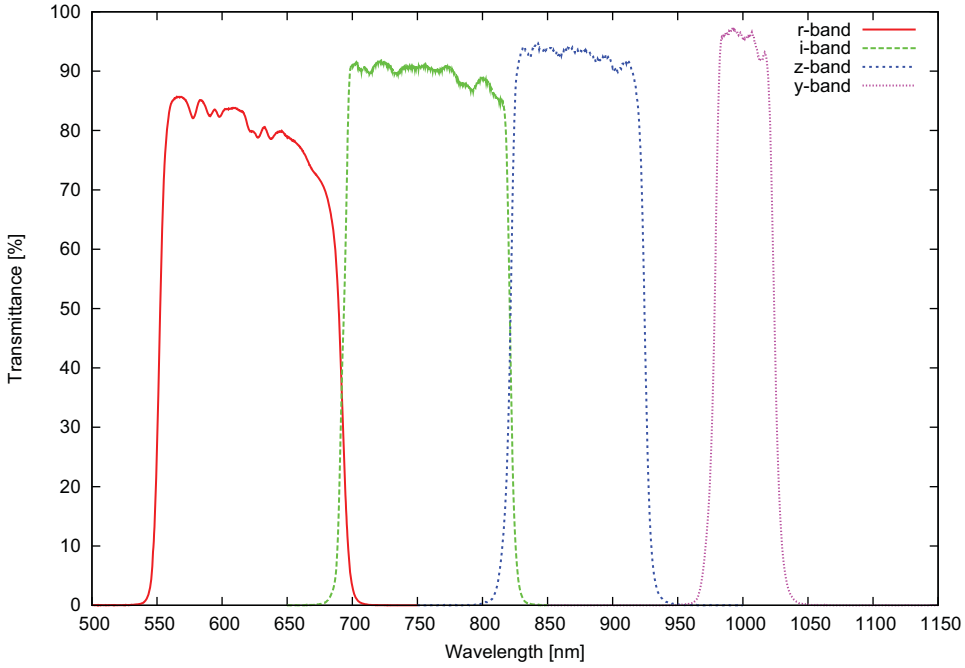

Figure 3: The transmittance properties of PS1 r', i', z', and y-band filters. The filter system of visible four-color simultaneous imager will be compatible with those of PS1 filter system. The filter transmittance data is obtained from PS1 Internal Wiki Page.

Kitt Peak National Observatory. Because of the larger thickness of the CCD, high back bias voltage is required to drive this type of CCDs for reasonablly small point spread function.

National Astronomical Observatory of Japan (hereafter, NAOJ) has also developed fully depleted CCDs in a collaboration with Hamamatsu Photonics[3] (Kamata et al. 2004, Fig. 4). The large formatted 4K × 2K fully depleted CCDs with the depletion layer thickness of 200 μm has been successfully fabricated, and this CCD has more than 40% quantum efficiency at $\lambda = 1.0$ μm under the operation temperature of −100°C (Kamata et al. 2008). NAOJ has replaced thinned back-illuminated CCDs of the prime focus wide-field imager "Suprime-Cam" for the 8.2-m Subaru telescope with newly developed fully depleted CCDs manufactured by Hamamatsu Photonics in summer 2008. NAOJ plans to utilize more than 100 fully depleted CCDs to develop the next generation wide-field imager "Hyper Suprime-Cam" (Komiyama et al. 2004). The Institute of Astronomy and Astrophysics at Academia Sinica (hereafter, ASIAA) is now collaborating with NAOJ on the development of this state-of-art instrument, and all the fully depleted CCDs are to be purchased and tested by ASIAA (Wang 2009). Fully depleted CCDs of Hamamatsu Photonics are commercially available. A company named e2v also developed fully depleted CCDs, and test devices are now being examined.

We finally decided to use a fully depleted CCD for y-band imaging, and three more deep depletion CCDs, with the depletion layer thickness of 40 μm, for r', i', and z'-band imaging. A CCD camera for y-band imaging is not commercially available, and we will need to develop it by ourselves. Three CCD cameras for r', i', and z'-band imaging are commercially available, and we plan to purchase these cameras. A possible candidate product is the CCD camera manufactured by Spectral Instruments, Inc.[4] Spectral Instruments, Inc. offers custum made CCD cameras, and one is able to order CCD cameras with specific CCD chips. Both kinds of CCDs have 4096 × 2048 pixels with 15 μm pixel size. The focal length of the 2-m telescope at Lulin is 16-m, and resultant pixel scale and field-of-view of the instrument is 0.19 arcsec per pixel and 13.2 × 6.6 arcmin, respectively. All the CCD chips for the four cameras will be cooled down to −100°C with cryogenic system to achieve lower noise.

For the CCD camera part, the key issue is the development of the readout electronics. For this part, we first use a commercially available product to drive a CCD. Astronomical Research Cameras, Inc.[5] provides number of controller boards for CCD drive. These products are known as GenIII boards or

[3]http://jp.hamamatsu.com/en/
[4]http://www.specinst.com/
[5]http://www.astro-cam.com/

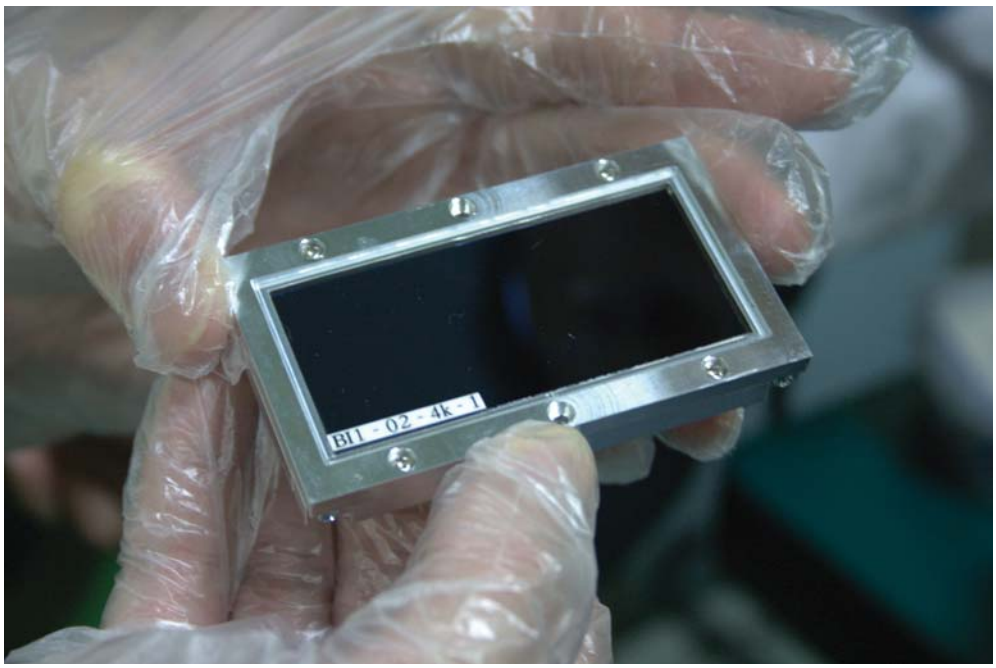

Figure 4: A fully depleted CCD manufactured by Hamamatsu Photonics. The photo was taken at the Institute of Astronomy and Astrophysics of Academia Sinica by courtegy of Dr. Wang Shiang-Yu.

Leach controller (Fig. 5). The GenIII controller has no experience of controlling fully depleted CCDs. Although, Astronomical Research Cameras, Inc. soon starts to manufacture high voltage bias board for fully depleted CCDs, we need some tests. We will collaborate on the driving of fully depleted CCDs using GenIII controller with the Solar Terrestrial Environment Laboratory[6] (hereafter, STE Lab.) of Nagoya University in Japan, because the STE Lab. has experiences of driving e2v CCDs using the GenIII system (Sako et al. 2008), and is also interested in developing a CCD imager with fully depleted CCDs for its 1.8-m telescope in New Zealand. At the same time, the instrumentation group at ASIAA plans to develop its own high voltage bias board for fully depleted CCDs (Wang 2009), and the use of this high voltage bias board may be an option in the future. A laboratory is necessary for the test of CCD driving, evaluation of CCD cameras, and integration of the instrument. We are currently preparing a laboratory with a clean room, dark room, optical bench, and electronics workshop. The detail of the laboratory set-up is reported by Wu Ching-Huang in the Annual Report of Lulin Observatory 2008. In the next step, we plan to collaborate with the Institute of Astronomy at University of Tokyo[7] to develop our own CCD controller.

2.2 Optics and Enclosure

The optics of the visible four-color simultaneous imager includes re-imaging optics, dichroic mirrors to split the beam, and band-pass filters. The instrument has a single shutter only. For the design of the optics part, Photocoding, Inc.[8] kindly provided a proposal of the preliminary optical design (Fig. 6). The sizes of the CCD cameras are taken account into the design. The optical design will be fixed shortly, and we will work on the mechanical design and enclosure design in 2009.

3 Development Strategy

For the development of the visible four-color simultaneous imager, we focus on two aspects: (1) in-house development of key components to accumulate our experiences, and (2) quick development of the instrument to give early science results right after the first-light of the 2-m telescope at Lulin observatory. These two aspects are somehow imcompatible with each other. If we emphasize the importance of in-house development of CCD cameras, it may take a while to complete the development of the instrument.

[6]http://www.stelab.nagoya-u.ac.jp/
[7]http://www.ioa.s.u-tokyo.ac.jp/
[8]http://www.photocoding.com/

Figure 5: The GenIII CCD controller (or Leach controller) manufactured by Astronomical Research Cameras, Inc. The photo was taken at Solar Terrestrial Environment Laboratory of Nagoya University in Japan by courtesy of Prof. Sako Takashi.

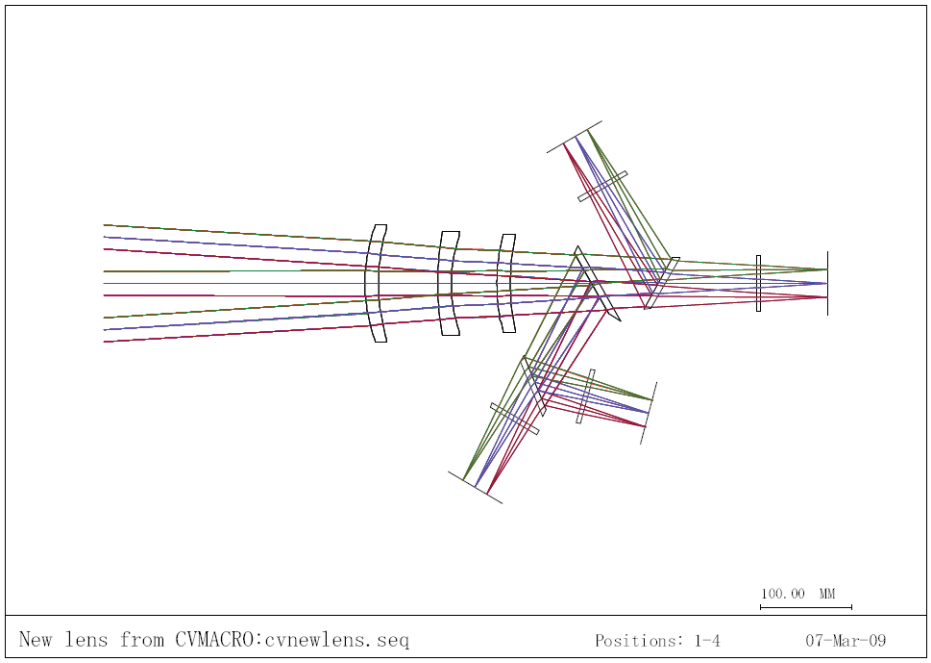

Figure 6: A preliminary optical design for visible four-color simultaneous imager proposed by Photocoding, Inc. A courtesy by Dr. Ikeda Yuji at Photocoding, Inc.

This means that the instrument may not be ready at the time of the telescope first-light, and we will lose the chance of quick scientific outputs. On the other hand, we will be able to start the scientific observations at the time of the telescope first-light, if we purchase commercially available products and assemble them into an instrument. In this case, we learn a little about the instrumentation, and we will not have enough skill and experience for future instrumentation programs. We noticed the balance between these two aspects is essential for the instrument development through the discussion among project members and our partners.

For the CCD camera part, we decided to purchase three cameras with deep depletion CCD chips for r', i', and z'-band and develop our own camera with the fully depleted CCD chip for the y-band. This secures the early scientific outputs by the three-color simultaneous imager at the time of the telescope first-light even if the development of the y-band camera is delayed a bit. It also provides us the opportunity to acquire a skill and accumulate experiences for the development of CCD readout electronics and vacuum chamber. We already started to consolidate the laboratory for the integration and in-house development of the CCD cameras.

4 Current Status of Development

In 2008, we spent significant fraction of time to fix the overall design of the instrument and development strategy. The current status of the instrument development is as follows. The specifications of three CCD cameras with deep depletion CCD is now fixed, and the purchase process is in progress. We expect the delivery of the first camera about six months after the order. We will be able to place an order in April 2009. We will complete the purchase of an engineering grade fully depleted CCD chip, cryocooler, vacuum pump, GenIII CCD controller, and tools such as oscilloscope and leakage detector in a few months, and the development of the fourth CCD camera will start in summer 2009. The optical design is roughly fixed, and we move on towards the mechanical design of the instrument.

5 Future Development Schedule

The target date of the first-light of the 2-m telescope is the end of 2010, and we plan to deliver the instrument in December 2010. The future schedule of the instrument development is summarized in Table 5.

Table 1: The future schedule of the instrument development.

Date	Event
Apr/2009	order of three deep depletion CCD cameras order of fully depleted CCD chip purchase of cryocooler and vacuum pump order of GenIII CCD controller
May/2009	completion of Instrument Laboratory consolidation
Jun/2009	delivery of fully depleted CCD chip
Jul/2009	start of driving tests of fully depleted CCD using GenIII controller
Aug/2009	order of optics and enclosure of the instrument
Oct/2009	delivery of deep depletion CCD cameras
Nov/2009	performance tests of deep depletion CCD cameras
Jan/2009	laboratory first-light of fully depleted CCD using GenIII controller
Mar/2010	first-light observation of deep depletion CCD camera with 1-m telescope
Jul/2010	first-light observation of fully depleted CCD camera with 1-m telescope
Aug/2010	delivery of optics and enclosure of the instrument
Oct/2010	integration of the instrument
Nov/2010	final tests of the instrument in the laboratory
Dec/2010	installation of the instrument to Lulin observatory

Acknowledgement

We would like to thank Prof. Chen Wen-Ping, Prof. Ko Chung-Ming, Prof. Hwang Chorng-Yuan, and Prof. Chou Yi for their valuable advices. This instrumentation program is supported by National Science Council of Taiwan (IDs: 96-2745-M-008-013 and 97-2911-M-008-010-MY2).

References

[1] Bebek, C. J., Bercovitz, J. H., Groom, D. E., Holland, S. E., Kadel, R. W., Karcher, A., Kolbe, W. F., Oluseyi, H. M., Palaio, N. P., Prasad, V., Turko, B. T., Wang, G., "Fully depleted back-illuminated p-channel CCD development", Proceedings of the SPIE, vol. 5167, pp. 50-62 (2004).

[2] Kaiser, N., "Pan-STARRS: a wide-field optical survey telescope array", Proceedings of the SPIE, vol. 5489, pp. 11-22 (2004).

[3] Kamata, Y., Miyazaki, S., Muramatsu, M., Suzuki, H., Miyaguchi, K., Tsuru, T. G., Takagi, S., Miyata, E., "Development of thick back-illuminated CCD to improve quantum efficiency in optical longer wavelength using high-resistivity n-type silicon", Proceedings of the SPIE, vol. 5499, pp. 210-218 (2004).

[4] Kamata, Y., Miyazaki, S., Nakaya, H., Tsuru, T. G., Tsunemi, H., Miyata, E., Muramatsu, M., Suzuki, H., Miyaguchi, K., "Evaluation of the fully-depleted back-illuminated CCD for Subaru Suprime-Cam", Proceedings of the SPIE, vol. 7021, pp. 70211S-70211S-9 (2008).

[5] Komiyama, Y., Miyazaki, S., Nakaya, H., Furusawa, H., Takeshi, K., "Subaru next-generation wide-field camera: HyperSuprime", Proceedings of the SPIE, vol. 5492, pp. 525-532 (2004).

[6] Kotani, T., Kawai, N., Yanagisawa, K., Watanabe, J., Arimoto, M., Fukushima, H., Hattori, T., Inata, M., Izumiura, H., Kataoka, J., Koyano, H., Kubota, K., Kuroda, D., Mori, M., Nagayama, S., Ohta, K., Okada, T., Okita, K., Sato, R., Serino, Y., Shimizu, Y., Shimokawabe, T., Suzuki, M., Toda, H., Ushiyama, T., Yatsu, Y., Yoshida, A., Yoshida, M., "MITSuME — Multicolor Imaging Telescopes for Survey and Monstrous Explosions", Il Nuovo Cimento C, vol. 28, issue 4, pp. 755-759 (2005).

[7] Sako, T., Sekiguchi, T., Sasaki, M., Okajima, K., Abe, F., Bond, I. A., Hearnshaw, J. B., Itow, Y., Kamiya, K., Kilmartin, P. M., Masuda, K., Matsubara, Y., Muraki, Y., Rattenbury, N. J., Sullivan, D. J., Sumi, T., Tristram, P., Yanagisawa, T., Yock, P. C. M., "MOA-cam3: a wide-field mosaic CCD camera for a gravitational microlensing survey in New Zealand", Experimental Astronomy, vol. 22, issue 1-2, pp. 51-66 (2008).

[8] Wang, S.-Y., personal comm. (2009).

附錄

NCU/LULIN LOT/1m OBSERVING PROPOSAL

Semester:

※ Observing time is allocated on a 5-month basis, September-January (B), for this semester.
※ The proposal, either in Chinese or English, should be sent to the Time Allocation Committee, preferably via email at tac_lulin@astro.ncu.edu.tw, or via post to Graduate Institute of Astronomy, National Central University, 300 Jungda Road, Chung-Li 32054 Taiwan. Inquiries regarding observing requests or instrumentation can be directed to the same email contact.
※ If time is granted, please fill out the Lulin Lodging Request Form before the observing run (http://www.lulin.ncu.edu.tw/TAC/LulinApplication.htm).
※ At times a time-honored event may require interruption of an ongoing project. The observer will be notified, and consulted for service observations if a mutual agreement can be reached.

---

1. Title of the Proposed Observing Program

---

2. Abstract (limited to 200 words)

---

3. Category

☐Solar System ☐Exoplanets ☐Stars Star Formation ☐Compact Objects
☐Interstellar Medium ☐Nearby Galaxies ☐AGN ☐Cosmology
☐Cluster of Galaxies ☐Gravitational Lenses ☐Large Scale Structure ☐Distant Galaxies
☐Others

---

4. Principal Investigator

Name:
Institute:
Address:
E-mail:
Phone/Fax:

5. Co-Investigators

Name / Institute	Name / Institute	Name / Institute

6. Link to Thesis Work

☐This observing program is linked to a PhD thesis

☐This observing program is linked to a master thesis

Name of the student(s):

7. Time Request

Instrument (LCI/LCS)	Number of Nights	Moon Phase (D/G/B)	Preferred Date	Acceptable Date	Remarks (Hi or Lo-Res for LCS)

Total requested number of nights:

Minimum acceptable number of nights:

8. Scheduling Constraints

9. Instrument Requirements

10. Observing Experiences

11. Backup Program in Poor Weather Conditions

12. Publications related to LOT usage

13. Status of Previous Observations if LOT observing time has been allocated to P.I. before

14. Target List

Object	RA (2000.0)	Dec (2000.0)	Magnitude	Angular Size	Exposure	Remarks

15. Scientific and Technical Justifications (limited to two additional A4 pages, including figures)

相關報導

東南亞最大中央大學建造 2M 光學望遠鏡

陳國維報導

中央大學今天（14）表示，將運用教育部五年五百億的經費，斥資 1 億 3 千萬元，在海拔 2862 公尺、位在南投縣和嘉義縣交界的鹿林天文台，建置 2 米光學望遠鏡，預計 2010 年完工，將成爲東亞最大的望遠鏡之一。

這項 2 米望遠鏡計畫已經在 2006 年啓動，分爲 4 大部分同步進行，包括望遠鏡本體製造、圓頂設計製作、天文台的建築與運輸系統，以及觀測和附屬儀器等。中央大學副校長葉永烜表示，目前已經完成修法和租地的工作，望遠鏡的主鏡片委託俄國的光學儀器廠商製作，天文台的圓頂也初步完成設計。

中央大學天文所所長黃崇源指出，鹿林天文台目前有 7 座望遠鏡，最大的是直徑 1 米長，未來 2 米望遠鏡建造完成後，將有著 4 倍一米望遠鏡的集光能力，可以觀測到銀河系更清楚、更深層的天體變化，開啓國內超新星搜尋的新視野，再搭配由國科會 3 年補助 4 千萬的可見光三波段同步成像儀，將使台灣在美國夏威夷大學所主導的泛星計畫（Pan-STARRS）中，有更密切的配合。

2 米望遠鏡的工程需要 1 億 3 千多萬元，中央大學表示，其中 9600 萬元來自教育部 5 年 5 百億元經費，另外還有 4000 萬由校方自籌來配合建設工程。

【原文轉載自 2008-03-14/國立教育廣播電台】

中大將建兩米望遠鏡追蹤天體獨步全球

中央社記者周永捷嘉義十四日電

二度獲得教育部「發展國際一流大學計畫」的中央大學今天展示鹿林天文台建置成果，並預計在 2010 年完成「兩米光學望遠鏡」，成爲東亞地勢最高、觀測條件最好的天文望遠鏡，屆時可配合美國夏威夷大學推動的泛星計畫，成爲全球唯一能持續追蹤迅速變化天體的望遠鏡。

中大連續兩次獲得教育部「發展國際一流大學計畫」，兩次分別獲得六億及七億元補助經費。中大副校長葉永烜今天帶領媒體記者及教育部官員至位於海拔兩千八百六十二公尺的鹿林天文台參觀計畫成果。

葉永烜表示，中大將斥資一億三千萬元，在鹿林天文台建置「兩米(口徑兩公尺)光學望遠鏡」，預計 2010 年完成天文台組裝測試，爲東亞地勢最高、觀測條件最好的天文望遠鏡。

中大天文研究所長黃崇源指出，兩米光學望遠鏡因口徑大，集光能力爲現行一米望遠鏡四倍強，可看到比一米望遠鏡可視亮度暗四倍的天體；在可視距離及範圍上，兩米光學望遠鏡可觀查到一米望遠鏡可視距離兩倍遠、可視範圍八倍大的銀河及天體活動情形。

黃崇源說，兩米光學望遠鏡完成後，將使台灣晉升全球中大型望遠鏡之列，配合與美國夏威夷大學推動「泛星計畫（Pan- STARRS）」，一旦夏威夷望遠鏡發現天體迅速變化時，台灣因時區緊接在夏威夷後，新望遠鏡將成爲全球唯一能持續追蹤天體變化的光學望遠鏡，有助台灣在全球天文觀測上佔有一席之地。

鹿林天文台設於海拔兩千八百六十二公尺的玉山國家公園旁，光害和塵害少，加上緯度低，可以觀測較寬廣的天域。鹿林天文台曾在 2002 年發現台灣第一顆小行星，迄今發現近四百顆，其中有六顆已取得正式編號，擁有命名權；2007 年台灣本土望遠鏡發現第一顆彗星，名爲「鹿林彗星」。

【原文轉載自 2008-03-14/中央社】

中央大學擬建天文望遠鏡教授捐畫義賣

【陳至中／嘉義報導】

中央大學預計於鹿林興建東亞最大的直徑二米天文望遠鏡，經費需求高達 1.3 億，五年五百億頂大計劃可挹注 9600 萬，中央得另自籌 40 00 萬，副校長兼天文所教授葉永烜決定捐出四幅個人畫作，希望藉此拋磚引玉，爲台灣二米望遠鏡圓夢。

爲發展國際一流大學，中央大學將斥資 1.3 億在海拔 2862 公尺的鹿林天文台建置二米光學望遠鏡，預計 99 年組裝測試完成，成爲東亞最大之望遠鏡之一，對於提昇我國天文研究國際地位有莫大助益。

中央目前在鹿林設置有一組直徑一米望遠鏡，及數組小型望遠鏡，參與國際天文計畫包括「中美掩星合作計畫」、「超新星巡天計畫」、「泛星計畫」等，迄今累計發現近 400 顆小行星，其中六顆取得正式命名權，爲東亞發現小行星最活躍的天文台。

鹿林天文台位於海拔 2862 公尺的嘉義鹿林前山，爲東南亞地區海拔最高、光害最少的觀測地點，地理位置相當優越。中央大學天文所所長黃崇源表示，裝置二米望遠鏡，可望比現有一米觀察範圍多 8 倍、距離遠 2 倍。

二米望遠鏡需經費 1.3 億，其中五年五百億計畫投注 9600 萬，其中購買望遠鏡就需 8000 萬，設置圓頂和施工費用需 1600 萬，中央大學另需自籌 4000 萬配合相關建設工程，尚有相當大的資金缺口。

爲此，中央副校長葉永烜捐出四幅畫作，希望能達到拋磚引玉的效果。葉永烜爲華人世界登上國際頂尖期刊《Nature》、《Science》論文篇數最多的學者，計有 41 篇，參與國際多項天文太空計畫。除了天文研究的貢獻，葉永烜也是油畫的創作者，作品多半呈現印象派畫風。

【原文轉載自 2008-03-15/中國時報/C4 版】

鹿林天文台高海拔低緯度觀測成果豐碩

陳國維報導

中央大學預計 2010 年在鹿林天文台，建造完成 2 米的光學望遠鏡，這座成立近 10 年的鹿林天文台，因爲海拔高、緯度低、接近赤道，可以觀測到較寬廣的範圍，尤其沿著夏威夷的大天文台，向西到台灣，中間沒有任何觀測站，因此，鹿林天文台成爲國際上重要的觀測點。

鹿林天文台在鹿林前山，橫跨南投縣和嘉義縣，海拔 2862 公尺，位於逆溫層之上，光害和塵害少，中央大學強調，這是目前台灣最高的天文台，由於接近赤道，可以觀測到日本、韓國等國家，觀測不到的南半球天體，中央大學天文所所長黃崇源說，靠著鹿林天文台的觀測系統，去年首次由台灣本土的望遠鏡發現第一顆彗星「鹿林彗星」，並從 2002 年起到現在，已經發現將近 400 顆小行星，其中有 7 顆取得正式編號，擁有命名權，當中已命名的 3 顆小行星分別叫「鹿林」、「中大」、「嘉義」。

中央大學表示，鹿林天文台也參與多項國際計畫，包括美國夏威夷大學天文所及美國空軍合作的「泛星計畫」、伽瑪射線爆可見光餘暉認定，以及亞洲大氣污染的長程輸送與衝擊研究等。另外，有關鹿林天文台的研究發現，也有 8 篇文章刊登在國際期刊「Nature」和「Science」。

【原文轉載自 2008-03-15/國立教育廣播電台】

捐畫助圓夢　設鹿林望遠鏡　中大義賣籌經費

【記者陳智華／嘉義報導】

由於內政部修法解套，中央大學昨天宣布，將建置鹿林天台文 2 米望遠鏡，由於需要經費 1.3 億元，該校還需自籌 4 千萬，目前仍不足近 2 千萬，該校副校長葉永烜也捐出 4 幅個人畫作，義賣籌款。

中央大學表示，海拔 2862 公尺的鹿林天文台已有 1 米光學望遠鏡，2 米望遠鏡將建置在 1 米望遠鏡的附近，預計 2010 年於天文台組裝測試完成，將成爲東亞最大的望遠鏡之一，建立台灣完整自主的光學觀測能力，對提升天文研究國際地位有很大助益。

中央大學天文所所長黃崇源表示，鹿林天文台使用 1 米望遠鏡已有多項重大發現，2 米望遠鏡集光能力是 1 米的 4 倍，可看到更暗的星星，看到星空的範圍，也將是 1 米望遠鏡的 8 倍，讓台灣晉升中大型望遠鏡之列。

黃崇源指出，目前 2 米望遠鏡預定地屬國土保安用地，要申請建照找不到主管關機，最近由立法院長王金平召開跨部會會議，內政部修法，在國土保安用地中增列用途可包括天文台，才讓此案解套。

葉永烜是國際知名天文學家，是華人世界登上國際頂尖期刊「Nature」及「Science」論文篇數最多的學者，爲替中大鹿林天文台 2 米望遠鏡募款，捐出 4 幅個人畫作義賣，希望民眾爲台灣的 2 米望遠鏡圓夢。

葉永烜中學畢業時，曾有進入藝專研習繪畫的念頭，最後選擇從事科學研究的工作，直到 1987 年，才重拾畫筆，早期用畫筆，後來改用畫刀，作品近 200 幅。

葉永烜作品以風景和人物爲主，在各地取景，這次義賣的 4 幅油畫，有 2 幅是和鹿林天文台遙遙相望的玉山，另兩幅是夏荷，都是他近期作品。

【原文轉載自 2008-03-15/聯合報/C4 版】

中央大學義賣籌款～全台首部 2 米望遠鏡 2010 年圓夢

記者葉正玲／嘉義報導

中央大學發展國際一流大學計劃，將在海拔 2 千 8 百多公尺的鹿林天文台，建置全台首部「2 米光學望遠鏡」，並預計 2010 年建置完成，開始科學觀測。由於需要經費 1.3 億元，該校還需自籌 4 千萬，中大副校長葉永烜也捐出 4 幅個人畫作，義賣籌款。

中央大學連續兩次獲得教育部「發展國際一流大學計畫」補助，葉永烜表示，鹿林天文台已有 1 米光學望遠鏡，2 米望遠鏡將建置在 1 米望遠鏡的附近，預計 2010 年於天文台組裝測試完成，成爲東亞地勢最高、觀測條件最好的天文望遠鏡。

中大天文研究所長黃崇源指出，2 米望遠鏡因口徑大、集光率強，可看到比 1 米望遠鏡可視亮度暗 4 倍的星星；在可視距離及範圍上，2 米光學望遠鏡可觀查到 1 米望遠鏡可視距離兩倍遠、可視範圍 8 倍大的銀河及天體活動情形。

由於 2M 望遠鏡預定地屬國土保安用地，中央大學在申請建照時，一度面臨找不到主管機關的困境，歷經

長達一年半的折衝，最近由立法院長王金平召開跨部會會議，內政部修法，在國土保安用地中增列用途可包括天文台，才讓此案解套。

中央大學表示，2 米望遠鏡所需經費高達 1.3 億元，該校還需自籌 4 千萬，目前仍不足近 2 千萬。爲了替中大鹿林天文台 2 米望遠鏡募款，副校長葉永烜捐出 4 幅個人畫作義賣，其中有兩幅爲玉山，和鹿林天文台遙遙相望，另兩幅是夏荷，希望藉此拋磚引玉，爲台灣第一座 2M 望遠鏡圓夢。

葉永烜是國際知名天文學家，是華人世界登上國際頂尖期刊「Nature」及「Science」論文篇數最多的學者，同時也是油畫藝術創作者；他 1987 年重拾畫筆，作品多半呈現印象派畫風，創作量高達百餘幅，曾於 1998 年於中央大學藝文中心舉辦個展。

【原文轉載自 2008-03-16/東森新聞報】

中大副校長葉永烜賣畫催生望遠鏡

〔記者謝文華／嘉義報導〕

「小時候，我幫同學畫一張坦克車或飛機，賺到兩張圖畫紙；現在也希望能靠著義賣畫作拋磚引玉，爲台灣首座兩米寬口徑的望遠鏡催生，期待將本土的天文研究推上另一高峰、與世界接軌！」

中央大學「發展國際一流頂尖計畫」，將斥資一點三億新台幣，在嘉義、南投交界，海拔兩千八百六十二公尺的鹿林天文台建置兩米口徑的光學望遠鏡。雖有五年五百億經費挹注和學校自籌款，但尚不足近兩千萬，副校長葉永烜昨天象徵性在鹿林天文台「登高一呼」，義賣四幅油畫籌措經費。

葉永烜是國際知名天文學家，還是華人世界登上國際頂尖期刊「Nature」、「Science」論文篇數最多的學者，至今已累積四十一篇之多。他曾是歐洲和美國合作「卡西尼」土星探測計畫的發起人之一，曾參與拍攝哈雷彗星彗核、美國太空總署「深太空一號」、歐洲太空總署ＥＳＡ的火星快車、水星計畫等任務。

葉永烜雖選擇科學研究做爲一生的志業，但並未忘記從小對畫畫的喜愛。四十歲時，他重拾畫筆，二十一年來，畫了近兩百幅油畫。

談起重新畫畫的過程，葉永烜透露，當時在德國的大學擔任研究員，每週開車送妻小到市中心購物，總被一家賣畫筆的小店吸引，但直到十年後，他才有勇氣推開那扇門。

六十一歲仍童心未泯的葉永烜解釋，德國的畫筆價格高，剛開始他拿孩子的蠟筆作畫，因深愛油畫，曾爲了省錢，拿燭火燒蠟筆，靠蠟滴作畫。

葉永烜說，有一陣子最愛畫「椅子」和「人的背影」，因爲永遠不會有人怪他：「你怎麼把我畫得這麼難看？」他的第一次畫展在德國一家鎮上的法院舉行，葉永烜笑說，鎮裡所有做壞事被抓進去的人，都看過他的畫。

天文研究所所長黃崇源表示，鹿林天文台九十二年啓用一米寬口徑的望遠鏡至今，已觀測到五百個小行星、十五個超新星。口徑愈大、集光力愈強，兩米口徑的望遠鏡可觀測到比一米望遠鏡暗四倍的星星、觀測範圍多出八倍！

亞洲目前也有兩米寬上下的望遠鏡，但台灣有其得天獨厚的觀測優勢，包括鹿林天文台海拔高，光害及塵害少，還接近赤道的低緯度，可觀測較寬廣天域，成爲西太平洋重要觀測據點。

【原文轉載自 2008-03-15/自由時報/A16 版】

鹿林彗星長尾巴一天比一天亮

李宗祐／台北報導

首顆由國內天文台觀測發現並命名的「鹿林彗星」，再度現身天際。中央大學鹿林天文台最近追蹤觀測，鹿林彗星逐漸長出尾巴，其繞行軌道明年一月通過近日點，二月廿七日距地球最近，亮度越來耀眼，屆時以肉眼就可觀測到。

鹿林天文台觀測員林啓生去年七月十一日利用四十一公分口徑天文望遠鏡進行例行性小行星巡天觀測時，經大陸廣州中山大學學生葉泉志協助分析資料，在寶瓶座附近發現、並經國際天文聯合會確認一顆新彗星，即「鹿林彗星」，成爲台灣本土發現、並命名的第一顆彗星。

鹿林天文台台長林宏欽表示，鹿林彗星因繞行軌道距離太遠，台灣地區一直未能再觀測到，最近才再度現身，從鹿林天文台一公尺口徑天文望遠鏡已隱約可見彗尾。以一般天文望遠鏡觀測，可能要等到今年底、明年初，彗星接近近日點，才有機會看到拖著尾巴的鹿林彗星。

林宏欽表示，根據目前粗估軌道來看，鹿林彗星將在明年一月通過近日點，明年二月廿七日（隨著更多觀測料資料，日期可能會有變更）最接近地球，距地球僅約六千萬公里，在獅子座方向。屆時整夜可見，亮度預計可達五到六等左右，以雙筒望遠鏡便可看到，在天氣晴朗、沒有光害的地方，肉眼便可見。

明年正好是「世界天文年」，紀念伽利略利用望遠鏡觀察星空，讓人類邁入現代天文觀測滿四百周年。而鹿林彗星被認爲是路長周期（周期超過二百年），或一去不復返的非周期彗星，明年距離地球最近，是現代人這輩子唯一可近距離觀測廬山真面目的機會。

【原文轉載自 2008-04-24/中國時報/A8 版】

北回歸線立標 100 年　嘉縣舉辦系列活動

（中央社記者江俊亮嘉義縣一日電）

為慶祝北回歸線立標一百週年，嘉義縣政府自今天起舉辦系列活動，首先登場的是「科技百年驚嘆號」科學展覽，並將舉辦「太陽能模型車競賽」，而中央大學鹿林天文台新發現的小行星「嘉義」，也將在夏至晚會中，贈送給嘉義縣政府。

今天登場的「科技百年驚嘆號」科學展覽，是由嘉義縣長陳明文、民進黨立委張花冠主持揭幕儀式，參觀民眾可在展場透過自行操控與螢幕互動方式，深入了解台灣這一百年來的科技演進與發展過程，從不同層面認識台灣的進步。

陳明文致詞表示，西元 1908 年（日本明治四十二年），當時在日本統治下的台灣，為了慶祝台灣鐵路全線通車，在目前的嘉義縣水上鄉下寮村縱貫鐵道旁，興建一座舉世首見的「北回歸線地標」，這是全世界第一座北回歸線標誌。

他說，在天文意義上，太陽直射地球最北端的位置，稱為北回歸線；在地理上，北回歸線是地球北半球熱帶與溫帶氣候的分界線；在人文方面，地標經歷了一百年的人世滄桑，如今已設立到第六代地標塔，雖然前四代地標塔已走入歷史，但北回文教基金會已根據老照片仿造成四座小型地標塔，與第五、六代地標塔並列。

今天揭幕的「科技百年驚嘆號」科學展覽，展出項目包括：台灣第一、水利中控室、化工黑板、機器版畫、我們住過的家、跳舞機、牽豬哥、稻米的一生、蘭花奇鏡、熱帶醫學等十項，內容涵蓋植物科學、動物科學、土木工程、電力水利、化工、機械、醫學生技與電腦資訊等。

陳明文指出，這項特展是由國科會設計規劃、高雄科工館巡迴至嘉義展出，其中的「蘭花奇鏡」，民眾只要以手碰觸鏡外的蝴蝶蘭模型，鏡子裡的蘭花都會隨著變色，相當新鮮有趣，陳明文也藉由實際操作，體會台灣「蝴蝶蘭王國」的美譽，並親自感受台灣科技進步的歷程。

由於夏至日是太陽直射北回歸線的日子，因此縣府將於夏至日（六月二十一日）舉辦「北回歸線盃」全國國中小學太陽能模型車競賽，以啓發學生們的創意思維、環保觀念，並培養學生們對綠色能源的重視。

此外，中央大學鹿林天文台新發現的小行星，經國際命名為「嘉義」，也將於夏至日在北回歸線太陽館前廣場舉辦的「夏至嘉義．北回一百」慶祝晚會中，由中央大學將「嘉義」行星模型贈送給嘉義縣政府，當晚也將邀請專家現場指導如何「觀賞嘉義的星空」。

【原文轉載自 2008-06-01/中央社】

北回歸線立標 100 年　嘉縣 21 日舉辦慶祝晚會

（中央社記者江俊亮嘉義縣三日電）

嘉義縣政府為了慶祝北回歸線立標一百週年，訂二十一日「夏至」晚上在北回歸線太陽館舉辦慶祝晚會，縣長陳明文今天召開記者會，公布限量發行的紀念衫，另有兩百二十個限量典藏包將在當晚抽獎送出。

陳明文表示，北回歸線矗立在嘉義縣水上鄉下寮村，西元 1908 年（日本明治四十二年），日本政府為了慶祝台灣鐵路全線通車，在北緯二十三點五度的水上鄉下寮村縱貫鐵道旁，興建一座舉世首見的「北回歸線地標」，成為全世界第一座北回歸線標誌。

他說，台灣是北回歸線經過的十六個國家中最大的海島，而嘉義縣則是北回歸線經過的物產最豐富而優質地區，雖然這是一條抽象的緯線，但縣府落實為具象的建築，民眾在北回歸線地標館前，可以得知正在跨越熱帶與副熱帶氣候區。

為了慶祝北回歸線立標一百週年，嘉義縣府除了自六月一日至八月三十日在北回歸線太陽館舉辦「科技百年驚嘆號」科學展覽之外，六月二十一日當天則有全國國中小學「太陽能模型車競賽」；中央大學鹿林天文台新發現的小行星「嘉義」，也將在夏至晚會中舉行贈星儀式，贈送給嘉義縣政府。

陳明文指出，為了配合北回歸線立標一百週年活動，縣府將發行限量紀念衫，總數只有一百件，六月九日起接受預訂，每人只限購一件；另外，縣府還發行一款「限量典藏包」，圖案以北回歸線第一代地標為主題，將在二十一日晚上的「夏至嘉義．北回一百」晚會中抽獎送出。

為了行銷嘉義，陳明文今天率領縣府官員及來賓，穿越象徵北緯二十三點五度的北回歸線，並敲響開幕鑼，為北回歸線立標一百週年系列活動揭開序幕，同時將第一代至第六代北回歸線地標塔模型放置在縣府中庭，讓民眾了解北回歸線百年來的歷史。

【原文轉載自 2008-06-03/中央社】

6/21 夏至　嘉縣北回歸線立標百年　活動多

〔龐清廉報導〕

今天是 6 月 21 日＜夏至＞，太陽直射北回歸線，也是嘉義縣北回歸線立標一百周年紀念日，嘉義縣政府舉行一系列慶祝活動．響應節能減碳，上午首先由別具意義的＜太陽能模型車競賽＞登場，另有＜科技百年驚

嘆號＞科學天文展，還有天文觀星慶祝晚會，而一顆由中央大學發現，以＜嘉義＞命名的行星，相關資料也展示於北回歸線天文館中。

日治時期，西元 1908 年，爲慶祝台灣鐵路全線通車，日本政府在嘉義縣水上鄉下寮村鐵道旁興建了全世界第一座「北回歸線地標」，距今剛好是一百年，這一個世紀以來，北回歸線地標歷經六次更替，現今的北回歸線太陽館是第六代標塔，也是唯一座可以讓民眾進出，兼具展覽、研習功能的標塔。

爲慶祝北回歸線立標一百周年，嘉義縣舉辦了一系列活動，上午首先登場的是有一百五十六所國中小報名，規模盛大的太陽能模型車競賽，主辦單位強調，節省減碳已成風潮，在太陽直射北回歸線的今天，希望學生能學習如何利用太陽能的方法和觀念，也培養他們的創意和設計實作能力。

學生們利用太陽板，搭配保特瓶、廢紙、不要的光碟片，現場創作造型奇特的太陽能模型車，環保又兼具創意，玩的不亦樂乎，正式比賽時，雖然雲量大，太陽偶而才露臉，模型車運動效果不如預期，但學生們還是樂在其中，現場加油聲不斷。

晚上，嘉義縣北回歸線廣場上，並有一場慶祝晚會，有精彩藝文表演還有文天觀星，而國立中央大學也正式將日前發現的一顆行星，命名爲＜嘉義＞，贈給嘉義縣，並在天文館內展示相關資料。

嘉義縣長陳明文強調，北回歸線天文館，兼具天文教育意涵與娛樂效果，縣府將列列特色觀光資源，全力行銷，以吸引更多遊客。

【原文轉載自 2008-06-21/中廣新聞網】

大氣汞傷人無形　台灣鹿林山成國際研究夥伴

（中央社記者陳舜協台北二十八日電）

「鮪魚、鯊魚等大型魚類不宜多吃」，大型魚類含汞濃度高，與食物鏈及生物累積作用有關，海水中的有機汞濃度增加，與大氣中的元素汞、氯化汞濃度息息相關，大氣汞能傷人於無形，近來引起國際重視，台灣的鹿林山監測站位置優越，成爲國際重要研究夥伴。

汞，是唯一可以液態、氣態同時存在自然界的重金屬，百分之九十五到百分之九十九的是以元素汞狀態存在於大氣之中，少部分透過降雨、沈積方式溶入水中、土壤，透過細菌、有機物質作用甲基化，成爲甲基汞，雖然可以被生物代謝，但代謝週期長，透過食物鏈方式累積，鯊魚、鮪魚等掠食魚類已被證實甲基汞含量高。人體攝入、累積過多甲基汞，一樣會引起汞中毒事件。台灣發生過有一家五口長期食用魚類，結果四人有慢性汞中毒症狀。

林口長庚醫院臨床毒物科主任林杰樑說，汞攝食過量會影響腦神經發展，成年人會動作遲緩、腎臟病變，兒童會危害智能、身心發展，而孕婦或哺乳的母親可能將汞傳給胎兒或嬰兒，造成神經病變、發育遲緩等。

汞對人體健康危害大，美國食品暨藥物管理局（FDA）2001 年一月發佈警訊，警告孕婦或準備懷孕婦女應 避免食用鯊魚、旗魚、馬頭魚、國王青花魚等大型魚類，2003 年將鮪魚追加列入警告名單內。因醫學研究證實及實際汞中毒案例出現，部分人對食用深海魚類態度保留。

衛生署藥物食品檢驗局副研究員陳石松表示，深海魚、近海魚及養殖魚，或多或少含甲基汞，「重點在於不要攝食過量」。衛生署建議深海魚類每週攝食量不要超過三百四十公克，平時要各種魚類混合食用，不點食用單一魚種，就可降低人體攝入過多甲基汞風險，並可攝入含量極高的不飽和脂肪酸及優良蛋白質。深海魚類甲基汞含量高，追根究底還是因爲大氣總汞濃度增加有關。

環保署監境監測及資訊處簡任技正張順欽表示，大氣汞的含量增加與人類經濟與工業活動快速成長高度正相關，而且大氣總汞濃度以 ppb（十億分之一）計量，經生物累積後濃度大幅增加百萬倍以上，進入人體後以 ppm（百萬分之一）計量，大氣汞對人體的危害及跨國傳輸問題，近年來已被國際高度重視。

中央大學大氣科學系教授許桂榮表示，中國大陸是全球大氣汞產出最多的地區，每年冬季來自中國的高濃度大氣汞會隨冷氣團、東北季風影響台灣及太平洋地區，因大氣汞沈降被植物、生物吸收後對人體造成的影響有待進一步研究，但不能不加以注意。

台灣的地理位置優越，在美國大氣與海洋署（NOAA）協助下，環保署 2006 年四月啓用標高達二千八百六十二公尺、東亞最高的鹿林山背景測站，其中一項重要任務就是監測空氣中的大氣總汞濃度，成爲國際研究重要夥伴。環保署表示，大氣總汞濃度監測資料將成爲國際規範「汞」削減量的基礎，鹿林山監測站可望爲國際環保、生態保育做出重大貢獻。

【原文轉載自 2008-06-28/中央社】

業餘天文學家　揚名星空

楊惠芳／臺北報導

由中央大學鹿林天文臺發現的小行星（編號 168126），最近經由國際天文聯合會小行星命名委員會審議通過，正式命名爲「Chengbruce（鄭崇華）」，以肯定鄭崇華追求環境永續、善盡綠色公民責任的努力。中央大學副校長葉永烜表示，這是國內首度以臺灣企業

家爲名的小行星，具有重要意義。

鄭崇華是臺達電子公司董事長暨創辦人。他從青少年就開始著迷天文，時常仰望星空，領略生命的價值，開啓對地球和宇宙的好奇。鄭崇華說，地球只有一個，因此，他許下重環保、愛地球的承諾，以節能減碳、珍愛地球爲努力的目標。

葉永烜表示，鄭崇華長期捐贈清大、成大及中央等大學，爲教育和公益奉獻，但從來不彰顯自己的名字，而以孫運璿、李國鼎等人名爲主，紀念他們對臺灣科技的貢獻。

葉永烜說，國際天文聯合會小行星命名委員會審議相當嚴格，這次小行星以「鄭崇華」命名，並獲得通過，主要是鄭崇華本身爲業餘天文學家，且符合「三 A 精神」，足爲青年學生的表率，「三 A 精神」是指 Ability（能力）、Attitude（態度）、Altruism（博愛）。

【原文轉載自 2008-07-09/國語日報/2 版/文教新聞】

台灣首位企業家命名爲小行星

鉅亨網記者葉小慧．台北

台達電董事長鄭崇華追求環境永續、善盡綠色公民責任的努力獲得肯定，由中央大學鹿林天文台所發現編號 168126 的小行星，經過國際天文聯合會 (IAU)小行星命名委員會審議通過，正式命名爲「Chengbruce (鄭崇華)」，這是國內首次以台灣企業家爲名的小行星。

對於自己名字被用來命名小行星，鄭崇華表示很意外，但感覺非常溫馨。他說，行星壽命至少比人類長，這會是他一輩子都永遠記得的一件事，開心的感覺很難用言語形容。

鄭崇華是在 2005 年秋天，在前中央大學校長劉全生的陪同下，以 70 歲高齡，一步一腳印步行登高 600 公尺，登上海拔 2862 公尺的玉山鹿林天文台，成爲台灣第 1 位登上中大鹿林天文台的企業家。

在寶來集團和交大產學合作鬧出風波之後，中央大學卻用台達電董事長的名字命名小行星，中央大學副校長葉永烜表示，中央大學和台達電的產學合作關係已經很久，不過將發現的小行星命名爲「鄭崇華」，主要是鄭崇華提倡「環保、節能、愛地球」的理念和中央大學環境永續理念一致。

葉永烜說，這次中央大學首次嘗試以個人命名，以後命名對象不限於企業家，只要是對年輕人有啓發性指標作用的對象，對社會、國際甚至全人類有貢獻，各領域人士或組織都考慮用來命名。最近還有另一顆也是由中央大學與他人合作發現的小行星，爲紀念中國汶川大地震，共同發現者以「汶川星」提出命名申請。

根據國際規則，小行星發現者擁有 10 年的命名權，但必須報請國際小行星中心和小行星命名委員會審議通過後，才成永久命名。而小行星命名也不是那麼簡單申請，微軟總裁比爾蓋茲就曾想以自己名字命名小行星，但 IAU 認爲比爾蓋茲就代表微軟，太過商業，就沒有通過。

用「鄭崇華」命名的 「168126 Chengbruce」小行星是在 2006 年 4 月 1 日，由中央大學天文所研究助理楊庭彰與中國廣州中山大學大二學生葉泉志合作發現，它位於火星和木星之間的小行星帶，大小約 3.6 公里，形狀屬不規則狀，預估今年 12 月左右，可再次透過 40 公分以上的望遠鏡拍攝到它的影像。

【原文轉載自 2008-07-08/鉅亨網】

小行星首次以台灣企業家鄭崇華命名

邱莉苓報導

宇宙中除了名爲「鹿林」、「中大」的小行星，最近還多了一顆「鄭崇華」。中央大學鹿林天文台發現的編號 168126 小行星，最近經國際天文聯合會（ＩＡＵ）審議通過，正式命名爲「Chengbruce（鄭崇華）」，這是首次以台灣企業家爲名的小行星。

鄭崇華是台達電子董事長暨創辦人，中央大學副校長葉永烜 8 日指出，鄭崇華符合中央對學生期許的三 A 精神—能力（ ability ）、態度（ attitude ） 和博愛（ altruism ），足爲世人和青年學子表率，先經校內審查委員會通過，再向ＩＡＵ申請以鄭崇華爲名，因其節能、愛地球受肯定而通過。

中央大學也表示，最近除了以鄭崇華命名小行星，另一顆小行星也以已過世的企業家溫世仁來命名，表彰他的慈善、愛心和無私的貢獻，還有一顆命名爲「汶川」，則是爲了紀念四川大地震。

中央大學天文所所長黃崇源說，這顆「168126 Chengbruce」小行星，是在 2006 年 4 月 1 日透過中大鹿林天文台 40 公分望遠鏡、由中大天文所楊庭彰與廣州中山大學葉泉志聯手發現，他們選定幾個天空區域，每間隔數分鐘觀測一次，共觀測 3 次。

中大天文所發現它在同一天區的比對影像中「跳動」，經確定其軌道位置，證實是新發現的天體。

「鄭崇華」小行星位於火星和木星之間的小行星帶，2006 年 4 月發現在室女座位置，目前位置在金牛座附近。大小約 3.6 公里，呈不規則狀，繞太陽 1 周約 4.14 年，預估今年 12 月左右，可再次透過 40 公分以上的望遠鏡拍攝影像。

【原文轉載自 2008-07-09/中央廣播電台新聞】

中央大學發現的小行星定名「鄭崇華」

由國立中央大學鹿林天文台所發現的編號 168126 小行星，經國際天文聯合會（IAU）審議通過，正式命名爲「Chengbruce 鄭崇華」，以肯定台達電董座鄭崇華追求環境永續、善盡綠色公民責任的努力，這也是國內首次有企業家名字躍上星空，成爲小行星的名字。中央大學副校長葉永烜表示，「鄭崇華」小行星能審議通過，主要因爲鄭董事長是業餘天文學家的背景，以後命名邀請對象可能朝向致力慈善、外交等各個領域人士，或是以組織來命名。

【原文轉載自 2008-07-08/國立教育廣播電台文教新聞】

鄭崇華小行星　即日起環繞天際

王中一報導

即日起，編號「168126 號」的小行星，將以「Chengbruce(鄭崇華)」名字環繞天際！這也是第一個由本土發現、經國際天文聯合會審議通過，且是第一個以國內企業家命名的小行星。這份榮譽，連微軟的比爾蓋茲至今都還享受不到。

就在寶來集團與交通大學因爲產學合作，引發連串風波之際，中央大學昨天舉行這項小行星的命名儀式，確實讓外界捏把冷汗！不過，中大副校長、同時也是國際知名天文學家的葉永烜，則完全不擔心。

葉永烜說，國際天文聯合會審議命名過程嚴格，之前比爾蓋茲曾想以自己名字命名小行星，但被該會以「比爾蓋茲就代表微軟、太過商業化」爲由，屢屢駁回申請案，可見通過審議之不易。鄭崇華本身就是業餘天文學家，是通過審核的關鍵。

鄭崇華在國內一向是環保、節能的代表性人物，此次小行星的命名，就是肯定他對追求環境永續、愛地球具體貢獻及善盡綠色公民責任的努力。他相信人們只要用心，就可以在不犧牲生活品質的前提下，節省一半的能源，「多試試，錯了也無妨；但不做就永遠無法改善。」

【原文轉載自 2008-07-09/工商時報/B4 版/上市櫃 2】

台達電董座鄭崇華　躍上星空成小行星

陳映竹報導

浩瀚的宇宙中，出現了一顆以台達電董座鄭崇華爲名的「鄭崇華」小行星！中央大學通過國際天文聯合會審議通過，將本土發現編號 168126 小行星，正式命名爲「Chengbruce 鄭崇華」，這也是國內首次有企業家名字躍上星空，成爲小行星的名字。

繼「鹿林」、「中大」、「嘉義」後，中央大學再度發現小行星，並且以台達電子董事長鄭崇華爲名。這顆小行星是在 95 年 4 月被中大鹿林天文台 40 公分望遠鏡所發現，同時也是台灣本土發現，「鄭崇華」小行星的位置目前在金牛座附近，預計在今年十二月可透過望遠鏡觀察。

在交大和寶來集團產學合作鬧出風波的節骨眼上，中大卻用企業家名字直接命名小行星。中央大學副校長葉永烜笑著說，雖然時機敏感，但卻沒有爭議，因爲「鄭崇華」小行星通過審議的關鍵爲：他是業餘天文學家的背景，中央大學位在玉山鹿林的天文台，鄭崇華就曾經以七十歲高齡，徒步登上。

葉永烜說，這次中央首次嚐試以個人命名，以後命名邀請對象不限於企業家，可能朝向致力慈善、外交等各個領域人士，或是以組織來命名。

根據國際規則，小行星發現者擁有十年的命名權，但必須報請國際小行星中心和小行星命名委員會審議通過後，才成永久命名。小行星命名也有一番學問，像是政治、軍事人物不行，商業名稱也不行，像是過去微軟總裁比爾蓋茲就曾想以自己名字命名小行星，但國際天文聯合會認爲比爾蓋茲就代表微軟，太過商業，最後都叩關失敗。

【原文轉載自 2008-07-08/中廣新聞網】

中央大學發現小行星　命名爲「鄭崇華」

(中央社記者韓婷婷台北 2008 年 7 月 8 日電)

由中央大學鹿林天文台所發現編號 168126 小行星，經過國際天文聯合會 (IAU) 小行星命名委員會審議通過，正式命名爲「Chengbruce(鄭崇華)」，以肯定台達電子 (2308)董事長鄭崇華追求環境永續、善盡綠色公民責任的努力。

這顆「168126 Chengbruce」小行星，是在 2006 年 4 月 1 日由中央大學天文所研究助理楊庭彰與中國廣州中山大學大二學生葉泉志合作發現。位於火星和木星之間的小行星帶，大小約 3.6 公里，形狀屬不規則狀，是台灣本土發且首次以台灣企業家爲名的小行星。

一般國際規則，彗星由發現者之名命名，小行星則是發現者擁有 10 年的命名權，必須報請國際小行星中心和小行星命名委員會審議通過後，才成永久命名。國外以企業家命名小行星情況常見，在台灣則是第一次。

自己名字首度被用來命名小行星，鄭崇華說：「很意外，但感覺非常溫馨，行星壽命至少比人類長，這會是他一輩子都永遠記得的一件事，那種開心的感覺很難用言語形容」。

鄭崇華與這顆小行星緣起於 2005 年秋天，在前中

央大學校長劉全生的陪同下，以 70 歲高齡，一步一腳印步行登高 600 公尺，登上海拔 2862 公尺的玉山鹿林天文台，成爲台灣第一位登上中大鹿林天文台的企業家。

【原文轉載自 2008-07-08/中央社】

太空探索／鄭崇華愛天文　168126 小行星以他爲名

財經中心／台北報導

提到鄭崇華，很多人都知道他是電子大廠台達電的董事長，從今天開始，「鄭崇華」也正式成爲星星的名字！就是因爲鄭崇華不只熱衷天文，還長期推廣環保節能，良好的企業家形象，讓中央大學決定所發現編號 168126 號小行星，未來將以「鄭崇華」三個字來命名。

雙手高舉小行星模型，台達電子董事長鄭崇華笑得樂開懷，因爲中央大學發現的這顆 168126 號小行星有了新的名字，國際天文聯合會 IAU 日前通過，這顆行星就叫做 Cheng bruce 鄭崇華。

鄭崇華表示，「我也很意外，沒有想到有這麼一件事情，那我聽到這個事情是蠻驚喜的，而且對我是個很大的鼓勵。」

用企業家名字來命名小行星，鄭崇華是台灣史上頭一個，因爲長期推展環保節能的他，形象備受肯定，加上從高中時期就愛仰望星空，還有研究天文，三年前甚至跟著中央大學天文所的師生，爬上海拔 2826 公尺的玉山鹿林天文台來觀星，企業大老闆對天文的熱衷，讓人很佩服。

鄭崇華表示，「(天文知識)書本以外，還有就是報紙，報紙偶然間你會看到天文一個新的發現，一般假如你不太會去注意的話，你看到了也就不會去注意。」

這顆位在火星跟木星之間小行星帶的「鄭崇華」小行星，今年 12 月透過 40 公分以上的望遠鏡，就可以觀測到它的蹤跡，到時候鄭崇華看「鄭崇華小行星」，對鄭崇華而言，屆時的感受肯定會更不同。

【原文轉載自 2008-07-09/NOWnews 今日新聞】

中央大學發現小行星　定名鄭崇華

【本報台北訊】

提倡環保、捐助興學，讓台達電子董事長鄭崇華的姓名高掛星空。國際天文聯合會通過將中央大學發現的一顆小行星定名爲「Chengbruce（鄭崇華）」，以肯定其追求環境永續、愛地球具體貢獻，與其善盡綠色公民責任的努力，這也是國內首次有企業家名字躍上星空，成爲小行星的名字。

「鄭崇華」小行星編號爲一六八一二六號，是民國九十五年四月由中央大學天文所研究助理楊庭彰與中國廣州中山大學大二學生葉泉志合作發現，位於火星和木星間的小行星帶，屬於 Main-belt 小行星。九十五年四月發現在室女座位置，目前位置在金牛座附近。大小約三點六公里，形狀屬不規則狀，繞太陽一周約四點一四年，預估今年十二月左右可再次透過四十公分以上的望遠鏡拍攝其影像。

台灣的小行星發現肇始於中央大學。中大鹿林天文台自國九十一年發現台灣第一顆小行星以來，累計目前已發現超過六百顆。自九十五年三月的「鹿林巡天計畫」有計畫性觀測以來，平均以每個月發現超過十五顆小行星之速度，成爲亞洲發現小行星最活躍的地方。其中有多顆已取得永久編號，並獲得到國際命名，除「鄭崇華」，還有「中大」、「鹿林」、「嘉義」等。

中央大學以鄭崇華爲小行星命名，除了環保理念相近外，多年捐助興學的背景，也讓中央大學決定以其名爲小行星命名。鄭崇華數次捐助大學都以他人之名命名，行事低調，如八十九年捐助清華大學設置孫運璿科技講座、九十年捐贈成大成立李國鼎科技講座、九十四年捐贈中央大學興建國鼎研發大樓、九十六年捐贈成大興建孫運璿綠建築研究大樓。

據國際規則，小行星由發現者擁有十年命名權，須報請國際小行星中心和小行星命名委員會審議通過後，才成永久命名。微軟創辦人比爾蓋茲曾想以自己名字命名小行星，但國際天文聯合會認爲比爾蓋茲代表微軟，太過商業，最後叫關失敗。中央大學副校長葉永烜表示，鄭崇華本身業餘天文學家的背景，是通過審議的關鍵。

【原文轉載自 2008-07-09/人間福報/2 版/焦點】

中大發現小行星　命名鄭崇華

台灣首度以企業家命名的小行星出現了！中央大學鹿林天文台在二〇〇六年發現編號 168126 小行星，並以台達電子董事長鄭崇華追求環境永續及愛地球的具體貢獻申請提名，經國際天文聯合會（ＩＡＵ）正式通過，命名爲「Chengbruce」。

中央大學副校長葉永烜表示，鄭崇華白手起家打造台達電，且力行節能減碳、珍愛地球，追求環境永續，足爲世人和青年學子表率，因此經校內審查委員會通過，向ＩＡＵ申請以鄭崇華爲名，且經審查通過，成爲台灣第一個以企業家爲名的小行星。

鄭崇華小行星位於火星和木星之間的小行星帶，屬於 Main-belt 小行星，二〇〇六年四月發現在室女座位置，目前位置在金牛座附近。（圖：中央大學提供／文：記者陳宣瑜）

【原文轉載自 2008-07-09/自由時報/A10 版/生活新聞】

鄭崇華小行星　照亮環保心

【記者 詹惠珠】

仰望浩瀚的宇宙，有一顆小行星已被國際天文聯合會 （IAU ）命名爲 Chengbruce（鄭崇華），今年底，只要透過 40 公分的望遠鏡，就可以看到這顆第一次以台灣企業家爲名的小行星，永恆的印記，這是對鄭崇華善盡綠色公民責任最直接的肯定。

這顆名爲鄭崇華小行星是中央大學鹿林天文台所發現的，國立中央大學副校長葉永烜說，鄭崇華所領導的台達電，在設計產品朝著節能著手，並不是爲了利益，而是爲了對環保的承諾，加上鄭崇華對天文的興趣，於是中央大學決定以鄭崇華來命名這顆小行星。

鄭崇華 14 歲時成爲流亡學生，隻身來台，當時在唸台中一中，常常在假日觀星看月，培養出對浩瀚宇宙的好奇心，體會出地球只不過是宇宙中的一顆小星星與人類的渺小，因而養成謙卑、與大自然和平相處的人格特質。

鄭崇華已到了從心所欲不逾矩的年紀，近年來積極投入環保，他認爲對地球的關心已比賺錢和股價來得重要，二氧化碳排放干擾人類的生活、極地冰山的融化及氣候的變遷等問題讓他感到憂心，於是他從自己開始身體力行，盡綠色公民的責任，追求環境的永續。

鄭崇華是國內第一個引進油電混合車的企業家，台達電目前的發展主軸全部以節能爲主，從太陽能、LED 照明、燃料電池、以及應用到電動車的鋰電池，並推動綠建築，以最自然的方式追求環保。

如今他要求台達電要在未來三年內節省二分之一的電力，鄭崇華認爲在不影響生活品質下，能夠節省一半的用電，最近他老家裝修，他全部更換省電燈泡代替傳統燈泡，只要有四分之一到五分之一的節能燈泡，就可以達到同樣的照明，未來使用 LED 燈泡，更只要十分之一的電力。鄭崇華認爲，要靠科技來節能，成爲台達電產品研發的驅動力。

即使台達電一年繳出每股 7 元的獲利能力，不過在談到現今的環境問題，鄭崇華仍感到很無力，更大聲疾呼這關係到後代子孫的生存，不能忽視。

《小辭典》 小行星命名

【記者詹惠珠】

小行星是目前唯一可以由發現者命名，並得到世界公認的天體，當一顆小行星至少四次在回歸中心被觀測到，並且精確測出其運行軌道參數後，就會得到國際小行星中心給予永久的編號。「鄭崇華」（Chengbruce）小行星的永久編號爲 168126。

發現者擁有對小行星的命名權，命名權在十年內隨時可以行使，所有小行星的命名，須報經國際小行星中心和小行星命名委員會審議通過後，才公諸於世，成爲該天體永久的名字，並爲世界各國公認。

【原文轉載自 2008-07-09/經濟日報/A12 版/話題新聞】

中大發現小行星命名「鄭崇華」

【陳怡靜／台北報導】

中央大學昨宣布，二〇〇六年中大鹿林天文台發現編號一六八一二六號小行星已通過國際天文聯合會審查，將以台達電董事長鄭崇華名字命名爲「Chengbruce（鄭崇華）」，這是國內發現新星中首度以企業家爲名的小行星。鹿林天文台發現新星中已有命名「中大」、「嘉義」、「鹿林」，新被命名的「Chengbruce」目前位置在金牛座附近。

推動環保獲肯定

中大副校長葉永烜說，將小行星命名「Chengbruce」是因鄭崇華致力推動環保節能，率先推行省能廠房，且鄭也是首名登上海拔兩千八百多公尺鹿林天文台的企業家。

台達電與中大長期產學合作，每年提供經費由數百萬元到千萬元不等，鄭崇華個人更捐二億元給校方蓋建國鼎研發大樓。中大昨被問到是否「捐款換星星」？葉永烜強調，以名人名字命名是看對社會的貢獻度，和捐款無關，這次通過國際天文聯合會審查的名人，還有已故英業達副董事長溫世仁，而溫從未捐款給中大。

鄭崇華昨開心地說，他從小就喜歡看星星，「天空中有星星以我爲名太榮耀了。」過去以名人命名的小行星還有武俠小說家金庸、藝人林青霞、導演徐克和諾貝爾物理獎得主楊振寧等。

◎鄭崇華小檔案
年齡：72 歲
現職：台達電子董事長
學歷：成大電機系畢
經歷：亞洲航空儀器工程師、美商精密電子品管經理
嗜好：散步、看 Discovery 頻道、參觀世界各地綠建築
資料來源：《蘋果》資料室

【原文轉載自 2008-07-09/蘋果日報/A11 版/生活】

董座名列小行星　中大：無利益交換

陳至中、實習記者蔡依珍／台北報導

在浩瀚的宇宙中，今後又多了 1 顆「鄭崇華」小行星高掛天際！中央大學發現的編號 168126 小行星，日前通過國際天文聯合會 IAU 審議，以台達電董事長鄭崇華命名，表彰其熱心環保、天文的精神。國外以企業家命名小行星並不罕見，在台灣是第 1 次。

但日前才爆發交通大學與寶來集團之間「買學位」的爭議，還鬧出人命，以企業家命名極爲敏感。中大昨天強調，絕無「利益交換」，且 IAU 審核極嚴格，禁止涉及商業行爲、政治、軍事人物，鄭崇華是「業餘天文家」，才能順利叩關。

台達電董座鄭崇華　業餘天文家

中大鹿林天文台是國內海拔最高的星象觀測站，擁有全國最大的 1 米口徑望遠鏡，自 91 年發現台灣第一顆小行星以來，至今已發現超過 600 顆小行星，全亞洲最活躍。其中通過 IAU 審查、獲得永久編號與國際命名權的小行星有「中大」、「鹿林」、「汶川大地震」等，近日增添 1 顆「鄭崇華(Chengbruce)」。

這顆編號 168126 的「鄭崇華」小行星位於火星與木星之間，由中大天文所專任助理楊庭彰與大陸廣州中山大學學生葉泉志合作發現，大小約 3.6 公里，呈不規則狀，繞行太陽 1 周約需 4.14 年。

比爾蓋茲想「登天」　IAU 拒絕

中大副校長葉永烜表示，鄭崇華以光電節能爲努力方向來帶領台達電，這種創新、務實的精神理念與該校相符，故以「鄭崇華」命名。

中大研究發展處處長劉振榮表示，94 年秋，高齡 70 歲的鄭崇華登上海拔近 3000 公尺的天文台，參觀中大的鹿林天文台，依舊健步如飛、羨煞旁人，也種下此次命名的因緣。

鄭崇華昨日直說，「星星壽命比人類長，這經驗一輩子難忘！」

近年國際以人名命名的小行星包括嫦娥、林則徐、蘇東坡；近代人物有金庸、林青霞、徐克、楊振寧等。微軟總裁比爾蓋茲也曾想以自己的名字命名小星生，IAU 認爲過於商業化而拒絕。

【原文轉載自 2008-07-09/中國時報/C4 版/教育新聞】

中大以鄭崇華命名 168126 小行星

【記者謝鎔鮮/台北報導】

浩瀚的宇宙裡除了「鹿林」、「中大」、「嘉義」外，從此多了一顆「鄭崇華」小行星！中央大學以台達電子董事長鄭崇華之名，經國際天文聯合會審議通過，將本土發現編號 168126 小行星正式命名爲「Chengbruce（鄭崇華）」，是國內首次以企業家名字命名小行星。

這顆編號 168126 小行星是 95 年 4 月由中央大學天文所研究助理楊庭彰與中國廣州中山大學大二學生葉泉志合作發現。鹿林天文台台長林宏欽表示，一般國際規則，彗星由發現者之名命名，小行星則是發現者擁有 10 年的命名權，必須報請國際小行星中心和小行星命名委員會審議通過後，才成永久命名。國外以企業家命名小行星情況常見，在台則是第一次。

在交大與寶來集團產學合作鬧出風波的節骨眼上，中大以企業家命名小行星，不怕引發爭議？葉永烜表示，時機的確有點敏感，但他不擔心，國際天文聯合會審議命名過程嚴格，微軟總裁比爾蓋茲曾想以自己名字命名小行星，國際天文聯合會認爲比爾蓋茲就代表微軟，太過商業，最後都叩關失敗，鄭崇華本身業餘天文學家的背景，是通過審議的關鍵。葉永烜說，這次首次嚐試以個人命名，以後命名邀請對象不限於企業家，可能朝向致力慈善、外交等各個領域人士。

全數個人捐贈

鄭都用孫運璿、李國鼎名義捐贈

【記者嚴珮華/台北報導】

台達電董事長鄭崇華對外的捐贈全數來自個人的捐贈，其捐贈分爲三種方式，一是個人捐贈股票，二是個人捐贈現金。三是由個人捐贈股票、現金給台達電文教基金會，再由基金會捐贈等三種方式。不論是股票、孳息、現金，或經由基金會捐贈，都是來自鄭崇華自掏腰包，與台達電企業公司無關。

鄭崇華是捐贈清大、成大或是中央大學，所用的名字，不是孫運璿就是李國鼎，從來不用自己的名字。鄭崇華說，李國鼎是台灣科技之父，非常感念他對台灣科技界的貢獻；而孫運璿更是台灣經濟發展的重要推手，爲紀念兩位對台灣的經濟與科技的重要貢獻，他的捐贈都以兩位先生命名。

追求環境永續另類產學合作

鄭愛天文　樂當綠色公民

【記者嚴珮華/台北報導】

國際天文聯合會（IAU）通過中央大學發現 168126 號小行星定名爲「鄭崇華（Chengbruce）」以肯定台達電子董事長鄭崇華追求環境永續、愛地球具體貢獻，以及善盡綠色公民責任的努力。

鄭崇華與這顆小行星的緣起爲，2005 年秋天，鄭崇華抱持著一顆求知的心，在前中央大學校長劉全生的陪同下，以 70 歲的高齡，一步一腳印步行登高 600 公尺，登上海拔 2,862 公尺的中央大學玉山鹿林天文台，成爲台灣第一位登上中大鹿林天文台的企業家。

鄭崇華喜歡天文，14 歲時，離鄉背井，隻身來台求學，最怕學校放長假，尤其是寒暑假，同學們大多返鄉過節，他常常深夜獨自一人坐在學校大操場仰望星空，從斗轉星移中領略生命價值，開啓他對宇宙的好奇，體認宇宙的浩瀚、與人類的渺小，從此他對天文結了不解之緣。

鄭崇華畢業於成大電機系，但是他對天文更感興趣，體認，地球只有一個，是現在台達電子以環保、節能爲企業文化及個人理想結合的重要主因，他並許下重環保、愛地球的承諾，產品追求環保節能，更將概念深化在日常運作中。

台灣的小行星發現肇始於中央大學。中大鹿林天文台自 2002 年發現台灣第一顆小行星以來，累計目前已發現超過 600 顆。自 95 年 3 月的「鹿林巡天計畫」(Lulin Sky Survey)有計畫性觀測以來，平均以每個月發現超過 15 顆小行星之速度，成爲亞洲發現小行星最活躍的地方。其中有多顆已取得永久編號，並獲得到國際命名爲「中大」、「鹿林」、「嘉義」、「鄭崇華」等。

鄭崇華小行星位於火星和木星之間的小行星帶，屬於 Main-belt 小行星。95 年 4 月發現在室女座位置，目前位置在金牛座附近。大小約 3.6 公里，形狀屬不規則狀，繞太陽一周約 4.14 年，預估在 97 年 12 月左右，可再次透過 40 公分以上的望遠鏡拍攝其影像。

【原文轉載自 2008-07-08/聯合晚報/A5 版/焦點】

小行星　多了一顆鄭崇華

【記者陳智華／台北報導】

宇宙中除了名爲「鹿林」、「中大」的小行星，最近還多了一顆「鄭崇華」。中央大學鹿林天文台發現的編號 168126 小行星，最近經國際天文聯合會（ＩＡＵ）審議通過，正式命名爲「Chengbruce（鄭崇華）」，這是首次以台灣企業家爲名的小行星。

鄭崇華是台達電子董事長暨創辦人，中央大學副校長葉永烜昨天指出，鄭崇華符合中央對學生期許的三Ａ精神—能力（ability）、態度（attitude） 和博愛（altruism），足爲世人和青年學子表率，先經校內審查委員會通過，再向ＩＡＵ申請以鄭崇華爲名，因其節能、愛地球受肯定而通過。

中央大學也表示，最近除了以鄭崇華命名小行星，另一顆小行星也以已過世的企業家溫世仁來命名，表彰他的慈善、愛心和無私的貢獻，還有一顆命名爲「汶川」，則是爲了紀念四川大地震。

中央大學天文所所長黃崇源說，這顆「168126 Chengbruce」小行星，是在九十五年四月一日透過中大鹿林天文台四十公分望遠鏡、由中大天文所楊庭彰與廣州中山大學葉泉志聯手發現，他們選定幾個天空區域，每間隔數分鐘觀測一次，共觀測三次。

中大天文所發現它在同一天區的比對影像中「跳動」，經確定其軌道位置，證實是新發現的天體。

「鄭崇華」小行星位於火星和木星之間的小行星帶，九十五年四月發現在室女座位置，目前位置在金牛座附近。大小約三點六公里，呈不規則狀，繞太陽一周約四點一四年，預估今年十二月左右，可再次透過四十公分以上的望遠鏡拍攝影像。

葉永烜強調，以往爲小行星命名，多以發現者或地名爲主，「鄭崇華」是中央大學首次以企業家名字命名，主要是鄭崇華長期對提倡環保及節能不遺餘力，也是天文愛好者，ＩＡＵ在核可這項命名案的說明中，表揚鄭崇華是具全球視野的創新者。

鄭老闆興奮：記得一輩子

【記者陳智華／台北報導】

愛好天文的鄭崇華昨天對有一顆自己名字的小行星，感到非常興奮，他說，這是「一輩子可永遠記得的事」，幕僚透露，他退休後，打算到大學修天文課。

鄭崇華跟中央大學因光電產學合作，結緣很早。二〇〇五年秋天，鄭崇華應邀在前校長劉全生陪同下，以七十歲高齡，登上海拔兩千八百六十二公尺的玉山鹿林天文台，成爲台灣第一位登上鹿林天文台的企業家。

鄭崇華說，小時候從福建隻身來台讀書，讀台中一中時，最怕學校放長假。寒暑假多數同學返鄉過節，他常在深夜時，獨自一人坐在學校大操場仰望星空，從此開啓對地球和宇宙的好奇。

鄭崇華說，「星星比人的生命要長久」，人的生命很短暫，鼓勵年輕人要努力學習，才不會白活。

行星命名 政治、商業都不行

【記者陳智華／台北報導】

天上的小行星名字有「林青霞」、「鄭崇華」等名人，但短期內不可能出現「馬英九」、「二次大戰」。根據國際天文聯合會（ＩＡＵ）規定，政治、軍事相關的事、物要發生一百年後，才可以拿來當小行星的名字，政治、軍事名人更要等過世後一百年後才行。

是否捐款給中央大學，學校發現的小行星就能以自己的名字命名，中央天文所所長黃崇源說，ＩＡＵ也規定命名不可有商業行爲及商業交易。

黃崇源表示，小行星是目前唯一可以由發現者命名並得到世界公認的天體。觀測到一顆小行星後，不能立刻確定是否爲新發現的小行星，必須在不同夜晚都觀

測到，報告國際小行星中心，確認是新發現的小行星後，才能得到一個「暫定編號」。精確測定運行軌道參數後，就會得到國際小行星中心給予的永久編號。

黃崇源表示，發現者小行星的命名權，十年內可行使，所有的小行星命名，須報經ＩＡＵ國際小行星中心和小行星命名委員會審議通過後，才公諸於世。

中央大學鹿林天文台台長林宏欽表示，有人曾提出要以微軟總裁比爾蓋茲來命名小行星，但ＩＡＵ認爲比爾蓋茲代表微軟，太過商業，扣關失敗。

【原文轉載自 2008-07-09/聯合報/A6 版/生活】

國際天文聯合會通過 168126 小行星定名「鄭崇華」

【記者柯安聰台北報導】

積極倡導節能減碳、珍愛地球的台達電子(2308)董事長暨創辦人鄭崇華（Bruce C.H. Cheng），在浩瀚的星海中，找到了相依相伴，永恆相繫的力量！由中央大學鹿林天文台所發現的編號 168126 小行星，最近經國際天文聯合會（IAU）小行星命名委員會審議通過，正式命名爲「Chengbruce（鄭崇華）」，以肯定鄭崇華先生追求環境永續、善盡綠色公民責任的努力。

這顆「168126 Chengbruce」小行星，是在民國 95 年 4 月 1 日被中大鹿林天文台 40 公分望遠鏡所發現，這同時也是台灣本土發現、首次以台灣企業家爲名的小行星，可謂從發現的那一刻起，這顆小行星就存在著非凡的意義。

中央大學副校長、國際知名天文學者葉永烜教授表示，鄭崇華先生符合三Ａ精神，足爲世人和青年學子表率，因此經校內審查委員會通過，特向 IAU 申請以鄭崇華先生爲名。這三 A 精神分別是 Ability（能力），鄭崇華先生白手起家，目前爲領導全球近 6 萬名員工的企業大家長；Attitude（態度），腳踏實地、視野開闊的企業家；Altruism（博愛）節能減碳、珍愛地球的環保先行者。IAU 核可的 50 字精簡文字當中，特別表揚鄭先生爲具全球視野的 Innovator（創新者）。

2005 年秋天，鄭崇華在前中央大學校長劉全生的陪同下，以 70 歲高齡，一步一腳印步行登高 600 公尺，登上海拔 2862 公尺的玉山鹿林天文台，成爲台灣第 1 位登上中大鹿林天文台的企業家。

站在國內最高的天文台、以及擁有全國最大 1 米口徑望遠鏡的星象觀測基地，鄭崇華回憶年少的自己，中學時代離鄉背井，隻身來台求學，最怕學校放長假，尤其是寒暑假，同學們大多返鄉過節，他常常深夜獨自一人坐在學校大操場仰望星空。別人是孤獨興嘆，但鄭崇華先生卻在斗轉星移中，領略生命的價值，開啓對地球和宇宙的好奇。

抱持著胸懷宇宙的寬廣視野，伴隨著生命的成長與企業的茁壯，鄭崇華先生許下重環保、愛地球的承諾，不只是產品追求環保節能，更將這些概念深化在公司日常運作中。

環保、節能長期以來一直是台達電子的經營使命，台達電子竭盡所能地降低溫室氣體的排放，以減緩地球暖化，其位在台南科學園區的黃金級標章「綠建築」廠辦就是最佳例證。多年來，台達電子在日常營運中，不斷專注地設法提高產品的效率，並開發新能源，這種創新、務實的精神，就像中大發現小行星一樣。

台灣的小行星發現肇始於中央大學。中大鹿林天文台自 2002 年發現台灣第 1 顆小行星以來，累計目前已發現超過 600 顆。自 95 年 3 月的「鹿林巡天計畫」(Lulin Sky Survey) 有計畫性觀測以來，平均以每個月發現超過 15 顆小行星的速度，成爲亞洲發現小行星最活躍的地方。其中有多顆已取得永久編號，並獲得到國際命名爲「中大」、「鹿林」、「嘉義」、「鄭崇華」等。

這顆「鄭崇華」小行星，是中央大學天文所楊庭彰與大陸廣州中山大學葉泉志連手發現，他們選定幾個天空區域，每間隔數分鐘觀測一次，共觀測三次。發現它在同一天區的比對影像中「跳動」，經確定其軌道位置，證實是新發現的天體。

鄭崇華小行星位於火星和木星之間的小行星帶，屬於 Main-belt 小行星。95 年 4 月發現在室女座位置，目前位置在金牛座附近。大小約 3.6 公里，形狀屬不規則狀，繞太陽 1 周約 4.14 年，預估在 97 年 12 月左右，可再次透過 40 公分以上的望遠鏡拍攝其影像。

中央大學以環境永續爲發展特色，首創地球科學學院、太空及遙測研究中心，守護著我們生存地球和台灣美麗家園；其中光電與光學領域發展領先群倫，環保節能成效卓著，這與台達電子提倡「環保、節能、愛地球」的理念相契合，目的無不希望留給後代子孫乾淨的生存環境。

【原文轉載自 2008-07-09/自立晚報】

發現小行星　中央大學命名鄭崇華

記者林靜梅 吳嘉堡台北報導

浩瀚的宇宙裡，有數不盡的星星，不過卻有一顆小行星，是以台灣的企業家來命名。這顆編號 168123、是由中央大學所發現，並且通過國際聯合會的審查，以台達電董事長鄭崇華的英文名字、Chengbruce 正式命名。

從中央大學副校長的手上，接下這顆小行星的模型，台達電董事長鄭崇華，喜悅全寫在臉上，因爲有一顆真正在宇宙中閃耀的小行星，用他的英文名字

Chengbruce 命名。

這顆小行星編號 168126，大小約 3.6 公里，位於火星和木星之間的小行星帶，繞行太陽一周要 4.14 年，比地球還要久，2006 年四月，由這位中央大學助理楊庭彰和另一位中國廣州大學的學生發現的。

發現了新的小行星，可是得精確算出它的運行軌道參數，才有命名權，這個過程通常曠日費時，也因此中央大學發現了六百多顆，現在也只有四顆的命名權。

另外，名字也不能隨便取，不能商業氣息濃厚或作爲利益交換，這次 Chengbruce、之所以能通過國際天文聯合會審查，是因爲鄭崇華長年推動環保的貢獻，也因此繼「鹿林」、「中大」、「嘉義」之後，「鄭崇華小行星」成了台灣第一顆、以企業家命名的小行星。

【原文轉載自 2008-07-08/公共電視】

中大發現小行星　命名鄭崇華

【本報台北八日電】

國際天文聯合會（IAU）通過中央大學發現 168126 號小行星定名爲「鄭崇華（Chengbruce）」以肯定台達電子董事長鄭崇華追求環境永續、愛地球具體貢獻，以及善盡綠色公民責任的努力。

鄭崇華與這顆小行星的緣起爲，2005 年秋天，鄭崇華抱持著一顆求知的心，在前中央大學校長劉全生的陪同下，以 70 歲的高齡，一步一腳印步行登高六百公尺，登上海拔 2862 公尺的中央大學玉山鹿林天文台，成爲台灣第一位登上中大鹿林天文台的企業家。

鄭崇華小行星位於火星和木星之間小行星帶，屬 Main-belt 小行星。2006 年 4 月發現在室女座位置，目前位置在金牛座附近。大小約 3.6 公里，屬不規則狀，繞太陽一周約 4.14 年，估在今年 12 月左右，可再透過 40 公分以上的望遠鏡拍攝其影像。

【原文轉載自 2008-07-08/世界日報——台灣新聞】

星星少了　太陽系天體只有預估的 1/100

【記者李樹人/台北報導】

浩瀚無窮的宇宙裡，究竟有多少星球呢？歷經兩、三年的天文觀察，分析超過 70 億筆恆星資料數據，國科會今天公布「中美掩星計畫」第一階段報告，發現了原來太陽系外天體數量不如天文科學家預估，甚至不到原先預測的百分之一。

這項發現讓全世界不少天文學家感嘆萬分，顯然過去大部分的學理推論，幾乎都是錯的，人類對於太陽系的形成，天體的軌道、數量及分布，幾乎是一無所知。

在中研院資助研究經費之下，國科會從 2005 年開始執行「中美掩星計畫」，利用鹿林天文台三台望遠鏡觀測，配備 400 萬畫素的高靈敏數位相機，入夜後自動觀測。

【原文轉載自 2008-10-03/聯合晚報/A8 版/生活】

TAOS 探測天涯盡頭原來太陽系外圍不擁擠！

劉靜瑀報導

台灣中研院、中央大學和來自美國及韓國的科學家參加中美掩星計畫(TAOS)，透過超廣角望遠鏡監測遙遠的恆星，卻發現，原來太陽系外圍天體數量沒有天文學家預期的多。研究團隊指出，雖然太陽系小型天體距離地球遙遠，但透過掩星技術，卻可以觀測直徑只有一公里的小型天體，廣受國際矚目。

台灣科學家現在已經可以觀測到太陽系周邊的小型天體，幾乎可以說是觀測到天涯盡頭！研究團隊指出，雖然這些小型天體和地球的距離太過遙遠，反射陽光微弱，不易觀測，不過，利用中美掩星技術，讓研究團隊達到這世界唯一的計畫。

中央大學天文所教授陳文屏：『我們觀測到太陽系外圍，因爲這些東西他很小，大小只有一公里，一般跑步的操場大一點點，這麼小的石頭擺在好遠的地方，平常用望遠鏡是看不到，但是用一種特殊的掩星技術，這技術是我們團隊開發出來的。』

透過台灣鹿林天文台 3 台望遠鏡，配備 4 百萬畫素的高靈敏數位相機，入夜後自動觀測，透過特殊程式控制，可以在 1 秒鐘內取得 5 次天體的亮度變化。

陳文屏：『他同時間可以看到幾百到幾千顆星，每一顆星一秒鐘可以量五次他的亮度，這是很難得的一種技術。因爲平常，就像數位相機，你打開可以看到很多顆星，可是你曝光一次可能要 1、2 分鐘，或者你只看一顆星，就可以讀很快，我們是兩者兼具，空間涵蓋率跟時間快速，同時可以達到。』

中央大學及中研院組成的研究團隊，自 2005 年開始收集資料，分析超過 70 億筆恆星亮度數據，但卻沒有看到任何掩星事件，這也表示，太陽系外圍的小東西，可能沒有想像中那麼多，比預期上限少了 10-100 倍。對於太陽系形成和早期演化提供了重要線索。而這項研究成果也刊登在國際頂尖期刊「天文物理通訊」(AstrophysicalJournalLetters)上。

【原文轉載自 2008-10-03/中央廣播電台_新聞】

中美掩星計畫觀測　太陽系外圍不擁擠

康紀漢報導

由行政院國科會及中央研究院資助中央大學研究

經費的中美掩星計畫，今天(3)公開發表研究成果，結果從分析超過 70 億筆的恆星亮度數據發現，太陽系外圍的天體數量比天文學家的預期上限少了 10 到 100 倍，並且這項研究成果也已刊載於「天文物理通訊」的國際期刊。

中美掩星計畫主要是運用背景恆星被古柏帶天體遮演時發生的亮度變化，來估計小型天體的數量，並透過鹿林天文台的三台 TAOS 廣角望遠鏡，以每秒 5 次的取樣頻率，進行監測大約一千顆恆星的光度變化。

研究團隊之一的中央大學天文所博士生張智威表示，這項研究主要是運用安裝於鹿林天文台的望遠鏡，觀測太陽系外圍的小型天體，通過恆星前方所造成的亮度變化，進以能夠估計太陽系外圍小天體的數量，並對行星形成與演化的瞭解更有幫助。

由於該項計畫是目前世界上唯一有系統研究太陽系小型天體的計畫，因而後續研究備受學界矚目。

【原文轉載自 2008-10-03/國立教育廣播電台文教新聞】

中美掩星計畫：太陽系外圍不如預期擁擠

陳奕華報導

觀測太陽系外圍天體數量，探索八大行星的演化過程，中研院與中央大學和來自美國及韓國的科學家合作的「中美掩星計畫(TAOS)」，透過超廣角望遠鏡進行觀查，結果發現，太陽系外圍的天體數量，沒有過去專家推估來的多，這項結論對太陽系形成和早期演化提供了重要線索，研究成果同時獲得國際肯定，刊登頂尖期刊「天文物理通訊」。

圍繞在太陽系外圍的小型天體由於距離地球遙遠，再加上只反射微弱的陽光，因此不容易觀測，不過由中央大學與中研院等單位組成的研究團隊，開發出的中美掩星技術，可以探測到太陽系外圍，直徑只有一公里的小型天體。

中央大學天文所教授陳文屏說：「我們觀測到太陽系外圍，因爲這些東西他很小，大小只有一公里，一般跑步的操場大一點點，這麼小的石頭擺在好遠的地方，平常用望遠鏡是看不到，但是用一種特殊的掩星技術，這技術是我們團隊開發出來的。」

研究團隊從 2005 年開始收集資料，分析超過 70 億筆恆星亮度數據，不過沒有看到任何掩星事件，這表示太陽系外圍的小型天體，沒有過去估計來的多，比預期上限少了 10 到 100 倍。對於太陽系形成和早期演化提供了重要線索。

中央大學天文所張智威博士說：「透過這些研究就可已知道太陽系的行星形成的過程，以及它形成以後的演化，一直到現在這個八大行星分布的樣子，這些小天體都是對於研究整個太陽系，是一個很重要的角色。」

「中美掩星計畫」是目前世界上唯一能夠有系統研究太陽系小型天體的計畫，研究成果備受國際注目，而且已經獲刊登在國際頂尖期刊「天文物理通訊」。

【原文轉載自 2008-10-03/中廣新聞網】

中美掩星計畫研究登上天文物理通訊

（中央社記者楊淑閔台北 2008 年 10 月 3 日電）

行政院國家科學委員會今天召開記者會表示，由國科會與中央研究院資助研究的中美掩星計畫研究發現，太陽系外圍天體的數量，沒有某些理論估計來得多，已刊登在今（2008）年 10 月 1 日出刊的國際期刊「天文物理通訊」。

中美掩星計畫（Taiwanese-American Occultation Survey，TAOS）爲由中央研究院、中央大學與美國勞倫斯利物摩國家實驗室、哈佛史密松天文物理中心、NASAAmes 研究中心、加大柏克萊分校、韓國研世大學等共同合作的計畫。

此計畫利用背景恆星被古柏帶天體（Kupier Belt Objects，KBOs）遮掩時發生的亮度變化，估計這類由冰塊及塵埃組成的小型天體數量。

TAOS 團隊成員、中央大學天文所博士生張智威說，此研究在鹿林天文台架設三台 TAOS 廣角望遠鏡（口徑 50cm，使用 2kx2k CCD 相機），每晚進行全自動觀測，以每秒 5 次的取樣頻率，同時監測近千顆恆星的光度變化。另一成員補充，此觀測占全天空 10 萬分之 1。

他指出，自 2005 年開始收集資料，今年取得第一批統計結果，共分析超過 70 億筆恆星亮度數據，結果沒有偵測到任何掩星事件，顯示太陽系外圍天體的數量，沒有某些理論估計來得多，對於太陽系形成與早期演化提供重要線索。此論文已刊登在今（2008）年 10 月 1 日出刊的國際期刊「天文物理通訊」AstrophysicalJournal Letters。

TAOS 團隊並說，此計畫第二代於 5 年後，至夏威夷架設三台口徑 1.3 米的望遠鏡，擴大觀測範圍。

【原文轉載自 2008-10-03/中央社】

中大天文所：太陽系外圍沒那麼擠

記者吳典叡／台北報導

由國科會資助中央大學天文所觀測太陽系外圍天體數量，與跨國科學家合作「中美掩星計畫(TAOS)」，昨日發表研究成果。結果發現天體數量，較天文學家的預期上限減少十至一百倍，該計畫證實太陽系外圍並非

異常擁擠，結論對太陽系形成和早期演化提供重要線索，並獲國際肯定，研究成果已刊載於「天文物理通訊」國際期刊。

中央大學天文所博士生張智威指出，中美掩星計畫主要運用背景恆星被「古柏帶」天體遮掩時，所發生的亮度變化來估計小型天體的數量，並透過鹿林天文台的三台 TAOS 廣角望遠鏡，以每秒五次的取樣頻率，進行監測大約一千顆恆星的光度變化。

張智威表示，這項研究主要是運用安裝於鹿林天文台的兩座望遠鏡，觀測太陽系外圍的小型天體，通過恆星前方所造成的亮度變化，進以估計太陽系外圍小天體的數量，對行星形成與演化的了解更有助益。

張智威說，透過這項研究可知太陽系行星形成的過程，及它形成後的演化，直到現在，這些小天體對於研究整個太陽系，都是很重要的角色。

「中美掩星計畫」是目前世界上唯一能夠有系統研究太陽系小型天體的計畫，因而後續研究成果備受國際矚目。

【原文轉載自 2008-10-04/青年日報/11 版/校園快訊】

太陽系外圍　星星數量不如預期

〔記者林嘉琪／台北報導〕

太陽系的外圍到底是什麼模樣呢？太陽系到底是如何形成與演化的呢？中美掩星計畫（Taiwan-America Occultation Survey, TAOS）分析超過七十億筆恆星數據後，迄今尚未偵測到任何掩星事件，顯示太陽系外圍天體數量並不如預期得多。

中美掩星計畫的目的，在透過觀察背景恆星被古柏帶天體遮掩時發生的亮度變化，計算出小型天體的數量。研究團隊在鹿林天文台架設四座廣角望遠鏡，以每秒五次的取樣頻率，在每天晚上監測近千顆恆星的光度變化，初步結果排除了在太陽系外圍存在大量一公里以上之小型天體。

中央大學天文所教授陳文屏表示，簡單來說，一旦有小型天體通過恆星前方時，恆星的亮度瞬間會變暗，在紀錄畫面上看來就像是「星星眨眼」，便是所謂的「掩星」事件，科學家只要統計小天體發生掩星的頻率，就可以推測出小天體的數量及大小。

中央大學天文所博士生張智威解釋，掩星觀測技術經由特殊程式控制，讀取相機感光元件上的電荷，可以在一秒鐘內取得五次天體的亮度變化，資料會儲存在電腦中，轉存於磁碟陣列，並進行天體的光變數據分析。

第一期的中美掩星計畫研究成果已經刊登在今年十月一日的國際期刊「天文物理通訊」，張智威更以台灣博士生的身分，以第一作者之姿躍上天文研究的舞台。

【原文轉載自 2008-10-04/自由時報/A8 版/生活新聞】

太陽系外天體數　比預期少數十倍

【李宗祐／台北報導】

太陽系外圍並不像天文科學家原先預測的那麼擁擠！由台美合作的「中美掩星計畫」研究團隊觀測評估，太陽系外圍的天體數量僅天文學過去推估的百分之一到十分之一，對太陽系的形成與早期演化提供重要線索。研究成果也已刊登在本月出版的《天文物理通訊》期刊。

國際知名天文學者、中央大學副校長葉永烜指出，太陽外圍天體數量不如天文學者原先預期的那麼多，「讓人感慨我們對於古柏帶、甚至是太陽系形成的一無所知。」這項研究發現是由「中美掩星計畫」（ＴＡＯＳ）在玉山國家公園內的鹿林天文台，設置的三座五十公分口徑望遠鏡，監測近千顆恆星光度變化的分析結果。

值得注意的是，參與這項計畫的研究團隊成員，包括中央大學、中央研究院、美國哈佛大學和瑩倫斯利物摩國家實驗室，以及韓國延世大學等國共廿四位學者，中大天文研究所博士班七年級張智威因負責撰寫電腦程式，分析七十億筆觀測資料，掛名研究論文的第一作者。

張智威表示，ＴＡＯＳ觀測研究的天體位於太陽系外圍，被喻爲彗星貯藏庫的古柏帶，利用掩星技術觀測太陽系外圍，直徑僅一公里的小型天體，在地球現有的最大型望遠鏡也無法看到這麼小天體的情形下，ＴＡＯＳ爲全球目前唯一能夠有系統研究太陽系小型天體的計畫。

中大天文所教授陳文屏指出，掩星技術是利用ＴＡＯＳ廣角望遠鏡監測遙遠的恆星光度變化，若有小型天體從恆星與地球之間穿越而過，恆星星光就會短暫消失，研究團隊即可據此估計太陽系外圍的小型天體數量。這次發表的論文是研究團隊根據ＴＡＯＳ建置的三座望遠鏡在二○○五年二月啓用以後，第一批（累積到二○○六年底）觀測資料的分析結果。

讓研究團隊訝異的是，在接近二年、監測近千顆恆星，高達近七十億筆觀測點資料中，竟然沒有偵測到任何掩星事件發生。張智威強調，這樣的結果顯示，太陽系外圍的天體數量並沒有天文學家過去所預期的那麼多。但張智威解釋，「零偵測」並不代表太陽系外圍完全沒有小型天體，就如同「毒奶粉事件」的「零檢測」，並不代表完全沒有三聚氰胺。

研究團隊以統計學模式還原「零偵測」在天體所

代表的數量意義，發現太陽系外圍的天體數僅有天文學家過去預期的百分之一到十分之一，每個平方度（相當於一個月亮所佔的天域）天體數量最多爲一億個，遠低於天文學家過去推估的十億到一百億個。

【原文轉載自 2008-10-04/中國時報/A11 版/生活新聞】

伽利略望向宇宙 400 年　天文館將與全球同慶

〔記者林曉雲／台北報導〕

義大利天文學家伽利略在距今約 400 年前（西元 1609 年），首次將望遠鏡指向夜空，全球天文機構爲紀念伽利略的重大貢獻，在 2009 年舉辦全球天文年活動，台北市立天文館共襄盛舉，從明年 1 月起將推出一整年的系列活動，第一波強打 16、17 世紀骨董望遠鏡特展活動，第二波則會推出 3.5 公噸的大殞石許願石活動，活動將會熱鬧精采一整年。

2009 全球天文年

天文館長邱國光表示，2009 全球天文年是全球矚目的活動，有 100 多個國家參加，台灣首座以天文專業爲主的台北天文館，也將會參與此一全球性的盛會。

邱國光表示，爲配合 2009 全球天文年活動，明年元旦當天將舉行全天域電影（IMAX） —「太空任務」（Destiny in Space）首映會，經由網路報名抽籤方式，天文館將提供數百名觀眾免費入場，首映會免費入場名單將由「影友會」網路報名名單中抽出，12 月下旬公告於天文館網站，民眾可上網報名。

北市伽利略季打頭陣

此外，天文館 2009 全球天文年活動，依時間先後分爲伽利略季、認識太陽系、探索宇宙與霹靂宇宙等 4 個單元，天文館組長陳俊良表示，伽利略使用的第一架望遠鏡真品目前收藏在義大利弗羅倫斯科學史博物館內，民眾可在弗羅倫斯科學史博物館內看到複製品，爲紀念伽利略，台北天文館在明年 1 到 3 月的伽利略季，以「小眼睛、大宇宙—窺天特展」爲主，強打和伽利略同時期的骨董望遠鏡特展，展品主要爲奇美博物館收藏的 16、17 世紀骨董天文儀器，奇美博物館目前收藏 40 多架骨董望遠鏡，天文館將商借 12、13 架骨董望遠鏡舉辦特展，再搭配台北圓山天文台時代的望遠鏡展出，中央大學天文研究所與鹿林天文台等也將提供相關的展品借展，是相當難得的機會。

陳俊良組長表示，第二季活動的主題爲探索太陽系，將以 3.5 公噸的太陽系殞石爲展出主角，除了讓民眾感受一下巨大殞石的神奇外，也可以作爲民眾的許願石；第三季活動則推出粒子展探索宇宙，而最特別的是從明年 4 月到 10 月的晚間，工作人員將帶著天文望遠鏡，到台北市 12 個行政區的公園，舉辦「路邊天文學」活動，讓民眾就近感受天文的奧秘。

【原文轉載自 2008-10-18/自由時報大台北新聞】

2009 全球天文年　網路報名免費看「太空任務」

生活中心／台北報導

2009 全球天文年是全球矚目的活動，有 100 多個國家參加，臺灣首座以天文專業爲主的臺北天文館，也將參與此一全球性的盛會。2009 年一整年將推出一系列的天文活動，元旦將舉辦「太空任務」首映會，採網路報名抽籤方式，提供數百位民眾免費觀賞。

天文館 2009 全球天文年活動內容依時間先後分爲「伽利略季」、「認識太陽系」、「探索宇宙」與「霹靂宇宙」等 4 個單元。其中伽利略季以「小眼睛、大宇宙-窺天特展」爲主，展品包括奇美博物館古董天文儀器，搭配臺北圓山天文台時代的望遠鏡。此外中央大學天文研究所與鹿林天文台等亦將提供相關的展品借展，伽利略季之後，其他天文年相關活動亦將陸續推出。

明年元旦舉辦的「太空任務」(Destiny in Space)首映會，經由網路報名抽籤方式，天文館將提供數百名觀眾免費入場觀賞，首映會免費入場名單將由「影友會」網路報名名單中抽出，12 月下旬公告於天文館網站，歡迎民眾一起來探索宇宙、瞭解宇宙的奧妙！

【原文轉載自 2008-10-17/NOWnews 生活新聞】

星星會閃爍　原來是大氣會擾動

記者羅智華採訪報導

美麗的滿天星斗讓許多天文迷看得目不轉睛，但對進行天文觀測的研究者來說，卻常因爲大氣擾動的問題，而使得望遠鏡影像產生模糊晃動、影響觀測準確度。周翊表示，這也是爲什麼我們從地面看星空，星星會一閃一閃亮晶晶的原因，主要就是因爲大氣擾動、導致空氣折射率不斷發生變化、造成星星看起來忽明忽暗，所以當我們抬頭仰望星空時，就容易覺得星星在閃爍。

爲何大氣會擾動？林琦峰表示，其實空氣本身就如同水一樣會流動，當光線通過大氣層時，會容易受到大氣層擾動的影響而使得望遠鏡所觀測的影像變得模糊，大氣擾動的原因主要是因爲大氣溫差所導致。

一般來說，大氣擾動可分爲高層大氣擾動、底層大氣擾動、望遠鏡附近的擾動等三類。當高層大氣擾動劇烈時，有時研究者只能先採取暫停觀測、等大氣穩定後再進行。若是望遠鏡附近的擾動，則可採取遠離熱

源、冷卻望遠鏡等措施來因應。

正因爲大氣擾動容易干擾觀測，因此一個穩定的天文觀測地點往往需要經過精挑細選，以鹿林天文台爲例，中央大學就經過長達十年的評估分析，才決定落腳在鹿林。周翊表示，良好的觀星地點須具備大氣擾動少、氣候乾燥、緯度近赤道、晴天率高等要素。綜合以上要素來看，不常下雨的高山地區是不錯的觀星點，具有大氣擾動少的優勢，所以每年流星雨來訪時，總會吸引不少天文迷一窩蜂往山裡跑。

哈伯望遠鏡　首開太空觀測先例

記者羅智華採訪報導

在眾多的天文望遠鏡中，最爲社會大眾所耳熟能詳的就是哈伯望遠鏡，周翊表示，哈伯望遠鏡執行太空任務多年來，不但爲人類觀測紀錄無數張珍貴的天文照片，更是全球第一台發射至太空中的反射式光學望遠鏡，在天文發展史中扮演舉足輕重的觀測角色。

哈伯望遠鏡是由美國航空暨太空總署與歐洲太空總署共同推動的天文計畫，於 1990 年將口徑達 2.4 公尺的反射式光學望遠鏡發射至太空軌道上。周翊表示，一般大型望遠鏡的壽命約 10 年，因此哈伯的年紀可說是諮老前輩矣，但由於戰績輝煌，因此迄今仍在服役中。

林琦峰表示，適逢 2009 年是國際天文年，臺北市立天文館也將舉辦小眼睛‧大宇宙—窺天特展等多項大型天文活動，家長除了可以帶著孩子前往天文館觀看哈伯望遠鏡模型外，亦可親耳聆聽解說員述說豐富有趣的天文發展史，活動詳情可上臺北市立天文館 http://www.tam.gov.tw/查詢。

【原文轉載自 2008-10-24/人間福報/13 版/科學】

2009 國際天文年　全球興起　觀星熱

記者羅智華採訪報導

2009 年是國際天文年，也是義大利科學家伽利略首次使用望遠鏡進行天文觀測滿 400 周年的紀念性時刻、對全球天文迷來說意義非凡。爲了迎接國際天文年的到來，世界各國的天文研究機構早已開始規畫各項暖身活動與天文觀測研究，希望讓大家更了解天文發展的來龍去脈與歷史沿革，透過天文觀測來領略穹蒼之美、星河浩瀚。

伽利略開啓天文觀測史

臺北市立天文科學教育館解說員林琦峰指出，進行天文觀測最重要的工具就是天文望遠鏡，回顧望遠鏡的發展史，最早可回溯到 1608 年，由荷蘭眼鏡製造商人立普塞所發明的第一架折射式望遠鏡。1609 年，則由伽利略第一次使用望遠鏡進行天文觀測，開啓人類採用望遠鏡觀星的歷史新頁。1668 年，英國科學家牛頓研發出全球第一架反射式面鏡望遠鏡，不只改善了折射式望遠鏡容易產生色差的缺點，而倍率增加也讓木星等主要星體的觀測更爲清楚。

而隨著歷史演進與技術改良，林琦峰指出，天文望遠鏡也在科技演化中不斷推陳出新。一般來說，望遠鏡可按接收的訊號來進行分類，例如可接收可見光波段的望遠鏡就稱之爲光學望遠鏡（optical telescopes）；而接收諮無線電波段的則稱爲無線電波望遠鏡（radio telescopes）。

以最常見的光學望遠鏡來說，主要結構可分爲光學系統、機械裝置、電控設備三個部分。依所用物鏡之不同可分爲折射式光學望遠鏡、反射式光學望遠鏡及折反射光學望遠鏡等三類。

林琦峰表示，折射式望遠鏡的原理主要是利用光線通過凸透鏡將光線集聚於一個焦點上，再利用焦點後端的目鏡將物體的影像放大。而反射式望遠鏡則主要是透過上頭有電鍍金屬的凹面玻璃來進行聚焦；再利用另一塊鏡片將所觀測的影像反射至鏡筒外、透過目鏡來達到放大的效果。

「天文望遠鏡的原理就如同照相機一般，光線是不可或缺的要素」中央大學天文研究所助理教授周翊表示，光源是最重要的條件，有了光線才能讓望遠鏡發揮效果。

歷經數百年的發展，周翊表示，人類從剛開始的一無所知到探索宇宙，所仰賴的除了對浩瀚星河的好奇與求知欲望外，最重要的就是望遠鏡技術的推陳出新。除了歐美等先進國家外，日本、台灣、韓國、中國、澳洲、印度也是在天文研究與觀測技術領域耕耘多年。

鹿林天文台觀星成果豐碩

以台灣爲例，中央大學在海拔 2862 公尺的嘉義鹿林前山設立鹿林天文台，是東南亞地區海拔最高也是光害最少的觀測點，而天文台內所架設的直徑 1 公尺望遠鏡則是國內目前規格最大的天文望遠鏡；多年來參與中美掩星合作計畫、泛星計畫、超新星巡天計畫等多項重大國際天文計畫、在宇宙中發現 600 多顆小行星，是東南亞發現小行星總數最爲活躍的國際天文台。

爲了讓台灣的天文觀測技術更上一層樓，周翊表示，目前中央大學正籌畫在鹿林天文台興建直徑達 2 公尺的大型天文望遠鏡，落成後將可比現有的 1 公尺望遠鏡觀測範圍再增加 8 倍、觀測距離增加兩倍，對於打造台灣成爲國際天文研究重鎮是一大助力。

【原文轉載自 2008-10-24/人間福報/13 版/科學】

歲末流星秀　天文館專人導覽

【記者周依禪整理報導】

流星雨熱潮即將到來，快到天文館充實你的知能！台北市立天文科學教育館 11 月每周末推出「假日主題導覽——歲末流星秀」，針對 12 月重大天象「雙子座流星雨」、「小熊座流星雨」及流星雨知識進行導覽解說。

天文館表示，流星是存在於地球附近的塵埃粒子等小天體，因爲被地球的引力吸引而進入大氣層，以高速與大氣摩擦燃燒發光的現象；每年相同時間流星都會一再出現，追蹤這些流星的軌跡，可知來自天空中相同的區域、彼此相關，稱爲流星群，如果流星群的數量很多，就稱爲流星雨。

今年「雙子座流星雨」極大值發生在 12 月 14 日上午 7 點；「小熊座流星雨」極大值發生於 12 月 22 日下午 3 點半，2 次流星雨極大值雖發生在白天，但極大值發生前後的夜晚，都有機會觀賞流星的飛逝。

天文館也預告 2009 全球天文年，爲紀念 1609 年義大利天文學家伽利略首次將望遠鏡指向夜空，全球天文年是全球矚目的活動，有 100 多個國家參加，天文館將於明年 1 月起推出一整年的系列活動，明年元旦當天將舉行全天域電影（IMAX）「太空任務」首映會，經由網路報名抽籤方式，供民眾免費入場觀賞，名單將於 12 月下旬公告於天文館網站。

天文館 2009 全球天文年活動，內容依時間先後分爲伽利略季、認識太陽系、探索宇宙與霹靂宇宙等 4 個單元。伽利略季以「小眼睛、大宇宙－窺天特展」爲主，展品包括奇美博物館古董天文儀器，搭配台北圓山天文台時代的望遠鏡，中央大學天文研究所與鹿林天文台也將提供相關的展品借展。

【原文轉載自 2008-11-04/立報新聞】

臺灣超新星巡天計畫

文/ 陳英同
陳婷琬

契 子

夜晚，當我們仰望星空，看到點點繁星，心中不禁會對這片夜空充滿許多疑問。星星可以數得清楚嗎?星星會消失嗎?會不會哪一天，天空中多出一顆星星呢?

當然，我們知道從古至今，星空並非一成不變，除了日升月落，斗轉星移，行星的移動，流星等等，也有突如其來的訪客—彗星的造訪，更有天體如同《宋會要輯稿》中所載：「至和元年五月，晨出東方，守天關，晝見如太白，芒角四出，色赤白，凡見二十三日」。也就是說，在西元1054年，有天早晨突然有顆亮星出現在東方天空，現在金牛座牛角的地方，白天就可以看見它，跟金星一樣亮，這顆星是赤白色的光芒，持續了23天白天都能看見。另外在《宋史．仁宗本紀》中則記載，這顆亮星在夜晚可見，直到快兩年的時間才消失。

這顆星星就是有名的「中國超新星」，編號SN 1054，它突然出現在天空，並且大放光芒，之後逐漸變暗直到看不見;現在我們還知道，它遺留下來的殘骸，就是「蟹狀星雲」與中間一顆快速自轉的中子星。

超新星現象

超新星在字義上像是新生成的恆星，但其實並非是新生的恆星，相反的，它是恆星轟轟烈烈的死亡過程。在超新星研究開啓之前，天文學家只觀測到亮度變化在千倍以下的短暫性突發新星(Nova)。有別於新星，超新星的亮度則是會突然增亮數十萬倍以上，所以當時的美國天文學家滋威基(Fritz Zwicky)稱其為超新星(SuperNova)

在經過理論與觀測天文學家的研究之後，我們慢慢對超新星有概念性的認識。當巨質量恆星演化到盡頭時，由於重力壓與內部量子壓力的不穩定，會產生劇烈爆炸的現象，在其劇烈的爆炸過程中，短短不到一秒鐘的時間，釋放出來的能量(10^{51} erg s^{-1})大約是一個太陽終其一生所產生的能量。如(圖一)，我們可以看到不同質量的恆星，其演化的命運極為不同：類似太陽的低質量恆星，演化到末期變成紅巨星，隨後外層物質往外拋出形成行星狀星雲，中間則遺留下一顆白矮星，直到溫度冷卻變成黑矮星，靜寂在宇宙中。

而10倍太陽質量以上的巨質量恆星可就不甘於此，演化到末期變成紅巨星之後，其核心由氫-氦-碳-氧…繼續融合到鐵。但鐵的融合是吸熱反應，無法再提供往外的熱壓力，此時自身重力獲勝，恆星開始往內塌縮，外層氣體往內碰撞到堅硬的核心產生反彈，形成超新星爆炸現象。核心則依照剩餘質量不同，形成中子星或是黑洞。而超新星爆炸的震波與周圍星際物質作用，則產生了雲狀般的超新星殘骸。

除了巨質量恆星的核塌縮爆炸模型之外，還有另外一種超新星爆發形式，如(圖二)，即一組密近雙星系統。其中一顆已經演化成碳-氧白矮星，白矮星不斷從其伴星吸積物質，直到超過錢卓極限(約1.4倍太陽質量)，白矮星的電子簡併壓承受不住自身重力，此時中心物質密度提高，溫度升高到足以點燃碳的核融合反應，這個碳爆燃火焰，將白矮星由內而外整個炸開，釋放出10^{53} erg s^{-1} 的能量，形成Ia型超新星的爆發。

圖二：碳爆燃型超新星，白矮星(右)正在對其伴星進行吸積。(圖片來源：http://physics.weber.edu/carroll/expand/accelerate.htm

為什麼要尋找超新星?

在我們自己的朋友當中，有著胖瘦高矮、老弱少壯等等不同年齡、體重等等的分類，而那些恆星也正是像我們所認識的人，有著不同的年齡、質量、組成(或許我們也可以說宇宙中的星際塵埃像是細菌般，看不見，卻布滿了四周)。其中影響最大的就是質量，不同質量的恒星會有不同的演化過程。可惜的是，恆星的整個演化過程通常長達數十億年，人的壽命相較於恆星的演化過程，是那樣的微不足道，不可能會有整個演化的完整觀測。所以比較來說，在全部恆星演化過程中，短暫時間的超新星爆炸便是我們很有興趣去研究的課題。

尋找的方法

第一步：制定巡天策略

目前在世界上已有不少的研究團隊在做超新星巡天的計劃，尤其是位於美國的研究團體或個人最多。以地理位置來看，雖然大致上在世界各個大洲都有觀測點，不過都是以北天為主，所以使得目前所發現的超新星比較集中在北天的星系，如(圖三);在南天除了澳洲與南非之外，少有南天國家是在做超新星巡天計劃。由於北京天文臺在2001年結束超新星巡天計劃，臺灣的地理位置剛好可替補亞洲的觀測點。臺灣的地理位置位於北緯23.5度，可視星場為北天全天，南天則可到達40度，我們以初學者去切入超新星巡天的研究，所鎖定的星場赤緯為DEC-20°~DEC-40°，一來不會與位於較高緯度的美國，已經對超新星巡天技術發展純熟的研究團體的觀測星場有所競爭，二來剛好切入南天超新星巡天研究團體少的優勢。

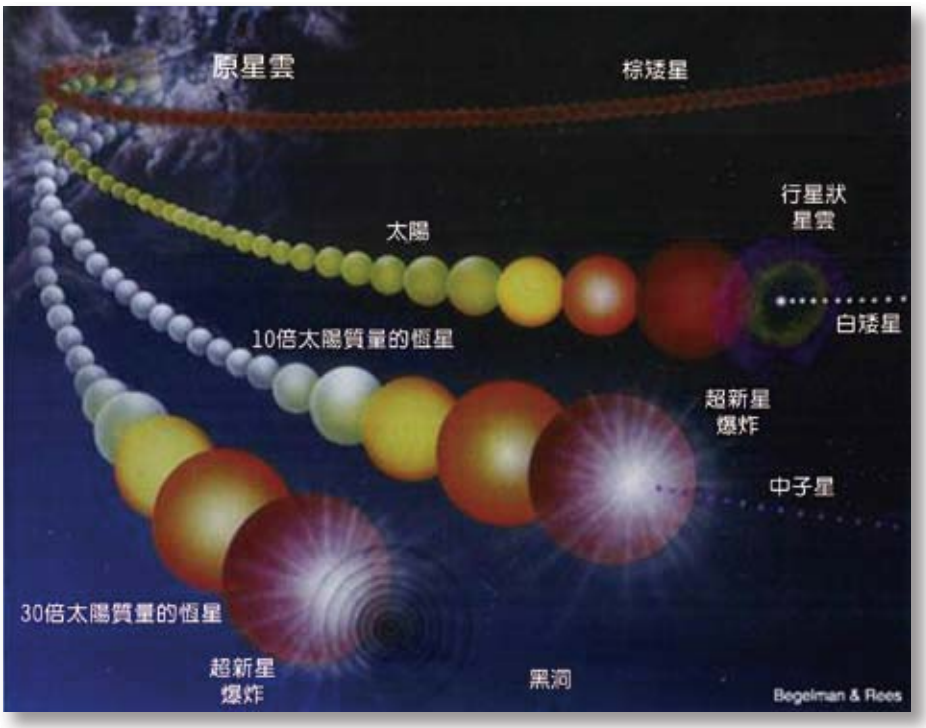

圖一：不同質量的恆星演化圖
圖片來源：http://aeea.nmns.edu.tw/geo_home/geo97/new_page_32.htm

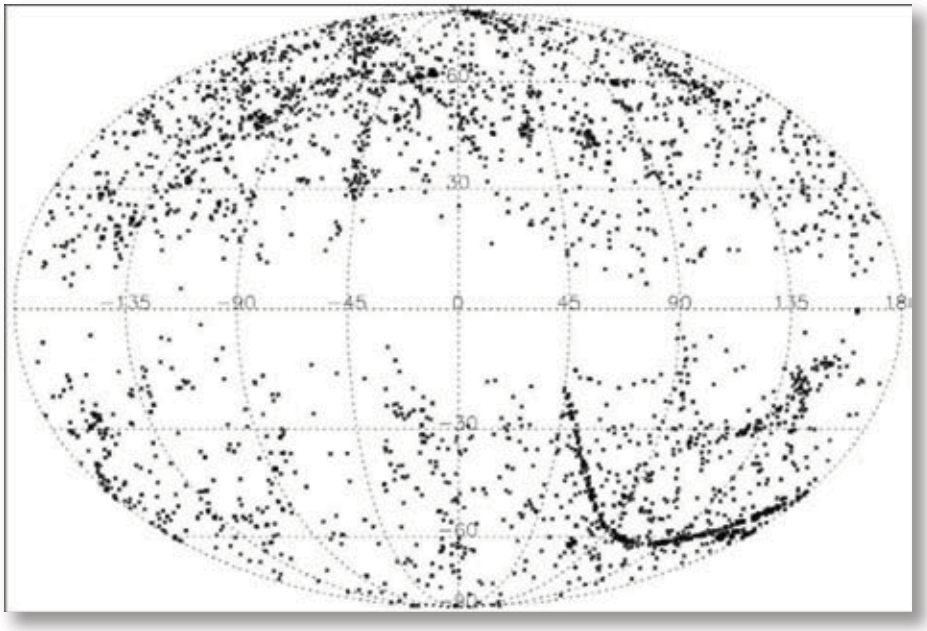

圖三： 從1885年到2006/4/23，所有有記錄的超新星在銀河坐標上的分佈。

第二步：選擇觀測目標

超新星原恆星在物理性質上，為大質量恆星以及白矮星-伴星之雙星系統，主要會發生在恆星密度最高的星系當中。在本銀河系跟河外星系均有發現超新星的可能性，不過對於超新星巡天而言，廣大並且消光嚴重的銀河盤面不是一個有效率的目標，就歷史上的本銀河系超新星的記錄而言，大約三百年會有一顆超新星產生，所以發現本銀河系超新星的機率是非常的低，所以我們主要是觀測發現機率較大的其他星系。

臺灣超新星巡天目前是利用國立中央大學鹿林山天文臺的一米望遠鏡(LOT)做巡天的觀測，如(圖四)，由於LOT算是小口徑的望遠鏡，其極限星等大約在20星等上下(天空背景在V-band(黃光波段)約20.72等，在B-band(藍光波段)約21.22星等)，所以我們在選取觀測星系時，均選取鄰近星系($z<0.02$)，並且挑選視直徑較大，視星等較亮的星系做為觀測星系表。

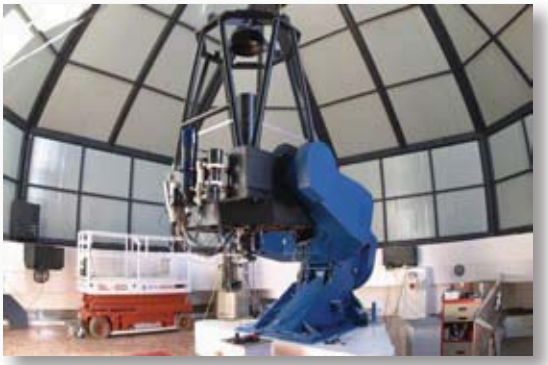

圖四：鹿林天文臺的一米望遠鏡 (LOT)
圖片來源：http://www.lulin.ncu.edu.tw

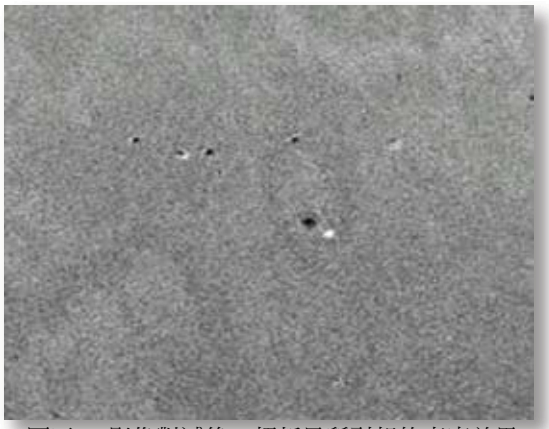

圖五： 影像對減後，超新星所引起的亮度差異，白點爲超新星候選者。

第三步：影像資料處理

臺灣超新星巡天計畫主要是利用不同時間所得到的影像去做影像對減，找出對減後的影像有無差異，區別有無超新星出現在影像裡。在短時間週期內，不同時間所照的影像中，假如沒有特殊發生天文事件的話，兩個時間的影像在對減後應該不會有特別奇怪的星點出現；反之，假如有一個亮度改變的天文事件發生在時間較晚的影像當中，在兩幅影像對減後，應該可以看到其不同的地方，如(圖五)。

第四步：確認超新星

在發現一個新的超新星候選者後，首先要先確定的是這個候選者是不是真的為一個超新星，因為會出現在影像中的候選者有許多的可能性，確認的方法主要為下列幾種：

1.已知超新星
2.已知小行星
3.未知小行星
4.宇宙射線
5.背景星

第五步：通報IAUC

IAUC(International Astronomical Union Circular)為國際天文聯合會IAU(International Astronomical Union)下的發行組織，利用Email及網頁通知特殊的天文事件，例如超新星、新星、彗星等等。在確認候選者為超新星後，就要向該單位通報新的超新星。

成果

臺灣超新星巡天計畫進行三年以來，總共發現了14顆超新星，並獨立完成通報的工作，成果如(表一)，分別列出該超新星獲得的國際編號、宿主星系、發現日期、發現時的星等、與超新星的分類。

另外，可參見(圖六)，左邊是星系IC 2531的基底影像，右邊則是超新星SN 2007cj爆發後所得到的影像。

未來展望

Pan-STARRS (the Panoramic Survey Telescope & Rapid Response System)是美國夏威夷大學天文所主持的大型巡天計畫，由四座1.8米望遠鏡所組成，約四天可對幾乎全天做一次完整巡天，其極限星等可深達24等星，其主要科學目標為找尋對地球有危險性的小行星，其資料庫還可應用於古柏帶星體、變星、系外行星，以及本文章的主要目的：超新星巡天。 Pan-STARRS預定在2008年完全正式上線(四座望遠鏡)後，將可取代大部分的超新星巡天計劃，而臺灣超新星巡天也將從合作的角色，轉換研究方向到超新星後續光變的研究。除此之外，可著手的研究還有離銀河較近星系中超新星的原恆星、超新星與化學豐度的關係、以及伽瑪射線爆(Gamma-Ray Burst, GRB)與超新星的關係等等研究。

陳英同、陳婷琬：分別為國立中央大學天文研究所博士班與碩士班研究生。

No.	Host Galaxy	Date	Mag	Type
SN 2003lz	ESO 428-G13	2003/10/30	17.1	?
SN 2004cy	ESO 403-G9	2004/04/05	15.6	?
SN 2004ee	ESO 298-G7	2004/07/31	17.2	Ia
SN 2004eq	ESO 404-12	2004/09/23	16.8	Ia
SN 2004fa	MCG -05-48-5	2004/09/01	16.8	Ia
SN 2004fb	ESO 340-G7	2004/10/07	18.3	II
SN 2004gv	NGC 856	2004/12/13	17.6	Ib
SN 2005O	NGC 3340	2005/01/16	15.2	Ib
SN 2005cd	IC 651	2005/05/16	17.4	?
SN 2005cw	IC 1439	2005/07/11	18.5	II
SN 2006V	UGC 6510	2006/02/04	18.0	II
SN 2007bh	PGC 54103	2007/04/13	18.6	?
SN 2007cj	IC 2531	2007/05/03	15.9	Ia
SN 2007fp	NGC 3340	2007/02/26	16.3	II

表一：超新星詳細資料表

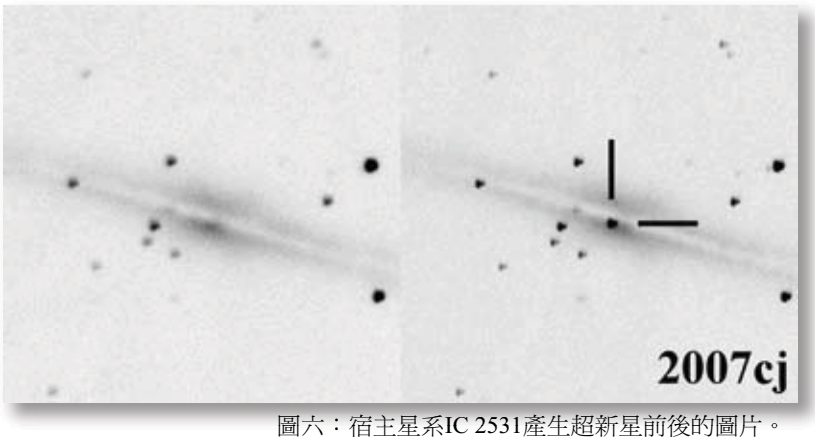

圖六：宿主星系IC 2531產生超新星前後的圖片。

天文觀測的新挑戰──談泛星計畫

Frontier Challenges in Astronomical Observations --- The Pan-STARRS Project

陳文屏
紐約州立大學石溪分校天文博士
現任 中央大學天文所、物理系教授

Wen-Ping Chen
PhD in Astronomy, State University of New York at Stony Brook

Current Position Professor of Graduate Institute of Astronomy, National Central University

摘要

天文觀測儀器發展日新月異──望遠鏡口徑增變大，偵測器靈敏度提升，焦平面覆蓋面積增加。本文介紹我國與美、德、英等國共同參與之「泛星計畫」 (Panoramic Survey Telescope And Rapid Response System; Pan-STARRS)，利用超廣角望遠鏡，新技術開發具備 14 億個像元之大面積對角轉移 (orthogonal transfer) CCD 電子相機，每週對全天域進行掃瞄一次，有效研究位置或亮度有變化的宇宙天體。為可見光觀測天文開創新紀元。

ABSTRACT

Advance in instrumentation in observational astronomy has been leaping---ever increase in the telescope aperture, improved sensitivity and larger focal-plane coverage in the detector technology. This article describes the hardware and software development of Pan-STARRS (Panoramic Survey Telescope And Rapid Response System), a telescope facility for which Taiwan is involved in the scientific operations, together with an elite group from the US, Germany and the UK, to patrol the entire visible sky once a week by employing wide-field optics, and a CCD camera with 1.4 gigapixels that makes use of an innovative orthogonal transfer technology. Pan-STARRS will be a powerful tool to identify celestial objects variable in position or in brightness, and will revolutionize optical observations in time-domain astrophysics.

1. 天文儀器的挑戰

天文學是門以觀測爲主的科學，藉由分析天體發出的訊號，透過理論解讀與統整，以瞭解天體的性質、來源與變化。除了觀測與理論外，有時候也利用實驗室模擬太空環境，觀察物質的物理與化學變化。除了隕石，以及少數機會送出太空船就近研究諸如月球、行星、衛星、彗星等天體，我們對於宇宙的瞭解，絕大多數來自於天文觀測。

天體發出的訊號以電磁波爲主，這些訊號經過了遙遠距離，受到星際物質吸收、散射，最後經過地球大氣層，被望遠鏡與偵測器接收。天體訊號通常極其微弱，因此天文觀測的挑戰，一直以來主要在於提高靈敏度與解析度。以靈敏度而言，一方面增加望遠鏡口徑，另方面提高偵測器效率。以解析度而言，諸如開發新技術克服大氣干擾，例如雷射導星、自適應光學，甚至把望遠鏡放在太空，以獲得清晰影像。另外改良光學技術，提高光譜分光的色散程度等。總而言之，觀測儀器，技術以及資料分析方法的發展，在於追求「看得遠、看得清楚」。距離遙遠的天體，其電磁波經過很長時間才抵達地球，因此提高觀測靈敏度，便能記錄到極爲遙遠的天體，也就能研究宇宙早年的情形。

爲了追求更高靈敏度與更佳解析度，天文觀測設備不斷挑戰最新技術。在無線電波波段，新一代的設備 Atacama Large Millimeter /submillimeter Array (ALMA) [1]，由美國、歐洲與日本合作，在南美洲智利北部沙漠安地斯山 ，海拔 5000 公尺 Chajnantor 高原建造數十座 12 公尺直徑之天線陣列，干涉儀基線從 150 公尺到 18 公里，解析度可以達到 0.005 角秒，比哈伯太空望遠鏡還好了十倍。在可見光、紅外線方面，歐美已經在規劃口徑 20 到 30 公尺的望遠鏡[2]，太空中則有接替哈伯望遠鏡的 James Webb Space Telescope (JWST) 都是研究宇宙極有威力的工具。

2. 研究宇宙的新領域──時變現象

泛星計畫 (Pan-STARRS, Panoramic Survey Telescope and Rapid Response System) 是因應新思維而開展的計畫 [1]。除了靈敏度與解析度，泛星計畫的特色在探索宇宙天體隨時間的變化現象。一九九四年彗星撞木星事件，讓人們體會到天體撞擊地球可能帶來的大規模災難，因此二００五年美國布希總統簽署法案，要求 NASA 在一年內提出可行性規劃，指認出軌道可能與地球相交的「近地小行星」，

[1] http://www.alma.cl/
[2] http://www.tmt.org/

並提出避免撞擊之解決方案與估計所需經費。泛星計畫應運而生，由美國國務院透過美國空軍斥資 6 千萬美金，建造超廣角望遠鏡進行巡天監測，由夏威夷大學執行，建造由四座口徑 1.8 公尺的望遠鏡構成觀測陣列 (PS 4)，各自配備最先進且具備 14 億個像元之電子數位相機。整個望遠鏡與相機組成的光學系統視野達到七平方度，每夜將巡天 6000 平方度，其深度可達 24 星等，每月掃瞄全天空數次，能夠有效辨識並研究位置（例如小行星、彗星）或亮度（例如超新星）產生變化的天體。

巡天觀測在取得大天區影像資料。評估巡天效率 (Survey Power) 的一項指標爲 $SP = A\Omega/\theta^2$。其中 A [m^2] 是望遠鏡主鏡的集光面積，Ω[deg2] 爲成像的立體角，由於集光面積越大相當於能夠看到距離越遠的天體，AΩ 的乘積相當於觀測所能涵蓋的空間體積。θ[arcsec] 則是望遠鏡點光源成像的半高全寬 (full-width at half maximum)，也就是一般說的「視相度」或大氣寧靜度 (seeing)。在視相度好的觀測地點，星光能量比較集中，靈敏度也就越好。表一列出數項巡天計畫的比較[2]，可以看出以巡天效率指標而言，泛星計畫要比口徑大得多的 CFHT 或是 Subaru 望遠鏡優越得多，也比現有搜尋小行星的望遠鏡，例如 LINEAR 或 Spacewatch 好了兩到三個數量級。美國正在規劃的 Large Synoptic Survey Telescope (LSST) 也是廣視野、高效率的巡天，其效率要比泛星計畫好得多，但是其經費昂貴且仍在設計階段。相比之下，泛星計畫已經落實，即將開始取得資料。

表一、望遠鏡的巡天能力 （取自 Jewitt 2003）

望遠鏡	口徑 [m]	集光面積 [m^2]	Ω [deg^2]	θ [角秒]	SP	狀態
LINEAR	1.0	0.8	2	2.5	0.2	進行中
Spacewatch	0.9	0.6	3	1.5	0.8	進行中
Palomar/QUEST	1.2	1.1	16.6	2	4.6	進行中
CFHT/Megacam	3.6	10	1.00	0.6	28	進行中
Subaru/Suprimecam	8.0	45	0.25	0.6	35	進行中
Pan-STARRS	3.6	10	7	0.5	280	2008+
LSST	8.3	54	7	0.6	1050	2012?

3. 泛星計畫的軟硬體設計

泛星計畫在軟、硬體方面有多項革命性研發，以下針對望遠鏡、偵測器、天文台地點、資料分析、觀測策略，以及主要科學目標等，簡單介紹。

3.1 望遠鏡

泛星計畫採取超廣角 Ritchey-Chretien 光學設計，由快焦比之主、次鏡，加上修正透鏡，構成 f/4 之卡賽格蘭成像系統（圖一）。完整的泛星計畫將建造四台這樣的望遠鏡 (PS4)，有可能放在同樣架台 (mount) 上。目前先導計畫已經建造一台 (PS1)，第二台望遠鏡也正在製作當中。

圖一：(a) Pan-STARRS 望遠鏡光路圖，最大的元件代表 1.8 公尺口徑之主鏡，反射光線到左方次鏡，之後經過三個修正鏡。最右方的紅色圓盤代表望遠鏡之卡賽格蘭焦平面。(b) 望遠鏡照片，可以看到次鏡與修正鏡。(c) 望遠鏡卡賽格蘭焦點儀器配掛示意圖。

圖二：望遠鏡遮罩、建築整合示意圖。

對於巡天計畫，超廣角視野爲觀測效率之關鍵因素。天文學界使用最廣泛的全天照片，大概算是 Digital Sky Survey (DSS)。其起源是位於美國加州帕羅馬山 (Mount Palomar) 的 48 吋史密特望遠鏡之巡天觀測 (Palomar Observatory Sky Survey, POSS)，於 1948 年起，使用藍光敏感 (Kodak 103a-O) 與紅光敏感 (Kodak 103a-E) 之照相玻璃底片做爲偵測器，這些底片利用化學反應感光，量子效應只有百分之幾，優點是視野寬廣，每張底片視野達 6.6 度平方，極限星等達 20～

22 星等（大約等於人類視覺靈敏度之百萬倍）。第一代 POSS 進行到約 1958 年，也就是整個巡天花了十年時間，共取得近千張底片。之後陸續有不同延伸或補充觀測，包括位於澳洲之 U.K. 史密特望遠鏡，於 1970 年代進行南半球巡天，完成全天空照片。這些底片經過掃瞄後便是 DSS 資料庫，乃天文研究必備工具。觀測人員需要查詢天空某塊天區，或是在其他波段觀測之前，必定先檢視 DSS 的影像。

泛星計畫同樣進行巡天觀測，雖然視野沒有 DSS 寬廣，但是由於使用電子相機，利用光電效應感光，量子效應達到 70%以上，與底片每張動輒小時的曝光時間相比，電子相機曝光 30 秒鐘便達到約 23.5 星等之靈敏度。注意 POSS 之所以成功，在於史密特望遠鏡的廣大視野，CCD 等電子偵測器除非尺寸能大幅增加，否則巡天效率受到很大限制。因此泛星計畫成功的技術關鍵在偵測器部分。

3.2 電子相機

泛星計畫採用拼接 CCD (charge-coupled device) 感光晶片做爲偵測器。整個電子相機由林肯實驗室 (Lincoln Laboratory) 與夏威夷大學共同研發，乃是整個泛星計畫在硬體技術方面最特殊的部分[3, 4, 5]。

爲了提高巡天效率，泛星計畫對於偵測器的設計包括以下幾項要求：（1）晶片尺度大，以增加視野，但仍有良好分辨力。泛星計畫目前的相機達 45 公分，一共有 14 億個像元 (pixel)，每個像元張角約 0.26 角秒。此相機稱爲 GigaPixel Camera (GPC)；（2）讀取快速，整個 GPC 讀出不超過兩秒鐘；（3）增加晶片製程良率 (yield rate)，因而節省經費；（4）能夠 on-chip guiding，也就是利用晶片本身進行導星；（5）減少亮星效應；（6）抵銷部分大氣擾動造成的影像飄移效應。這當中（2）到（5）需要嶄新的「陣列」(array) 偵測器概念，而第（6）項則必須採用「對角轉移」 (orthogonal transfer, OT) 技術。

一般 CCD 晶片的原理，是入射光子藉由光電效應，使得半導體（一般是矽）產生成對之電子與空洞。這些電子受到電力偏壓束縛，累積在位能井 (potential well) 當中，最後改變電壓，依序將電荷讀出。通常同一列的像元，它們個別的電子沿著該列方向，順序讀出。有些相機爲了加快讀出速度，使用不只一個讀出電極。

GPC 之設計在接合傳統大面積 CCD 晶片，組成陣列，而各個單格 (cell) 可以獨立讀取 (independently addressable)。每 64 個單格安置於單一矽晶上，組成一個 Orthogonal Transfer Array (OTA)，邊長約五公分（圖三）。整個相機共有 60 個 OTA（去除了離光軸距離遠之正方形四個角落）。

採取獨立單格設計，可以大爲提供製程成功率，例如一般 2K x 4K 15-微米像元的 CCD 晶片成功率只有約 25%，而 GPC 每 8 x8 構成的 OTA 可以允許 2-3 個單元有瑕疵，而不致因爲局部短路、放大器故障等瑕疵而報銷整個晶片。而由於每個單格有各自讀出電路，讀取速度也大爲提升。獨立單格也解決了亮星的問題，某個單格理的亮星造成飽和，可以用較快速度讀出，用來當作導星之用，而不致影響其他單格中的暗星（圖五），大爲提高訊號的動態範圍 (dynamical range)。

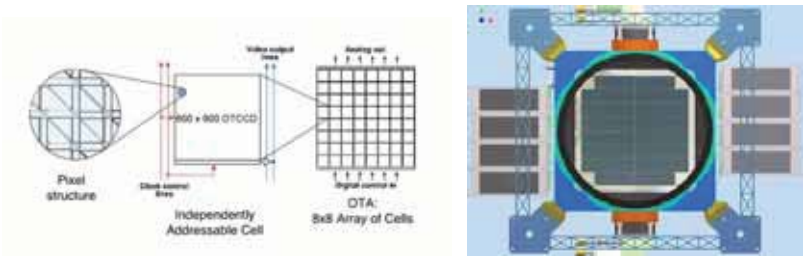

圖三：(a) 單格晶片配置圖，每個 OTA 由 64 個 OTCCD 組成，而每個 OTCCD 則有 600 x 600 個像元。(b) GPC 相機共有 60 個 OTA。

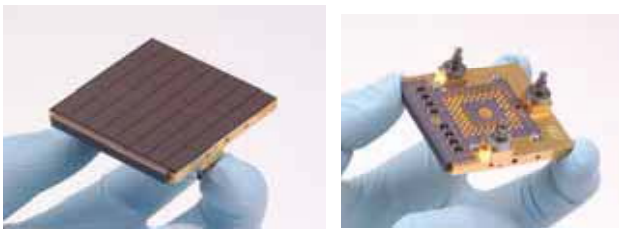

圖四：OTA 之正面與背面。每個 OTC 由 8 x 8 個單個組成，可以各自控制與讀出。GPC 一共有 60 個 OTA。

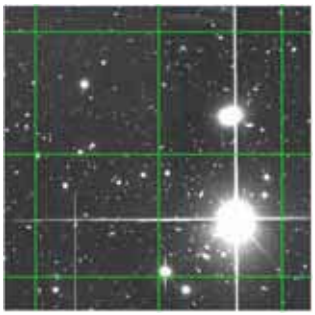

圖五：利用 OT 技術，個別單格之內的亮星，雖然飽和，但是電荷不會滿溢，影響其他單格。綠色格線表示 OTA 單格的範圍。圖中最亮的星為九等星。

一般相機快門打開後，由於大氣擾動，星點影像模糊，一般偵測器保持相同狀態收集光線，因此輸出影像便受到影響。利用自適應光學 (adaptive optics)，可以偵測並計算大氣所造成影像模糊，快速調整光路（例如一面小反射鏡）變形，以抵銷變形。OT 則是利用在晶片上移動電荷的技術，達到類似的效果。

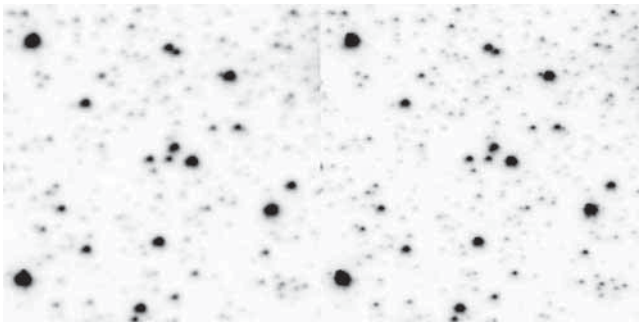

圖六：（左）沒有抵銷影像運動的影像，以及（右）利用 OT 技術取得之影像，可以看到暗星的訊號比較清晰。

3.3 天文台地點

泛星計畫的四座望遠鏡預計將安置在美國夏威夷群島之「大島」(Big Island，也稱夏威夷島）之基亞峰 (Mauna Kea)，該處爲公認世界上最佳天文觀測地點之一，已經有多座國際級大型天文台。至於目前已經建置之 PS1，包括整套望遠鏡、GPC 與資料處理系統，做爲先導計畫，安置於「毛伊」(Maui) 島之「哈里阿卡拉」(Haleakala) 山頂（圖七）。此址已經有太陽觀測站，以及美國空軍之人造天體監測站，雖然無論晴天率或視相度都不如基亞峰，但使用取得比較容易（圖八）。由於夏威夷之低緯度地理位置（與台灣緯度相當），全年可見全天球約四分之三的範圍（也就是約 3 π steradian 立體角）。

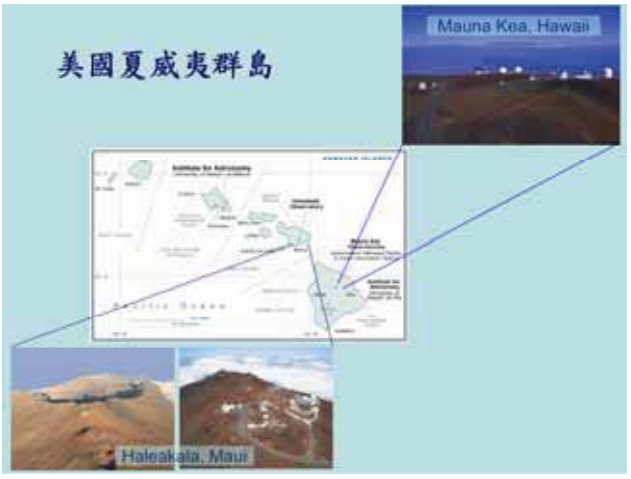

圖七：泛星計畫望遠鏡所在，為於美國夏威夷。PS1 安裝於 Haleakala 天文台，日後 PS4 預計放置在 Mauna Kea。

圖八：毛伊島之哈里阿卡拉山頂已有多座天文台，此為從 PS1 天文台所見之景觀。

3.4 資料分析

每幅 GPC 影像大小爲 2 Gigabytes。在巡天模式下，一般每幅曝光時間爲 30 秒，所以一個晚上所累積的資料量達數 Terabytes，如此大量資料，無論是處理、分析、儲存、分配等，都是資訊工程上極大挑戰。

以往天文觀測著重在望遠鏡，自然希望口徑越大越好。到了廿世紀中期，製作大口徑望遠鏡的技術，受到重量限制，達到口徑五公尺之瓶頸。之後的技術發展朝向偵測器，從底片到單元探測器（例如光電倍增管），再到高效能 CCD，量子效應在某些波段可達 90%以上。廿世紀末期，望遠鏡製造技術有了突破，採用組合式鏡片，或望遠鏡陣列組成干涉儀，同時提高靈敏度與解析力。偵測器的發展，除了減少噪音，則主要朝大尺寸發展。泛星計畫的 GPC 爲箇中翹楚，有多項嶄新技術，也是目前全世界最大的數位相機。

泛星計畫的資料流程如圖九。來自望遠鏡的光子，經過相機記錄，原始檔案首先經過 Image Processing Pipeline (IPP) 處理，分析影像，將點光源（星球）與沿展光源（星系）分開，並分析其位置與亮度，進而產生天體目錄，提供不同科學群組使用。比對不同時期所拍攝的影像，便挑選出有變化的天體，其中位置產生變化者，由 Moving Object Processing System (MOPS) 流程處理，例如與已知太陽系天體比對，計算軌道等。將「變化」的天體去除後，「不變」的夜空影像則可以長期疊加，相當於長時間曝光的全天空影像，除了提供未來天文學家普遍使用外，也是諸如 Google Sky 等軟體的良好資料庫。泛星計畫的資料最後建成資料庫，將透過 Published Science Product Subsystem (PSPS) 介面，提供給使用者。可以說天文觀測繼望遠鏡與偵測器之後，隨著資料量暴增，尤其類似泛星計畫這

樣研究時變現象，下一個革命就是資料庫。執行科學計畫不能僅止於開始的硬體建設，還應該把軟體開發、日後營運，以及資料後續使用等經費，都包括在規劃內。

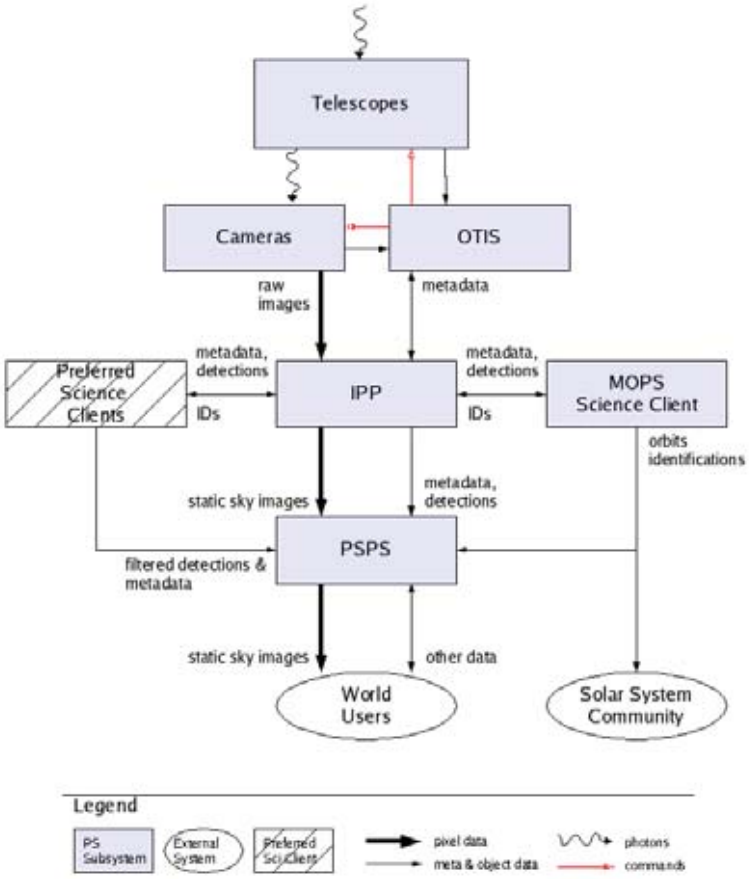

圖九：泛星計畫資料流程。

3.5 主要科學目標

泛星計畫的英文直譯爲「全天域觀測望遠鏡及快速反應系統」，顧名思義，基本上是個觀測設備。PS1 預期將進行三年半，產生史無前例的大量資料，可以提供極多科學課題使用。圖十爲巡天所使用的濾光片，藉由觀測天體在不同波段的亮度，來研究其性質。

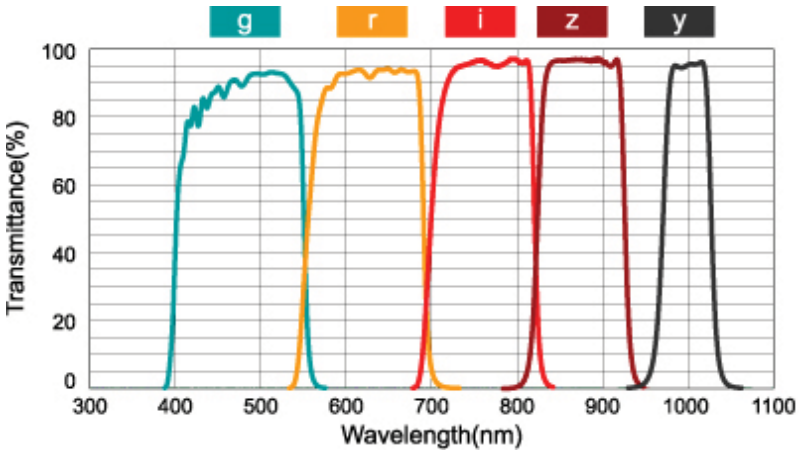

圖十：泛星計畫所使用之濾光片 (Asahi 公司設計、製作)，最長波達 1 微米。

在太陽系中，從地球周圍的近地小行星、各式小型天體，外圍的古伯帶天體(Kuiper-belt Object)，甚至尚未發現的行星，都是研究的好課題。例如現在發現上千個近地小行星，PS1 預期可以找到上萬個，對於保衛地球文明做出具體貢獻。在銀河系尺度，泛星計畫的數據提供全天星體的亮度、距離、運動速度等，除了推敲銀河系結構，以及形成與演化，也可以挑選出無偏差之特殊星體樣本，例如光度極弱之天體，加以研究。在更大尺度，還可以研究相互碰撞的星系，或是成團的星系等宇宙大尺度結構。

在亮度變化方面，除了無以數計的變星，還有恆星死亡時產生的超新星爆發，或是至今仍然神秘的迦瑪射線爆發的光學對應源等。泛星計畫的每個像元對應不到 0.3 角秒，而預計視相度可以達到 0.7 角秒左右，這樣良好的影像品質，對於至於「不變」的宇宙，例如研究物質分佈所造成的空間微小變形等，也將提供極珍貴的資料。

4. 計畫進度及結語

夏威夷大學所獲得的經費，僅限於建造，營運部分則組成「科學委員會」(Science Council)，負責巡天之經費籌措、操作模式，以及計畫管理等。望遠鏡、GPC 於 2007 年底取得初步影像（圖十一），目前複雜的光學系統仍繼續調整當中（圖十二），預計 2009 年初開始正式科學觀測。

科學團隊除了夏威夷大學外，還包括德國 Max Planck Institute for Astronomy in Heidelberg, 以及 Max Planck Institute for Extraterrestrial Physics in Garching，美國 Harvard-Smithsonian Center for Astrophysics/ the Las Cumbres Observatory、Johns Hopkins University 約翰霍普金斯大學、英國 Durham University/University of

Edinburgh/Queen‘s University Belfast，以及台灣。我國團隊成員共有約 20、30 位教授與研究生，來自中央大學、清華大學、台灣大學、成功大學、中央研究院等，除了天文學家，還包括資訊工程學者加入資料庫技術、分散式計算等課題，爲我國光學天文學較具規模之國際合作計畫。泛星計畫預期將引發出大量新發現，甚至在時間尺度方面發現前所未知的現象，中央大學目前正在鹿林天文台建造兩公尺口徑望遠鏡，由於我們與夏威夷有 5、6 小時時差，廣大太平洋缺乏其他天文台，完成後將在經度上取得優勢，於第一時間追蹤觀測泛星的可疑結果，第一手驗證這些發現。且讓我們摩拳擦掌，拭目以待泛星計畫正式開展，揭開研究時變宇宙的新紀元！

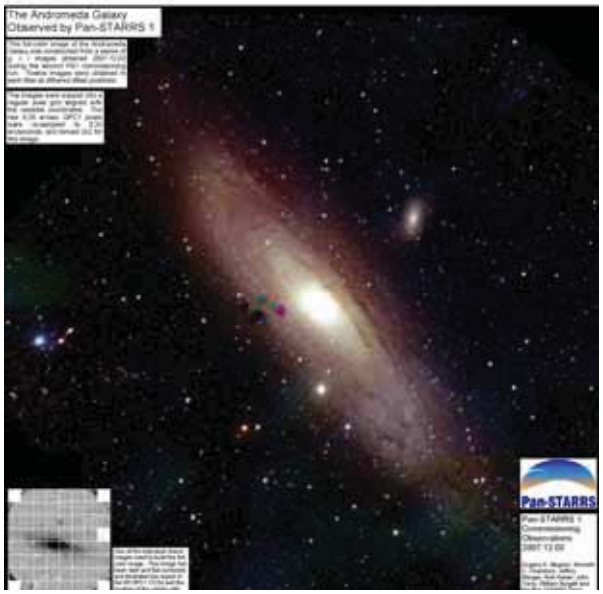

圖十一：PS1 於 2007 年 12 月 2 日取得第一張影像。超廣角視野可以將仙女座星系 M31 完全攝入。

圖十一：泛星計畫所拍攝之 M51 螺旋星系及其衛星星系，影經過光學調整，影像品質明顯改良。

參考資料

1. N. Kaiser, et al. "*Pan-STARRS --- A Large Synoptic Survey Telescope Array*", in "*Survey and Other Telescope Technologies and Discoveries*", Ed. J. Anthony Tyson, Sidney Wolf, Proceedings of SPIE, **4836**, 154 (2002)
2. D. Jewitt, "*Project Pan-STARRS and the Outer Solar System*", Earth, Moon, and Planets, **92**, 465 (2003)
3. J. L. Tonry, Burke, B. E., & P. L. Schechter, "*The Orthogonal Transfer CCD*", Pub. of the Astronomical Society of the Pacific, **109**, 1154 (1997)
4. J. L. Tonry, G. A. Luppino, N. Kaiser, B. Burke, & G. H. Jacoby , "*Rubber Focal Plane for Sky Surveys*", Proceedings of the SPIE, **4836**, 206 (2002)
5. J. L. Tonry, B. Burke, P. M. Onaka, G. A. Luppino, & M. J. Cooper, "*Orthogonal Transfer Array*", in ``*Scientific Detectors for Astronomy 2005*", Astrophysics and Space Science Library, **336**, 281 Kluwer (2006)

老中青三代談臺灣高等天文教育(上)

沈君山教授

沈君山教授是早年國內推動天文學發展的教父，不論是主持天文學會或在校任教，都著有功績、誨人無數。沈教授才華洋溢，足球、籃球、圍棋、橋牌無一不精。1973年毅然放棄美國普渡大學物理系教授之職，返國任教於清華大學，歷任教授、院長、校長；亦曾獲政府延攬，受聘為行政院政務委員。退休後，目前定居於在新竹清華園。

採訪/ 葛必揚、劉愷俐

葛：請問您是如何接觸到國內的天文？

沈：我是1973年返國任教，當時我們國家剛退出聯合國。我從前沒有搞過天文的東西，到了普林斯頓後碰了一點，也是天文物理。在回國之前我寫了兩本有關天文的小書，「天文漫談」和「天文新語」；那個時候還沒有人寫科普的東西。回來後在清大開課，在臺大和東海也兼任開課，開的課是天文物理，不是天文學；當年國內還沒有其他大學校開這個課。

葛：所以您是開風氣之先，那當時有觀測方面的環境嗎？

沈：邱宏義先生曾帶領清大的學生動手，自己磨製一個16吋的望遠鏡。這比中央大學24吋的望遠鏡還要早，但是它的主軸沒弄好，所以雖然可以看得遠，但對天體的定位有問題。

葛：既然條件不盡理想，您為什麼還會選擇天文、天文物理來推動教學？

沈：天文是一門古老的科學，能啓發人的好奇心，人類最早產生好奇的對象就是天，我們知道好奇是科學萌芽的基礎。天文本身要用到所有的基礎物理的知識，把這些基本的工具一一打好基礎後，再在天文的課題上應用出來。我回國後並沒有從事這方面的研究工作，因為效果與意義不大，那個時候條件與環境都不理想；我記得很清楚，蔡臺長要找木星的衛星給我看，結果一直找不到，我當時就在想，人家伽利略時代就看見了。但是我認為作為一個知識份子應該要具備有天文方面的素養，所以我開課、寫書把它當作是文化傳承的一部份在做。

葛：您回國後除了在大學任教，也主持天文學會的運作，請您談談那個時期的情況。

沈：當時國內天文的工作者很少，只有如戴運軌先生、曹謨先生、蔡章獻先生等少數；我回國後參加中國天文學會，在中山堂開年會，只有十幾個人，當時會長是戴運軌先生，他推舉我繼任會長，可能他們認為我比較有辦法，可以找到經費資助，這一做就是11年。之後交給中央大學的吳心恆先生。後來他們的任期就短了，3年、2年甚至1年。

葛：在您主持天文學會時，兩岸與國際的天文交流互動情形如何？

沈：天文學會會長的工作之一，就是要代表國家出席國際天文學聯合會(International Astronomy Union, IAU)，當時中國大陸也在積極參與。因此雙方在名稱的稱謂上就必須有所研究。那一年在加拿大蒙特婁開會，他們的代表是張鈺哲先生，張先生人很好，是屬於老一輩的學者，但是大陸的政治體制關係，張先生有時並不能完全作主；國際聯合會的主席Dr. Brown, 提出了一個建議，就是我們用「China, Taipei」，在China 與Taipei之間用一個逗號隔開，大陸方面用的是「China, Nanjing」，表示雙方對等的關係。這在當時並沒有提到大會去討論，只是一個協議，因此沒有定案做成會議結論。至於以後有沒有再變動，我就不知道了。

這與奧會的模式不一樣，奧會用的是「Chinese Taipei」；另外就我所知道，有的地方用的名稱則是特別在臺北之前加上「located」一字，比方中央研究院就是如此。

至於兩岸之間的交流，早年我們觀測方面基礎很弱，只有圓山一處天文臺，大陸方面情況比我們要好一點，尤其他們在古代天文學這一領域做的有些成績。這幾年兩邊在推動天文名辭的翻譯統一上，也有往來討論。

葛：我們知道您曾經促成天文與氣象的分離，請您回憶當時的情形。

沈：當時在政府看來天文是屬於氣象的一部份，蔡臺長他們認為不方便。可能他們認為我比較會講話，所以有一天讓我到立法院給立法委員上了一堂課，講述天文與氣象是兩門不同的學科，我對立法委員講，從前欽天監的職權很大，甚至可以管到皇帝的生活作息，今天把它放到氣象局底下，綁在同一個法規裡面，實在不合適，也太委屈了天文自古以來的地位了。後來就立法通過，將天文的內容從氣象法中剔除了。

葛：也請您談談對圓山天文臺的回憶。

沈：早期國內只有圓山天文臺，在圓山天文臺之前，還在中山堂的樓上，一架小小的望遠鏡。蔡先生對推動臺灣的天文教育有很大的貢獻。但平心而論，圓山的觀測條件並不好，光害嚴重，望遠鏡的口徑也不大。我在開課的那些年，每年都帶修課的學生到圓山參觀，但常常是把望遠鏡對準到圓山大飯店屋簷上的龍飾，讓學生體驗一下望遠鏡的功用而已。

葛：最後請您談談國內天文環境數十年來的變化，並請您揭示未來應該發展努力的方向。

1958年6月中國天文學會在臺復會的成立大會留影紀念

1982年在圓山天文臺舉辦的天文儀器展示會，沈君山蒞臨開幕剪彩。

沈：天文發展這幾年大有進步，比起以前當然不一樣。不過談到未來發展的方向，就見仁見智，每個人看法不同。我一直認為以臺灣的客觀條件，應該推動的是天文的教育，而不是天文的研究。

天文是一門很純粹的科學，太空方面的研究還可以帶動一些周邊的科技發展，但天文學能帶動的應用科技就很有限。所以像天文館這樣的社會推廣工作，我就贊成；至於對於那些有興趣於天文學的學生，我們現在也有研究所，可以在學校裡教育、栽培他們，他們將來可以到國外進修，從事研究工作；或者也可以到學校教書，中學裡就需要這樣背景專長的教師，把天文的知識當作種籽傳遞給下一代。但要國家花大筆的經費，蓋現代化的大型天文臺，自己來從事大的研究科目，我個人一直持保留態度。這不是研究本身不對，而是要想一想我們的條件，我們這樣發展投資的目的何在。這些年的天文發展比較偏向於國際大型的研究題目，當然與人有關係，我們的研究人員都是從美國學成回來，自然受到美國的環境影響，把那邊的東西搬回來用。不過談到自己的方向，總要仔細評估一下才對。(整理/ 葛必揚)

葛必揚、劉愷俐：皆任職於臺北市立天文科學教育館

吳心恆教授

吳心恆教授在一連串機緣巧合下，不小心成為天文學家，卻對臺灣高等天文教育有著舉足輕重的影響。他是早期少數在大學中開設天文通識教育課程者，主導臺灣第一座研究用天文臺的建置，並曾參與天文標準名詞的修定工作。他幽默的行事風格，及對各類科學敏捷的反應最讓人印象深刻。吳教授自中大退休後，目前任職於吳鳳技術學院電子工程系。

採訪/ 張桂蘭

我早年是從事大氣與極光領域的物理研究。我在匹茲堡大學的指導教授受基特峰天文臺（Kitt Peak Observatory）之邀，在1970～1975年航海家號太空船升空之前，模擬太空船拍出的行星高層大氣光譜，以便協助測試儀器性能。因此取得物理博士學位後，我也到基特峰天文臺位在亞利桑納大學的總部訪問一年，期間曾參加他們的研習營，學習如何磨製望遠鏡鏡片。

中央大學在臺復校後便已成立物理系，後來申請設立物理研究所時，受到中國天文學會與教育部的「關切」，1977年決定改為設立「物理與天文研究所」，成為臺灣第一個設立專業天文研究的機構。

申請回中央大學時，校方以為我在基特峰天文臺工作過就應該是天文學家而聘用；1976年回臺後，直接指定我在大學部開設普通天文學和天文觀測實習課。後來更在當時的物天所所長倪祖偉教授的帶領下，一同加入了中國天文學會。當時除了我之外，還有郭富雄教授有在地球物理系開普通天文學的課。

我第一年開設普通天文學時，因是選修課，只有3個人選修。當時天文最厲害的不是我，而是中大天文社。我為了準備課程到圖書館借書時，發現每一本書都有同一個人借過，想說這個人怎麼這麼厲害-這個人就是蔡文祥！直到後來才知道學校規定天文社於學期初需由社長出面將整批書借回，到學期末再整批歸還。由此可見當時中大天文社之蓬勃！

中國天文學會的沈君山、李太楓等人藉1986年哈雷彗星76年一次的回歸籌畫了許多活動，推廣天文知識，將天文炒熱，許多學校因而希望開設天文相關通識課程。

但當時臺灣地區開設天文課程的教授不多，且內容非常專業，例如沈君山教授開的是恆星內

部結構和溫度變化之類的課，當他在臺上講得愈高興時，臺下一臉茫然的人就愈多，與一般大學生只想知道那是什麼星座？它的神話故事是什麼？這類可以「把妹」的知識需求差距很大。所以當時普通天文的課程一般是由物理系和圓山天文臺的人負責上。我也有在中原、淡江等大學兼任開課，也許他們較少接觸天文而覺得稀奇，最多曾有約100人同時修課。

不過，臺灣因無大學天文系，25歲出國留學才開始認北斗七星在哪裡，天文功力與國外大學就已唸天文的人怎麼比？而且臺灣地區的天文機構也不多，真的有人想唸，回來也會找不到工作。所以當時留學生多半從事理論研究，少有天文觀測人才；沈君山教授曾笑說：這是「雞生蛋、蛋生雞」的問題，總要有人先出去唸，未來天文機構成立後，才有人能回來教。蔡文祥老師等大概是第一批出去學習天文觀測方面的人。

至於中大天文臺24吋望遠鏡的建造，也是個機緣巧合的機會。當時物理系和物天所要申請下一年度的預算時，各實驗室都有提出申請。在1980年左右，中大物理系只有一支教學用的C8望遠鏡，倪祖偉教授提議申請一支16吋左右的望遠鏡，預估預算約需新臺幣50萬，相當於整個物理系所預算的1/4。結果教育部可能在中國天文學會的推動下，不僅將相關經費提升為第一順位，更專案撥款800萬來建造研究級的望遠鏡。

除了校內組成一個專案小組外，倪祖偉所長商請基特峰天文臺第一任臺長A. B. Meinel夫婦幫忙，在他們的大力協助下進行望遠鏡評選和天文臺規劃工作，讓我們省了很多冤枉路。最後選定Perkin-Elmer公司的24吋反射式望遠鏡及德式赤道儀，希望承載能力高、用途廣泛，後續國際合作時做儀器擴增替換也較方便。

當時恰好中大科一館進行擴建工程，便選定在科一館頂樓蓋天文臺。我們向建築師提出一些奇怪的要求，譬如說：要在建築物中蓋一根不能和牆壁接觸的柱子，柱子和建築物之間要用保麗龍隔開，防止有人在房間中走動產生的震動影響觀測結果。當時的工程師就是幫圓山天文臺蓋圓頂的人，有了圓山的一次經驗，蓋中大天文臺時溝通上就比較沒問題。當時並曾聘請呂克華教授為訪問教授，教授一些天文觀測和理論方面的課程。

經歷2年的規劃建設，1981年中大天文臺終於完成。後來利用24吋望遠鏡以光度計進行變星觀測，此外因當時的4X5大型底片很貴，所以利用縮攝相機，將影像縮小5倍，才可利用135底片進行拍攝月亮、M42星雲等比較亮的天體，除做天文推廣教育外，並可做最暗星等、追蹤精度、像差等的基本測試。國內第一個研究用天文臺終於成形，持續培養天文人才。

張桂蘭：任職於臺北市立天文科學教育館

1990年4月開始修訂，1992年出版的「天文學名詞」。

上圖：中央大學24吋望遠鏡曾是全臺灣最大的研究教學望遠鏡，下圖爲其安裝時的情景。

老中青三代
談臺灣高等天文教育(中)

蔡文祥教授

號稱「中大小虎隊」之一的蔡文祥教授是國內第一個專攻天文觀測的學者，臺灣天文社教圈中許多人都是他的學徒。他於碩士研究生期間全程參與中大天文臺的建設，學成歸國後又一手包辦鹿林天文臺的選址探勘工作，並注重臺灣光學設計人才的培養。現居美國，仍持續利用親自動手於自家後院蓋的天文臺進行變星觀測，及天文科普教科書的撰寫工作。

採訪/ 張桂蘭

我是國中第一屆有地球科學課程的學生，但當時大都是地理老師兼任，有時甚至是課本放在旁邊、卻在上別的課程。那時的地科課本封面是馬頭星雲，大學之前對天文的印象僅止於此。

圖1.蔡文祥教授攝於鹿林山莊前

中央大學天文社約在民國59年成立，天文社的小天文臺與4吋望遠鏡均由地球物理研究所借給天文社使用。當時天文相關書籍很少，天文社社長每年學期初至圖書館整批借出，放在小天文臺中供社員參考，至學期末再整批歸還，接任的新社長再決定要不要去整批借書。我大二至大三時，吳心恆老師回中大物理系任教；他在接任天文社指導老師之前都不知書會被天文社借走，一直到暑假期間才看到書而得以備課。

天文社每年都會自費從國外郵購一些帕洛瑪天文臺的彩色漂亮星雲海報或卡片，每學期新生入學時到新生宿舍去兜售並招攬新社員；我就是被這些圖片「騙」去參加天文社。我於大二時接任天文社第7屆的社長。後來每一屆都會去結匯票向國外購買，當時匯票還受管制。

當年可進行天文科普演講的人只有沈君山教授、蔡章獻或陳正鵬等人-不過他們當初講的內容很簡單，就是現在科普演講都還在講的東西。而鄒志剛老師與郭富雄老師回中大任教時，只曾在地球物理研究所開設宇宙線有關的高能物理及天文物理課程。所以在此之前，大學天文教育幾乎都尚未開始，直到吳心恆老師回來為止。

吳老師在我大四時開普通天文學，僅三人修課。他向物理系申請經費購買一支C8望遠鏡做為教學設備；當時以新臺幣20萬元購買，那時美金匯率約1:40，所以相當於美金5000元之多。我和另一個修課的同學楊開越常將C8搬出來用。

當時望遠鏡是管制品，軍方怕被用來偷窺軍方設施，在學期結束時，管區警察都要來檢查C8有沒有妥善地鎖在保險櫃中。

中央研究院在大陸時有天文研究所，可是來臺後卻沒有任何高等天文教育的機構。沈君山與蔡章獻等人擔任中國天文學會理事長期間，與中研院院長、教育部科導會的吳大猷博士一同推動臺灣高等天文教育，希望在大學成立天文系，可是一直沒通過。那時臺灣已有5個「物理研究所」，使得中大申請了好幾年要設立物理研究所都過不了；剛好中國天文學會在推動要有高等天文教育，教育部的人因而告知中大最好改一個他校沒有的名字，中大將之改為「物理與天文研究所」後再送出，終於在我大三時通過審核而正式成立，第一屆招生只有2個人去唸，而且都是攻讀固態物理領域。後來我考上成為第二屆學生，同期進入物天所的10人中，只有我攻讀天文，其他人都在物理領域，因而少有開設天文課程。所以我那時除了修過一年呂克華老師的光譜光度學，另外只得去地球物理所修鄒志剛老師的天文物理課。

當時的所長兼系主任倪祖偉教授曾在美國亞利桑納州立大學教過書，於該地認識蓋美國基特峰國家天文臺（Kitt Peak）的Meinel博士，便在準備蓋中大天文臺時邀請他來幫忙。1978年大陸開放，Meinel受邀到上海天文臺去幫他們設計1.5米望遠鏡，故上海天文臺1.5米望遠鏡的規劃年代與中大天文臺24吋望遠鏡很接近。之後他順道到臺灣，曾在中大開過一學期課。我大四時，天文臺開始動工；按Meinel建議將望遠鏡臺柱從地下室打到三樓，與建築物分離，為臺灣第一個標準天文臺臺柱。

確定考上研究所後，有一天接到倪祖偉教授託人打來的電話，問我是否要回學校當助教；當時教育部剛好有個條款，研究生可擔任領全薪的專任助教，但得多唸一年才能畢業。我評估過天文臺蓋好到望遠鏡可以用約需兩年時間，考量之下就答應接下這個工作。中大天文臺從開始蓋到完成望遠鏡安裝的這三年，恰好是我待在中大當助教兼研究生的時間，全程參與了天文臺基礎工程建設。

現已退休的中大物理系曾祥光教授曾有一次到美國芝加哥一帶，倪祖偉老師託他詢問當地華人圈中是否有做天文的華人，有人介紹呂克華老師。我研一時望遠鏡採買定案，天文臺圓頂的工程則正在進行中，呂克華教授被聘為客座教授，我擔任他的助教，也當他的研究生。呂老師當年在天文臺圓頂規格與望遠鏡極軸定位方面，大力協助了包商改善工程。

我的論文題目是呂老師在南美智利觀測的恆星自行資料，他在中大一年期間教我如何分析；當時的電腦速度非常慢，花了一整學期的時間，將資料初步分析完，至研二時他已回美，我只好陸續將分析完的資料用航空郵寄去美國給他，他再將修改的意見寄回給我，每次一來一往都得花上一個多月。好在研三時呂老師又回中大客座，不僅協助24吋望遠鏡的測試工作，論文也終於在他親自指導下完成。

24吋雖在我研三時已設置完成，儀器卻只有一套4X5玻璃片照相機，無法進行正式天文觀測；望遠鏡和光度計等儀器待我當兵後才全部建構完成，使得我不曾用24吋望遠鏡觀測資料來寫論文，這是我唯一的遺憾。

中大天文臺中的赤道儀其實承載量可達36吋望遠鏡的重量；只做到24吋，是因為原本規劃用庫德式鏡片來導光到三樓的光譜儀平臺上，考量庫德式鏡片很重之故，因而用較大的赤道儀裝載較小的望遠鏡。24吋望遠鏡焦長很長，架在德式赤道儀上。Perkin-Elmer這種型式望遠鏡是1970年代美國大學天文臺中的標準品，而美國國家天文臺的小型望遠鏡大都是標準德式赤道儀或叉式赤道儀；經緯儀則一般都用在4米以上的大望遠鏡。由於中大天文臺是個標準天文臺，但受限於經費只能買小望遠鏡，所以Meinel建議買這種望遠鏡。

在臺柱下方有準備放光譜儀的平臺，是所有標準天文臺的標準設計。Meinel當初設計時，建議也設置這樣的平臺，可以放光度計，也可以放光譜儀；因光譜儀很重，故在臺柱下方有個洞，可將星光經庫德式鏡片穿過這個洞導到3F實驗室的平臺上。

圖2.鹿林天文臺空照圖(2002年)
圖3.建設前的鹿林天文臺址，荒草一片，中立者爲蔡文祥教授，一旁背影爲王敏生教授。
圖4.鹿林選址時期的鐵皮屋(觀測站)，沒水沒電沒廁所。
圖5.「國立中央大學鹿林觀測站 民國八十年十一月建臺」
圖6.觀測站內部：選址用的望遠鏡和電腦等設備，也是生活的空間，。

當時物理系梁忠毅老師曾打算利用24吋望遠鏡進行「雷射測距」的研究。但庫德鏡片要多花美金20萬元（約新臺幣400萬元），等於整個專案經費的一半都需花在庫德式這樣的特殊光學系統上，實在不划算。其次，當時的雷射還在最早期開發的年代，而進行這項研究必須用染料雷射開關（dye Laser switch）這種新技術才能達成，染料雷射開關與僅發出5mW的雷射就至少各需美金10-20萬元左右。由於將耗資甚鉅，使得這個計畫不了了之。雖然這個計畫很有挑戰性也很有趣，但終究只是一個遙遠的夢想而已。

孫維新教授、闕志鴻教授和我是同時期回中大的。當初中大找我回去的目的，是校內有教授認為24吋望遠鏡使用效率太低而建議要把它丟掉，吳心恆老師和郭富雄老師誓死反對。吳老師研究氣象局的資料後，認為恆春一帶晴天率很高，希望我能詳細評估24吋望遠鏡搬到墾丁的可能性。

我們三人回中大的第一個學期就南下墾丁做

選址勘查，結果發現：恆春半島近海，鹽分將會讓電子系統嚴重鏽蝕；此外恆春的落山風很強，我們勘址時恰遇一臺箱型車被落山風吹翻了；而且初夜海陸風交換時，雲朵常飄來飄去，視相度（seeing）沒想像中好，因而可能不太適合。

之後，臺灣一些天文愛好者如陳培堃、林啓生等人開始提供資料，於是我開始往山上找點。陳培堃當時正好完成「玉山星空」第一階段、正在執行第二階段的拍攝計畫；鹿林前山是管制區，一般人進不去，只有陳培堃實際在鹿林觀測過。他幫我們與玉管處聯繫，我和王敏生老師隨他上鹿林勘查地形；當時是秋季，為鹿林最棒的季節，感覺很舒服，因此決定在此重點發展。

後來申請經費，買了一套C14設備，聘請專任助理藍文隆在鹿林山莊後方、阿里山和自忠等地，進行選址的長期觀測。當初我還打算申請一部可移動式的天文觀測車，以便能載望遠鏡和觀測儀器到處觀測。教育部雖答應給100萬專用款，但因那個年代買車一定要配司機，養個司機2、30年的經費相當龐大，所以該專款不准中大買車。

中大遙測中心主任陳哲俊教授當時給了一個很「實用」的指導，他說：「拿到錢，不能買車，那就買個車、但把4個輪胎拿掉嘛！」這就是鹿林山頂上的平頂觀測站的由來。100萬經費中的40萬是雇用人工背了一兩噸鐵皮、建材等材料上山的工資；平頂觀測站中共有3個水泥臺墩和12個水泥臺柱，那是我一生中做過最貴的水泥臺柱。負責工程的陳老闆因要揹水和水泥上山，共雇用了4位山青幫忙，後來陳老闆就地取材、用塑膠盆接鹿林山上小天池的水來拌水泥，省去揹水的工作。最後才成就了臺灣的第一個高山觀測站。

蓋天文臺要考慮的因素很多。鹿林特殊之處是它在環山之間，並非在最高峰處；因空口無憑，要證明這個地點的好壞，必須由長期累積的seeing觀測資料做科學性說明。後來鹿林選址勘測共花了3～4年的時間取得資料。

我們本來也考慮在阿里山做選址觀測，雖然阿里山交通食宿方便，但是顧慮到該處未來的觀光發展將帶來光害影響，加上阿里山比鹿林前山低了五百多公尺，經常處於雲海中，因而作罷。陳培堃另外還曾介紹自忠一帶，此處有許多簡易工寮可供食宿，早期許多無法進入玉管處管制區的天文同好大都在此處拍攝。

許多同好也會在合歡山進行天文攝影。合歡山雖好，但它的致命傷就是會下雪-會下雪代表平均水汽很重；水汽重且會積雪的地方都代表天氣不是大好就是大壞。我當初曾做過雨量和雲圖分析，合歡山恰好在濁水溪以北，鹿林則在濁水溪之南，東北季風期間，北來的水汽大都被海拔高的合歡山擋掉，再加上鹿林以東有玉山山脈會將颱風等較激烈的風擋掉，從西邊上來到鹿林的颱風幾十年才會發生一次，危害不大。此外，合歡山不在國家公園管制區內，車輛容易進出，易產生光害，設施也易被破壞。所以從各方考量，選擇了鹿林這個點。

我從學生時期到回臺教書，對學生的天文學習態度的第一個觀點是：今昔年輕人對天文的愛好一直沒變，一樣好奇、一樣想探究；但這種探究分兩個階段，一是對拍照片方面的探究，另一是對天文物理方面的探究；如傅學海老師說的，要有基本的觀眾群，才能在其中挑出一兩個真正對天文有興趣者。我早期認識對天文有興趣的人多集中在天文攝影方面，當他們踏進天文之門後，天文物理方面的潛力不夠，要讀書、要考試的都掛了。到後來，學生的潛力夠了，但大多是想念個學位，天文只是個跳板而已。真正潛力夠，對天文又很執著的，與物理的人相比，目前比例大概是1：40，與美國相當。亦即，學物理天文者，真正對天文有興趣、會繼續待在天文領域的，比例大約是1：40，已經比以前多很多了。

教育是很難評斷的，現在臺大、中大、清大都有天文研究所，分食這個學生比例大餅，所以各系所如何提升學生的素質，得視還在教育線上的大老們如何努力了。

張桂蘭：現任職於臺北市立天文科學教育館

老中青三代談臺灣高等天文教育(下)

陳文屏教授

陳文屏現任中央大學天文研究所教授及中國天文學會理事長。聰明、專業、做事認真而親切，是他給人常留下的印象。不僅在天文所所長任內大力推動鹿林天文台與TAOS計畫的建置，之後又陸續與世界各地2米左右望遠鏡和重要觀測計畫洽談合作事宜。除了研究工作，對於推動高等天文教育也具有滿腔熱誠。

採訪/ 張桂蘭

1970-80年代的中大天文教育概況

民國65～69年我念大學時，還在圓山天文臺時代，偶爾會去那裡參加活動、聽演講或開會，也是那時候認識了蔡章獻臺長。現在想起來，以前的圓山天文臺真的有點簡陋。

念中央大學時，當時天文社有個4吋望遠鏡。不知有多少晚上我們躺在小天文臺外看星星，真的好舒服。那時認識了趙寄昆老師，而鄒志剛老師也才剛回國。當時天文社相當蓬勃，常舉辦演講或望遠鏡觀星活動。雖然我從小喜歡天文，念過一些書，但從未真正用望遠鏡看星星。直到大學天文社透過望遠鏡看了許多星雲、星團、行星等。尤其是土星，覺得美麗又奇妙到不可思議，奠定了我研究天文的意願。

大四之前，我修過吳心恆老師的普通天文學，學習時間座標，及一些天文現象。後來呂克華老師回中大客座一年，所以我大四9學分全修了呂老師的課。呂老師從美國帶回一套玻璃光譜，要用顯微鏡分析測量以進行光譜分類，他另外還教授光度系統、高等研究等之前沒聽過的東西。

當時蔡文祥老師是研究生，也修呂老師的

位於鹿林天文台的TAOS計畫其中的兩架望遠鏡

課，只我們倆上課，跟家教一樣。上課時，呂老師說他在國外申請望遠鏡觀測時間，去過基特峰（Kitt Peak）、智利等天文臺，他說：「連我這種沒名氣的人，也照樣可能申請到觀測時間，到世界其他地方使用大型天文臺。」當時我好羨慕，直到自己到美國當研究生也做同樣的事，才體會到箇中的辛苦與樂趣。

蓋中大天文臺時，我正在服兵役，沒有參與建設過程；偶有一次回到中大，第一次看到24吋望遠鏡正式運作。有兩位國外天文學家準備做掩星觀測。我問他們為什麼要到臺灣，用這麼小的望遠鏡觀測，他們回答說因為那次的掩星事件只有臺灣才看得到，讓我體會到天體動態的一面。

(上)陳文屏大學時擔任天文社社長，於演講時由呂克華教授（右一）補充說明
(左)陳文屏於大學時以天文社天文臺4吋望遠鏡觀測的情形。

由國外經驗，引進新的天文課程模式

天文物理導論課程的開設

到美國念研究所那年4個入學生全都得補修大學部的課。臨畢業時，老師問我：「入學時先有個入學考，決定學生應補修什麼課程的這種制度，你認為如何？」現在想起來那個入學考很難，因為大學時學的電磁學是高斯定理、平行電板等，但天文用的電磁學一開始就是馬克斯威方程（Maxwell equation）或輻射轉移（radiative transfer）等，都是電磁學最後兩章、老師不太教的東西。

國外天文的研究生，他們大學時候多半曾經修過天文學與天文物理，或日常生活已經接觸，但是我在臺灣只接觸非常基本的天文學，研究所就跳到高等天文物理，沒有接觸過中間課程。因此1989年闕志鴻、孫維新、蔡文祥老師來中大任教後，認為需要在大三、四開設天文物理.....並不只有定性敘述而已。

天文非常依賴語言來溝通

當時在國外念書很辛苦。一來因為在臺灣以中文學習，雖稍有用望遠鏡看星星的經驗，吳老師也要求拍攝月亮當作業，但這些都只是業餘的訓練，許多專有名詞都沒聽過。在美國不僅要當助教帶課，而且上課都聽不懂，英文不懂，天文也不懂，上完課都非常沮喪。

天文學家描述事件都用「大概～」，和物理學家的風格不同。我在紐約州立大學石溪分校念研究所時，前後共有大陸、韓國、香港等地共10個東方學生也來念，最後除了我以外都轉系離開。造成這種現象的原因，一方面是就業市場，另方面可能是東方學生不適應，總覺得只要書讀好了就不成問題，因此著重在可以推導、可以考試的公式、定理等，文字說明就比較不細究。但物理學已經清楚區分電磁學、熱學或力學，天文則還是問題導向的應用學科，例如談到星際物質，必須同時用到電磁學、熱學與力學的知識，常沒有標準教科書，因此在學習時，幾乎無法關著門讀書，而必須透過討論、閱讀期刊來瞭解問題，探討答案。

研一時修專題課，每3個星期就輪一次上臺報告最近讀的論文。另外當助教每星期有一晚要花一小時教學生課堂上來不及講的內容，這些在在都需要語言表達，在臺灣時卻沒有這種訓練。現在我們學生的表達機會明顯比其他系所多，經過訓練後，站在臺上的表現也很好，經由演講、問答、爭辯來釐清概念是很重要的學習過程。

所以演講聽不懂一點都不奇怪。我以前在美國聽演講時常聽不懂，一方面是語言問題，一方面是天文問題。慢慢地，我訓練自己思索並演繹演講內容，再看看是否猜對一些內容，經年累月下來，發現慢慢聽懂的越來越多，而且不限天

留著小鬍子的陳文屏於紐約大學石溪分校時期，利用懷俄明的紅外線望遠鏡(Wyoming Infrared Telescope)觀測。

文，其他題目都可以聽懂一些。這種「用腦筋聽別人說話」的訓練是無價的，真正學到多少天文知識倒是其次。

養成解決問題的習慣

出國念書之前，我請吳心恆老師寫推薦信，並請教應該要加強什麼科目，吳老師說：「電子學！」當時非常納悶。多年之後我才瞭解為何不是近代物理或電磁學，這是因為中大天文臺那時剛蓋好，最需要電子與儀器方面人才。這給了我啓發：天文是個實際操作的學科，而科學家是要解決事情的，我們所受的訓練，是要讓我們不怕問題！真的碰到問題時，即使不是自己專長，也要有能力找答案，否則就尋求協助，想辦法解決問題。

博士資格考時，我筆試第一名，口試卻沒過。經向系上爭取後得以重考，結果我把普通天文學從頭到尾讀一遍，唸完後，有如打通任督二脈，對我後來研究天文幫助非常大。我現在教普通天文學時，第一堂課會告訴學生：「普通天文學有如第二外國語」。我告訴學生：「你們其實已經很有本事，可以解決很多問題了。你們所學的群論或偏微分方程，連大學老師都不一定常用」。普通天文學用的都是淺顯的基礎物理，甚至高中物理就足夠，只不過對象是宇宙天體。例如力學，物理中描述兩個彈珠彈性或非彈性碰撞，天文中卻是星球、星系甚至黑洞碰撞等。所以，真正要解決問題的時候，常常不需要非常深奧的知識，為了解決問題，去修課或翻書、查資料、和別人討論，養成這些解決問題的習慣相當重要。當然，要是有了深奧的知識，就能解決更多、更艱難的問題。

在帶學生方面，能得英才而教之，當然是樂事。我要求學生清楚知道自己在做什麼。有些小孩子不懂事，是因為他們父母太能幹，幫他們把事情都處理好了。所以父母不要太勤勞，孩子就有機會獨立，否則即使考了100分，也是父母的；同樣道理，當老師的要讓學生有自己領悟的機會，就算考試只有80分，也全是他們自己的。

電腦是天文必備的能力

天文領域在使用電腦方面相當領先。美國軍方一開始用網路時，天文界便已開始使用。所以讀書期間，除了天文學外，我覺得電腦的訓練也很重要。

早年推動2米望遠鏡建設的計畫

在美國念研究所時，我曾寫信給當時中央研究院吳大猷院長，建議國內要發展天文學，他回了一封很厚的信，讓我好感動。後來我也曾寫信給期刊上看到的一些大陸天文學家。這樣主動接觸，奠定了日後我和很多大陸天文學家合作研究的基礎，有些也有深厚私交。

當時從臺灣出去念天文的人非常少，呂克華老師是其一。他也認識吳大猷院長，不知這是否推動24吋望遠鏡建設的原因。呂老師從很早以前就要在臺灣建構2米望遠鏡，直到1990年「十年規劃」也曾列入討論。1992年我在美國華盛頓特區的卡內基學院當博士後研究員，申請當時中央大學正要成立天文所教職，有天早上劉兆漢校長打電話，問我是否有意協助2米望遠鏡計畫，笑說我答應，他才要簽聘書！後來評估2米望遠鏡在國際上已沒有競爭力，因此沒有繼續推動。現在臺灣蓋2米望遠鏡，又晚了10幾年，更需要針對特定課題，集中研究能量，才能有成果。

極為成功的十年規劃

1990年代臺灣天文界的「十年規劃」由李太楓院士發起，與徐遐生 (Frank Shu) 院士一起領軍，由國科會資助，找海外華人天文學家寫白皮書，企圖讓臺灣天文的發展不再迂迴前進，而能跳躍邁入世界前緣。當初參與十年規劃者尚有—袁旂 （Chi Yuan）、魯國鏞（Fred Lo）、賀曾樸（Paul Ho）、郭新（Sun Kwok）、朱有花（You-Hua Chu）、譚英元（Erick Young）、林潮（Doug Lin）、呂克華（Phillip Lu）、余光超（Howard Yee）、譚遠培 (Ronald Tamm)、顧植元 (David Koo)等，以及當時屈指可數的國內天文學者—鄒志剛、吳心恆、闕志鴻、周定一、孫維新、蔡文祥、高仲明等，我趕上最後一班車。。

那時候臺灣天文有如白紙，規劃的自由度很寬廣。研究領域在發展時，常常科學與技術輪流前進，連儀器設備、波長也一樣。電波天文當時已快速發展干涉術，例如特大天線陣列（Very Large Array），光學觀測卻停頓在4～5米望遠鏡長達50年之久。直到這十幾年狀況才不一樣，光學開始建設8～10米望遠鏡，甚至規劃30米望遠鏡。所以15年前要蓋2米望遠鏡，是真的沒什麼競爭力。那時成功的海外華人天文學家做電波的較多，他們認為不要走回頭路，因此十年規劃中決定發展電波和紅外干涉術。

第一個十年規劃的確將我國天文快速啓動，邁向世界前緣，不但有具挑戰的科學問題，也推動了尖端工程技術。同時在策略方面，干涉儀不需要完全從零開始，以Sub-Millimeter Array (SMA) 為例，美國原規劃6個天線，臺灣再加2個，不僅整組儀器效率增加2倍，臺灣也學到技術和儀器使用權，這非常符合經濟效應。在此之前，臺灣先參加Berkeley-Illinois-Maryland Array (BIMA)，花錢買觀測時間來訓練人員。SMA的成功，奠定了執行Atacama Large Millimeter Array (ALMA) 的基礎。這一路走來是對的，雖然的確不便宜，不過一流的科學從來沒有便宜過。

第一個十年規劃雖成功，但如何訓練自己的學生及如何不遺漏本土的基礎建設等配套措施卻

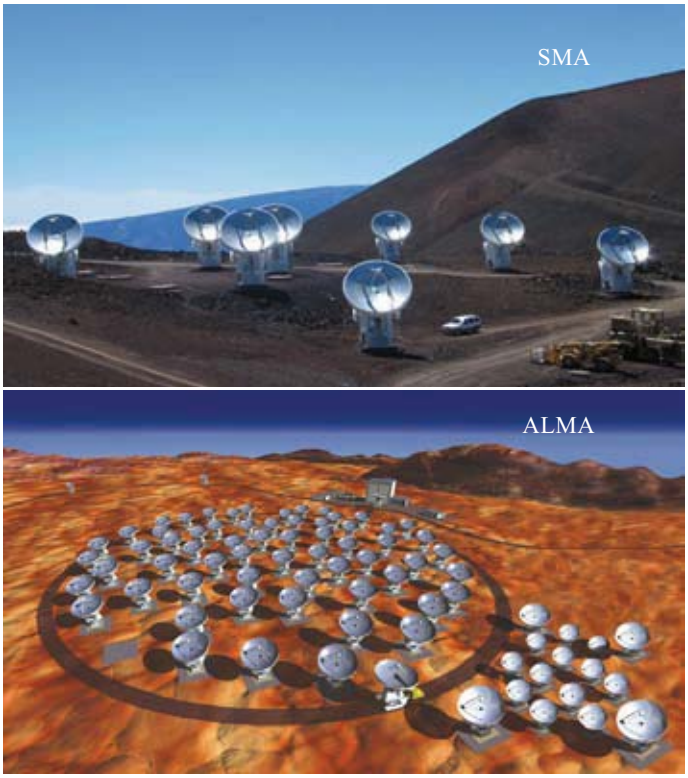

圖片來源：中研院天文所網頁

嫌不足，使得國內增加的天文學家數量遠低於所需要的。現在SMA中有很多國外天文學家，雖說可以吸取世界人才，且海外華人天文學家認為卓越是不分國界的！然而事情不這麼簡單，不僅卓越的定義可能因人而異，達到卓越的手段絕對因人、時、地而有不同。

第2個十年規劃已開始啟動

由於電波天文已發展得不錯了，自當繼續進行，例如ALMA就屬於這部份。大約於3～5年前開始啓動臺灣天文第2個十年規劃則主要集中在OIR（可見光/紅外波段）。但在OIR領域，朱有花、郭新、余光超、顧植元等在國外都有自己的工作，也都做得很好，沒有人回臺灣主持大局而無法推動，再加上沒有既成的好計畫可以像SMA這樣讓我們搭便車，所以當時曾做很多規劃、開很多會，但OIR一直沒有起飛，一直到參與泛星計畫（Panoramic Survey Telescope And Rapid Response System; Pan-STARRS），雖然並非整個天文界的共識，但算是有個著力點。

Pan-STARRS 泛星計畫的第一架1.8米望遠鏡。」。
圖片來源：泛星計畫網頁

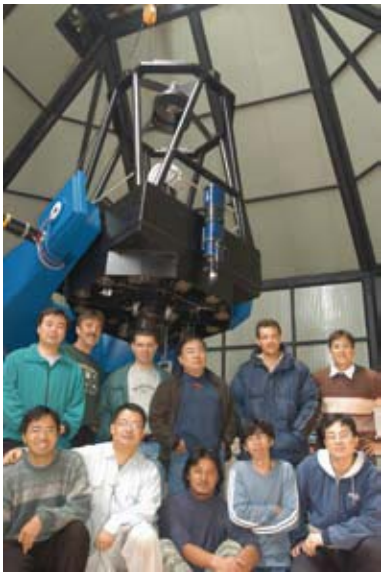

鹿林一米望遠鏡安裝團隊合影

國際上不乏類似泛星這種大計畫，但它特別之處在於以廣角且高分辨的儀器，大約每星期完成一次全天搜尋，因此適合用來研究「變化」的天體，包括位置的變化（小行星、彗星、古伯帶天體、地外行星）或是亮度的變化（變星、超新星、伽瑪線爆發源）等。我們參與泛星計畫無須分攤約6000萬美金的硬體建設費用，而與其他國家的優秀團隊分攤運作經費，就可使用Pan-STARRS全部觀測資料，進行我們專長的課題研究，培養迫切需要的新一代人才，做為躍進OIR殿堂的踏板石。

鹿林天文臺
1米與2米望遠鏡的推動

過去幾年由教育部與國科會支持的「學術追求卓越」計畫中，葉永烜老師主導爭取建設鹿林天文臺的經費，把它從一個小觀測站，躍升成為國際上具能見度的天文臺。其中一筆經費是TAOS 計畫第4座50公分望遠鏡，但後來韓國投入TAOS望遠鏡，因此追求卓越的那筆錢就用來買了一個舊的1米望遠鏡，當時望遠鏡屬德國一個社區天文臺，他們要升級為1.2米，因此我們取得優惠價錢買到鏡片，經過重新加工望遠鏡本體，才有鹿林天文臺1米望遠鏡（LOT, Lulin One-meter Telescope），成為過去幾年的主要設備。

鹿林本身並不卓越，這我們得承認。但整個卓越計畫做完，鹿林的基本建設留下了，也培育了一些人才，好好走下去，有機會成為卓越的第一步。追求卓越計畫結束後，有一次遇到徐遐生，他拍拍我肩膀說：「我覺得當年還是該蓋個2米望遠鏡！」當年為什麼沒有蓋？因為沒有資深的人堅持要蓋，電波能推動大型計畫，就是因為徐遐生、魯國鏞、賀曾樸等人願意來臺灣執行計畫，而人才是一切計畫之本。

當時國外天文學家認為不值得在臺灣蓋2米望遠鏡，一心追求最前沿，是他們忘了美國很多大學都有2米望遠鏡，當年總得有人做。如果目的是要做科學，那每年花錢買大型望遠鏡觀測時間就好了，不但可以選擇種類不同的設備，效率又好。雖然鹿林天氣狀況並非極佳，但有了自己的設備後，視野不一樣了，有了實際觀測、資料分析的經驗後，我們才知道4米、6米望遠鏡的價值，或申請8米、10米望遠鏡時才有所本。LOT發展到現在，已成為研究生常態性或論文的訓練；真正需要再深入研究，就必須申請國際上大型望遠鏡，目前臺灣與加法夏望遠鏡(CFHT)、日本Subaru望遠鏡合作就很好。有了優秀的設備，才能挑戰尖端課題，取得突破性成果。但是大望遠鏡時間極其珍貴，有人開玩笑，在寫觀測申請書時，就已經預期會看到什麼結果。然而使用自己的設備，大家不但有很多實際動手的經驗，也敢於嘗試新的想法，若再結合大望遠鏡「驗證」，可以取得非常好的成績。

鄰近的日本、韓國、中國早有兩米級望遠鏡，雲南和泰國不久另有2.4米望遠鏡，我們這幾年和烏茲別克天文臺、智利 Cerro Tololo天文臺的小型望遠鏡合作，可以進行聯合觀測，或是光譜與光度，可見光與紅外波段互補觀測等，讓鹿林的小望遠鏡發揮最大影響。

鹿林天文臺除了小行星巡天、超新星巡天這樣的工作外，我們也用LOT參加全球聯測等工作，但是因為口徑小，只能觀測比較明亮的天體，也就是幾乎限於銀河系內的天體。但以後2米望遠鏡

陳文屏及其博士後、研究生、助理...。左圖後排最右邊爲木下大輔，目前爲中大天文所助理教授。

就不一樣了，有了四倍的集光能力，相當於涵蓋八倍的宇宙體積，可以研究的課題增加很多。鹿林2米望遠鏡所規劃的電子相機，可同時在多波段進行觀測，以後甚至將開發紅外波段儀器，大幅增加望遠鏡的效能。

近年臺灣的天文教育

我回臺灣15年了，臺灣在天文方面的成長很多。學習環境變好了，學生的學習狀況呢？現在的學生的確不如以前用功，原因是他們的生活非常多元，而這也是他們的優點。如果他們清楚知道自己在幹嘛，利用資源的方法與思考的方式跟我們這輩不一樣，所以可以有不一樣的成功方式。現在電視廣告、年輕人演的話劇，有創意極了！他們敢嘗試新的東西，這是我們以前不敢、沒有能力、格局不同之處，這些創意配合適當的學問，能夠學、又能思，其實很有前途，絕對可以青出於藍。

但在臺灣光靠我們自己訓練出一流的天文學家，並不容易，必須充分利用全球的資源，才能訓練出跟全世界競爭的人才。中大天文所成立十幾年了，畢業生表現很好，其中有些留在學術界繼續努力。他們未來如何發展，並非只看能力，還要看有沒有企圖心。國內年輕學者普遍企圖心不夠，原因在於國內碩士、博士念太久，再加上男生有兵役問題，平均年齡都比國外大；在國外大學畢業直攻博士平均需時5、6年，已經比別的領域還慢了，可是國內卻要花到10年，站在研究崗位上，就已經35歲左右了，除了必須面對家庭、經濟問題，個人創造力與膽識也比較缺乏了。我建議年輕學生專心，在最短時間內取得學位，因為學習乃一輩子的事情，拿到學位才開始而已！

對未來天文教育的期許

現在我們博士生暑假都出國移地訓練，即使做的是與在臺灣一樣的課題，也要出去接觸第一流科學家，體會「事情總可以做得更好」，即使我們目前不是一流，也要知道一流是怎麼回事！希望他們培養深而廣的學問基礎，然後以大格局想新的問題，不要受限制；以使用大望遠鏡為例，並不是與用小望遠鏡做一樣的科學題目，只是曝光時間短一點而已，而是要發揮儀器特長，做重要的課題。我們自己沒有先進觀測設備，所以盡量尋求資源，讓學生能夠使用國際大型望遠鏡，並且送他們到國外跟隨優秀的學者學習。日後他可以看不起我「原來老師也只懂這麼多」，那就對了，學問就是這樣往前走。等到有一天，當學生告訴我格局不夠，眼光不足，或是胸襟不廣之時，就是我退休的時候了。

我常提醒自己：什麼樣的老師教出什麼樣的學生。當老師的本分就是要認真備課，讓學生不致空手而回；否則老師們抱怨學生素質低落，學生們同樣也抱怨老師上課不認真。老師不做研究、外務太多，學生自然不專心做學問。我小孩形容我做什麼事都很認真，一直讓我引以為傲，也以此為戒。我希望有一輩子熱誠，以樂觀態度敦促自己不斷進步，在長大成一棵小樹的同時，也能播下無數種子。

張桂蘭：任職於臺北市立天文科學教育館

小行星觀測

主講、審校/ 陳文屏教授
整理/ 蔡穎仁

小行星是什麼？如何觀測小行星？有那些研究可以做？這裡介紹如何利用掩星估計小行星的大小，監測小行星亮度變化可以獲得哪些資訊。

何謂小行星？

小小行星分佈在整個太陽系當中(圖1)，其中絕大多數集中在火星與木星軌道之間，這個區域稱為「小行星帶」。有些特殊小行星與木星軌道相同，位於木星前後與太陽成60度夾角之處，位在所謂的拉格朗基點上，這些稱為「特洛伊小行星」。最大的小行星為「穀神星」，直徑略小於一千公里，被歸類於「矮行星」。目前偵測到最小的小行星為軌道行經地球附近的「近地小行星」，大小只有幾百公尺。除了軌道以外，小行星也可以光譜來分類，例如C（碳）、S（矽）與M（金屬）類型。目前已知小行星超過幾十萬顆，分佈在上述寬廣的空間中，全部加起來的質量只有月球的百分之四；事實上小行星的分佈很稀疏，所以外行星探測太空船能順利通過小行星帶。

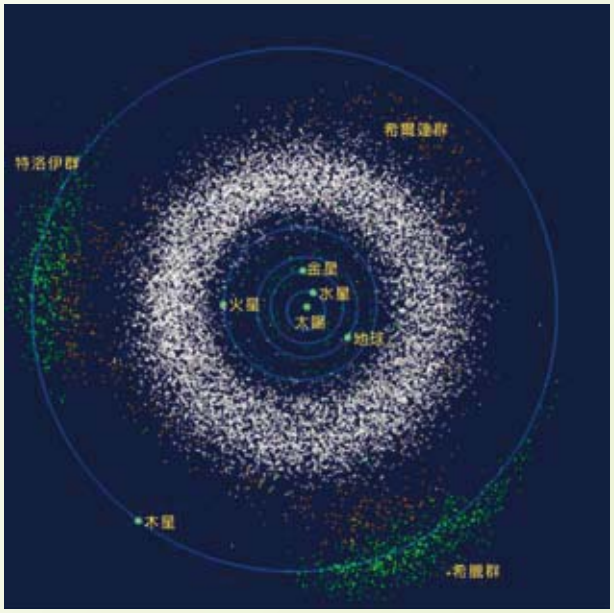

圖1.小行星分佈示意圖。絕大多數小行星集中於小行星帶中。本圖取自 http://upload.wikimedia.org/wikipedia/commons/f/f3/InnerSolarSystem-en.png

小行星帶中存在「柯克伍德縫隙」(圖2)，在這些區域的天體其軌道周期與木星軌道周期成簡單整數比，受到木星引力持續影響而成為橢圓軌道，或是遠離黃道面，容易受到進一步擾動而被散射掉，造成該區域缺乏小行星。可以把小行星想像成是沒有成形的行星，一般相信是因為受到木星引力的影響。有些則是小行星彼此撞擊而散開。小行星的公轉方向大都與八大行星及矮行星相同，這符合太陽系形成的星雲學說，認為太陽系天體皆源於一團旋轉的分子雲。

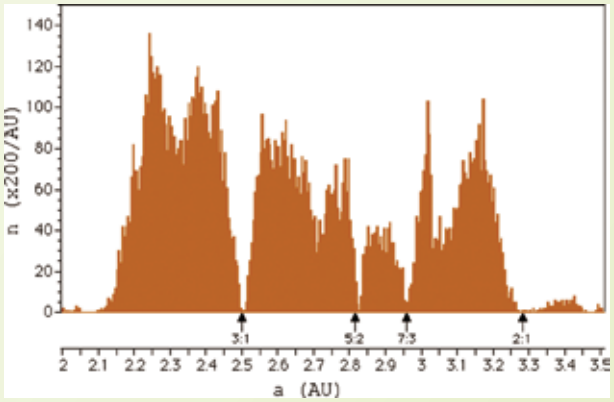

圖2.小行星帶中有些區域明顯缺乏小行星，稱爲「柯克伍德縫隙」。圖中所示爲小行星個數密度隨離太陽距離的分佈。縫隙所在處爲與木星軌道共振的區域，該區域的軌道週期與木星軌道週期成簡單整數比，如圖中標示之3:1, 5:2等。

觀測天體時，天體之張角 θ 大小，與天體實際大小（直徑）d，以及觀測者與天體之間的距離 r 有關： $\theta = d / r$，這裡的張角單位是弧度 (radian)。由於投影面積愈小，視角愈小，所以某天體離觀測者愈遠，其視角愈小。天文觀測常用的角度單位為角度、角分、角秒。一角秒為一度的3600分之一，是個很小的張角，在三角形中，一角秒的對邊只有邊長的約20萬分之一，相當於在五公里之外，一個十元硬幣的張角。太陽系天體之視直徑，太陽為 32'、月球約30'，兩者都約半度，也就是伸直手臂，大約半根食指的寬度。行星就小得多，例如金星約0.56'、木星0.68'、土星0.3'，火星則差不多是0.17'。

小行星當中，體積最大，也是第一個發現的小行星為「穀神星」(Ceres)，於1801年發現，直徑為960公里，已於2006年8月24日升級為矮行星，與冥王星及鬩神星 (Eris) 成為同類；而體積小的小

行星，例如 1991BA，只有6公尺寬。圖3為幾個大型小行星的影像，附表則為它們的部分參數。小行星的數量大約與其直徑的3到4次方成反比，也就是愈小的小行星數量愈多得多。

有一種小行星研究，是找出軌道在地球軌道附近，可能撞擊而危害地球的「近地小行星」，對這類小行星，我們希望盡量把它們全部指認出來，然後精確預測其軌道—這很不容易，因為它們很容易受到其他天體引力影響—以提供防範措施，這攸關整個地球文明，是很重要的工作。當然，如何減少小行星撞擊所造成的災害，甚至能排除撞擊，是更關鍵的課題。

以科學課題來說，我們探討小行星的數量、大小與空間分佈，或是它們的組成等等。小行星體積小，不像地球有地熱，造成火山、板塊運動等活動，因此地球已經不再是當初形成時候的情形，然而小行星有如化石，記錄了太陽系誕生以及撞擊的過程。小行星的大小是基本的物理參數之一，下面我們討論怎麼測量小行星的直徑。

圖3

穀神星
經過色調加強後的影像
(HST)

智神星
影像顯示其非正圓的形狀 (HST)

灶神星
(HST)

編號	名稱	發現年份	發現者	長軸(km)	自轉周期(hr)	反光率	平均日距(AU)	軌道週期(年)	軌道橢圓率	軌道傾角(度)
1	穀神星(Ceres)	1801	G. Piazzi	960	9.08	0.1	2.767	4.61	0.08	10.6
2	智神星(Pallas)	1802	H. Olbers	570	7.81	0.14	2.771	4.61	0.23	34.8
4	灶神星(Vesta)	1807	H. Olbers	578	5.34	0.38	2.362	3.63	0.09	7.1

如何測量小行星直徑

估計小行星直徑有以下幾種方法：（1） 測量小行星的反光與發光能力；（2）利用無線電波雷達取得影像；（3）太空船飛到附近直接測量；（4）利用掩星事件。

小行星的亮度來自反射陽光，這與小行星與太陽的距離，以及小行星與地球的距離有關。另外影響反射光強度的，是小行星本身大小與反射率。另一方面，小行星除了反光，也吸收陽光而本身發出熱量，這也與小行星大小及反射率有關。所以我們可以在可見光波段測量小行星反射強度，另外在長波（遠紅外或微波波段）測量其熱輻射強度，便能求得小行星的大小及反射率。由於來自小行星的熱輻射非常微弱，因此非得需要大型電波望遠鏡與專業儀器不可。只有少數情況，能夠在可見光直接解析出表面大小，例如圖4是哈伯太空望遠鏡觀測觀測9 Metis 的小行星影像，經過特殊影像還原處理，所得到的結果，小行星明顯不為圓形，其大小為 235 公里 x 165 公里。

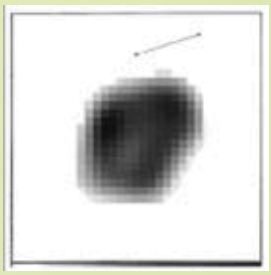

圖4. 小行星 9 Metis 由哈伯太空望遠鏡拍攝，經過處理後的影像。Storrs (1999) Icarus, 137, 260,

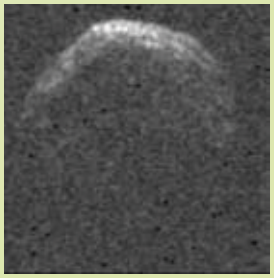

圖5.1950 DA 的雷達反射影像，本圖取自 http://www.planetary.org/html/news/articlearchive/headlines/2002/1950DA.htm (S. Ostro, JPL)，動畫檔可見 http://neo.jpl.nasa.gov/1950da/radar_movie.html

順帶一提，以上這篇研究論文發表在 Icarus 期刊，專門登載研究行星科學的學術論文。Icarus 源於希臘神話人物，以蠟製翅膀飛行，因為太接近太陽，翅膀融化而墜海。Icarus 也是顆小行星的名字，編號1566。

直接以雷達可以取得小行星的影像，以估計其大小。例如圖5是2001年3月4日利用波多黎各的電波望遠鏡取得之編號 1950DA 小行星的影像，當時

這顆小行星距離我們約地月距離的22倍，算是對地球具潛在威脅的小行星 (Potentially Hazardous Asteroids, PHAs) 之一。1950DA 小行星直徑約一公里，據估計在西元2880年有三百分之一的機會撞擊到地球。

在太空船測量方面，圖6是 Gaspra 小行星，編號 951，其三軸尺寸為19x12x11 公里，首先於1991年被「伽利略號」太空船近距離觀測，可以看到這顆約20公里大小之小行星，表面有許多撞擊痕跡，是被更小的太空碎片撞擊的結果。伽利略號快速經過 Gaspra 小行星後，繼續飛往木星。

圖6.小行星 Gaspra 的影像（伽利略號拍攝）

另外一提，我們看到小行星的形狀不規則。為什麼大型天體，例如太陽、地球，甚至月球都成球型，而小型天體總是形狀不規則呢？這個現象，居然和烤肉時把煤炭打碎才容易點燃的原理類似！這是因為東西打碎了，相同的體積便有了更大的表面積。因此，體積大的天體，熱容量大，受到撞擊加熱，之後由於表面積相對小，冷卻速率慢，因此引力能夠將天體拉縮成最穩定狀態的球型。相反的，直徑小於約 200～300 公里的小天體，例如小行星、彗星核等，形狀多不規則。

以下介紹如何藉由小行星掩過背景恆星，以掩星的時間估計小行星的大小。

利用掩星估計小行星大小與形狀

發生小行星掩星時，小行星的影子投影在地球上(圖7)，如果觀測者記錄下恆星消失與復出的時間，由於我們知道小行星的軌道，便可以由影子的速度來估算小行星的大小。當然，個別觀測者看到的只是某個影子當中的一個截切線段，要是能結合不同位置的觀測者，組成觀測網，整合他們記錄的時間，便能繪製出小行星的大小與形狀。圖8是小行星掩星時，不同觀測者各自測量掩星時間與長短(上圖)，便能繪出小行星的形狀與大小 (下圖) ，左邊 a是地面歐洲南方天文臺8米望遠鏡取得的影像，中央 b 是掩星觀測的結果，右邊 c 則是太空船前往小行星附近所拍的照片。可以看出掩星觀測不需要大型昂貴設備，但藉由有組織的紀錄，一堆小兵也可以立大功！

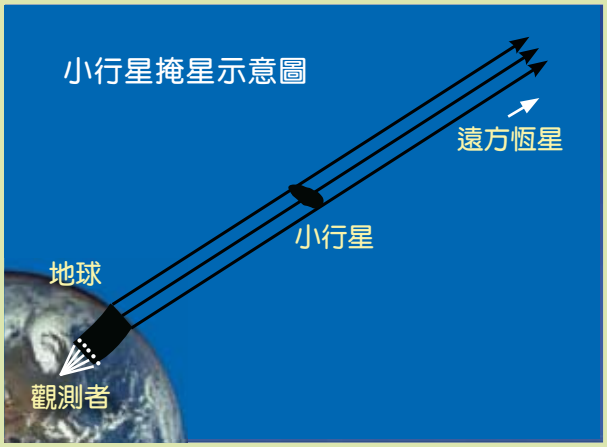

圖7.小行星遮掩遙遠恆星時，小行星的陰影投影在地表

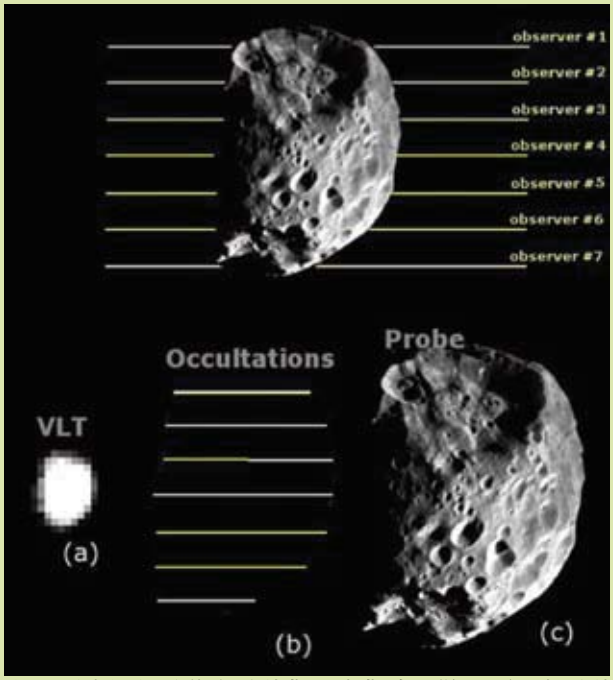

圖8.（上圖）分佈各地的觀測者觀察到陰影不同部分的截切線段，其記錄到的掩星開始、結束時間不同，掩星期間長短也不同。（下圖）a 是超大望遠鏡 (Very Large Telescope) 取得的小行星影像； b 是利用上圖掩星觀測網所估計出來的小行星大小與形狀；c 是太空船前往小行星附近所取得的影像。http://www.occultations.net/occultations-asteroids.htm

觀測小行星掩星時，由於我們監測的是恆星的亮度變化，因此重點在於能看到恆星，但是並不需要看得到小行星，這表示即使小望遠鏡也可以進行觀測。較為關鍵的是計時，這在臺灣也不是問題。國際的掩星組織 IOTA (International Occultation Timing Association) 宣稱，即使只有簡單望遠鏡、沒有數位相機，只要能計時，就能從事掩星觀測。圖9,10是Richard Nugent 先生網站介紹他的設備，包括望遠鏡、數位相機等一共只有大約10公斤而已，架設簡單。國內的觀測者，例如科博館林志隆博士也開發出適合觀測掩星的設備，值得參考。

在臺灣能觀測到的小行星掩星事件，可以參閱 http://asteroidoccultation.com/ 這個網站的預報，內容包括日期、時間、小行星編號、背景恆星編號及可觀察地點等。

舉例而言，在2007年12月12日國際時間17：21 UT，會有一顆12.0等的恆星被一顆12.6 等的小行星遮掩(圖11)，這是小行星暗，背景星亮的例子，而每一星等相差2.51倍，臺灣本地時間要把UT 加上8小時。對於這個事件，小行星已知直徑61公里，它在太空就會形成一個61公里為直徑的柱

圖11

圖9.Richard Nugent 的可攜式掩星觀測裝備，包括望遠鏡、錄影機、收音機（對時），以及電池組。國內對時可以使用手機報時，裝備更精簡。http://www.lunar-occultations.com/iota/video/rnvideosetup.htm

圖10.圖9的輕簡裝備可以架設在後車廂上方，方便操作。

狀陰影，投影在地球表面，依照預測陰影會經過臺灣南端（圖12），所以墾丁就適合觀測。要注意這樣的預測只提供參考，因為小行星越大其陰影軌跡就預測得愈準，而較小的小行星預測得較不準，但這些小天體不容易用其他方法測量，反而是掩星觀測發揮功效之處。但是要布置全臺觀測網，來觀測只有幾十公里的小行星掩星，其預測誤差可能超過全臺灣範圍，困難可見，不過要是觀測成功，科學回報卻非常可觀。

圖12

NEAR太空船於1996年2月17日從美國佛羅里達州發射，在1999年2月遭遇到 433 Eros 小行星，當時距離1800公里。由於受到其他天體的引力干擾，小行星的自轉常不規則(圖13)。

圖13. 小行星 Eris 自轉後我們看到不同面向。其動畫可參見 http://nssdc.gsfc.nasa.gov/planetary/image/eros_movie_20000208.gif，在此網站可以看到 Eros 的動畫影像。

接著我們再看一個有趣的小行星。小行星 243 Ida 本身只有50幾公里，卻有個小月亮 Dactyl，大小只有 1.4 公里，彼此互繞（圖14）。藉由軌道半徑及周期，可以計算出小行星的質量。如同太陽質量可由地球軌道半徑及周期求得，而地球質量可由月球軌道求得，月球質量則要靠人造天體軌道求得。

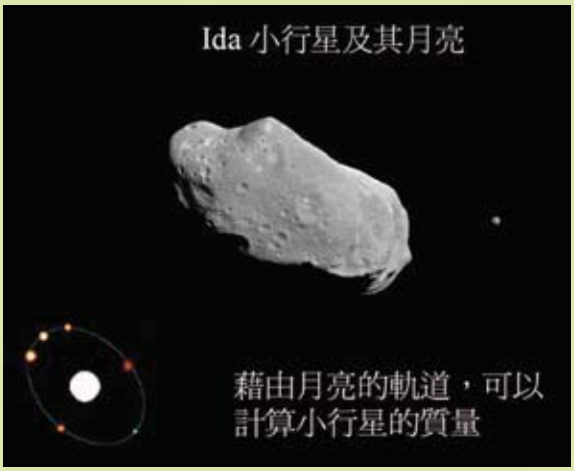

圖14. Ida 小行星及其衛星 Dactyl

小行星 87 Sylvia 就更有意思了。這顆小行星於2001年由夏威夷 Keck II 口徑十公尺的望遠鏡發現第一個月亮 Romulus，直徑18km，2005年歐洲南方天文臺發現第二個月亮Remus，直徑7km，成為第一個已知擁有兩個小月亮的小行星。由質量、體積可以求出密度，發現 87 Sylvia 的密度為1.2g/cm3，結構鬆散，像個「石頭堆」（rubble pile）。距推論這類小行星曾遭受劇烈撞擊，碎散之後又因為自身引力而重新聚集。

87 Sylvia 於2006年12月18日遮掩 BD +29 1748號恆星。當時中美掩星計劃 TAOS 的其中兩座望遠鏡，TAOS–A, TAOS-B 測得大約20秒的掩星(圖15) 。同樣位於鹿林天文臺的40 cm 望遠鏡觀測同樣事件，也測得大約20秒的掩星持續時間(圖16) 。但是從距離鹿林天文臺40公里外，位於臺中的林志隆博士用望遠鏡及DV拍攝，卻測得兩次掩星事件，持續時間分別為23.9秒及10.8秒(圖17)。經過分析，發現 BD +29 1748 原來是顆緊密相距0.1" 的雙星，之前不知道，但是經由這次掩星事件，居然用簡單的儀器，得到了一般大型望遠鏡都沒有的解析力。我們雖然沒有多學到有關於小行星的知識，但卻學到背景恆星的知識！

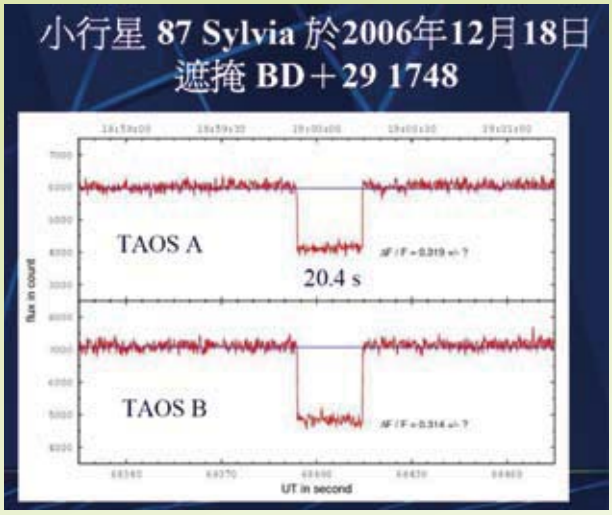

圖15. 小行星87 Sylvia 於2006年12月18日掩過恆星 BD+29 1748，鹿林天文台兩台 TAOS 望遠鏡成功記錄到該次掩星事件。

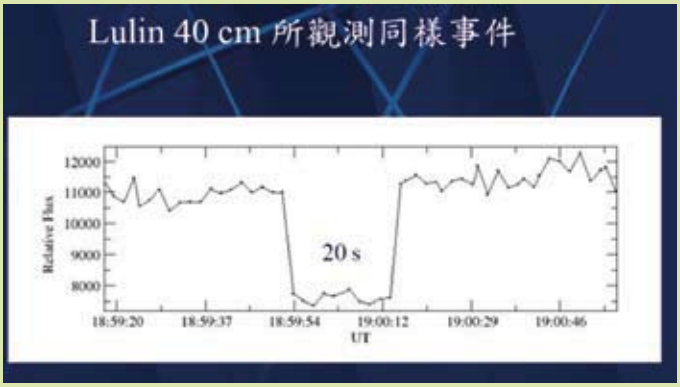

圖16. 與圖15相同的掩星事件，同樣位於鹿林天文台的40公分望遠鏡也記錄到約20秒的掩星事件。

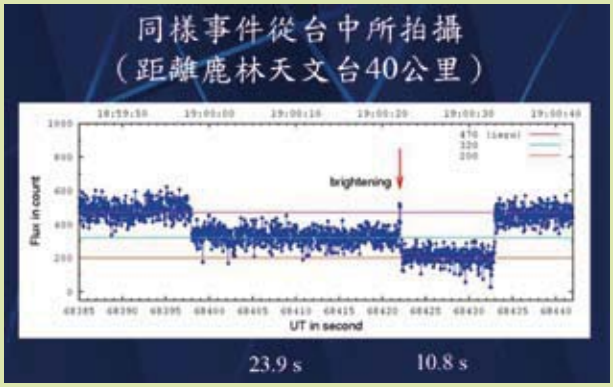

圖17. 與圖15、16相同的掩星事件，在台中市觀測，卻看到不一樣的光變曲線，顯示發生了兩次掩星，分別長達23.9秒與10.8秒。

業餘天文學家除了觀測掩星，以估計小行星大小，另外還可以監測小行星亮度變化。小行星的亮度變化源於其不規則形狀以及表面不均勻的成分。當小行星自轉時，不同面向反射陽光到地球，亮度變化周期等於小行星自轉週期。有些小行星的亮度變化起因於表面成分不同，這些會造成顏色也有同樣週期變化(圖18)。一般小行星亮度變化週期約4到12小時。

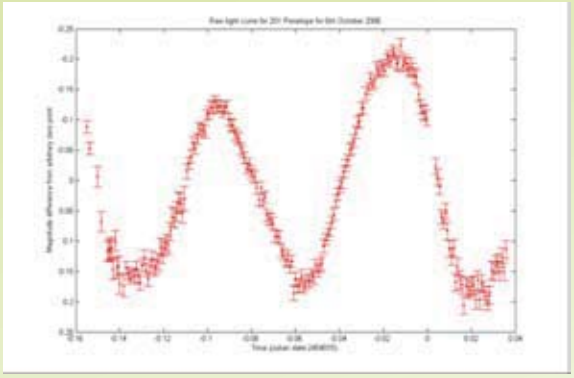

圖18. 小行星亮度變化來自於自轉以及表面的反射物質不均

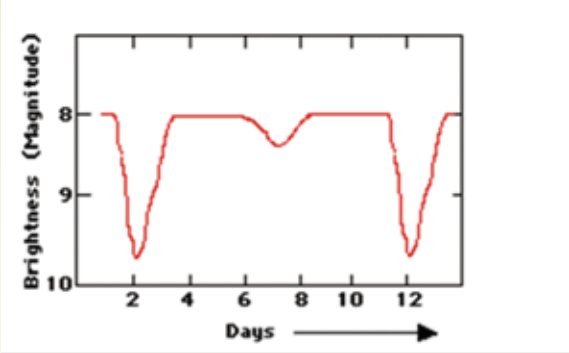

圖19. 食雙星光變曲線一例

光變曲線 (lightcurve) 是亮度隨時間的變化，例如食雙星是兩顆星互繞（圖19)，或是超新星因星球爆炸而突然變亮（圖20），都有明顯容易辨認的光變曲線。

結論

即使只用簡單的設備，甚至沒有望遠鏡、電子相機，也可以進行有用的天文觀測。小行星掩星或月掩星觀測門檻低，適合一般業餘同好從事。若是能有組織規劃，建立局部，甚至大規模觀測網，可以取得具影響力的科學成果。

陳文屏教授：任教於國立中央大學天文所
蔡穎仁：任職於臺北市立天文科學教育館

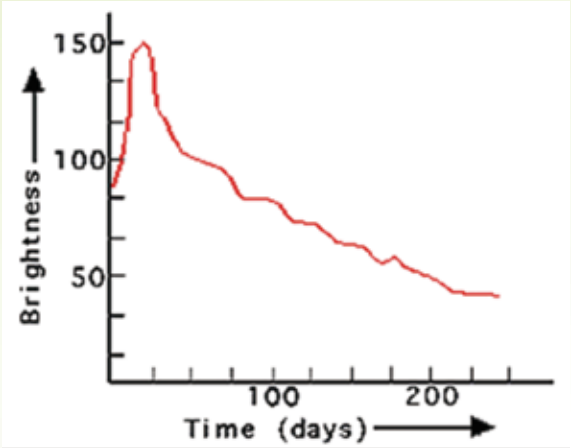

圖20. 超新星光變曲線一例